THE UNIVERSITY OF ADELAIDE

Department of Chemistry

DIORGANOPHOSPHINOTHIOFORMAMIDES: DERIVATIVES AND METAL COMPLEXES

A thesis submitted by

Georgios Siasios B.Sc. (Hons)

for the degree of Doctor of Philosophy

March, 1995

VOLUME 1

DECLARATION

This thesis contains no material that has been submitted previously for a degree or diploma in any university and to the best of my knowledge contains no material published or written by another person, except where due reference is made.

I consent to this thesis being made available for photocopying and loan.

9/3/95

ACKNOWLEDGMENTS

I would like to extend genuine gratitude to my supervisor, Dr E.R.T. Tiekink, who through his continual guidance, immeasurable assistance and helpful conversation has contributed significantly to the essence of this research.

The assistance and friendship of my fellow research workers: Ernst Horn, John Faamau, Peter Cookson, Andrea Collins, Michael Cox and especially Veronica Hall, have been appreciated immensely.

I am heavily indebted to my parents for their support and sacrifices during these years which has made this work possible.

The receipt of a Commonwealth Postgraduate Research Award is gratefully acknowledged.

ABSTRACT

This thesis reports the preparation and characterisation of oxygen, sulfur and selenium derivatives of diorganophosphinothioformamides, i.e. $R_2P(Y)C(S)N(H)R'$, R, R' = alkyl and/or aryl and Y = O, S or Se. The compounds were characterised by infrared, multinuclear magnetic resonance and mass spectroscopic techniques as well as single crystal X-ray crystallographic methods. The detailed structural study of these derivatives revealed that the central P(1)-C(1) bonds in the R = Ph compounds were systematically longer than the corresponding distances in the R = Cy compounds. This difference in bond strength correlates with the different chemical behaviour of the compounds.

The second part of this thesis examined the coordination of the diorganophosphinothioformamides, i.e. $R_2PC(S)N(H)R'$, R, R' = alkyl and/or aryl, and their derivatives to metal centres employing spectroscopic methods and crystallography. The deprotonated diorganophosphinothioformamides were found to coordinate to metal centres, such as nickel, cobalt, gold and palladium, as bidentate ligands utilising the sulfur and phosphorus donor atoms forming four-membered MPCS rings. Of particular interest was the observation of a P-, S-chelation mode in two of the ligands as well as a S-, N- coordination mode in the structure of $\{Co[Cy_2PC(S)NPh]_3\}$. In the structure of $\{Au[Cy_2P(O)C(S)N(H)Me]Cl\}$ the ligand coordinated in a monodentate mode *via* the sulfur atom exclusively. A S-, S- chelation mode was found for the deprotonated $[Ph_2P(S)C(S)N(H)Ph]$ ligand in the structure of the nickel complex which resulted in the formation of a five-membered NiSPCS ring. Similar S-, Se-coordination was observed in the structures of the nickel and cadmium complexes involving the $R_2P(Se)C(S)N(H)Ph$ ligands which resulted in the formation of novel MSePCS five-membered rings.

ABBREVIATIONS

The following abbreviations are used in this thesis:

Å	Angström
b. pt	boiling point
°C	degree Celsius
^{13}C NMR	carbon-13 nuclear magnetic resonance
Cy	cyclohexyl
dec.	decomposition point
Et	ethyl
FAB-MS	Fast Atom Bombardment - mass spectroscopy
^{1}H NMR	proton nuclear magnetic resonance
Hz	hertz
IR	infrared spectroscopy
$^{x}J_{AB}$	coupling constant between nuclei A and B over x bonds
$[M]^{+}$	molecular ion
Me	methyl
m. pt	melting point
m/z	mass to charge ratio
NMR	nuclear magnetic resonance (Fourier Transform)
^{31}P NMR	phosphorus-31 nuclear magnetic resonance
Ph	phenyl
ppm	parts per million
thf	tetrahydrofuran
TMS	tetramethylsilane
δ	chemical shift
λ	wavelength
υ(A–B)	stretching frequency of A–B bond

TABLE OF CONTENTS

Chapter 1

INTRODUCTION

1.1 General Introduction

Metal phosphine complexes, in particular transition metal phosphine complexes, form a most important class of compound. Phosphines, themselves, may be employed in organic synthesis and transition metal phosphine complexes are used extensively as hydrogenation catalysts [1]. A more recent development, and pertinent to this thesis, is the use of certain metal phosphine complexes in medicine; a brief overview of this aspect is given in Chapter 5. Triorganophosphine ligands normally coordinate metal centres exclusively *via* the lone pair of electrons residing on the phosphorus atom. The incorporation of an additional potential donor atom(s) in the organo residue(s) gives rise to additional coordination possibilities and therefore different chemical reactivities. One such class of phosphine is the diorganophosphinothioformamides (**I**), shown below.

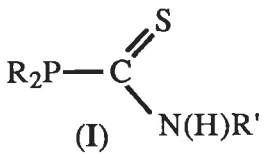

(**I**)

R, R' = alkyl, aryl

These ligands have the potential to coordinate a metal centre(s) *via* the phosphorus and/or sulfur atoms. Owing to the presence of an acidic proton on the nitrogen atom, these ligands have the additional facility of being deprotonated leading to uninegative anions. The derived ligands may utilise one of, or some combination of, the phosphorus, sulfur and nitrogen atoms in coordination to metal centres.

Three of the neutral diorganophosphinothioformamide ligands (R = Ph or Cy, R' = Ph and R = Ph, R' = Me) have been characterised crystallographically. Further, a limited number of metal complexes with the neutral ligand and its deprotonated form have also been analysed crystallographically (see later).

Diorganophosphinothioformamides may be synthesised by the insertion of an alkyl or aryl isothiocyanate into the P-H bond of a dialkyl- or diaryl-phosphine in an inert atmosphere [2, 3], Scheme 1. The reaction proceeds readily without the necessity of base to

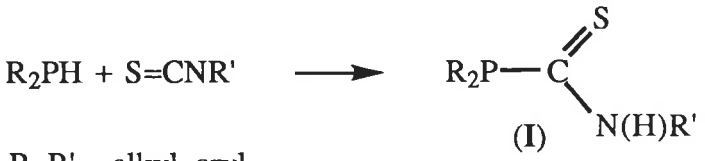

Scheme 1

initiate the process. The deprotonated diorganophosphinothioformamide can also be incorporated directly into a metal complex by the insertion of an isothiocyanate into a metal-phosphorus bond in which monodentate coordination to the metal centre occurs *via* the sulfur or nitrogen atom [4-9]; see Scheme 2. An investigation of the chemistry of these ligands shows that when R = Cy the reactivity of the ligands is greatly enhanced compared to the R = Ph counterpart [10-11]; in some cases no reaction occurs when this latter ligand is employed [12]. A review of the literature of the diorganophosphinothioformamide ligands (**I**) and their metal complexes is given in Sections 1.4-1.9.

M = Sn or Tl; R, R' = alkyl, aryl; R'' = alkyl; n = 2 or 3

Scheme 2

The oxidation of the phosphorus(III) atom in (**I**) by oxygen, sulfur or selenium gives rise to a new class of potential ligands, these are known as the diorganophosphinylthioformamides (**II**), diorganothiophosphinylthioformamides (**III**) and diorganoselenophosphinylthioformamides (**IV**), respectively. These phosphorus(V) ligands can also be prepared by

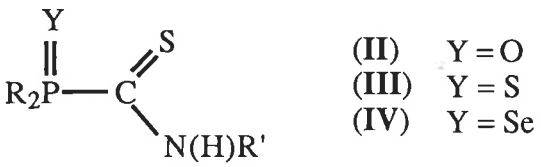

reacting a diorganophosphine, R_2PH, with either oxygen, sulfur or selenium, and to the resulting species, isothiocyanate is inserted into the P-H bond.

The phosphorus(V) centre in each of (**II**), (**III**) and (**IV**) is no longer available for coordination, however, the phosphorus-bound hetero atom, Y, is. The coordination

potential of these ligands is largely unexplored and non-existent for Y = Se. Only three metal complexes have been characterised structurally with the ligands being deprotonated in each case; a review of the available structures in the literature is given in Sections 1.5-1.6.

The aim of the work embodied in this thesis is to i) ascertain the coordination potential of both neutral and deprotonated diorganophosphinothioformamide (**I**) ligands towards a variety of metal centres, ii) to prepare and characterise both spectroscopically and crystallographically the diorganophosphinylthioformamide (**II**), diorganothiophosphinylthioformamide (**III**) and diorganoselenophosphinylthioformamide (**IV**) compounds, and iii) to examine the coordination properties of (**II**), (**III**) and (**IV**) in both their neutral and deprotonated forms towards a variety of metal centres. A particular focus of this work has been an examination of gold coordination complexes of these ligands.

1.2 Gold-based Pharmaceuticals, Chemistry

As mentioned above, metal phosphine complexes are known to possess useful pharmaceutical properties. In particular gold(I) phosphines have shown activity against rheumatoid arthritis and more recently, good cytotoxicity. Hence, as stated above, the interaction of the diorganophosphinothioformamides and their oxidised derivatives with gold centres has been examined. In this section, a brief overview of gold chemistry is given, in particular in the context of pharmacology.

Gold can exist in several oxidation states, -I, 0, I, II, III and V, however, gold chemistry is dominated by the oxidation states 0, I and III. The gold(III) nucleus is a very powerful oxidising agent, and as such is toxic in the reducing environment of the mammalian body; the gold(I) centre is not as oxidising. Nevertheless, the gold(I) species needs to be stabilised as in an aqueous medium gold(I) centres disproportionate into inactive metallic gold and gold(III) according to the following equation:

$$3Au(I) \longrightarrow 2Au(0) + Au(III)$$

Gold(I) is a soft metal ion and shows a preference for soft donor atoms such as sulfur, phosphorus and carbon, over hard donor atoms such as nitrogen and oxygen. Thus, gold(I) is stabilised by ligands such as cyanide, phosphines (e.g. R_3P), and a range of sulfur-

containing ligands (e.g. sulphydryl). The same ligands also stabilise gold(III). An anti-arthritic compound containing gold(I), phosphorus and sulfur, e.g. *S*-2,3,4,5-tetraacetyl-1-β-D-thioglucose triethylphosphinegold(I), known as auranofin [13], is in wide clinical use.

The gold(I) centre prefers a linear arrangement but coordination numbers of three and four are also known. In the linear geometry, as found in auranofin, incoming ligands can approach the gold atom without steric interference and bind to the gold atom to form an intermediate three coordinate gold centre. It is possible that over a period of time that one of the original ligands can cleave off the gold resulting in a new linear gold(I) system as represented below.

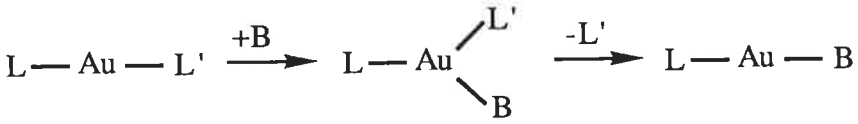

This could be the mechanism of ligand exchange which occurs on the gold(I) centre for gold drugs in the biological medium, see Chapter 5. For the above reasons, only gold(I) coordination chemistry has been examined in this thesis (with one exception).

1.3 Coordination Properties of Diorganophosphino-, Diorganophosphinyl- and Diorgano-thiophosphinyl- thioformamides

In the following sections the available crystallographic data for the diorganophosphino-thioformamide, diorganophosphinylthioformamide, and diorganothiophosphinylthioform-amide compounds are summarised. All diagrams have been redrawn with the ORTEP program [14] using arbitrary thermal ellipsoids; hydrogen atoms have been omitted for most diagrams for reasons of clarity. A common numbering scheme has been adopted throughout this thesis as shown in Fig. 1.3a. This section is organised such that the neutral diorganophosphinothioformamides are discussed first followed by their metal complexes with the neutral and deprotonated ligands, respectively. The metal complexes with the phosphorus(V) derivatives will follow. The few metal complexes with the phosphorus(V) derivatives will be described directly after their phosphorus(III) counterparts.

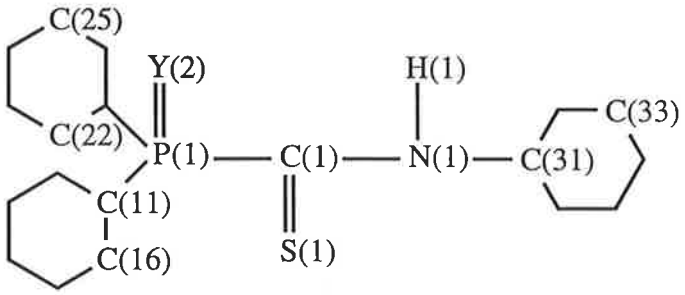

Fig. 1.3a Numbering scheme adopted for the $R_2P(Y)C(S)N(H)R'$ compounds

1.4 $[Ph_2PC(S)N(H)Ph]$ and Metal Complexes

1.4.1 The Molecular Structure of $[Ph_2PC(S)N(H)Ph]$

The molecular structure of $[Ph_2PC(S)N(H)Ph]$ [15], is illustrated in Fig. 1.4.1, which shows that the conformation about the C(1)-N(1) bond is *Z*, and that the central P, C(1), S and N chromophore is essentially planar. The P(1)-C(1) distance of 1.862(3) Å is similar to the distance of a normal P-C single bond of 1.87 Å [16]. The expected C=S double bond distance is about 1.61 Å [16] and the distance found in $[Ph_2PC(S)N(H)Ph]$ of 1.650(3) Å is longer than this value. The C(1)-N(1) bond distance of 1.334(3) Å is shorter than the N(1)-C(31) distance of 1.422(3) Å which suggests some double bond character in the former bond. The deviation of the C(1)=S(1) and C(1)-N(1) bond distances from their expected C=S and C-N values is indicative of significant delocalisation of π-electron density over the C(1), S and N moiety which is consistent with the canonical forms shown in Scheme 1.4. The angles about the central C(1) atom, i.e. S(1)-C(1)-P(1), S(1)-C(1)-N(1) and P(1)-C(1)-N(1), are 114.4(2), 128.8(2) and 116.8(2)°, respectively, consistent with a sp^2 carbon atom. The nitrogen bound-phenyl group and the central P, C(1), S and N chromophore form a dihedral angle of about 6°.

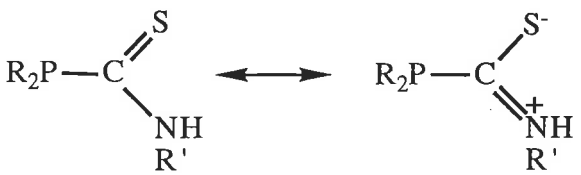

Scheme 1.4

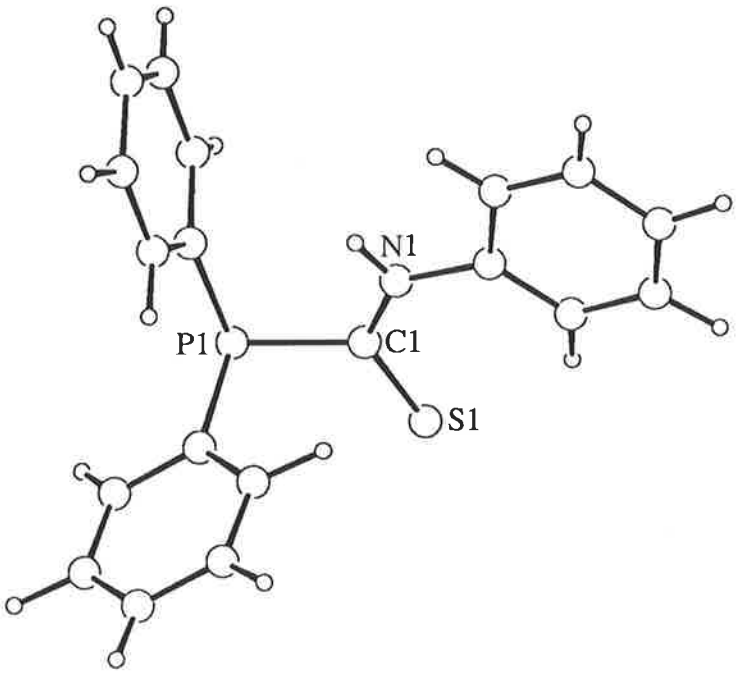

Fig. 1.4.1 The molecular structure of [$Ph_2PC(S)N(H)Ph$]

1.4.2 The Molecular Structure of fac-{MnBr(CO)$_3$[Ph$_2$PC(S)N(H)Ph]}

The sole example of a crystal structure with the diphenylphosphinothioformamide ligand, i.e. [Ph$_2$PC(S)N(H)Ph], coordinated to a metal centre in the neutral form is that for the complex *fac*-{MnBr(CO)$_3$[Ph$_2$PC(S)N(H)Ph]}, as shown in Fig. 1.4.2 [17]. The ligand maintains the *Z* configuration about the C(1)-N(1) bond upon coordination. The manganese atom is chelated by the ligand *via* the phosphorus (Mn-P(1) 2.315(3) Å) and sulfur atoms (Mn-S(1) 2.381(3) Å) which leads to the formation of a four-membered ring. A bromide atom and three carbonyl groups, which define one octahedral face, complete the coordination polyhedron around the manganese atom. Some noteworthy distances involving the diphenylphosphinothioformamide ligand are: S(1)-C(1) 1.68(1), P(1)-C(1) 1.851(9) and C(1)-N(1) 1.30(2) Å. The angles around the manganese atom are close to the ideal octahedral with the exception of S(1)-Mn-P(1) chelate angle of 72.5(1)° which is significantly less than the expected angle of 90°. This observation is attributed to the restricted "bite angle" of the [Ph$_2$PC(S)N(H)Ph] ligand. Other angles of note in the structure are S(1)-C(1)-P(1), S(1)-C(1)-N(1) and P(1)-C(1)-N(1) of 103.6(6), 130.7(5) and 125.6(5)°, respectively.

1.4.3 The Molecular Structure of {Mn(CO)$_4$[Ph$_2$PC(S)NPh]}

The structure of the {Mn(CO)$_4$[Ph$_2$PC(S)NPh]} complex was determined independently by two different groups [17,18], equivalent parameters were found in the two reports. The details presented below are from reference 18. The structure is displayed in Fig. 1.4.3 where it can be seen that coordination to the manganese atom by the [Ph$_2$PC(S)NPh]$^-$ ligand is *via* the sulfur and phosphorus atoms, Mn-S(1) 2.383(3) and Mn-P(1) 2.310(1) Å, the remaining positions being occupied by the carbonyl ligands. The manganese atom exists in a distorted octahedral environment, the distortion arising owing to the restricted bite angle of the [Ph$_2$PC(S)NPh]$^-$ ligand, S(1)-Mn-P(1) 73.00(4)°. The presence of the four-membered ring also distorts the tetrahedral geometry about the phosphorus atom, Mn-P(1)-C(1) 91.9(1)°. The S(1)-C(1) 1.755(4) Å, P(1)-C(1) 1.834(3) Å, and C(1)-N(1) 1.270(4) Å

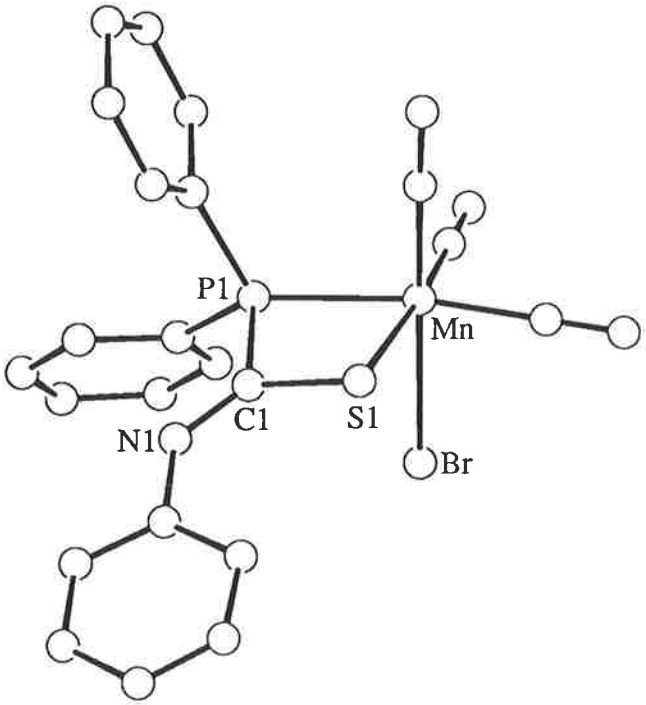

Fig. 1.4.2 The molecular structure of *fac*-{$MnBr(CO)_3[Ph_2PC(S)N(H)Ph]$}

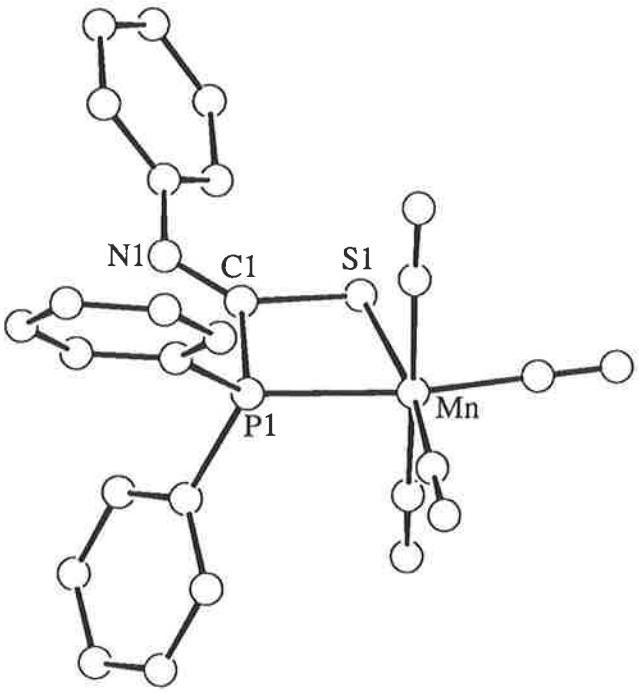

Fig. 1.4.3 The molecular structure of $\{Mn(CO)_4[Ph_2PC(S)NPh]\}$

bond distances have expanded, contracted and contracted, respectively compared to those in the neutral ligand, $[Ph_2PC(S)N(H)Ph]$ [15]. The S(1)-C(1) distance has changed from a formal double bond to one with more single bond character while the reverse has occurred for the C(1)-N(1) bond which has acquired additional double bond character. The P(1)-C(1) separation has decreased by some 0.03 Å from the free ligand indicating that this is a relatively stronger bond in the complex. There are also notable differences in the angles about the C(1) atom compared to the uncoordinated ligand, these having expanded, expanded and contracted to 102.1(2), 134.0(3) and 123.8(3)° for S(1)-C(1)-P(1), S(1)-C(1)-N(1) and P(1)-C(1)-N(1), respectively. These angles are indicative of a sp^2 carbon.

1.4.4 The Molecular Structure of {$Ph_3PRu(MeCp)[Ph_2PC(S)NPh]$}

The deprotonated form of the $[Ph_2PC(S)N(H)Ph]$ ligand appears in the molecular structure of the organometallic ruthenium complex, $\{Ph_3PRu(MeCp)[Ph_2PC(S)NPh]\}$, where MeCp is the methylcyclopentadienyl ligand, as shown in Fig. 1.4.4 [19]. The ruthenium atom is chelated by the phosphorus and sulfur atoms of the $[Ph_2PC(S)NPh]^-$ ligand (Ru-P(1) 2.295(1), Ru-S(1) 2.401(2) Å) which define a chelate angle of 72.14(6)°. The third coordination site is occupied by the phosphorus atom of the triphenylphosphine ligand (Ru-P(2) 2.299(1) Å). If the MeCp ligand is assumed to occupy three coordination sites, the ruthenium atom geometry is that of a distorted octahedron. Distortions from the regular geometry may be related to the restricted bite angle of the $[Ph_2PC(S)NPh]^-$ ligand and the steric bulk of the PPh_3 ligand. The S(1)-C(1) and C(1)-N(1) bond lengths have elongated and contracted to 1.762(5) and 1.263(6) Å, respectively, while the S(1)-C(1)-P(1) angle has decreased to 100.3(2)°, compared with the equivalent parameters for the neutral ligand $[Ph_2PC(S)N(H)Ph]$ [15]. These parameters follow similar trends to what was observed above for the $\{Mn(CO)_4[Ph_2PC(S)NPh]\}$ complex.

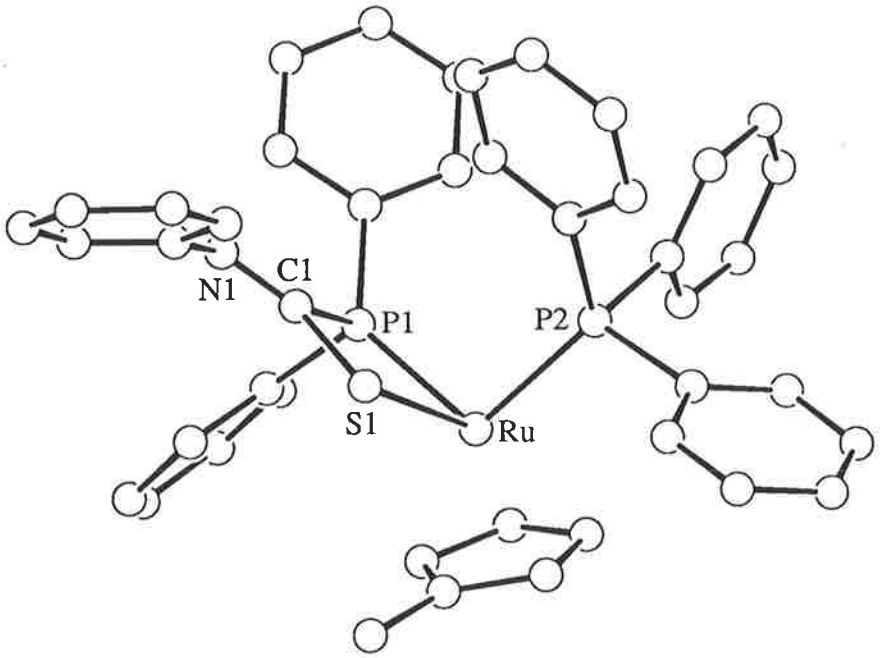

Fig. 1.4.4 The molecular structure of {$Ph_3PRu(MeCp)[Ph_2PC(S)NPh]$}

1.4.5 The Molecular Structure of {$Ph_3Sn[Ph_2PC(S)NPh]$}

The structure of the {$Ph_3Sn[Ph_2PC(S)NPh]$} complex is illustrated in Fig. 1.4.5 [20]. The deprotonated ligand coordinates the tin centre *via* the sulfur atom (Sn-S(1) 2.463(1) Å) which results in the elongation of the S(1)-C(1) bond distance (1.746(4) Å *cf.* 1.650(3) Å for the free ligand [15]). The sulfur atom and the three carbon atoms derived from the three phenyl substituents define a distorted tetrahedral geometry about the tin atom. There is, however, a weak secondary interaction between the nitrogen atom and the tin centre of 2.728(3) Å which is well within the sum of the van der Waals radii for the tin and nitrogen atoms (3.75 Å [21]) but this has been attributed to packing in the crystal lattice rather than representing a significant interaction; no evidence was found for intra- or inter-molecular coordination between phosphorus and tin. Hence, the $[Ph_2PC(S)NPh]^-$ ligand can be described as coordinating exclusively in the monodentate mode and functioning as a thiolate ligand. The C(1)-N(1) bond length of 1.278(4) Å is indicative of a formal double bond between these two atoms. Additional important parameters are P(1)-C(1) 1.860 Å, S(1)-C(1)-P(1) 112.0(2), S(1)-C(1)-N(1) 117.1(3) and P(1)-C(1)-N(1) 122.9(3)°.

1.5 Molybdenum Complex with $[Ph_2P(O)C(S)N(H)Ph]$

1.5.1 The Molecular Structure of {$Ph_3PMo(CO)_2[Ph_2P(O)C(S)NPh]_2$}

The structural analysis of {$Ph_3PMo(CO)_2[Ph_2P(O)C(S)NPh]_2$} showed that the molybdenum atom exists in a seven-coordinate environment as represented in Fig. 1.5.1 [22]; the phosphorus- and nitrogen-bound phenyl substituents were omitted for clarity. The ligand is present in its deprotonated form. The complex was isolated as a dichloromethane solvate, however, the dichloromethane molecule is not shown in the diagram. Two $[Ph_2P(O)C(S)NPh]^-$ ligands coordinate the molybdenum atom *via* the thiolato sulfur atom and the oxo function (Mo-S(1) 2.525(2) and 2.555(2) Å, Mo-O(2) 2.220(6) and 2.210(4) Å) which result in chelate angles, S(1)-Mo-O(2), of 80.0(1) and 77.9(1)° for each five-membered ring, respectively. The other three positions around the molybdenum atom are occupied by two carbonyl ligands and a PPh_3 group (Mo-P(2) 2.503(2) Å). The geometry

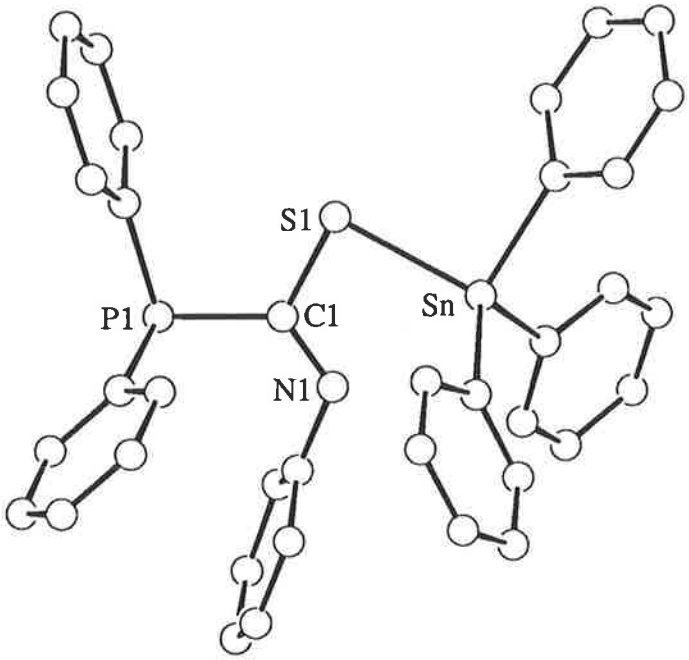

Fig. 1.4.5 The molecular structure of $\{Ph_3Sn[Ph_2PC(S)NPh]\}$

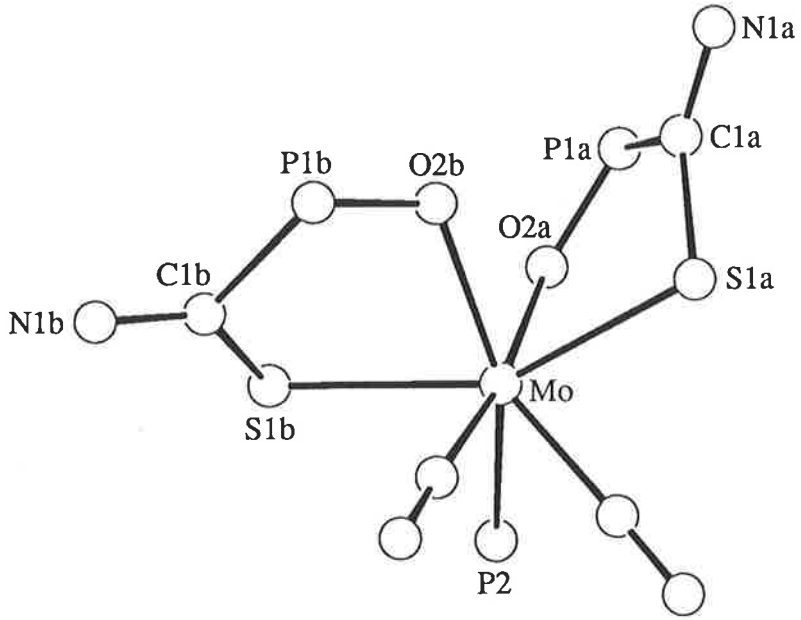

Fig. 1.5.1 The molecular structure of $\{Ph_3PMo(CO)_2[Ph_2P(O)C(S)NPh]_2\}$

about the molybdenum atom can be described as a 4:3 piano-stool configuration. The two anionic, bidentate ligands adopt essentially the same configuration about the metal atom and their parameters are almost equal within experimental error. The P(1)-O(2) bond length is 1.500(5) and 1.516(5) Å for each of the two molecules which are longer than the average P=O bond distance found in phosphine oxide structures of 1.46 Å [23]. The C(1)-N(1) bond length is shorter than the corresponding N(1)-C(31) distance, i.e. 1.290(8) and 1.278(9) vs 1.48(2). The C(1)-S(1) separations of 1.740(8) and 1.750(6) Å are consistent with the presence of thiolate atoms. The angles surrounding the P(1) atom of the $[Ph_2P(O)C(S)NPh]^-$ ligand are approximately 109° indicating a tetrahedral arrangement about this atom.

1.6 Metal Complexes with $[Ph_2P(S)C(S)N(H)Ph]$

Two complexes have been structurally characterised with the $[Ph_2P(S)C(S)N(H)Ph]$ ligand in its deprotonated form, i.e. $[Ph_2P(S)C(S)NPh]^-$. Two different coordination modes are adopted in the two complexes.

1.6.1 The Molecular Structure of {$Mn(CO)_4[Ph_2P(S)C(S)NPh]$}

The $[Ph_2P(S)C(S)NPh]^-$ anion coordinates the manganese atom in a bidentate manner *via* the thiophosphinyl S(2) atom and the thiolato S(1) atom resulting in the formation of a five-membered ring, as depicted in Fig. 1.6.1 [18]. The Mn-S(1) and Mn-S(2) bond distances are 2.390(1) and 2.410(1) Å, respectively. The Mn, P, C(1), S(1) and N atoms are coplanar with the S(2) atom lying above this plane (*ca.* 0.90 Å). The remaining sites about the central atom are occupied by four carbonyl ligands which complete an almost regular octahedral geometry about the manganese atom. No significant distortion from the ideal environment occurs owing to the chelate angle, S(1)-Mn-S(2), being 90.01(3)°. The five-membered ring is not as strained as the four-membered counterpart seen above for the {$Mn(CO)_4[Ph_2PC(S)NPh]$} complex. The bond distances in the two manganese complexes are equal within experimental error. There are, however, significant distortions in the angles, particularly around the C(1) atom. The S(1)-C(1)-P(1), S(1)-C(1)-P(1) and S(1)-C(1)-P(1) angles for the {$Mn(CO)_4[Ph_2PC(S)NPh]$} complex [18] are 116.9(2), 129.2(3)

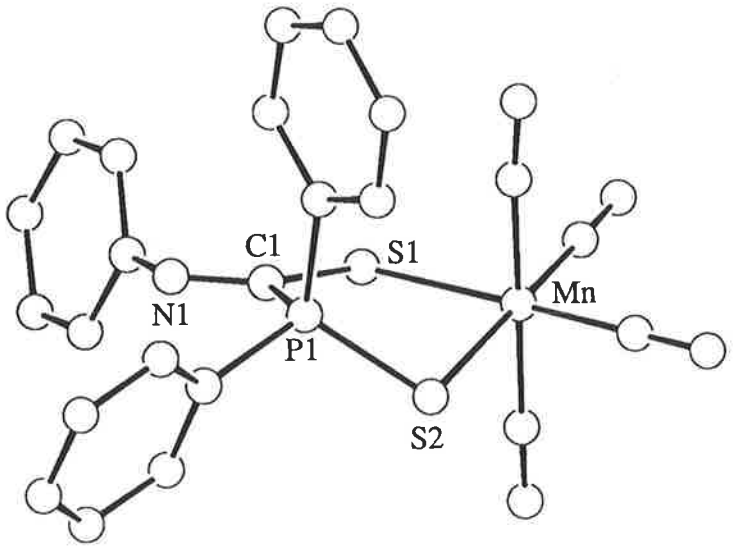

Fig. 1.6.1 The molecular structure of $\{Mn(CO)_4[Ph_2P(S)C(S)NPh]\}$

and 123.8(3)°, respectively while the same angles are 102.1(2), 134.0(3) and 113.9(3)°, respectively in the {$Mn(CO)_4[Ph_2P(S)C(S)NPh]$} complex. The variations in the angles for the two molecules can be attributed to the different strain experienced by the C(1) atom in the formation of the chelate ring with the manganese atom.

1.6.2 The Molecular Structure of {$Mo(CO)_2(\eta^5\text{-}C_5H_5)[Ph_2P(S)C(S)NPh]$}

In Fig. 1.6.2 the molecular structure of {$Mo(CO)_2(\eta^5\text{-}C_5H_5)[Ph_2P(S)C(S)NPh]$} [24] is shown. The $[Ph_2P(S)C(S)NPh]^-$ ligand is in its anionic form and chelates the molybdenum centre *via* the thiolato S(1) atom and the amido nitrogen atom (Mo-S(1) 2.490(2), Mo-N(1) 2.175(5) Å) which results in the formation of a four-membered ring. The pendant S(2) atom is directed away from the metal centre and is not involved in any kind of interaction to the molybdenum atom; P(1)-S(2) 1.942(2) Å. The C(1)S(1)N(1) moiety and the molybdenum atom form a planar four-membered ring. Two carbonyl groups occupy *cis* positions and the coordination about the molybdenum atom is completed by a cyclopentadienyl group which occupies three positions. The coordination geometry has been described as tetragonal pyramidal, however, consistent with the structure of {$Ph_3PMo(CO)_2[Ph_2P(O)C(S)NPh]_2$} [22], a 4:3 piano-stool configuration.

1.7 $[Ph_2PC(S)N(H)Me]$ and Metal Complexes

1.7.1 The Molecular Structure of $[Ph_2PC(S)N(H)Me]$

Two independent molecules of $[Ph_2PC(S)N(H)Me]$ comprise the asymmetric unit of $[Ph_2PC(S)N(H)Me]$, one of these is depicted in Fig. 1.7.1 [25]. The molecules adopt the *Z* configuration about the C(1)-N(1) bond, as was observed for the R' = Ph analogue, but have a different conformation of the phenyl groups. The values for the second molecule will follow those for the first in parentheses in the following description. The parameters about the central C(1) atom are as follows; S(1)=C(1) 1.656(5) [1.656(4)], P(1)-C(1) 1.848(5) [1.850(5)], C(1)-N(1) 1.315(6) [1.319(6)] Å, S(1)-C(1)-P(1) 115.9(3) [116.2(3)], S(1)-C(1)-N(1) 124.6(4) [125.1(4)] and P(1)-C(1)-N(1) 119.2(3) [118.2(3)]°. These parameters

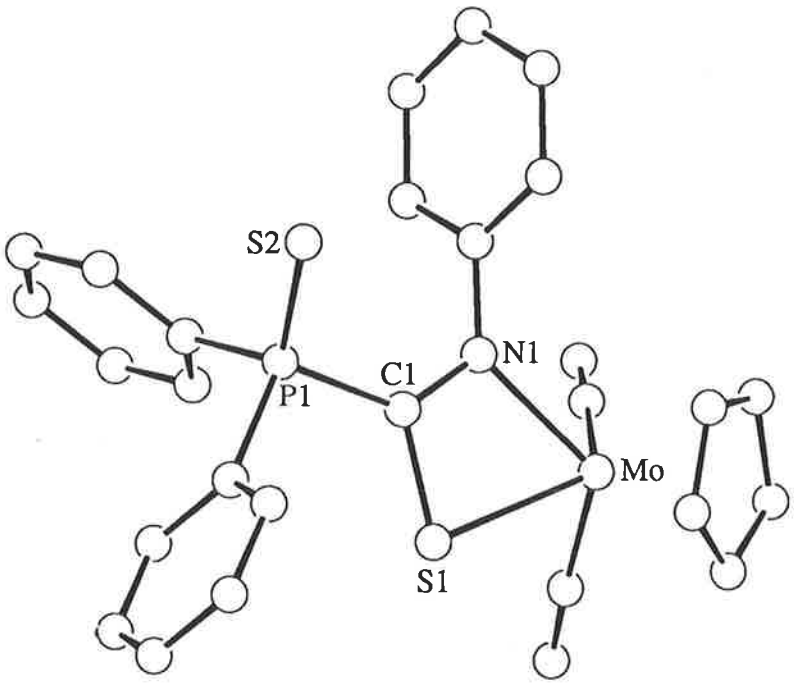

Fig. 1.6.2 The molecular structure of $\{Mo(CO)_2(\eta^5\text{-}C_5H_5)[Ph_2P(S)C(S)NPh]\}$

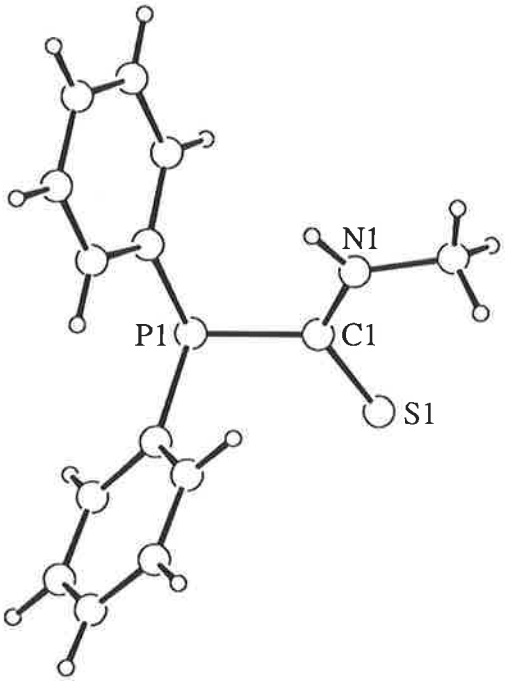

Fig. 1.7.1 The molecular structure of [$Ph_2PC(S)N(H)Me$]

are equal within experimental error for the two molecules and are comparable to those values found in the structure of [$Ph_2PC(S)N(H)Ph$] [15]. The derived results are consistent with the delocalisation of π-electron density on the SC(1)N chromophore as described earlier. Evidence that two independent molecules comprise the asymmetric unit was obtained from the solid state cross-polarised magic angle spinning ^{13}C-NMR spectrum on the bulk material which showed two signals in the N-Me region, one peak due to each of the molecules [26].

1.7.2 The Molecular Structure of {$Cr(CO)_4[Ph_2PC(S)N(H)Me]$}.thf

The reaction of $Cr(CO)_6$ with an equimolar amount of [$Ph_2PC(S)N(H)Me$] in thf solution yields the 1:1 adduct {$Cr(CO)_4[Ph_2PC(S)N(H)Me]$}.thf [27]. The structure of the complex is shown in Fig. 1.7.2 from which it can be seen that the neutral [$Ph_2PC(S)N(H)Me$] ligand, in the *Z* configuration, coordinates the chromium atom *via* the sulfur and phosphorus atoms (Cr-S(1) 2.507(1) and Cr-P(1) 2.348(1) Å) defining a chelate angle, S(1)-Cr-P(1), of 71.01(4)° and results in a four-membered CrSC(1)P ring. The chromium atom exists is in a distorted octahedral geometry with the remaining four positions being occupied by carbonyl ligands. Distortions from the ideal octahedral environment might be related to the restricted bite angle of the [$Ph_2PC(S)N(H)Me$] ligand. The central PSC(1)NC(31) moiety is planar (mean deviation 0.03 Å) with distances S(1)-C(1), P(1)-C(1), C(1)-N(1) and N(1)-C(31) of 1.653(5), 1.833(5), 1.319(5) and 1.446(7) Å, respectively, and angles S(1)-C(1)-P(1), S(1)-C(1)-N(1) and P(1)-C(1)-N(1) of 126.4(4), 108.0(2) and 125.4(4)°, respectively. The compound crystallises as a thf solvate with a N(1)-H(1)...O(thf) separation of 1.91Å (the N(1)-H(1)-O(thf) angle is 164°, and N(1)...O(thf) is 2.809(1) Å) indicative of a hydrogen bond between these atoms; this is represented by the dashed line in diagram.

1.7.3 The Molecular Structure of {$Mo(CO)_2[Ph_2PC(S)NMe][\mu\text{-}Ph_2PC(S)NMe]$}$_2$

The structure analysis of the orange-red crystals of {$Mo(CO)_2[Ph_2PC(S)NMe][\mu\text{-}Ph_2PC(S)NMe]$}$_2$ [28, 29] reveals a very different coordination behaviour of the

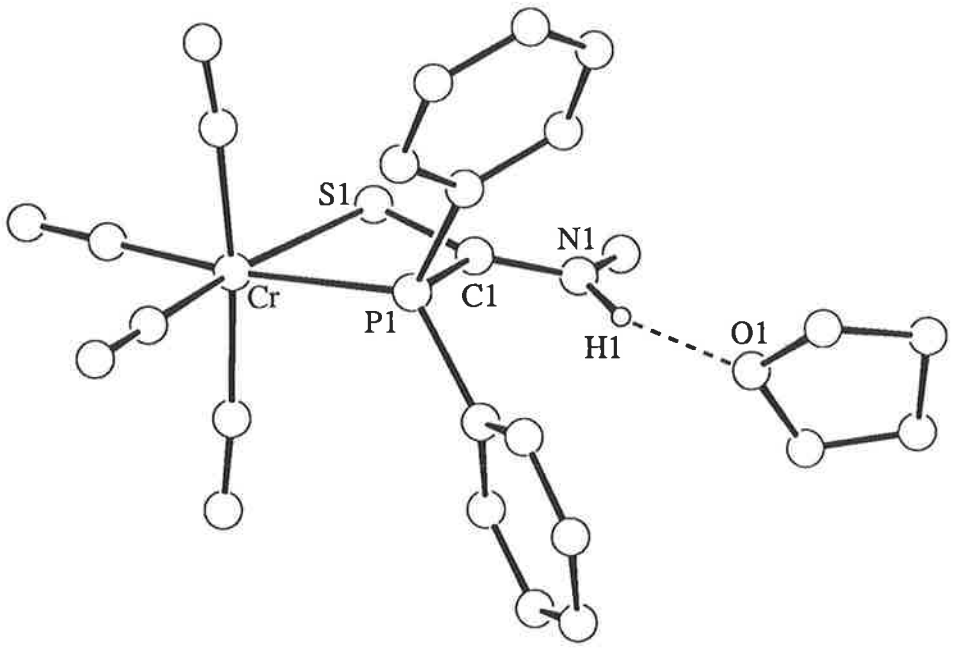

Fig. 1.7.2 The molecular structure of $\{Cr(CO)_4[Ph_2PC(S)N(H)Me]\}.thf$

deprotonated $[Ph_2PC(S)NMe]^-$ ligand, as shown in Fig. 1.7.3; the phosphorus-bound phenyl groups have been excluded for reasons of clarity. The dimer, which crystallises as a dichloromethane solvate, has a two-fold axis of symmetry. The molybdenum atom exists in a seven-coordinate environment and is coordinated by two carbonyl ligands and two deprotonated $[Ph_2PC(S)NMe]^-$ ligands. One $[Ph_2PC(S)NMe]^-$ ligand is bidentate, chelating a molybdenum atom *via* the sulfur and phosphorus atoms (the Mo-S(1) and Mo-P(1) bond distances are 2.512(4) and 2.453(5) Å, respectively). The second $[Ph_2PC(S)NMe]^-$ ligand chelates the same molybdenum atom *via* the sulfur and nitrogen atoms (Mo-S(1) and Mo-N(1) bond lengths are 2.523(4) and 2.607(4) Å, respectively) and at the same time coordinates the symmetry related molybdenum atom *via* the phosphorus atom, P(1)-Mo' 2.25(2) Å. This second $[Ph_2PC(S)NMe]^-$ ligand is thus tridentate, bridging two molybdenum atoms. The result of this mode of coordination is the formation of a central eight-membered MoSC(1)PMo'S'C(1)'P' ring which incorporates two four-membered MoSC(1)N rings. The geometry about the molybdenum atom is best described as a 4:3 piano-stool configuration. In the bidentate ligand, the PC(1)SN chromophore is planar with the molybdenum atom lying 0.58 Å out of this plane while in the tridentate $[Ph_2PC(S)NMe]^-$ ligand, the molybdenum and phosphorus atoms are 0.27 and 0.35 Å, respectively above the plane defined by the S, C(1) and N atoms. The phosphorus atom of the bidentate ligand exists in a distorted tetrahedral environment due to it being involved in the four-membered ring, Mo-P-C(1) 93.8(5)°. The S(1)-Mo-P(1) chelate angle of 68.2(2)° is wider than the S(1)-Mo-N(1) chelate angle of 63.7(3)° by 4.5°. Additional parameters for the bridging and bidentate $[Ph_2PC(S)NMe]^-$ ligands are listed below:

Bidentate $[Ph_2PC(S)NMe]^-$ ligand

S(1)-C(1) 1.76(2) Å; P(1)-C(1) 1.82(2) Å; C(1)-N(1) 1.28(2) Å

S(1)-C(1)-P(1) 102.0(9)°; S(1)-C(1)-N(1) 131(2)°; P(1)-C(1)-N(1) 127(2)°

Bridging $[Ph_2PC(S)NMe]^-$ ligand

S(1)-C(1) 1.72(2) Å; P(1)-C(1) 1.86(2) Å; C(1)-N(1) 1.32(2) Å

S(1)-C(1)-P(1) 117.6(8)°; S(1)-C(1)-N(1) 112(1)°; P(1)-C(1)-N(1) 129(2)°

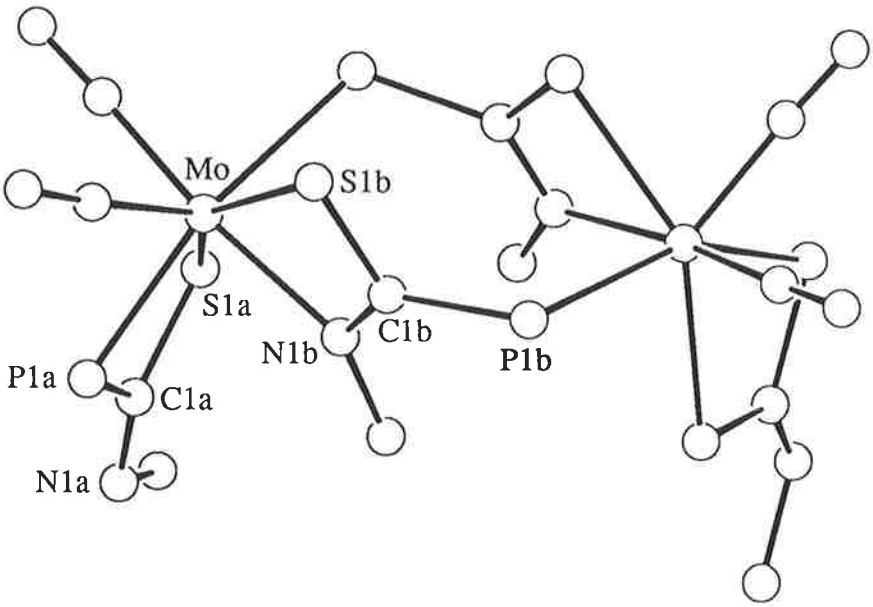

Fig. 1.7.3 The molecular structure of $\{Mo(CO)_2[Ph_2PC(S)NMe][\mu\text{-}Ph_2PC(S)NMe]\}_2$

1.7.4 The Molecular Structure of {$Mo_2[Ph_2PC(S)NMe]_4$}

Two isomers of {$Mo_2[Ph_2PC(S)NMe]_4$} [30] have been characterised crystallographically and are represented in Figs 1.7.4a and b. The recrystallisation of {$Mo_2[Ph_2PC(S)NMe]_4$} from dichloromethane solution resulted in green crystals of isomer A and yellow crystals of isomer B; both isomers crystallised as CH_2Cl_2 solvates. Crystals of isomer A are monoclinic and the molecule is disposed about a centre of inversion. Crystals of isomer B are triclinic with no molecular symmetry. Both molecules are dimeric and five-membered rings are formed when each $[Ph_2PC(S)NMe]^-$ ligand bridges two molybdenum centres. In isomer A one of the independent $[Ph_2PC(S)NMe]^-$ ligands coordinates the two molybdenum atoms (Mo-Mo 2.104(2) Å, i.e. a Mo-Mo quadruple bond) *via* the sulfur and nitrogen atoms (Mo-S(1) is 2.439(3) Å and Mo-N(1) is 2.117(8) Å) and the other ligand coordinates *via* the phosphorus and nitrogen atoms (Mo-P(1) is 2.571(3) Å and Mo-N(1) is 2.182(8) Å). The Mo-N(1) bond distance involving the nitrogen atom *trans* to the phosphorus atom is significantly longer than the Mo-N(1) bond distance opposite the S(1) atom, i.e. 2.182(8) *cf.* 2.117(8) Å. The arrangement of bridging $[Ph_2PC(S)NMe]^-$ ligands results in a N_2PS donor set about each molybdenum atom. Important parameters for the S- and N- chelating ligand (the values for the P- and N- chelating ligand follow in curly brackets) are: S(1)-C(1) 1.69(1) {1.65(1)}, P(1)-C(1) 1.89(1) {1.86(1)}, C(1)-N(1) 1.34(1) {1.35(1)} Å, S(1)-C(1)-P(1) 119.5(6) {121.9(6)}, S(1)-C(1)-N(1) 121.7(8) {128.6(8)} and P(1)-C(1)-N(1) 118.6(8) {109.5(7)}°; the relatively high errors associated with these parameters preclude a detailed comparison with those of the free ligand. In isomer B of {$Mo_2[Ph_2PC(S)NMe]_4$} the coordination of each of the four $[Ph_2PC(S)NMe]^-$ ligands to the dimolybdenum unit (Mo-Mo 2.083(1) Å) is through the sulfur and nitrogen atoms with the average Mo-S(1) distance being 2.466(8) Å and the average Mo-N(1) distance being 2.124(5) Å. The arrangement of the ligands in the dimeric structure is such that like atoms occupy opposite positions; i.e. nitrogen atoms are always *trans* to other nitrogen atoms. The geometric parameters defining the four independent $[Ph_2PC(S)NMe]^-$ ligands are equal within experimental error with important mean parameters being S(1)-C(1)

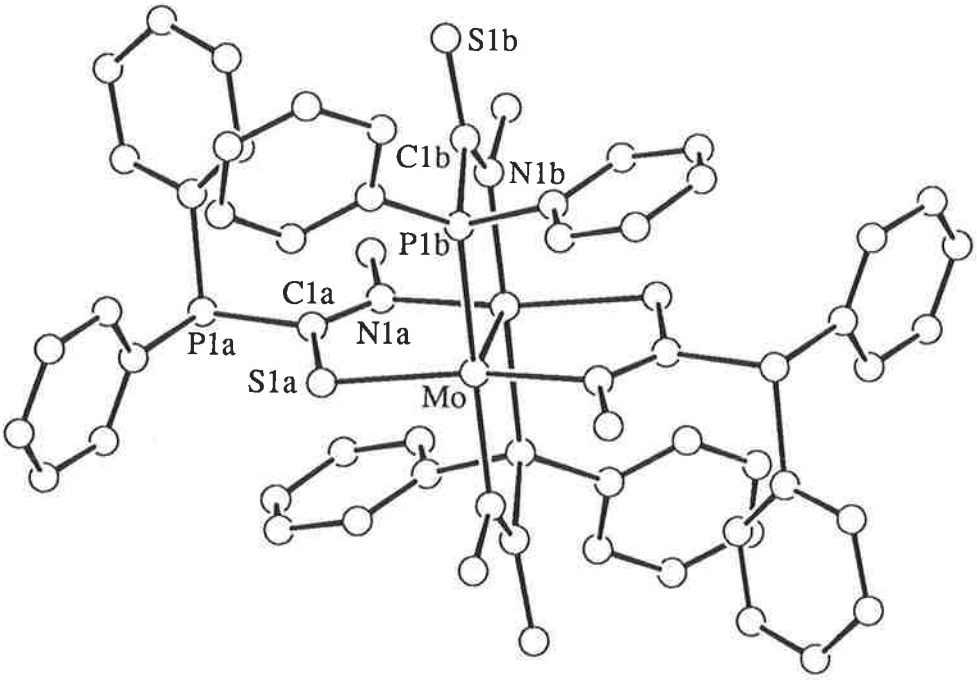

Fig. 1.7.4a The molecular structure of isomer A of $\{Mo_2[Ph_2PC(S)NMe]_4\}$

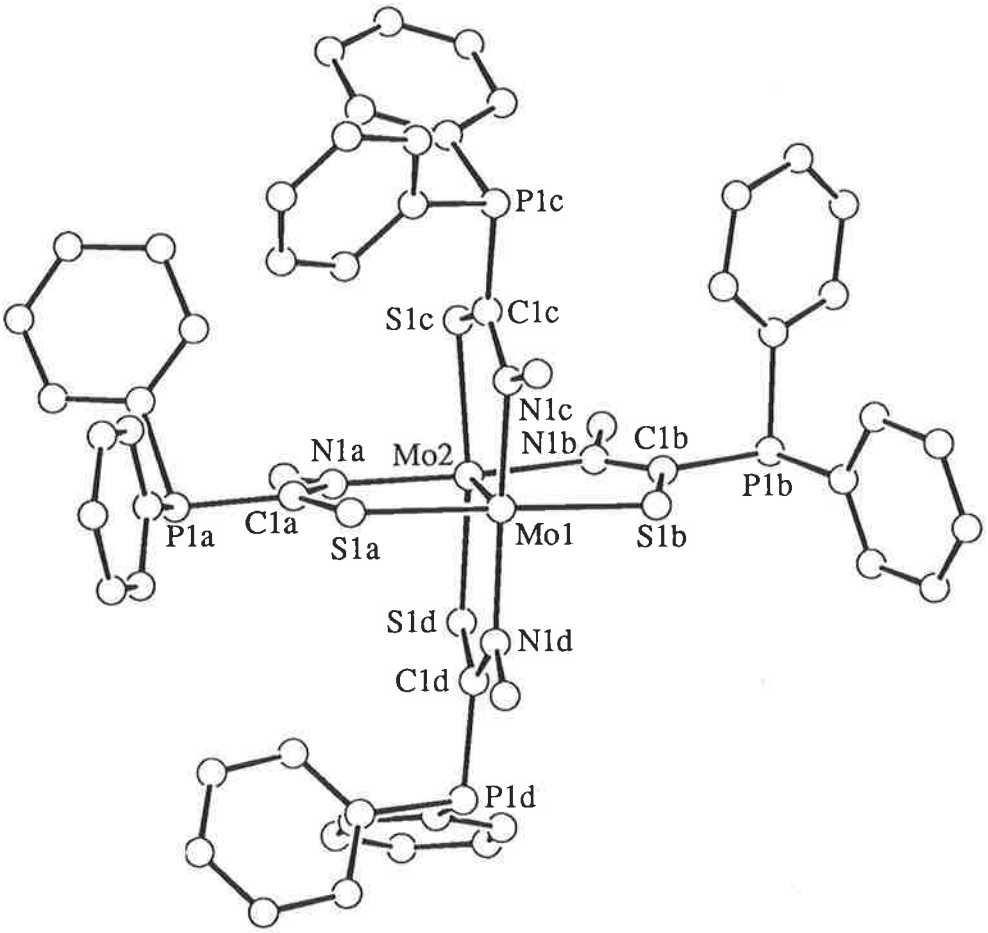

Fig. 1.7.4b The molecular structure of isomer B of $\{Mo_2[Ph_2PC(S)NMe]_4\}$

1.724(8), P(1)-C(1) 1.851(5), C(1)-N(1) 1.304(9) Å, S(1)-C(1)-P(1) 118.1(2), S(1)-C(1)-N(1) 120.0(4) and P(1)-C(1)-N(1) 121.8(3)°.

1.8 [$Cy_2PC(S)N(H)Ph$] and Metal Complexes

1.8.1 The Molecular Structure of [$Cy_2PC(S)NHPh$]

In the structure of [$Cy_2PC(S)NHPh$] [15], the conformation about the C(1)-N(1) bond is *Z* as found for [$Ph_2PC(S)N(H)R'$], R' = Ph and Me. There are two independent molecules in the crystallographic asymmetric unit of [$Cy_2PC(S)N(H)Ph$], which do not differ greatly from each other. The molecular structure for one of these molecules, molecule *a*, is displayed in Fig. 1.8.1. Similar features as found in [$Ph_2PC(S)N(H)Ph$] [15] are also observed for the structure of [$Cy_2PC(S)N(H)Ph$]. The central P, C(1), S and N chromophore is essentially planar. The P(1)-C(1), C(1)=S(1) and C(1)-N(1) bond distances are 1.859(7) [1.877(7) for molecule *b*], 1.661(6) [1.658(7)] and 1.356(8) [1.349(9)] Å, respectively. These distances, coupled with the planarity of the central P, C(1), S, N chromophore, indicate delocalisation of π-electron density over the P, C(1), S and N moiety. The angles about the central C(1) atom, i.e. S(1)-C(1)-P(1), S(1)-C(1)-N(1) and P(1)-C(1)-N(1) are 124.7(4) [124.1(4) for molecule b], 125.1(5) [125.6(5)], and 110.2(4) [110.3(4)]°, respectively. An approximate 10° increase in the S(1)-C(1)-P(1) angle of [$Cy_2PC(S)N(H)Ph$] compared to the equivalent angle in the structure of [$Ph_2PC(S)N(H)Ph$] is ascribed to the increased steric bulk of the phosphorus-bound cyclohexyl rings. The dihedral angles formed between the least-square planes through the P, C(1), S and N moiety and the nitrogen-bound phenyl ring is 18° and [32° for molecule *b*].

The following three structures are examples in which the [$Cy_2PC(S)N(H)Ph$] ligand coordinates in the neutral form and the only examples of any of the diorganophosphinothioformamides coordinating in a monodentate mode *via* the phosphorus atom exclusively. The adopted configuration about the C(1)-N(1) bond is *Z* in all three structures.

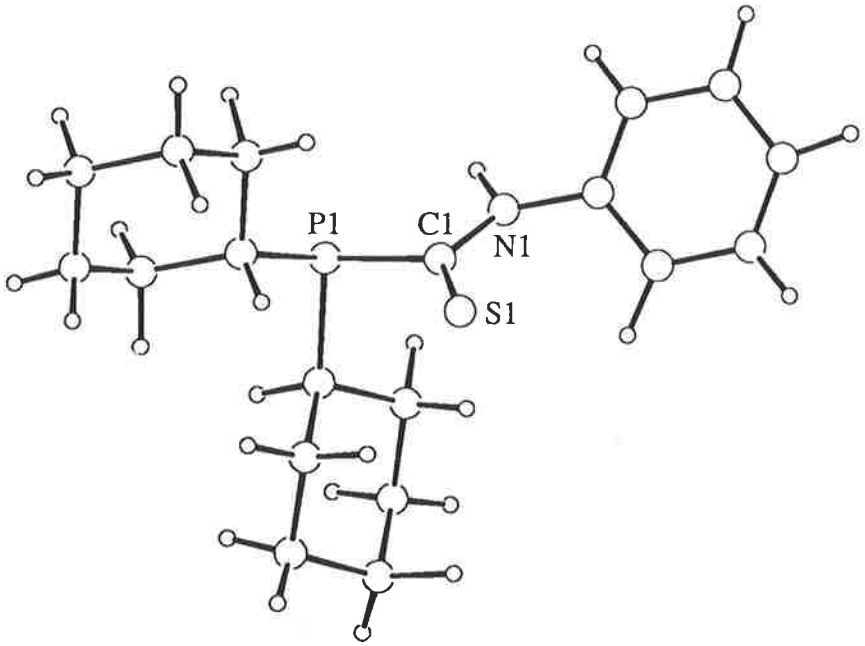

Fig. 1.8.1 The molecular structure of [$Cy_2PC(S)N(H)Ph$]

1.8.2 The Molecular Structure of {$CdI_2[Cy_2PC(S)N(H)Ph]$}$_2$

The structure of {$CdI_2[Cy_2PC(S)N(H)Ph]$}$_2$ [31] is constructed about a centrosymmetric (crystallographically imposed) Cd_2I_2 ring with Cd-I(2) 2.856(1) Å and I(2)...Cd' 2.887(1) Å; the Cd...Cd' separation of 4.024(1) Å is not indicative of a significant interaction between these atoms. The molecular structure is depicted in Fig. 1.8.2. The approximate tetrahedral geometry about the cadmium atoms is defined by the two bridging iodide atoms (I-Cd-I' 91.01(3)°), a terminal iodide atom (Cd-I 2.680(1) Å), and the phosphorus atom derived from the monodentate ligand, Cd-P(1) 2.593(3) Å. The parameters of the dicyclohexylphosphinothioformamide ligand in the coordinated derivative and the free ligand are very similar and will not be discussed further. The H(1) atom on the nitrogen atom is close enough to the bridging I(2) atom to indicate some hydrogen bonding between these atoms [31]; I(2)...H'(N') 2.933(1) Å, I(2)...N' 3.792 Å. The sum of the van der Waals radii for iodine and hydrogen is 3.15 Å [21]. No interactions with other atoms in the ligands are apparent and therefore coordination is exclusively by the phosphorus atom.

1.8.3 The Molecular Structure of {$HgCl_2[Cy_2PC(S)N(H)Ph]_2$}

Monodentate coordination to the mercury atom by both [$Cy_2PC(S)N(H)Ph$] ligands occurs through the phosphorus atoms, Hg-P(1a) 2.452(6) and Hg-P(1b) 2.457(7) Å, in the structure of {$HgCl_2[Cy_2PC(S)N(H)Ph]_2$}, represented in Fig. 1.8.3 [31]. The two independent, coordinated ligands have parameters equal within experimental error to each other and are also very similar to the values in the free ligand [15]. Two chloride atoms complete the approximate tetrahedral geometry about the mercury atom which is distorted significantly from the ideal geometry as shown in the magnitude of the P(1a)-Hg-P(1b) angle, 149.4(2)°. Hydrogen bonding to the chloride atoms is implied by the observed short Cl...N(a, b) separations of 3.28(2) and 3.29(2) Å for the two ligands, respectively. Coordination of the [$Cy_2PC(S)N(H)Ph$] ligand *via* the phosphorus atom exclusively is indicated by the absence of significant inter- or intra-molecular Hg...S bonds.

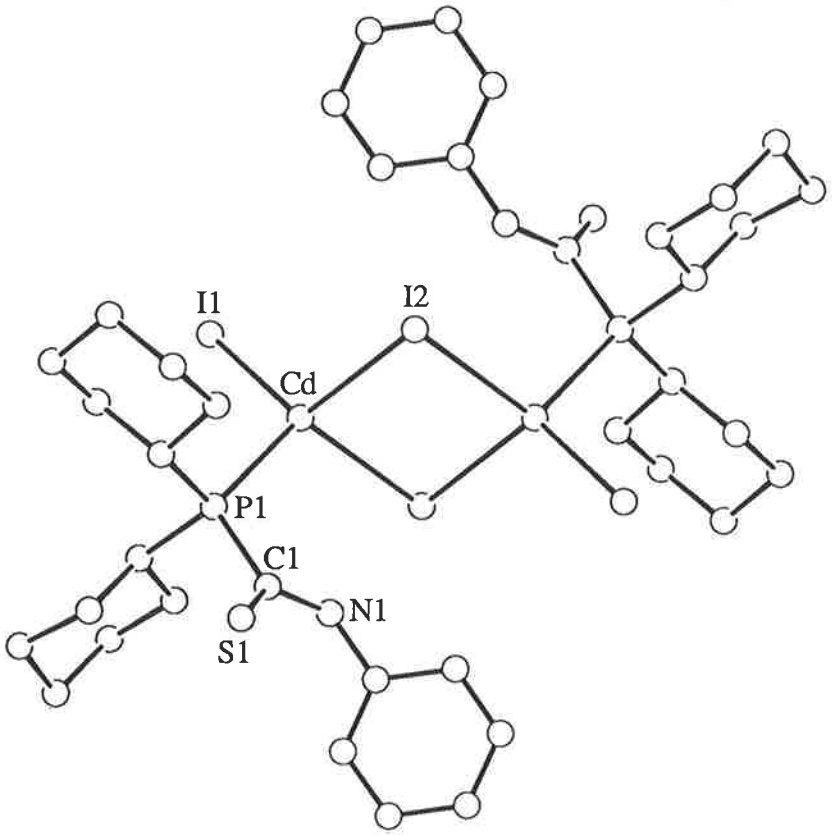

Fig. 1.8.2 The molecular structure of $\{CdI_2[Cy_2PC(S)N(H)Ph]\}_2$

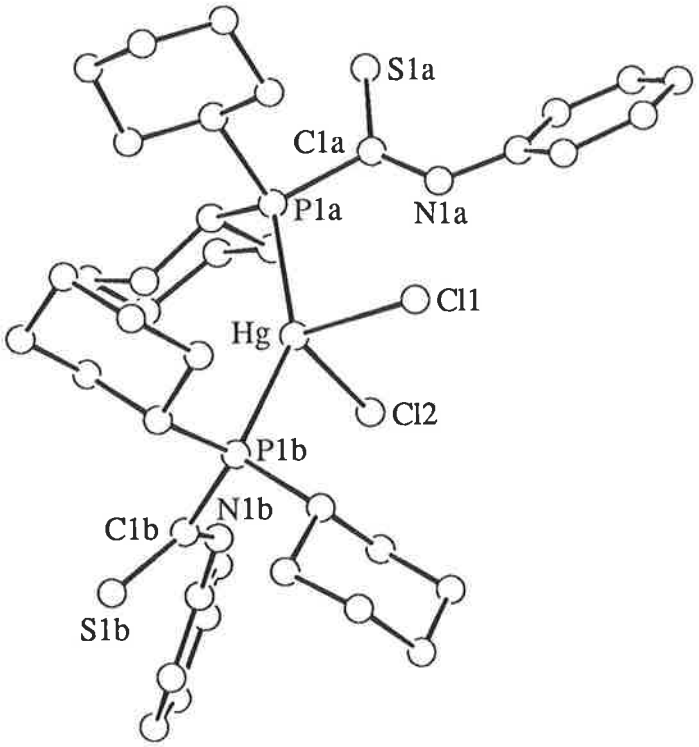

Fig. 1.8.3 The molecular structure of $\{HgCl_2[Cy_2PC(S)N(H)Ph]_2\}$

1.8.4 The Molecular Structure of {$HgCl_2[Cy_2PC(S)N(H)Ph]\}_2$

Two independent molecules of the compound $\{HgCl_2[Cy_2PC(S)N(H)Ph]\}_2$, labeled, A and B, respectively, and two CH_2Cl_2 molecules of solvation comprise the crystallographic asymmetric unit, one of these molecules is represented in Fig. 1.8.4 [31]. There is a central centrosymmetric Hg_2Cl_2 ring, as was the case for the analogous cadmium iodide structure mentioned above; Hg-Cl(2) 2.748(7) (A), 2.719(7) Å (B), Cl(2)-Hg-Cl(2)' 84.5(2) (A), 89.2(2)° (B). There is monodentate coordination of the ligands *via* each phosphorus atom to the mercury atom such that Hg-P(1) is 2.400(7) (A) and 2.393(7) Å (B). The three chloride atoms [two bridging, one terminal, i.e. Hg-Cl(1) 2.352(8) (A) and 2.348(8) Å (B)] and the phosphorus atom from the $[Cy_2PC(S)N(H)Ph]$ ligand complete an approximately tetrahedral geometry around the mercury atom. The tetrahedral geometry is severely distorted, as can be seen by the magnitude of the Cl(1)-Hg-P(1) angle of 144.8(3) (A) and 142.9(3)° (B). Short intramolecular contacts between the bridging chloride atoms, i.e. Cl(2), and the nitrogen atoms suggest hydrogen bonding between the amine proton and this bridging chloride atom; Cl(2)...N(1) 3.22 (A) and 3.21 Å (B). There was no evidence found for any interaction between the mercury and sulfur atoms.

1.8.5 The Molecular Structure of {$Ph_3Sn[Cy_2PC(S)NPh]$}

The molecular structure of $\{Ph_3Sn[Cy_2PC(S)NPh]\}$ [32] has almost similar features to the related complex $\{Ph_3Sn[Ph_2PC(S)NPh]\}$ which differs only by the nature of the phosphorus-bound substituents [20]. A monodentate mode of coordination of the $[Cy_2PC(S)NPh]^-$ anion to the tin atom occurs through the sulfur atom (Sn-S(1) 2.437 Å) as shown in Fig. 1.8.5. The nitrogen atom is positioned in close proximity to the tin atom (Sn...N(1) 2.788(3) Å), however, it is there as a result of the packing in the lattice as was the case for the $\{Ph_3Sn[Ph_2PC(S)NPh]\}$ structure and not due to the presence of a significant Sn...N(1) interaction. A tetrahedral arrangement is found about the tin atom which is defined by the monodentate thiolate ligand and the three phenyl groups. Important

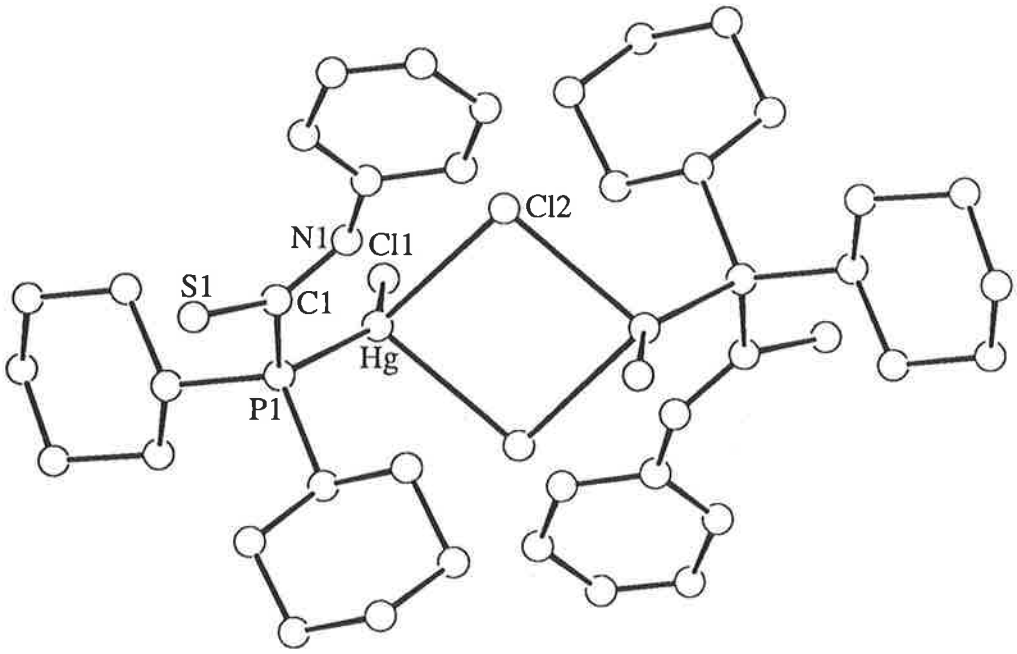

Fig. 1.8.4 The molecular structure of $\{HgCl_2[Cy_2PC(S)N(H)Ph]\}_2$

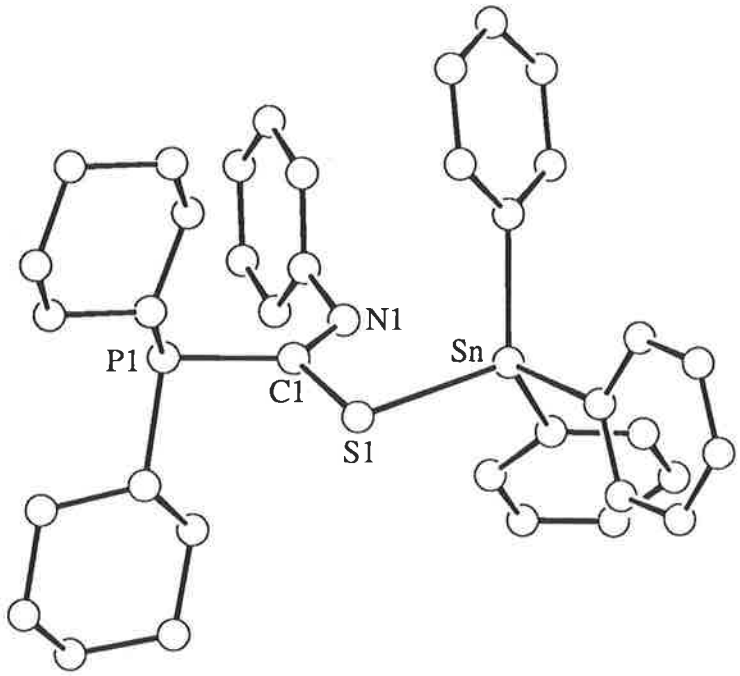

Fig. 1.8.5 The molecular structure of {$Ph_3Sn[Cy_2PC(S)NPh]$}

parameters of note are S(1)-C(1) 1.774(3), P(1)-C(1) 1.852(3), C(1)-N(1) 1.284(4) Å, S(1)-C(1)-P(1) 119.8(2), S(1)-C(1)-N(1) 115.2(2) and P(1)-C(1)-N(1) 125.0(3)°.

The {$Ph_3Sn[Cy_2PC(S)NPh]$} compound was the first compound of the two tin derivatives mentioned thus far for which a structure was determined. Only one isomer was observed in solution for {$Ph_3Sn[Cy_2PC(S)NPh]$} as determined by a ^{31}P and ^{119}Sn NMR study [22]. The NMR data indicated the presence of two isomers, however, for the {$Ph_3Sn[Ph_2PC(S)NPh]$} compound, when prepared from the reaction of [$Ph_2PC(S)N(H)Ph$] with Ph_3PSnCl in the presence of Et_3N. The structural analysis of {$Ph_3Sn[Cy_2PC(S)NPh]$} revealed a similarity to {$Ph_3Sn[Ph_2PC(S)NPh]$} (Section 1.4.5), however. By contrast the {$Ph_3Sn[Ph_2PC(S)NPh]$} complex was synthesised from the reaction between phenyl isothiocyanate and $Ph_3PSnPPh_2$ only one isomer was observed in solution. These results indicate the fickle nature of these compounds.

1.8.6 The Molecular Structure of trans-{Pt[$Cy_2PC(S)NPh]_2$}

The crystal structure of the complex *trans*-{$Pt[Cy_2PC(S)NPh]_2$} has been determined [33] and the platinum atom, located on a crystallographic centre of inversion, exists in a square planar geometry as can be seen in Fig. 1.8.6. The deprotonated $[Cy_2PC(S)NPh]^-$ ligand chelates the platinum centre *via* the sulfur and phosphorus atoms with Pt-S(1) 2.322(1) and Pt-P(1) 2.282(1) Å; the bite angle, S(1)-Pt-P(1) is 74.7(1)°. The PC(1)SN moiety is planar with the platinum atom lying 0.3316 Å above this plane. Other important parameters are S(1)-C(1) 1.763(4), P(1)-C(1) 1.834(3), C(1)-N(1) 1.268(4) Å and S(1)-C(1)-P(1) 101.9(2)°.

1.9 Tin Complex with [$Cy_2P(O)C(S)N(H)Me$]

1.9.1 The Molecular Structure of {$Ph_3Sn[Cy_2P(O)C(S)N(H)Me]Cl$}

The reaction between Ph_3SnCl and the [$Cy_2P(O)C(S)N(H)Me$] ligand results in the isolation of the {$Ph_3Sn[Cy_2P(O)C(S)N(H)Me]Cl$} adduct [12], as shown in Fig. 1.9.1. The tin atom is coordinated by three phenyl groups, a chloride atom and the O(2) atom (Sn-

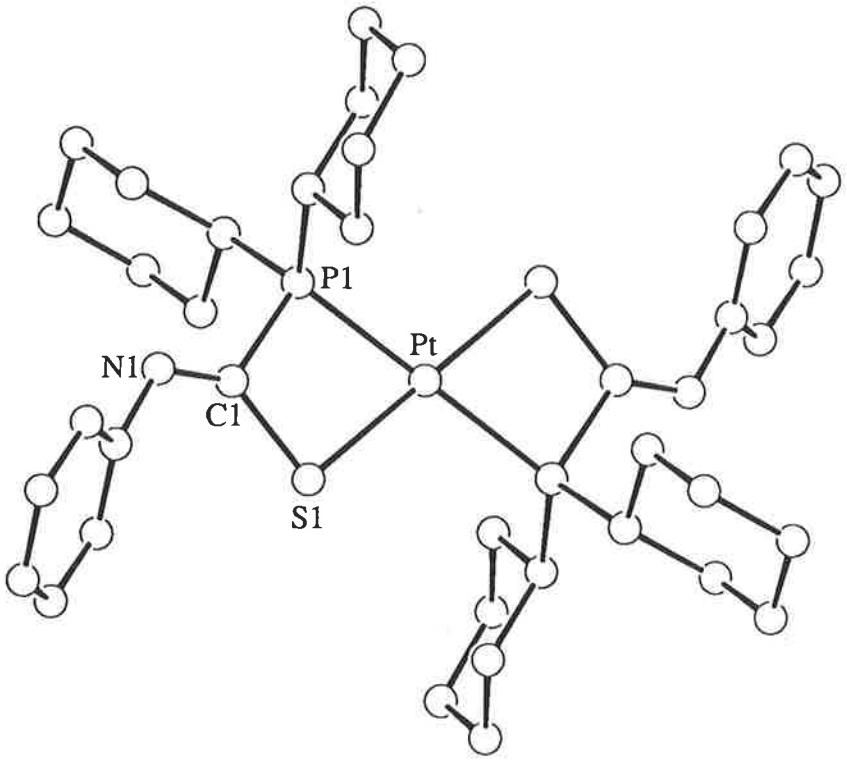

Fig. 1.8.6 The molecular structure of *trans*-{Pt[$Cy_2PC(S)NPh]_2$}

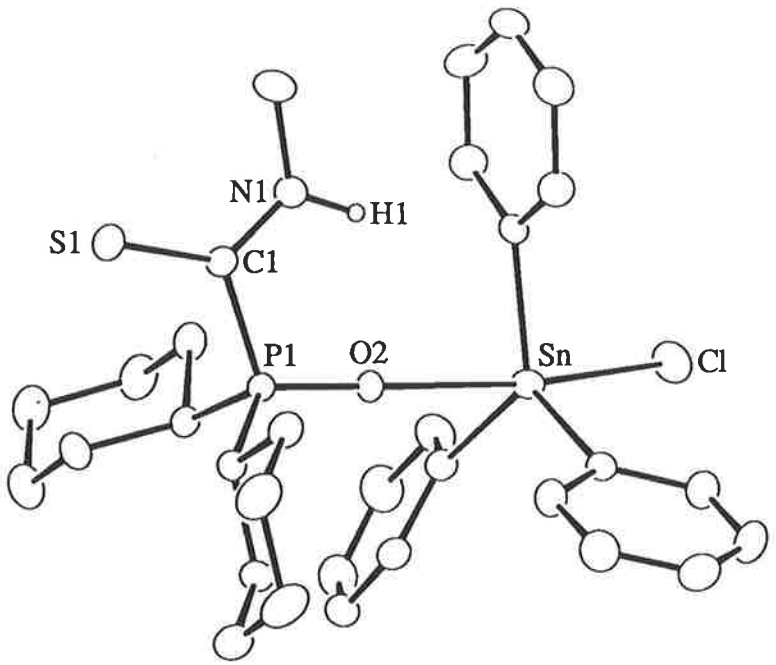

Fig. 1.9.1 The molecular structure of {$Ph_3Sn[Cy_2P(O)C(S)N(H)Me]Cl$}

O 2.523(2) Å) derived from the neutral [$Cy_2P(O)C(S)N(H)Me$] ligand, which has the *Z* configuration. This arrangement leads to a five-coordinate tin centre which has a distorted trigonal bipyramidal geometry with the O(2) and chloride atoms defining the axial positions; O(2)-Sn-Cl 172.73(5)°. The P(1)-O(2) bond distance of 1.490(2) Å is indicative of a double bond between these atoms. It has been noted in the literature [34-36] that the length of the P=O separation in triorganophosphine oxide adducts of tin is independent of the strength of the tin to oxygen bond, however, the structure of [$Cy_2P(O)C(S)N(H)Me$] is not available for comparison to verify this conclusion.

1.10 Summary

An inspection of the structures described above in 1.4 to 1.9 reveals a number of coordination modes for the diorganophosphinothioformamides (**I**), diorganophosphinylthioformamides (**II**) and diorganothiophosphinylthioformamides (**III**) compounds with the ligands in their neutral or deprotonated forms. Clearly, however, there is enormous scope for further work, in particular for the phosphorus(V) derivatives, (**II**), (**III**) and the diorganoselenophosphinylthioformamides (**IV**).

1.11 Aims

The aim of this thesis is to explore the coordination potential to metal centres of ligands with general structural features shown in diorganophosphinothioformamides (**I**), diorganophosphinylthioformamides (**II**), diorganothiophosphinylthioformamides (**III**) and diorganoselenophosphinylthioformamides (**IV**). A particular focus of this work is an investigation of the coordination possibilities of these ligands with gold. Essential to the understanding of the effects coordination has on the electronic structure and geometrical arrangement of the atoms in these ligands, is a knowledge of the precise interatomic parameters of the ligands themselves. As a consequence of the above, the thesis is divided into three major sections.

The first section explores the chemistry, spectroscopic characterisation and X-ray crystal structures of the phosphorus(V) ligands, diorganophosphinylthioformamides (**II**), diorgano-

thiophosphinylthioformamides (**III**) and diorganoselenophosphinylthioformamides (**IV**). The second section examines the interaction of the phosphorus(III) ligands (**I**) and their phosphorus(V) derivatives (**II-IV**) with gold(I) salts. The third section describes the X-ray crystal structures of a variety of metal complexes of **I-IV** prepared by the author or supplied by Professor R. Kramolowsky, University of Hamburg, Germany.

The spectroscopic methods utilised during the course of this study included infrared (IR), multinuclear magnetic resonance (NMR), fast atom bombardment (FAB) and electron impact (EI) mass spectroscopy. A number of compounds have also been investigated using single crystal X-ray diffraction methods.

Owing to the large volume of crystallographic data accumulated during this study, this thesis is divided into two volumes. The primary crystallographic data, i.e. crystal and refinement details, fractional atomic coordinates, thermal parameters, all bond distances, all bond angles and listings of observed and calculated structure factors have been included in Volume 2.

Chapter 2

EXPERIMENTAL METHODS AND PREPARATIONS

General Information

All preparations and reactions, where appropriate, carried out during this study were performed under an inert atmosphere of either argon or nitrogen. Glassware was flame-dried and evacuated before use. The flash column used for the chromatographic separations and the technique employed was as according to the literature [37].

Care should be taken when handling phosphines and selenium-containing compounds, as these are potentially hazardous chemicals and hence should be used in a fume-hood with appropriate protection being worn.

Microanalysis

Elemental analyses for C, H and N were performed by the Chemical and Microanalytical Services Pty Ltd, Essendon, Victoria.

Instrumentation

2.1 Infrared Spectroscopy (IR)

Infrared spectra for all compounds were recorded as KBr discs on a Perkin-Elmer 1720X FT spectrometer in the range of 4000 - 400 cm^{-1} and calibrated with the polystyrene absorption at 1601 cm^{-1}.

2.2 Nuclear Magnetic Resonance Spectroscopy (NMR)

Proton (^{1}H) and carbon-13 proton decoupled (^{13}C) NMR spectra were recorded on a Bruker ACP-300 NMR spectrometer with deuterated chloroform, $CDCl_3$, as the solvent. The recording frequencies used were 300.13 MHz for ^{1}H NMR and 75.47 MHz for ^{13}C NMR. The internal reference used was $SiMe_4$ (TMS). Proton decoupled phosphorus-31 (^{31}P) NMR spectra were recorded on a Bruker CXP-300 NMR spectrometer at 121.5 MHz, as chloroform solutions, with the internal reference being 85% H_3PO_4 in D_2O.

2.3 Mass Spectroscopy (MS)

Fast atom bombardment (FAB) mass spectra were obtained using a VG ZAB-2HF spectrometer. The excitation gas was argon at a source pressure of typically 10^{-6} mbar. The FAB voltage was 7 kV with a current of 1 mA, the ion accelerating potential being 8 kV. A drop of a *ca* 0.5 mol dm^{-3} solution of the complex in dichloromethane was added to a drop of 3-nitrobenzyl alcohol matrix and applied to the probe tip. The spectra were recorded as a mass to charge ratio, m/z. Relative abundance was calculated by designating the most abundant peak as 100% and determining the abundance of the other peaks based on their relative heights in the spectra to the most abundant peak. FAB mass spectra were obtained with the assistance of Mr Tom Blumenthal of the Department of Chemistry, University of Adelaide. Mr Blumenthal recorded the electron impact (EI) spectra.

2.4 Melting Points

All melting points were determined using a Gallemkamp melting point apparatus calibrated with benzil (m. pt 94-95°C).

2.5 Crystallography

Crystal data and refinement details for all structures are listed in Volume 2 of this thesis. This section outlines the general procedures employed for each analysis. Two different methods were utilised to collect data for the crystal structures presented in this thesis as given below in a) and b). All crystals were mounted on a glass fibre using cyanoacrylate glue and all data collections were performed at room temperature (293 K).

a) Intensity data for the following five compounds: $[Ph_2P(Y)C(S)N(H)Ph]$, Y = O, S, Se, $[Ph_2P(O)C(S)N(H)Me]$ and $\{Au[Ph_2PC(S)NPh]\}_2$ were measured on an Enraf-Nonius CAD4*F* diffractometer fitted with Mo$K\alpha$ radiation; $\lambda = 0.7107$ Å. The ω:2θ scan technique was employed to measure data for the compounds up to θ_{max} 25.0° (27.5° for $[Ph_2P(O)C(S)N(H)Me]$). Two standard reflections were measured every 7200 seconds of X-ray exposure time and this revealed that no decomposition of any of the crystals had

occurred during their respective data collection. Each data set was corrected for Lorentz and polarisation effects and an analytical absorption correction was applied in each case [38]. Only reflections which satisfied the $I \geq 3.0\sigma(I)$ criterion of observability were used in the subsequent analysis.

b) Intensity data were measured on a Rigaku AFC6R diffractometer fitted with either Mo$K\alpha$ (graphite monochromator) radiation, λ = 0.71073 Å, or Ni-filtered Cu$K\alpha$ radiation, λ = 1.5418 Å. The ω:2θ scan technique was employed to measure data up to a maximum Bragg angle of 25-27.5° for Mo$K\alpha$ or 60-65° for Cu$K\alpha$ radiation. The net intensity values of three standard reflections, remeasured after every 400 intensity measurements, showed no significant change in any of the data collections. The data sets were corrected for Lorentz and polarization effects [39] and for absorption effects employing an empirical correction [40]. Of the reflections measured only those that satisfied the $I \geq 3.0\sigma(I)$ criterion of observability were used in the subsequent analysis.

The unit cell dimensions were determined from the least squares refinement of 25 (20 for Cu radiation) carefully-centred reflections in all cases.

All the structures were solved by direct-methods using SHELXS86 [41] and each refined by a full-matrix least-squares procedure based on F [39]. The function minimised was

$$\sum_{i=1}^{n} w_i \left(|F_{obs}|_i - |F_{calc}|_i\right)^2$$

where n is the number of reflections, and

$$w = \frac{1}{\sigma^2(F_{obs})}$$

Non-hydrogen atoms were refined with anisotropic thermal parameters (where possible) and hydrogen atoms were either located and refined or included in their calculated positions (C-H 0.97 Å and N-H 0.95 Å). A sigma weighting scheme was applied (in some cases unit

weights were employed) and the refinement continued until convergence in each case. At convergence, the values of R and R_w were obtained, where

$$R = \frac{\sum_{i=1}^{n} (|F_{obs}|_i - |F_{calc}|_i)}{\sum_{i=1}^{n} |F_{obs}|_i} \quad \text{and} \quad R_w = \left\{ \frac{\sum_{i=1}^{n} w_i (|F_{obs}|_i - |F_{calc}|_i)^2}{\sum_{i=1}^{n} w_i |F_{obs}|^2} \right\}^{1/2}.$$

The analysis of variance for each refinement revealed no special features indicating that an appropriate weighting scheme was applied in each case.

In some cases a correction was applied for secondary extinction effects [42]. Scattering factors for all the atoms were those incorporated in the teXsan software package [39] which was installed on a Silicon Graphics Iris Indigo computer system. Tables of bond distances and bond angles, fractional atomic coordinates, anisotropic thermal and hydrogen atom parameters, and structure factors for all determinations are located in the Appendices, Volume 2. The expression for the anisotropic thermal parameter is

$$T_{aniso} = \exp[-2\pi^2(h^2a^{*2}U_{11} + k^2b^{*2}U_{22} + l^2c^{*2}U_{33} + 2hka^*b^*U_{12} + 2hla^*c^*U_{13} + 2klb^*c^*U_{23})]$$

and the expression for Beq is

$$B\text{eq} = \frac{8\pi^2(U_{11} + U_{22} + U_{33})}{3}.$$

All diagrams were drawn utilising the ORTEP program [14] with thermal ellipsoids specified in the relevant sections.

When appropriate, the absolute configuration of a structure was determined by refining each hand and comparing the final values of R_w and examining their significance employing the Hamilton significance test [43]. As a matter of course, each chiral compound was examined by the 'Look for Centres of Symmetry' routine in teXsan [39].

2.6 Chemicals

The chemicals used in the syntheses of the complexes and their sources were: dicyclohexylphosphine (Aldrich and Strem), diphenylphosphine (Aldrich), triphenylphosphine (B.D.H.), phenyl- and methyl-isothiocyanate (Aldrich), thiodiglycol (Aldrich), nickel nitrate (Unilab), cadmium chloride (Albright and Wilson), and were used without further purification. In addition, diphenylphosphine was prepared following the literature procedure [44]. All the solvents employed were of analytical grade and dried over molecular sieves before use.

2.7 Preparation of Starting Materials

2.7.1 Red Selenium

Red selenium [45] was prepared by the reduction of SeO_2 in an hydrochloric acid medium with SO_2 gas being passed into the solution with the desired product precipitating out in a few minutes. The selenium was collected by filtration, washed with cold water, ethanol and then with a small amount of ether. It was stored in a desiccator, over phosphorus pentoxide, and kept in the refrigerator.

2.7.2 Diphenylphosphine, Ph_2PH

The phosphine was prepared by the literature method [44]. It essentially involved the cleavage of one P-Ph bond in triphenylphosphine with sodium metal in liquid ammonia, followed by hydrolysis of the resulting sodium diphenylphosphide with water to obtain the phosphine. The diphenylphosphine was vacuum distilled: b.pt 134°C at 3 mm Hg, to give a yield of 130 g (72%), *cf.* literature results; b.pt 103°C at 1 mm Hg (or at 75-79°C at *ca* 3 x 10^{-4} mm Hg), yield of 150 g (80%).

2.7.3 $HAuCl_4$

Gold metal was dissolved in aqua regia to generate $HAuCl_4.xH_2O$ (x = 2 or 3) in accordance with the literature method [46].

2.8 Preparation of Diorganophosphinothioformamides, $R_2PC(S)N(H)R'$

The procedure followed was the literature method reported by Issleib and Harzfeld [2, 3] and involved the addition of the appropriate diorganophosphine to the appropriate organo-isothiocyanate (both liquids) with stirring for at least one hour to generate the desired compound. The sticky solid obtained was dissolved in the minimum amount of hot acetonitrile from which crystals were grown. The compounds prepared had R = Ph or Cy and R' = Ph or Me. Yields and melting points of these compounds are listed in Table 2.8. It was found that the R = Cy compounds were very difficult to isolate in a pure form, especially for the R' = Me compound (see later).

2.9 Preparation of Diorganophosphinyl-, Diorganothiophosphinyl- and Diorganoseleno-phosphinyl-thioformamides, $R_2P(Y)C(S)N(H)R'$

2.9.1 Preparation of the $R_2P(O)C(S)N(H)R'$ compounds

Following the published procedure by Ojima et al [47], the oxidation of the $R_2PC(S)N(H)R'$ compounds with oxygen resulted in the formation of the $R_2P(O)C(S)N(H)R'$ compounds, R = Ph or Cy, R' = Ph or Me. Molecular oxygen was passed into an ethanolic solution of the precursor ligand for about three hours with stirring. The solvent was removed *in vacuo* and the resultant solid was dissolved in a small amount of dichloromethane and purified by passing the solution through a flash column with silica gel. The ligand was eluted with ethylacetate : petroleum spirit 40/60°C (1/1 *v/v*), isolated by evaporating the solvent and was used without further purification. Physical data can be found in Table 2.8.

Table 2.8: Melting Points, Yields and Physical Appearance for the $R_2P(Y)C(S)N(H)R'$, Y = 0, O, S or Se, R = Ph or Cy, R' = Ph or Me, Compounds

Compound	colour	% yield	m. pt (°C)
$[Ph_2PC(S)N(H)Ph]$	bright yellow	92	117-118
$[Ph_2PC(S)N(H)Me]$	light yellow	93	139-140
$[Cy_2PC(S)N(H)Ph]$	bright yellow	95	99-101
$[Cy_2PC(S)N(H)Me]$*	pale yellow	90	98-101
$[Ph_2P(O)C(S)N(H)Ph]$	bright yellow	82	157-158
$[Ph_2P(O)C(S)N(H)Me]$	pale yellow	86	186-188
$[Cy_2P(O)C(S)N(H)Ph]$	bright yellow	90	205-207
$[Cy_2P(O)C(S)N(H)Me]$	pale yellow	87	194-197
$[Ph_2P(S)C(S)N(H)Ph]$	bright yellow	75	129-130
$[Ph_2P(S)C(S)N(H)Me]$	pale yellow	72	96-98
$[Cy_2P(S)C(S)N(H)Ph]$	bright yellow	81	111-113
$[Cy_2P(S)C(S)N(H)Me]$	pale yellow	85	212-214
$[Ph_2P(Se)C(S)N(H)Ph]$	bright yellow	75	100-102
$[Ph_2P(Se)C(S)N(H)Me]$	yellow/green	71	101-103
$[Cy_2P(Se)C(S)N(H)Ph]$	yellow	82	120-122
$[Cy_2P(Se)C(S)N(H)Me]$	yellow	57	213-215

* crude product before recrystallisation (see text)

2.9.2 Preparation of the $R_2P(S)C(S)N(H)R'$ compounds

The published procedure by Ojima et al [47] was used to prepare the sulfur derivatives $R_2P(S)C(S)N(H)R'$. To a benzene solution of $R_2PC(S)N(H)R'$ (1 mole equivalent) was added elemental sulphur (1.1 mole equivalent) and the resulting solution was refluxed for three hours. The solution was filtered and the benzene removed *in vacuo*. The compound was recrystallised from ethanol and the crystals were dried *in vacuo* over phosphorus pentoxide for 12-24 hours. The compound was then purified by passing a dichloromethane solution of the compound through a flash column and eluted with ethylacetate : petroleum spirit 40/60°C (1/4 *v/v*). The pure, solid compounds, $R_2P(S)C(S)N(H)R'$, R = Ph or Cy, R' = Ph or Me, were obtained and used without further purification. Physical data can be found in Table 2.8.

2.9.3 Preparation of the $R_2P(Se)C(S)N(H)R'$ compounds

The reactions of the parent ligands with selenium were performed in an analogous manner as for $R_2P(S)C(S)N(H)R'$ and a general description of the preparation is given.

To a benzene or tetrahydrofuran solution of $R_2PC(S)N(H)R'$ (1 mole equivalent) was added freshly prepared elemental red selenium (1.1 mole equivalent). The solution was stirred for 1 hour at room temperature and then refluxed for a further three hours. The solution was filtered, the solvent was removed *in vacuo* and the $R_2P(Se)C(S)N(H)R'$ compound was isolated. Crystals were obtained from ethanol and dried *in vacuo* over phosphorus pentoxide for 12-24 hours. The compound was then purified by passing a dichloromethane solution of the compound through a flash column and eluted with ethylacetate : petroleum spirit 40/60°C (1/3 *v/v*). The $R_2P(Se)C(S)N(H)R'$, R = Ph or Cy, R' = Ph or Me, compounds were used without further purification. Physical data can be found in Table 2.8.

2.10 Preparation of Gold(I) Complexes with Diorganophosphino-, Diorganophosphinyl-, Diorganothiophosphinyl- and Diorganoselenophosphinyl-thioformamides

Tables 2.10.1 - 2.10.4 and 2.11.3 summarise the physical properties and the percentage yields of the complexes prepared.

2.10.1 Reaction of $HAuCl_4$ with $R_2PC(S)N(H)R'$

The reactions of $HAuCl_4$ with the phosphorus(III) compounds [$Ph_2PC(S)N(H)Ph$], [$Ph_2PC(S)N(H)Me$], [$Cy_2PC(S)N(H)Ph$] and [$Cy_2PC(S)N(H)Me$] were performed in an analogous manner. Details for the reaction involving [$Ph_2PC(S)N(H)Ph$] are given below. Physical data and percentage yields are given in Table 2.10.1.

2.10.1a Reaction of [$Ph_2PC(S)N(H)Ph$] with $HAuCl_4$

Under an inert atmosphere and at a temperature of 0°C (ice-bath) one molar equivalent of $HAuCl_4.3H_2O$ (150 mg, 0.38 mmol) was dissolved in a solution of acetone and water (4/1 *v/v*, 5 cm^3). Three molar equivalents of thiodiglycol (0.12 cm^3, 1.15 mmol) was then added dropwise to the yellow-orange solution over a period of 2 hours. Extra drops were added, if necessary, until a clear and colourless solution was obtained. A 1.1 molar equivalent of [$Ph_2PC(S)N(H)Ph$] (134 mg, 0.42 mmol) was dissolved in hot ethanol (*ca* 5 cm^3) and added dropwise over a period of 10 minutes to the stirred solution. A solid product precipitated out almost immediately and after the completion of the addition, the complex was collected by vacuum filtration and washed with cold ethanol. The crude product was recrystallised from a chloroform/ethanol solution (4/1 *v/v*, 5 cm^3) and the resulting crystals were dried over anhydrous phosphorus pentoxide under vacuum. The complex was a pale yellow solid and was air-stable, the yield obtained was 178 mg (91%).

2.10.2 Reaction of $HAuCl_4$ with $R_2P(O)C(S)N(H)R'$

The procedure employed was as for 2.10.1a. Reaction of $HAuCl_4$ with the [$Ph_2P(O)C(S)N(H)Ph$], [$Ph_2P(O)C(S)N(H)Me$] and [$Cy_2P(O)C(S)N(H)Ph$] compounds resulted in no new products. Reaction of the [$Cy_2P(O)C(S)N(H)Me$] compound with

Table 2.10.1: Physical Data for the Gold(I) Diorganophosphinothioformamido Complexes, $\{Au[R_2PC(S)NR']_2\}$, R = Ph and Cy, R' = Ph and Me

Complex	colour	% yield	m. pt (°C)
$\{Au[Ph_2PC(S)NPh]_2\}$	pale yellow	91[a], 80[b], 59[c]	250 (dec.)
$\{Au[Ph_2PC(S)NMe]_2\}$	white	78[a], 75[b], 44[c]	205-210 (dec.)
$\{Au[Cy_2PC(S)NPh]_2\}$	pale yellow	80[a], 84[b], 47[c]	116-118
$\{Au[Cy_2PC(S)NMe]_2\}$	pale yellow	nr[a], 78[b], 38[c]	145 (dec.)

a Reaction of $R_2PC(S)N(H)R'$ ligand with $HAuCl_4$

b Reaction of $R_2PC(S)N(H)R'$ ligand with Ph_3PAuCl

c Reaction of $R_2P(Se)C(S)N(H)R'$ ligand with Ph_3PAuCl

nr = no reaction

Table 2.10.2: Physical Data for the Gold(I) Dicyclohexyl-N-methyl-thiophosphinyl-thioformamido Complex

Complex	colour	% yield	m. pt (°C)
$\{Au[Cy_2P(O)C(S)N(H)Me]Cl\}$	pale green	53	163-165 (dec.)

Microanalysis

Found: C, 32.8; H, 5.0; N, 2.6 %. $C_{14}H_{26}AuClNOPS$ requires C, 32.3; H, 5.0; N, 2.7 %

Table 2.10.3: Physical Data for the Products of $HAuCl_4$ with $R_2P(S)C(S)N(H)R'$, R = Ph and Cy, R' = Ph and Me

Complex	colour	% yield	m. pt (°C)
$\{Au[Ph_2P(S)C(S)NPh]\}_\infty$	dark yellow	88	94-99
$\{Au[Ph_2P(S)C(S)NMe]\}_\infty$	yellow/brown	95	115-120

Table 2.10.4: Physical Data for the Products of $HAuCl_4$ with $R_2P(Se)C(S)N(H)R'$, R = Ph and Cy, R' = Ph and Me

Complex	colour	% yield	m. pt (°C)
$\{Au[Ph_2P(Se)C(S)NPh]\}_\infty$	black	85	96
$\{Au[Ph_2P(Se)C(S)NMe]\}_\infty$	black	97	130
$\{Au[Cy_2P(Se)C(S)NPh]\}_\infty$	black	86	120

Table 2.11.3: Physical Data for the Products of Ph_3PAuCl with $R_2P(S)C(S)N(H)R'$ R = Ph or Cy, R' = Ph or Me

Complex	colour	% yield	m. pt (°C)
$\{Ph_3PAu[Ph_2P(S)C(S)NPh]\}$	orange	58	113-115
$\{Ph_3PAu[Ph_2P(S)C(S)NMe]\}$	orange	64	127 (dec.)
$\{Ph_3PAu[Cy_2P(S)C(S)NPh]\}$	orange	68	185 (dec.)
$\{Ph_3PAu[Cy_2P(S)C(S)NMe]\}$	orange	51	154 (dec.)

$HAuCl_4$ resulted in the formation of {Au[$Cy_2P(O)C(S)N(H)Me$]Cl}. This gold(I) complex was air-stable but when left in solution elemental gold precipitated out after a few days. Physical data can be found in Table 2.10.2.

2.10.3 Reaction of $HAuCl_4$ with $R_2P(S)C(S)N(H)R'$

The reaction of the $R_2P(S)C(S)N(H)R'$ compounds with $HAuCl_4$ employed the same procedure as outlined in 2.10.1a. Insoluble products formed with the $Ph_2P(S)C(S)N(H)R'$ compounds which were dark yellow in colour and were air-stable. The reaction with the $Cy_2P(S)C(S)N(H)R'$ derivatives did not result in the formation of any new detectable products. Physical data can be found in Table 2.10.3.

2.10.4 Reaction of $HAuCl_4$ with $R_2P(Se)C(S)N(H)R'$

The reaction of the $HAuCl_4$ species with the $R_2P(Se)C(S)N(H)R'$ compounds was identical to the one used in 2.10.1a. Similar insoluble, polymeric complexes as seen for the Y = S derivatives above were isolated. These complexes were of a dark brown/black colour and were also air-stable. Gold(I) complexes formed with three of the ligands, [$Ph_2P(Se)C(S)N(H)Ph$], [$Ph_2P(Se)C(S)N(H)Me$] and [$Cy_2P(Se)C(S)N(H)Ph$], whereas with the [$Cy_2P(Se)C(S)N(H)Me$] compound, addition to the gold(I) solution resulted in the immediate precipitation of elemental gold and selenium. Physical data can be found in Table 2.10.4.

2.11 *Reaction of Ph_3PAuCl with Diorganophosphino-, Diorganophosphinyl-, Diorgano-thiophosphinyl- and Diorganoselenophosphinyl-thioformamides, $R_2P(Y)C(S)N(H)R'$*

The reaction of the Ph_3PAuCl species [48] with each of the $R_2PC(S)N(H)R'$, $R_2P(O)C(S)N(H)R'$, $R_2P(S)C(S)N(H)R'$ and $R_2P(Se)C(S)N(H)R'$ ligands was essentially the same and hence, a general description only will be given.

2.11.1 Reaction of Ph_3PAuCl with $R_2PC(S)N(H)R'$

The reactions of Ph_3PAuCl with the [$Ph_2PC(S)N(H)Ph$], [$Ph_2PC(S)N(H)Me$], [$Cy_2PC(S)N(H)Ph$] and [$Cy_2PC(S)N(H)Me$] were performed in an analogous manner. Details for the reaction involving [$Ph_2PC(S)N(H)Ph$] are given below. Physical data and percentage yields are given in Table 2.10.1.

2.11.1a Reaction of Ph_3PAuCl with [$Ph_2PC(S)N(H)Ph$]

One molar equivalent of Ph_3PAuCl (200 mg, 0.40 mmol) was dissolved in a tetrahydrofuran solution with stirring. To this solution was added a 1.1 molar equivalent of solid [$Ph_2PC(S)N(H)Ph$] (141 mg, 0.44 mmol). Stirring was continued until the solids dissolved and then triethylamine (*ca.* 2 cm^3) was added dropwise over a few minutes after which the colour of the solution faded. After 45 minutes of stirring, the solution was filtered and then the solvent was removed *in vacuo*. The product was washed with ethanol and then recrystallised from a small quantity of an ethanol/dichloromethane mixture (1/4 *v/v*, 5 cm^3) to give a colourless/pale yellow microcrystalline, air-stable product. The melting point of the complex was 250°C (dec.) and 165 mg (80%) was recovered.

2.11.2 Reaction of Ph_3PAuCl with $R_2P(O)C(S)N(H)R'$

The procedure employed for the attempted reaction of the $R_2P(O)C(S)N(H)R'$ ligands with Ph_3PAuCl was the same as 2.11.1a, however, no detectable reaction was observed in any case.

2.11.3 Reaction of Ph_3PAuCl with $R_2P(S)C(S)N(H)R'$

The reaction of the $R_2P(S)C(S)N(H)R'$ ligands with the Ph_3PAuCl species employed the same procedure as in 2.11.1a. The crude product obtained was pale white in colour. On dissolving the product in chlorinated solvents (the only solvent the complexes were soluble

in) elemental gold precipitated out and a dark-orange residue remained. Physical data can be found in Table 2.11.3.

2.11.4 Reaction of Ph_3PAuCl with $R_2P(Se)C(S)N(H)R'$

The procedure for the reaction of the $R_2P(Se)C(S)N(H)R'$ ligands with the Ph_3PAuCl species followed the same route as in 2.11.1a. Characterisation of the gold(I) complexes found them to be the same products as obtained for the reaction with the $R_2PC(S)N(H)R'$ ligands, i.e. $\{Au[R_2PC(S)NR']\}_2$. Physical data can be found in Table 2.10.1.

2.12 Reaction of Nickel Nitrate with selected Diorganophosphino-, Diorganophosphinyl-, Diorganothiophosphinyl- and Diorganoselenophosphinyl-thioformamides, $R_2P(Y)C(S)N(H)R'$

2.12.1 Reaction of $NiNO_3$ with $R_2PC(S)N(H)R'$

The reactions of the $NiNO_3$ species with $[Ph_2PC(S)N(H)Ph]$, $[Ph_2PC(S)N(H)Me]$, $[Cy_2PC(S)N(H)Ph]$ and $[Cy_2PC(S)N(H)Me]$ were performed in an analogous manner. Details for the reaction involving $[Ph_2PC(S)N(H)Ph]$ are given below. Physical data and percentage yields are given in Table 2.12.1.

2.12.1a Reaction of $NiNO_3$ with $[Ph_2PC(S)N(H)Ph]$

To a stirred ethanolic solution (35 cm^3) of 1 molar equivalent of $NiNO_3.6H_2O$ (200 mg, 0.69 mmol) was added 2.1 molar equivalents of solid $[Ph_2PC(S)N(H)Ph]$ (464 mg, 1.44 mmol). The solution was stirred for about ten minutes with slight warming (45-50°C) until all solids had dissolved. Et_3N (2 cm^3) was added dropwise over one minute. After 30 minutes stirring, a characteristic red precipitate appeared. The complex was collected by vacuum filtration and washed with cold ethanol and diethyl ether. The nickel complex could only be dissolved in hot chloroform or dichloromethane solutions. Recrystallisation of the complex was from chloroform and the orange/red crystalline product was dried in a desiccator over P_2O_5, 457 mg (95%). Physical data can be found in Table 2.12.1.

Table 2.12.1: Physical Data for the Nickel(II) Diorganophosphinothioformamido Complexes, $\{Ni[R_2PC(S)NR']_2\}$, R = Ph or Cy, R' = Ph or Me

Complex	colour	% yield	m. pt (°C)
$\{Ni[Ph_2PC(S)NPh]_2\}$	orange/red	95	150 (dec.)
$\{Ni[Ph_2PC(S)NMe]_2\}$	orange/red	88	153 (dec.)
$\{Ni[Cy_2PC(S)NPh]_2\}$	orange/red	83	210 (dec.)
$\{Ni[Cy_2PC(S)NMe]_2\}$	orange/red	79	158-160

Table 2.12.2: Physical Data for the Nickel(II) Complexes with $R_2P(O)C(S)N(H)R'$, R = Ph or Cy, R' = Ph or Cy

Complex	colour	% yield	m. pt (°C)
$\{Ni[Ph_2P(O)C(S)NPh]_2\}$	pale yellow	36	154-157 (dec.)
$\{Ni[Ph_2P(O)C(S)NMe]_2\}$	pale green	70	120-140
$\{Ni[Cy_2PC(S)NPh]_2\}$	orange/red	45	210 (dec.)
$\{Ni[Cy_2PC(S)NMe]_2\}$	orange/red	56	158-160

2.12.2 Reaction of $NiNO_3$ with $R_2P(O)C(S)N(H)R'$

The reaction of $NiNO_3$ with the [$R_2P(O)C(S)N(H)R'$] ligands was analogous to the procedure outlined in 2.12.1a. The products for the R = Ph ligands were green or yellow in colour. The red/orange products isolated for the R = Cy ligands were of the form {$Ni[Cy_2PC(S)NR']_2$}. Physical data can be found in Table 2.12.2.

2.12.3 Reaction of $NiNO_3$ with $[Ph_2P(S)C(S)N(H)Ph]$

The reaction of $NiNO_3$ with [$Ph_2P(S)C(S)N(H)Ph$] was the same as the procedure employed in 2.12.1a. The precipitate obtained from solution had a very dark green/brown colour. Recrystallisation of the air-stable complex was from hot chloroform layered with petroleum spirit 40/60°C. Physical data can be found in Table 2.12.3.

2.12.4 Reaction of $NiNO_3$ with $[Ph_2P(Se)C(S)N(H)Ph]$

The reaction of $NiNO_3$ with [$Ph_2P(Se)C(S)N(H)Ph$] utilised the method as outlined in 2.12.1a. The product was dark green/brown in colour. Recrystallisation of the complex was achieved from hot chloroform layered with petroleum spirit 40/60°C. Upon standing for two of weeks, the precipitation of elemental selenium occurred. Physical data can be found in Table 2.12.4.

2.13 *Reaction of Cadmium Chloride with Dicyclohexyl-N-phenyl-selenophosphinylthio-formamide, $[Cy_2P(Se)C(S)N(H)Ph]$*

2.13.1 Reaction of $CdCl_2$ with $[Cy_2P(Se)C(S)N(H)Ph]$

One molar equivalent of $CdCl_2$ (100 mg, 0.55 mmol) was dissolved in a dichloromethane/ethanol solution (1/1 *v/v*, 40 cm^3) to which 2.1 molar equivalents of the solid ligand, [$Cy_2P(Se)C(S)N(H)Ph$], (368 mg, 1.15 mmol) was added. After about 5 minutes of stirring Et_3N was added (2 cm^3) and the colour faded until there was a slight yellow tinge. The solution was allowed to stir for an additional 30 minutes and was then

Table 2.12.3: Physical Data for the Nickel(II) Diphenyl-N-phenyl-thiophosphinothioformamido Complex

Complex	colour	% yield	m. pt (°C)
$\{Ni[Ph_2P(S)C(S)NPh]_2\}$	brown	65	134-136 (dec.)

Table 2.12.4: Physical Data for the Nickel(II) Diphenyl-N-phenyl-selenophosphinothioformamidophosphinothioformamido Complex

Complex	colour	% yield	m. pt (°C)
$\{Ni[Ph_2P(Se)C(S)NPh]_2\}$	brown	75	135 (dec.)

Table 2.13.1: Physical Data for the Cadmium(II) Dicyclohexyl-N-phenyl-selenophosphinylthioformamido Complex

Complex	colour	% yield	m. pt (°C)
$\{Cd[Cy_2P(Se)C(S)NPh]_2\}$	white	73	163-165 (dec.)

filtered, the solvent removed *in vacuo* and the complex was recrystallised from chloroform (10 cm^3). The white crystals had a melting point of 163-165°C (decomposition point) and 299 mg (73%) of the product was obtained. After about two weeks at room temperature, red selenium precipitated out, however, the complex was stable when kept in an inert atmosphere. Physical data are given in Table 2.13.1.

Chapter 3

STRUCTURAL ANALYSIS OF DIORGANOPHOSPHINYL-, DIORGANOTHIOPHOSPHINYL- AND DIORGANO-SELENOPHOSPHINYL- THIOFORMAMIDES

In this chapter, the crystal and molecular structures of the $R_2P(Y)C(S)N(H)R'$ compounds where Y = O, S or Se; R = Ph or Cy; R' = Ph, Me, Et or Cy are described. The details concerning the data collection procedures used for the crystal structure determination of the following compounds are outlined in Chapter 2. This chapter comprises three sections, i.e. Section 3.1: the description of the $R_2P(O)C(S)N(H)R'$ structures (**II**), Section 3.2: the $R_2P(S)C(S)N(H)R'$ structures (**III**), and Section 3.3: the $R_2P(Se)C(S)N(H)R'$ structures (**IV**).

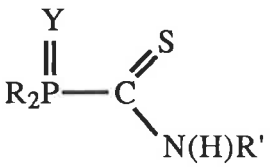

(**II**) Y = O
(**III**) Y = S
(**IV**) Y = Se

R, R' = alkyl, aryl

No structural information for any of the compounds has appeared in the literature, however, several metal complexes with the deprotonated forms of $[Ph_2P(O)C(S)N(H)Ph]$ and $[Ph_2P(S)C(S)N(H)Ph]$ are available; see *Introduction* (Chapter 1).

3.1 The Structures of $R_2P(O)C(S)N(H)R'$

Four compounds of the type $R_2P(O)C(S)N(H)R'$ have been structurally characterised for R = Ph or Cy and R' = Ph or Me. The compounds will be discussed in the following order: R = Ph, R' = Ph (3.1.1); R = Ph, R' = Me (3.1.2); R = Cy, R' = Ph (3.1.3) and R = Cy, R' = Me (3.1.4). A listing of selected bond distances and bond angles for the four structures described in this section are collected in Table 3.1.

3.1.1 The Structure of $[Ph_2P(O)C(S)N(H)Ph]$

Bright yellow crystals of *P,P*-diphenyl-*N*-phenyl-phosphinylthioformamide, $[Ph_2P(O)C(S)N(H)Ph]$, were obtained from the slow diffusion of ether into an acetonitrile solution of the compound. Crystals are triclinic, space group $P\bar{1}$ with unit cell dimensions a = 8.785(1), b = 12.004(2), c = 8.741(1) Å, α = 110.06(1), β = 94.63(1), γ = 100.82(1)°, V = 839.9(2) Å^3, Z = 2 and D_x = 1.334 g cm^{-3}. The structure was refined to final R = 0.050, R_w = 0.054 for 2036 reflections with $I \geq 3.0\sigma(I)$.

Table 3.1: Selected bond distances (Å) and angles (deg.) for $R_2P(O)C(S)N(H)R'$, R = Ph or Cy and R' = Me or Ph

Atoms	R = Ph R' = Ph	R = Ph R' = Me	R = Cy R' = Ph	R = Cy R' = Me
P(1)-O(2)	1.476(3)	1.487(2)	1.479(4)	1.480(2)
P(1)-C(1)	1.852(4)	1.837(3)	1.817(5)	1.814(4)
P(1)-C(11)	1.799(5)	1.801(4)	1.786(6)	1.781(4)
P(1)-C(21)	1.796(5)	1.796(3)	1.809(6)	1.786(4)
C(1)-S(1)	1.623(4)	1.652(3)	1.618(5)	1.630(3)
C(1)-N(1)	1.329(5)	1.319(3)	1.327(6)	1.306(4)
N(1)-C(31)	1.426(5)	1.451(4)	1.423(6)	1.445(6)
O(2)-P(1)-C(1)	111.4(2)	110.2(1)	111.3(2)	110.8(2)
O(2)-P(1)-C(11)	111.6(2)	111.8(2)	110.4(3)	111.2(2)
O(2)-P(1)-C(21)	111.8(2)	112.5(1)	115.1(3)	112.4(2)
C(1)-P(1)-C(11)	106.6(2)	106.9(1)	105.7(3)	107.4(2)
C(1)-P(1)-C(21)	104.9(2)	105.5(1)	101.8(3)	105.1(2)
C(11)-P(1)-C(21)	110.2(2)	109.6(1)	111.9(3)	109.6(2)
S(1)-C(1)-P(1)	119.9(2)	121.6(2)	119.8(3)	121.0(2)
S(1)-C(1)-N(1)	126.8(3)	125.5(2)	128.9(4)	126.0(3)
P(1)-C(1)-N(1)	113.3(3)	112.9(2)	111.4(4)	113.0(3)
C(1)-N(1)-C(31)	127.5(4)	124.0(3)	128.1(5)	124.0(3)

The structure determination of [$Ph_2P(O)C(S)N(H)Ph$] confirms the stoichiometry of the compound as formulated. The molecular structure showing the numbering scheme employed is shown in the ORTEP diagram [14], 15% thermal ellipsoids, in Fig. 3.1.1a.

The conformation about the C(1)-N(1) bond in [$Ph_2P(O)C(S)N(H)Ph$] is *Z* as it is for all the other Y = O derivatives mentioned in this thesis. The atoms P(1), O(2), C(1), S(1) and N(1) are essentially coplanar with deviations from the least-squares plane through these atoms being -0.007(1), 0.047(4), -0.003(4), 0.008(2) and -0.020(4) Å, respectively. This planarity can also be seen in the values of 177.3(3) and -3.1(4)° for the respective S(1)/C(1)/P(1)/O(2) and O(2)/P(1)/C(1)/N(1) torsion angles. The three phenyl groups C(11)-C(16), C(21)-C(26) and C(31)-C(36) form dihedral angles of 58.8, 69.7, and 36.7°, respectively, with the P(O)C(S)N plane. The last angle indicates that there is no conjugation between the P(O)C(S)N chromophore and this phenyl group. Considering the bond distances about the P(1) atom first (Table 3.1), and comparing these to the average bond distances found in related systems [23], it is noted that the P-C(phenyl) bonds are comparable to the average distance of 1.801 Å found in similar arrangements, and that the P(1)=O(2) distance of 1.476(3) Å is shorter than the average P=O distance of 1.489 Å [23]. The P(1)-C(1) distance of 1.852(4) Å is significantly longer than the P-C(phenyl) bond distances but this fact may be related to the nature of the remaining substituents bound to the C(1) atom. In the 'parent' compound [$Ph_2PC(S)N(H)Ph$] [15], the P(1)-C(1) distance was determined to be 1.862(3) Å and the P-C(phenyl) bond distances were found to be 1.837(2) and 1.837(3) Å. So while the P-C(phenyl) distances in [$Ph_2P(O)C(S)N(H)Ph$] have contracted by nearly 0.04 Å, the P(1)-C(1) bond distance has contracted by only 0.01 Å. The contractions are expected as the parent compound contains phosphorus in the +III oxidation state and in the [$Ph_2P(O)C(S)N(H)Ph$] compound, the phosphorus atom is in the +V oxidation state. What is not expected is the disparity of the contractions in the P(1)-C(1) bond distances in [$Ph_2P(O)C(S)N(H)Ph$] and, indeed, in the remaining structures described in Chapter 3. The disparity in contraction indicates that the P(1)-C(1) bond in [$Ph_2P(O)C(S)N(H)Ph$] is significantly weaker than the comparable bond in

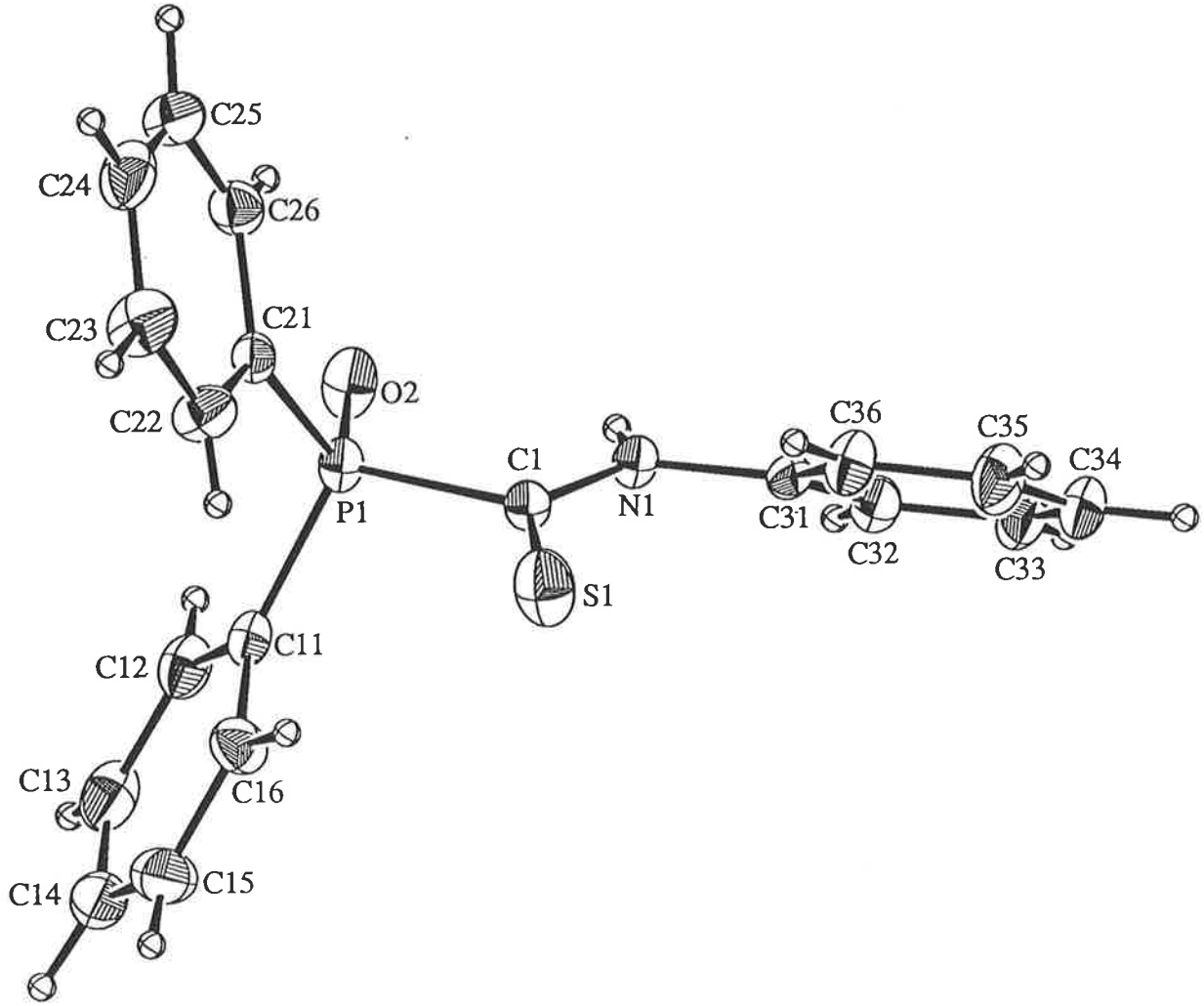

Fig. 3.1.1a The molecular structure of $[Ph_2P(O)C(S)N(H)Ph]$

[$Ph_2PC(S)N(H)Ph$] (see later). The geometry about the phosphorus atom is distorted tetrahedral with the range of angles being 104.9(2) to 111.8(2)°.

The sp^2 C(1) atom exists in a distorted trigonal planar geometry with the S(1)-C(1)-P(1) angle being 119.9(2)°, S(1)-C(1)-N(1) 126.8(3)°, and P(1)-C(1)-N(1) 113.3(3)°. The latter two angles have expanded and contracted, respectively compared to the equivalent angles in [$Ph_2PC(S)N(H)Ph$] owing to the presence of intermolecular hydrogen bonding (discussed below). The C(1)=S(1) distance of 1.623(4) Å is significantly shorter than that found in [$Ph_2PC(S)N(H)Ph$] of 1.650(3) Å and the C(1)-N(1) bond distance of 1.329(5) Å indicates some multiple bond character in this bond. The C=S distance in [$Ph_2P(O)C(S)N(H)Ph$] is also significantly shorter than comparable bonds in related systems, i.e. 1.656(5) Å in [$Ph_2PC(S)N(H)Me$] [25] and 1.663(4) Å in [$Ph_2P(S)C(S)NMe_2$] [49]. While at first inspection it may seem enigmatic that the presence of a short C(1)-N(1) bond is not accompanied by lengthening of the C(1)=S(1) bond, there are two related features in the structure which may help to explain this phenomenon.

The first feature relates to the comparative weakening of the P(1)-C(1) bond mentioned above and the other to the presence of intermolecular hydrogen bonding in the lattice. Fig. 3.1.1b shows a view of the association of two centrosymmetrically related [$Ph_2P(O)C(S)N(H)Ph$] molecules *via* the N(1)-H(1)...O(2)' (symmetry operation 1-*x*, -*y*, -*z*) hydrogen bonds (dashed in Fig. 3.1.1b); the H(1)...O(2)' distance is 2.13(4) Å, N(1)...O(2)' 2.823(5) Å and the N(1)-H(1)...O(2)' angle is 164(4)°. The unit cell contents for [$Ph_2P(O)C(S)N(H)Ph$] are illustrated in Fig. 3.1.1c. The intramolecular separation between the O(2) and H(1) atoms is not indicative of a significant interaction between these atoms in this structure and the same is true for the remaining $R_2P(O)C(S)N(H)R'$ compounds. The presence of the intermolecular hydrogen bond has the effect of withdrawing electron density from the N(1) atom, which is compensated by delocalisation of electron density from the P(1)-C(1) bond to the C(1)-N(1) bond.

The [$Ph_2P(O)C(S)N(H)Ph$] compound has been characterised as its anion in the structure of {$Ph_3PMo(CO)_2[Ph_2P(O)C(S)NPh]_2$} [22]. The anion was found to coordinate *via* the oxygen and sulfur atoms with substantial changes in geometric parameters compared

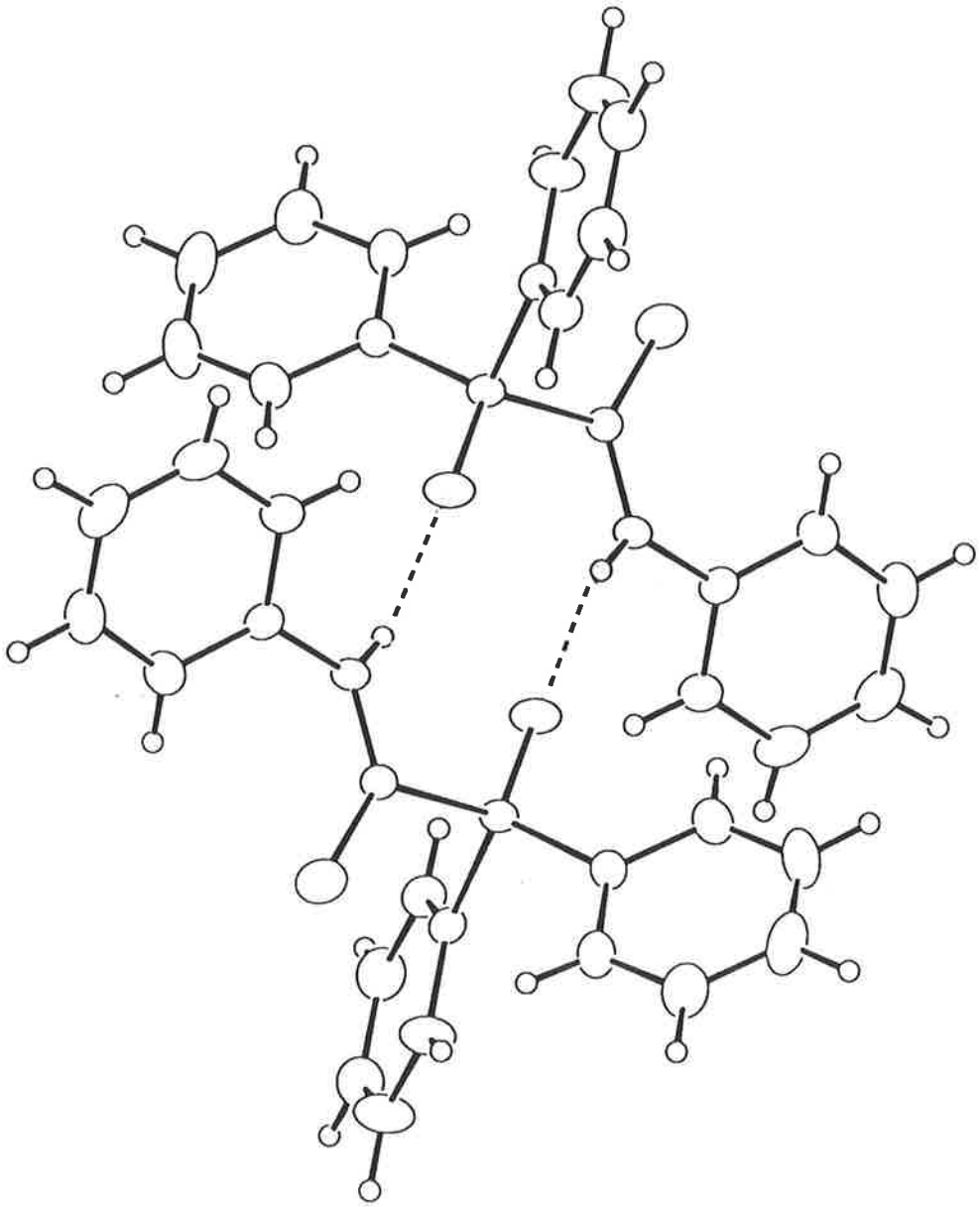

Fig. 3.1.1b Mode of association between centrosymmetrically related molecules of $[Ph_2P(O)C(S)N(H)Ph]$

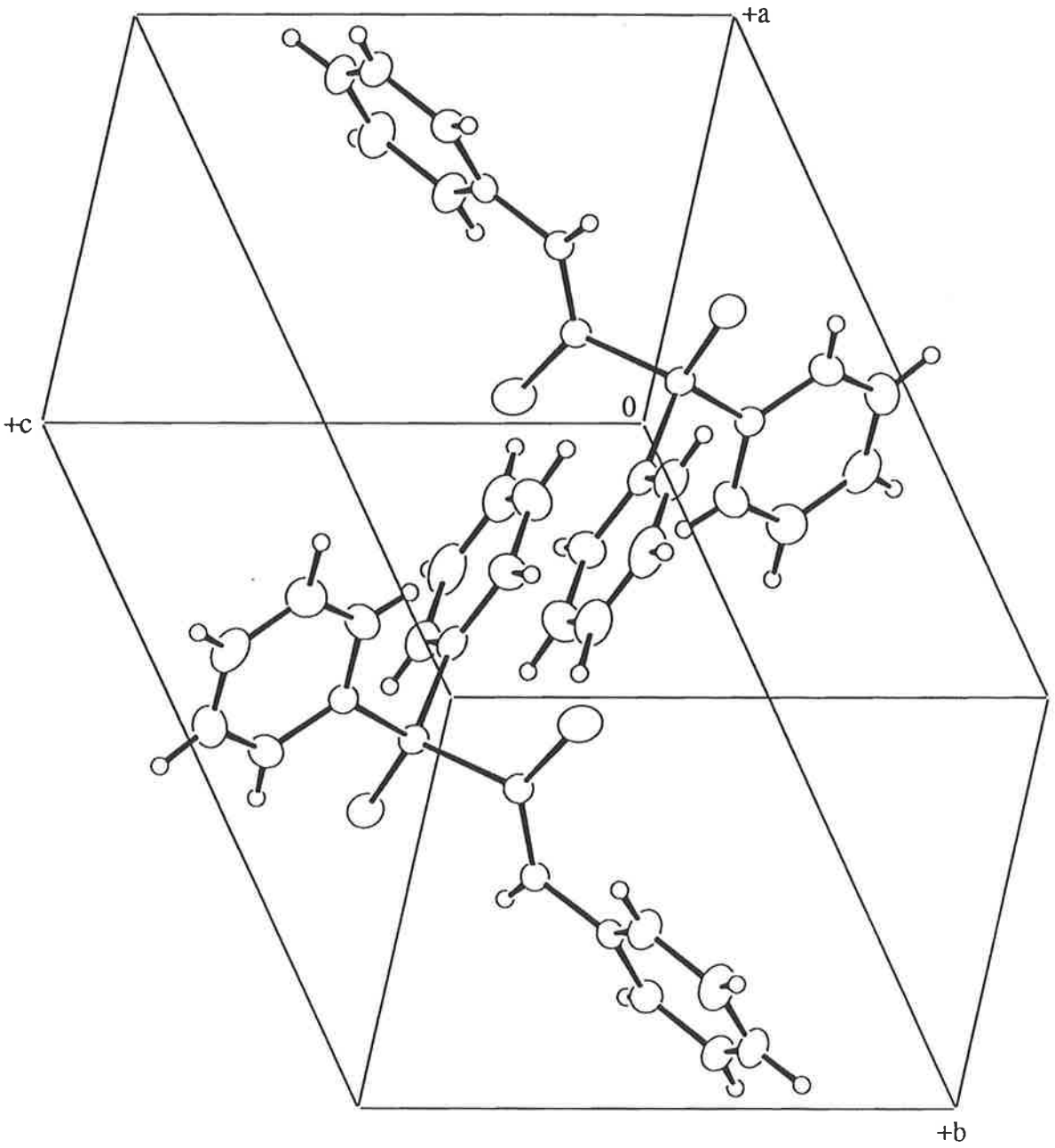

Fig. 3.1.1c The unit cell contents for [$Ph_2P(O)C(S)N(H)Ph$]

to the free ligand [$Ph_2P(O)C(S)N(H)Ph$]. Notably, the P=O distances have increased to 1.500(5) and 1.516(5) Å, the C-S distances have increased to 1.740(8) and 1.750(6) Å, and the C=N distances have decreased to 1.290(8) and 1.278(9) Å for each of the ligands. Of particular interest are the P(1)-C(1) bond distances, which are 1.822(6) and 1.842(5) Å, emphasising the relatively weak nature of the P(1)-C(1) bond in the uncoordinated, neutral ligand.

The observation that the P(1)-C(1) bond in [$Ph_2P(O)C(S)N(H)Ph$] is weak is borne out by the fact that [$Ph_2P(O)C(S)N(H)Ph$] has been found to be susceptible to hydrolysis. In the presence of moisture the [$Ph_2P(O)OH$] species may be isolated, as verified by comparison to an authentic compound [50, 51], as a significant impurity.

3.1.2 The Structure of [$Ph_2P(O)C(S)N(H)Me$]

The pale-yellow crystals of *P,P*-diphenyl-*N*-methyl-phosphinylthioformamide, [$Ph_2P(O)C(S)N(H)Me$], were obtained from the slow diffusion of ether into a chloroform solution of the compound. Crystals are monoclinic, space group $P2_1/c$ with unit cell dimensions a = 10.775(1), b = 14.073(2), c = 9.663(1) Å, β = 105.78(1)°, V = 1410.0(3) Å^3, Z = 4 and D_x = 1.297 g cm^{-3}. The structure was refined to final R = 0.036, R_w = 0.032 for 1458 reflections with $I \geq 3.0\sigma(I)$.

The molecular structure of [$Ph_2P(O)C(S)N(H)Me$] is shown in Fig. 3.1.2a [14] at 15% thermal ellipsoids. The conformation about the central chromophore is essentially planar with deviations from the least-squares plane through the P(1), O(2), C(1), S(1) and N(1) atoms being -0.0113(8), 0.107(3), -0.026(3), 0.010(1) and -0.046(3) Å, respectively; where the C(31) atom lies -0.072(4) Å out the plane. The two torsion angles, O(2)/P(1)/C(1)/S(1) and O(2)/P(1)/C(1)/N(1) are 173.4 and -5.5°, respectively, emphasising the planarity of this moiety. The phosphorus-bound phenyl groups, C(11)-C(16) and C(21)-C(26), form dihedral angles of 59.6 and 77.6°, respectively with this POC(1)SN plane. The availability of two structures of the general formula [$Ph_2P(O)C(S)N(H)R'$], R' = Me or Ph enables an examination of the electronic structure of the acid as the N-bound substituent is varied which in turn may explain the different

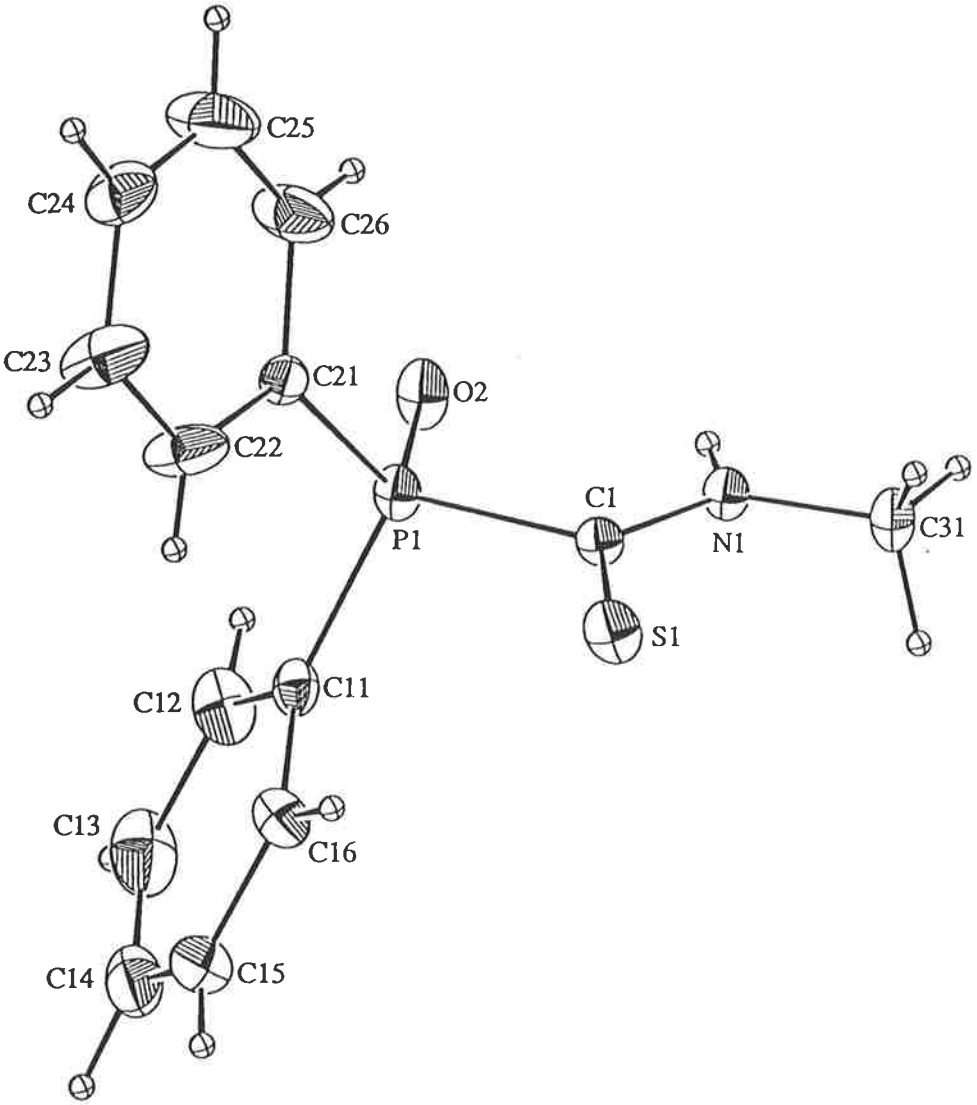

Fig. 3.1.2a The molecular structure of $[Ph_2P(O)C(S)N(H)Me]$

stabilities/reactivities of these ligands. Of particular interest in this context is an apparent systematic variation in the derived parameters describing the central P(O)C(S)N chromophore in the R' = Me and Ph compounds.

Although the estimated standard deviations associated with some of the bond distances suggest experimental equivalence at the three sigma level, the trends in the variations suggest a reorganisation of π-electron density in the [$Ph_2P(O)C(S)N(H)R'$] compounds as the nature of the N-bound substituent is varied. For [$Ph_2P(O)C(S)N(H)Me$], the P(1)=O(2) and P(1)-C(1) bond distances of 1.487(2) and 1.837(3) Å, respectively are longer and shorter to the comparable values in the R' = Ph compound of 1.476(3) and 1.852(4) Å, respectively. More noteworthy, however, are the differences in the C(1)=S(1) and C(1)-N(1) bond distances. Whereas the C(1)=S(1) bond distance of 1.652(3) Å is longer than the equivalent distance in the R' = Ph structure of 1.623(4) Å, the C(1)-N(1) distance is shorter, at 1.319(3) Å, than the comparable separation in the R' = Ph derivative of 1.329(5) Å. The variation in these parameters suggest that the resonance structure in which π-electron density is localised in the C(1)-N(1) bond, leading to S^- and N^+ centres (as shown in 3.1.2), is of more significance in the R' = Me compound.

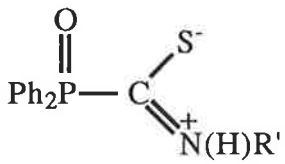

3.1.2

It is likely that it is the smaller inductive effect of the nitrogen-bound methyl substituent that is responsible for the variations in the geometric parameters defining the central chromophores in the two [$Ph_2P(O)C(S)N(H)R'$] structures.

An examination of the intermolecular contacts in the lattice of [$Ph_2P(O)C(S)N(H)Me$] shows the presence of hydrogen bonding between centrosymmetrically related molecules (symmetry operation: 1-*x*, 1-*y*, 1-*z*) involving the O(2) and H(1) atoms, i.e. N(1)-H(1)...(O2)' 2.03(3) Å (N(1)...O(2)' 2.778(3) Å, the angle O(2)'...H(1)-N(1) is 147(3)°); see unit cell contents in Fig. 3.1.2b.

The crystal structure of the parent phosphorus(III) compound, [$Ph_2PC(S)N(H)Me$] ([25]; Section 1.6.1), is also available for comparison with [$Ph_2P(O)C(S)N(H)Me$]. In the

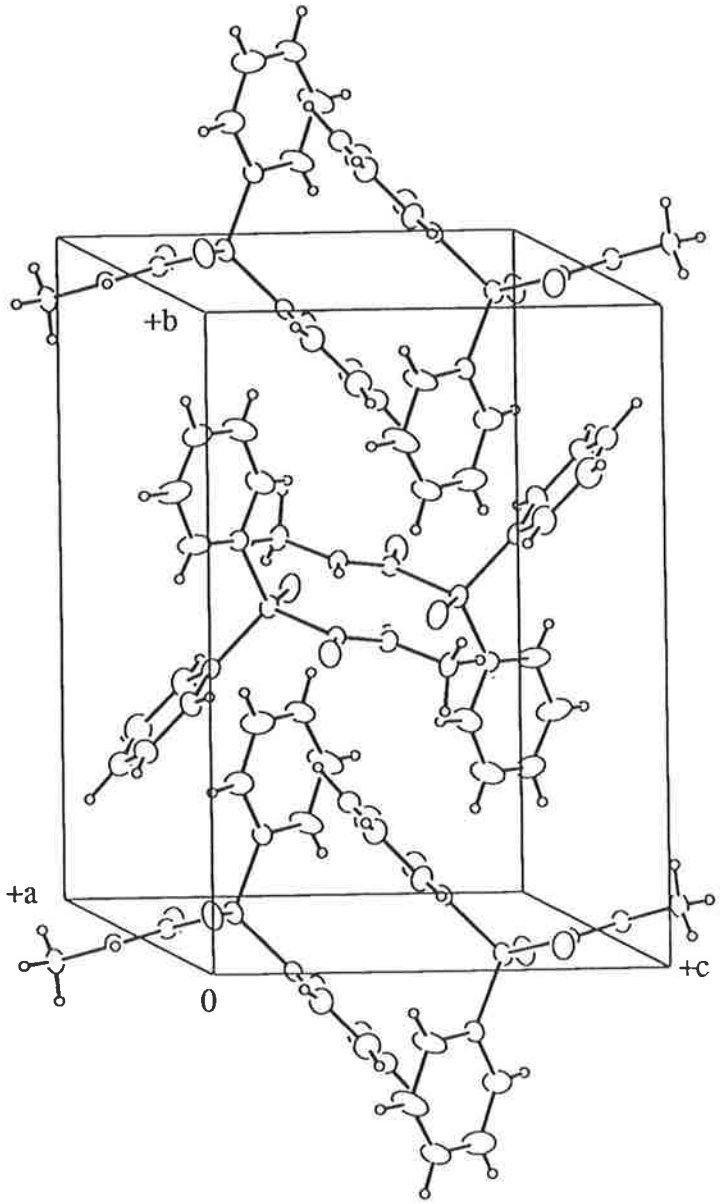

Fig. 3.1.2b The unit cell contents for [$Ph_2P(O)C(S)N(H)Me$]

structure of [$Ph_2PC(S)N(H)Me$] there are two independent molecules in the crystallographic asymmetric unit with the two P(1)-C(1) bond distances of 1.848(3) and 1.850(5) Å being equal within experimental error to that found in the phosphorus(V) compound reported herein. These data support the conclusion made in Section 3.1.1 which stated that the P(1)-C(1) bond in the phosphorus(V) compound is comparatively weaker than the P(1)-C(1) bond in the phosphorus(III) compound from which it is derived.

3.1.3 The Structure of [$Cy_2P(O)C(S)N(H)Ph$]

The yellow crystals of *P,P*-dicyclohexyl-*N*-phenyl-phosphinylthioformamide, [$Cy_2P(O)C(S)N(H)Ph$], were obtained from the slow evaporation of an ethanol solution of the compound. Crystals are monoclinic, space group *C*2/*c*, with unit cell dimensions a = 14.856(4), b = 11.666(4), c = 22.039(3) Å, β = 95.59(1)°, V = 3801(1) Å^3, Z = 8 and D_x = 1.221 g cm^{-3}. The structure was refined to final R = 0.046, R_w = 0.040 for 1257 reflections with $I \geq 3.0\sigma(I)$. The crystallographic numbering scheme is shown in Fig. 3.1.3a ([14]; 30% thermal ellipsoids).

The S(1), P(1), O(2), N(1) and C(1) atoms are effectively coplanar with the mean deviation from the least-squares plane being 0.005(3) Å. This planarity is reflected in the torsion angles of -179.2(3) and -0.7(9)° for S(1)/C(1)/P(1)/O(2) and S(1)/C(1)/N(1)/C(31), respectively. The nitrogen-bound phenyl substituent is not coplanar with the central chromophore as evidenced in the C(1)/N(1)/C(31)/C(32) torsion angle of 145.1(6)°; the dihedral angle between the least-squares planes through the central chromophore and the phenyl ring is 36.7°. The geometry about the phosphorus atom is distorted tetrahedral with the range of angles being 101.8(3) to 115.1(3)°. The P(1)=O(2) bond distance of 1.479(4) Å is marginally shorter than the average P=O bond distance of 1.489 Å found in related systems [23] but is equal within experimental error to the P=O bond distances found in the structures of [$Ph_2P(O)C(S)N(H)Ph$] and [$Ph_2P(O)C(S)N(H)Me$] of 1.476(3) and 1.487(2) Å, respectively. The average P-C(Cy) bond distance of 1.798(4) Å is approximately 0.06 Å shorter than the average distance of 1.856(3) Å found in the structure of the parent acid, i.e. [$Cy_2PC(S)N(H)Ph$], and the P(1)-C(1) bond distance of 1.817(5) Å is approximately 0.05

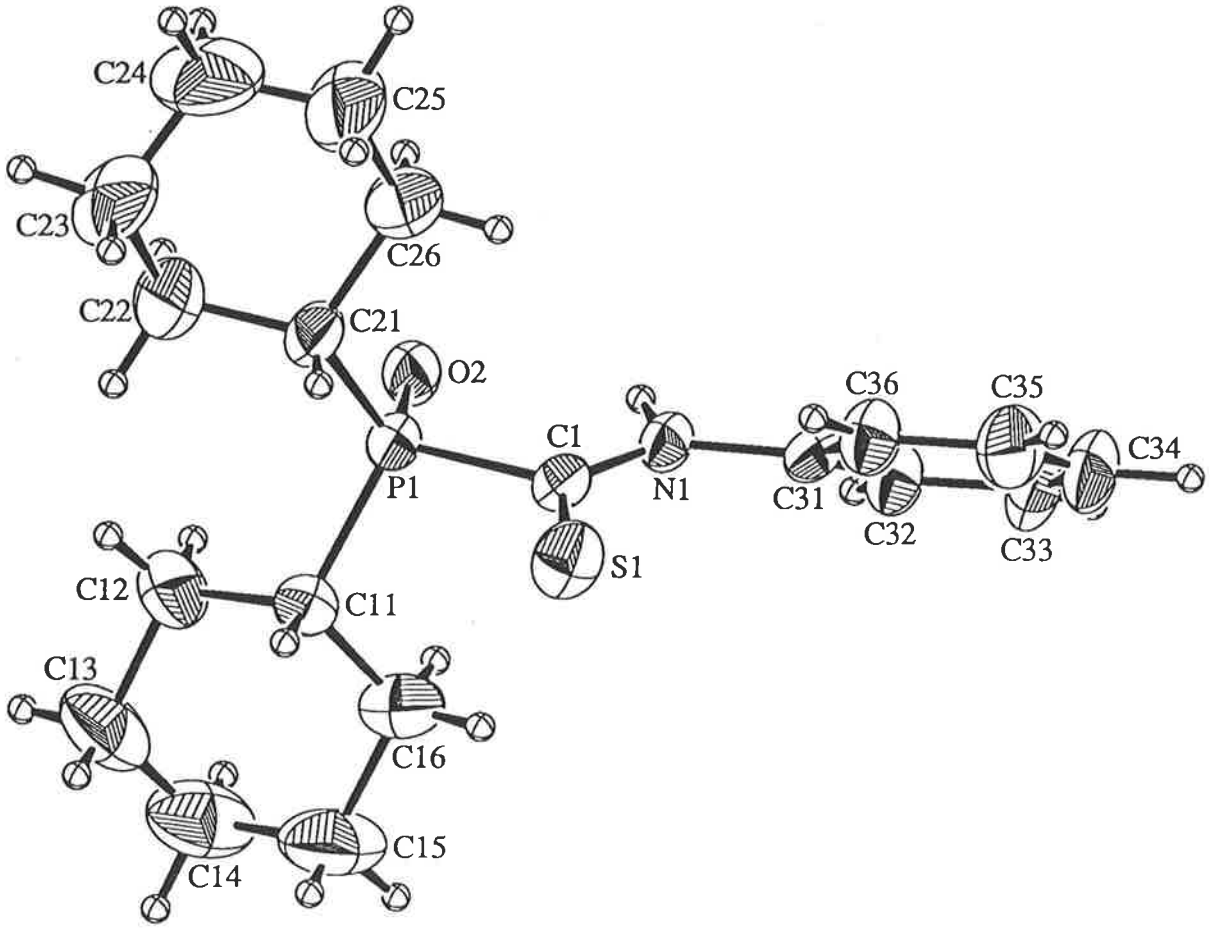

Fig. 3.1.3a The molecular structure of $[Cy_2P(O)C(S)N(H)Ph]$

Å shorter than the comparable distance (average : 1.868(5) Å) in the parent compound [15]. Hence, the contraction in the P-C bond distances that is expected as the oxidation state of the phosphorus atom is increased from +III to +V is not uniform. This variation suggests that the P(1)-C(1) bond is comparatively weaker in the phosphorus(V) compound, an observation that has been noted above, although more pronounced between the [$Ph_2PC(S)N(H)Ph$] and [$Ph_2P(O)C(S)N(H)Ph$] compounds.

The C(1)=S(1) and C(1)-N(1) bond distances of 1.618(5) and 1.327(6) Å, respectively are comparable to those found in [$Ph_2P(O)C(S)N(H)Ph$] of 1.623(4) and 1.329(5) Å, respectively which shows that changing the R groups on the phosphorus atom from phenyl to cyclohexyl has little or no effect on these parameters.

The unit cell contents for the [$Cy_2P(O)C(S)N(H)Ph$] compound are shown in Fig. 3.1.3b. The lattice is comprised of symmetry related pairs of the compound associated *via* hydrogen bonding contacts such that N(1)-H(1)...O(2)' is 1.884(4) Å (N(1)...O(2)' is 2.765(6) Å) and the angle subtended at the H(1) atom is 153.0(3)° (symmetry operation: 1-x, +y, 1.5-z).

3.1.4 The Structure of [$Cy_2P(O)C(S)N(H)Me$]

The green crystals of *P,P*-dicyclohexyl-*N*-methyl-phosphinylthioformamide, [$Cy_2P(O)C(S)N(H)Me$], were obtained from the slow evaporation of an ethanol solution of the compound. Crystals are monoclinic, space group $C2/c$, with unit cell dimensions a = 10.247(2), b = 16.025(4), c = 19.358(4) Å, β = 97.75(2)°, V = 3149(1) $Å^3$, Z = 8 and D_x = 1.212 g cm^{-3}. The structure was refined to final R = 0.036, R_w = 0.031 for 1383 reflections with $I \geq 3.0\sigma(I)$. The crystallographic numbering scheme is shown in Fig. 3.1.4a ([14]; 30% thermal ellipsoids).

The deviations of the S(1), P(1), O(2), N(1) and C(1) atoms from the least-squares plane through these atoms are 0.014(1), -0.015(1), 0.088(3), -0.047(3) and -0.024(3) Å, respectively (for reference the C(11) atom lies -1.519(5) Å out of this plane). The S(1)/C(1)/P(1)/O(2) and S(1)/C(1)/N(1)/C(31) torsion angles are 174.1(2) and 0.2(6)°, respectively indicating planarity throughout this chromophore. The distortion from

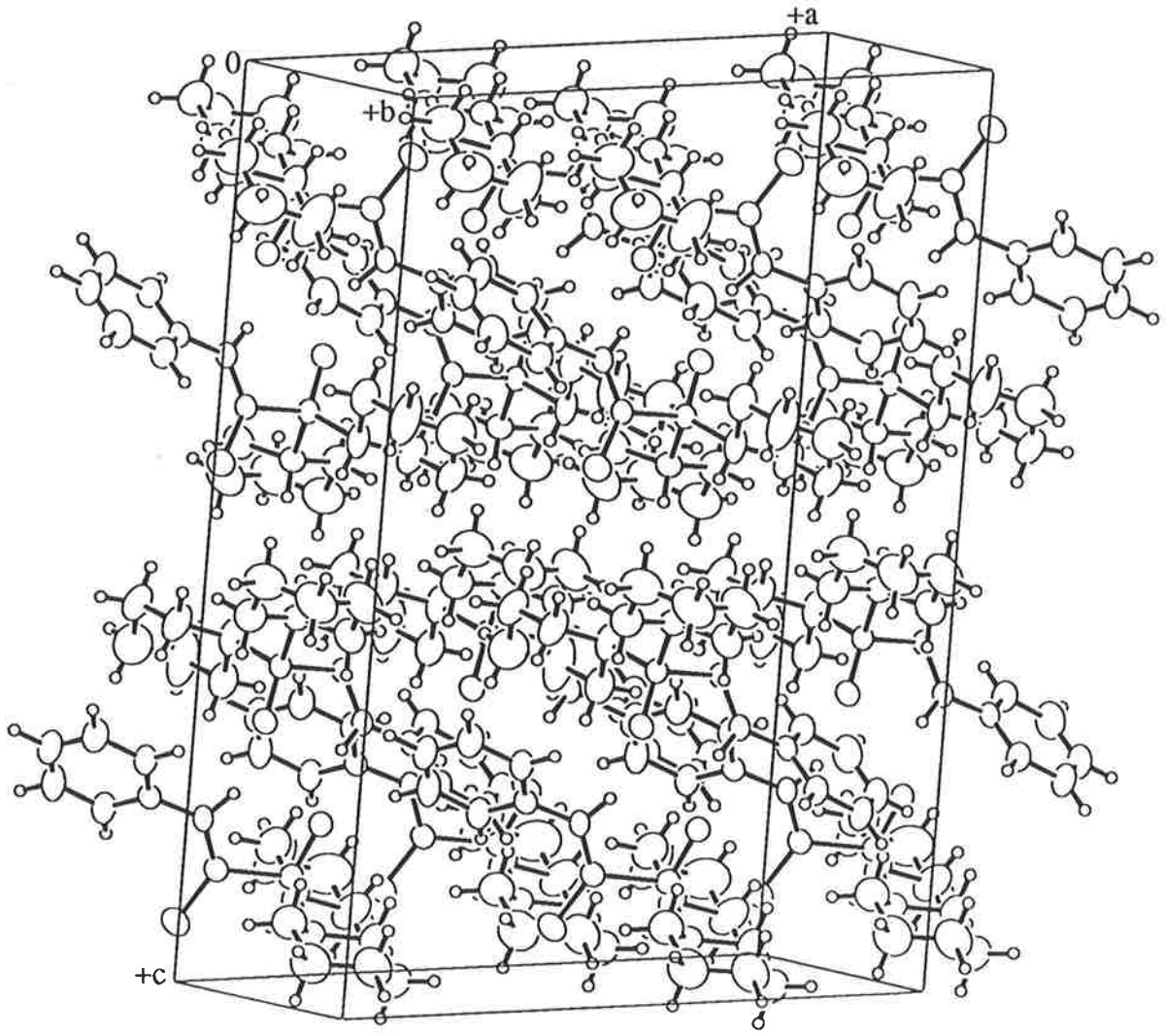

Fig. 3.1.3b The unit cell contents for [$Cy_2P(O)C(S)N(H)Ph$]

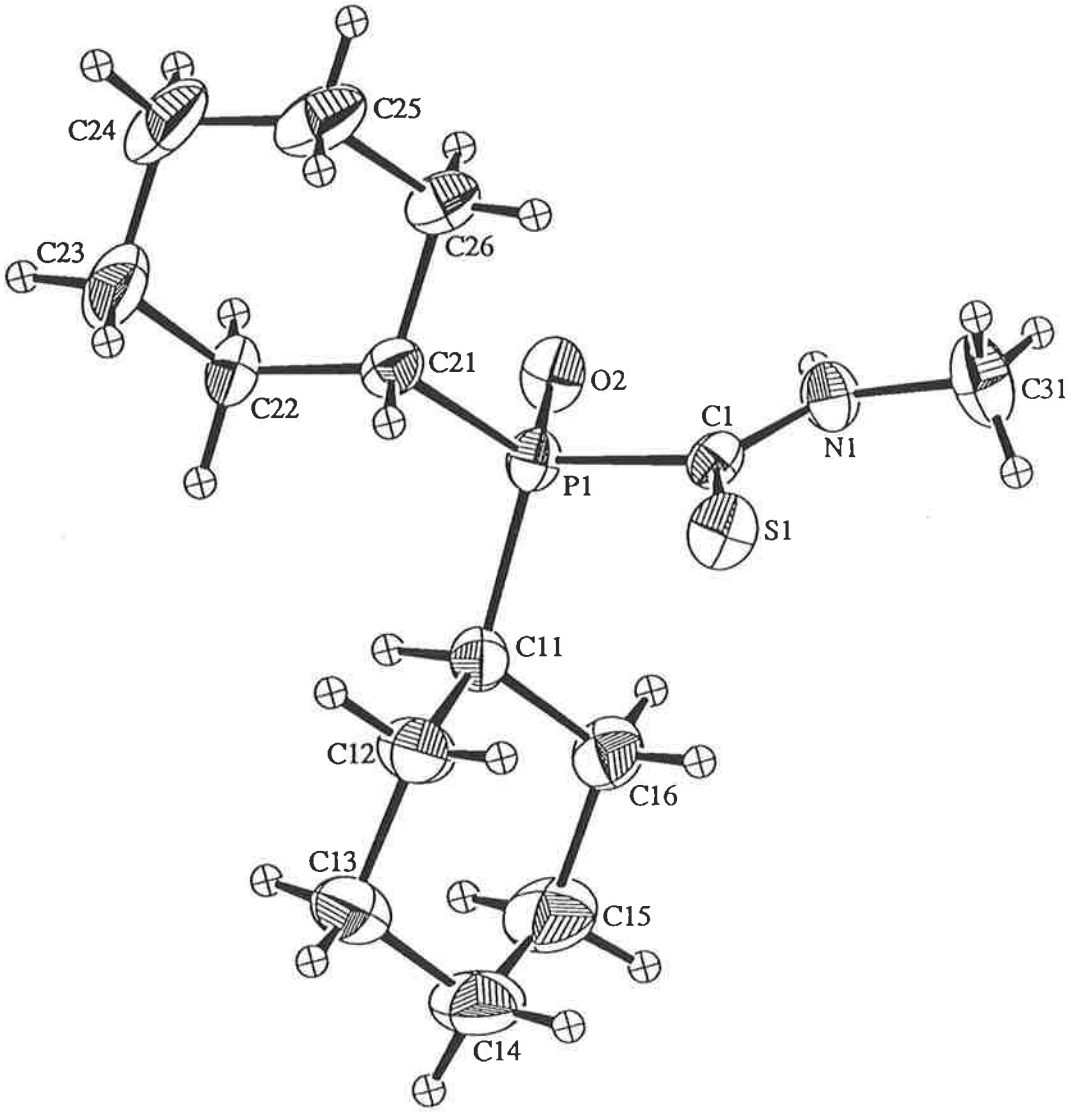

Fig. 3.1.4a The molecular structure of $[Cy_2P(O)C(S)N(H)Me]$

tetrahedral geometry about the phosphorus atom in [Cy_2P(O)C(S)N(H)Me], with angles in the range 105.1(2) to 112.4(2)°, is less than that in the [Cy_2P(O)C(S)N(H)Ph] analogue 105.7(3) to 115.1(3)°. The P(1)=O(2) bond distance of 1.480(2) Å, however, is equal within experimental error to that found in the R' = Ph analogue. The crystal structure of the parent acid, [Cy_2PC(S)N(H)Me], is not available for comparison of derived interatomic parameters. The C(1)=S(1) bond distance of 1.630(3) Å is comparable to that found in [Ph_2P(O)C(S)N(H)Ph] of 1.623(4) Å.

The P-C bond distances in [Cy_2P(O)C(S)N(H)Me] are equal within experimental error to the comparable distances in the structure of [Cy_2P(O)C(S)N(H)Ph] described in Section 3.1.3. This observation suggests that the nature of the nitrogen-bound substituent, i.e. methyl or phenyl, has little effect on the phosphorus atom parameters. However, the same is not true for the C(=S)N(H)R portion of the molecule.

The estimated standard deviations associated with the remaining part of the molecule are relatively high making correlations quite difficult, however, definite trends may be ascertained from the systematic variation of the interatomic parameters defining the C(=S)N(H)R' moieties. The C(1)=S(1), C(1)-N(1) and N(1)-C(31) bond distances in [Cy_2P(O)C(S)N(H)Me] are longer, shorter and longer, respectively than those in [Cy_2P(O)C(S)N(H)Ph]. Given that the P(1)-C(1) bonds distances are experimentally equivalent in the two molecules, these trends may be rationalised in terms of the greater inductive effect of the phenyl substituent over that of the methyl group. This has the result that less π-electron density is localised in the N(1)-C(31) bond in the R' = Me compound, leading to a comparatively stronger C(1)-N(1) bond and a weaker C(1)=S(1) bond. The relatively small size of the methyl group in [Cy_2P(O)C(S)N(H)Me] also has the effect of reducing the S(1)-C(1)-N(1) angle by approximately 3° compared to the equivalent angle in [Cy_2P(O)C(S)N(H)Ph] which results in a concomitant decrease in the other angles about the C(1) atom.

An interesting difference exists between the two R = Cy structures, namely in the relative disposition of the cyclohexyl groups. In [Cy_2P(O)C(S)N(H)Ph] the molecule has approximate mirror symmetry in that the two methine hydrogen atoms lie to the same side of

the molecule whereas in the R' = Me compound the two methine hydrogen atoms are orientated in opposite directions. There are some minor variations in the angles about the P(1) atom in that the O(2)-P(1)-C(21) and C(1)-P(1)-C(21) angles are smaller and greater, respectively in the R' = Me compound compared with the R' = Ph analogue. The reason for the different relative orientations of the cyclohexyl groups is not clear.

As with the previous Y = O compounds, there are intermolecular hydrogen bonds between symmetry related molecules in the crystal lattice of [$Cy_2P(O)C(S)N(H)Me$]; unit cell contents are shown in Fig. 3.1.4b. The N(1)-H(1)...O(2)' separation is 1.95(4) Å, N(1)...O(2)' is 2.768(4) Å and the N(1)-H(1)...O(2)' angle is 149(3)° (symmetry operation: $-x$, $+y$, $0.5-z$); there are no other notable intermolecular contacts. The intramolecular O(2)...H(1) separation is 2.36(4) Å and is the shortest such contact observed in the four $R_2P(O)C(S)N(H)R'$ compounds.

3.2 The Structures of $R_2P(S)C(S)N(H)R'$

Four compounds of the type $R_2P(S)C(S)N(H)R'$ have been structurally characterised for R = Ph or Cy, R' = Ph or Me. The compounds will be discussed in the following order: R = Ph, R' = Ph (3.2.1); R = Ph, R' = Me (3.2.2); R = Cy, R' = Ph (3.2.3) and R = Cy, R' = Me (3.2.4). The conformation about the C(1)-N(1) bond in the four compounds is *Z* as found for the $R_2P(O)C(S)N(H)R'$ structures described in Section 3.1. A listing of selected bond distances and bond angles for the four structures described in this section can be found in Table 3.2.

3.2.1 The Structure of [$Ph_2P(S)C(S)N(H)Ph$]

Yellow crystals of *P,P*-diphenyl-*N*-phenyl-thiophosphinylthioformamide, [$Ph_2P(S)C(S)N(H)Ph$], were grown by the slow evaporation of a chloroform solution of the compound. Crystals are orthorhombic, crystallising in the *Pbca* space group with unit cell dimensions a = 11.922(2), b = 8.742(1), c = 34.043(2) Å, V = 3548.0(8) Å^3, Z = 8 and D_x = 1.323 g cm^{-3}. The structure was refined to final R = 0.041, R_w = 0.045 for 1295

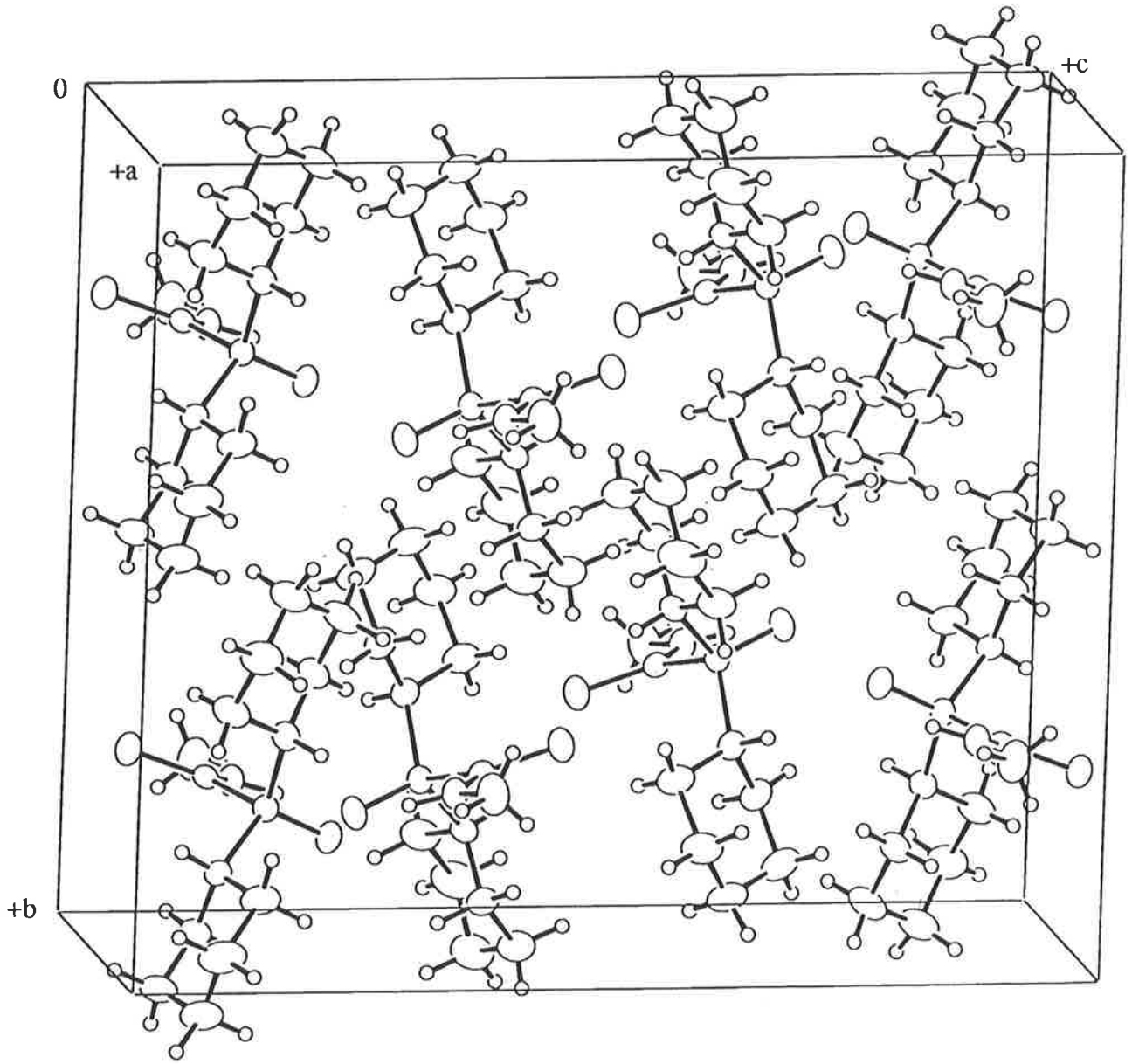

Fig. 3.1.4b The unit cell contents for [$Cy_2P(O)C(S)N(H)Me$]

Table 3.2. Selected bond distances (Å) and angles (deg.) for $R_2P(S)C(S)N(H)R'$, R = Ph or Cy and R' = Me or Ph

Atoms	R = Ph R' = Ph	R = Ph R' = Me	R = Cy R' = Ph	R = Cy R' = Me
P(1)-S(2)	1.951(2)	1.959(1)	1.9495(9)	1.942(1)
P(1)-C(1)	1.855(5)	1.847(4)	1.846(3)	1.823(4)
P(1)-C(11)	1.797(5)	1.813(4)	1.817(3)	1.806(3)
P(1)-C(21)	1.819(4)	1.791(4)	1.803(3)	1.806(3)*
C(1)-S(1)	1.633(4)	1.642(4)	1.624(2)	1.644(4)
C(1)-N(1)	1.338(5)	1.326(5)	1.317(3)	1.290(5)
N(1)-C(31)	1.420(6)	1.448(7)	1.401(3)	1.433(6)
S(2)-P(1)-C(1)	110.8(2)	111.8(1)	110.38(9)	110.5(1)
S(2)-P(1)-C(11)	114.6(2)	113.5(1)	111.53(9)	114.3(1)
S(2)-P(1)-C(21)	112.6(2)	112.7(1)	114.07(9)	114.3(1)*
C(1)-P(1)-C(11)	104.5(2)	103.6(2)	106.5(1)	103.8(1)
C(1)-P(1)-C(21)	106.7(2)	106.7(2)	104.7(1)	103.8(1)*
C(11)-P(1)-C(21)	107.0(2)	108.1(2)	109.2(1)	109.2(2)*
S(1)-C(1)-P(1)	120.4(3)	121.0(2)	118.2(1)	119.7(2)
S(1)-C(1)-N(1)	128.0(4)	125.8(3)	130.2(2)	124.6(3)
P(1)-C(1)-N(1)	111.5(3)	112.9(3)	111.6(2)	115.6(3)
C(1)-N(1)-C(31)	132.6(5)	123.3(4)	132.3(2)	126.3(4)

* the C(21) atom is related across crystallographic mirror plane

reflections with $I \geq 3.0\sigma(I)$. The molecular structure of [$Ph_2P(S)C(S)N(H)Ph$] is illustrated in Fig. 3.2.1a ([14]; 15% thermal ellipsoids).

The P(1)S(2)C(1)S(1)N(1) moiety has significant deviations (-0.057(1), 0.062(1), -0.111(4), 0.075(2) and -0.278(4) Å for the respective atoms) from planarity in contrast to that found for the analogous P(1)O(2)C(1)S(1)N(1) moiety in $Ph_2P(O)C(S)N(H)Ph$ (see Section 3.1.1). This point is emphasised in the torsion angles of -168.3(2)° for S(2)P(1)C(1)S(1) and 10.2(4)° for S(2)P(1)C(1)N(1) and suggests little delocalisation of π-electron density over the respective groups. The P(1)C(1)S(1)N(1) atoms are planar, however, to ± 0.004 Å. The least-squares plane through these atoms forms a dihedral angle of 165.3° with the nitrogen-bound phenyl group again indicating little conjugation between the two groups of atoms. The dihedral angles formed with the phosphorus-bound phenyl groups defined by the C(11)-C(16) and C(21)-C(26) atoms are 103.1 and 117.2°, respectively. The P(1)=S(2) bond distance of 1.951(2) Å is equal to the average P=S bond distance of 1.954 Å found in C_3P=S systems [23] and the P-C(phenyl) distances are as expected. The P(1)=S(2) separation is also equal, within experimental error, to the P=S bond distance found in the related structure, [$Ph_2P(S)C(S)NMe_2$] of 1.950(2) Å [49]. The range of angles about the phosphorus atom is 104.5(2) to 114.6(2)° and these differ marginally from those found in the Y = O analogue, i.e. the increased size of the sulfur atom is compensated by an increase in the P(1)=S(2) separation.

The length of the P(1)-C(1) bond of 1.855(5) Å in [$Ph_2P(S)C(S)N(H)Ph$] is equal within experimental error to the equivalent distance of 1.852(4) Å found in [$Ph_2P(O)C(S)N(H)Ph$]. This observation suggests that the P(1)-C(1) bond in [$Ph_2P(S)C(S)N(H)Ph$] is relatively weak and, by analogy with [$Ph_2P(O)C(S)N(H)Ph$], may indicate that this compound would be susceptible to hydrolysis.

The closest hydrogen contact in the unit cell occurs between the S(2) and H(14)' atoms of 3.00(5) Å (symmetry operation: 1-x, 0.5+y, 0.5-z) which is within the sum of the van der Waals radii of these atoms [21], but is not indicative of a significant interaction. The closest non-hydrogen interaction is between the C(21) and C(32)' atoms of 3.524(7) Å

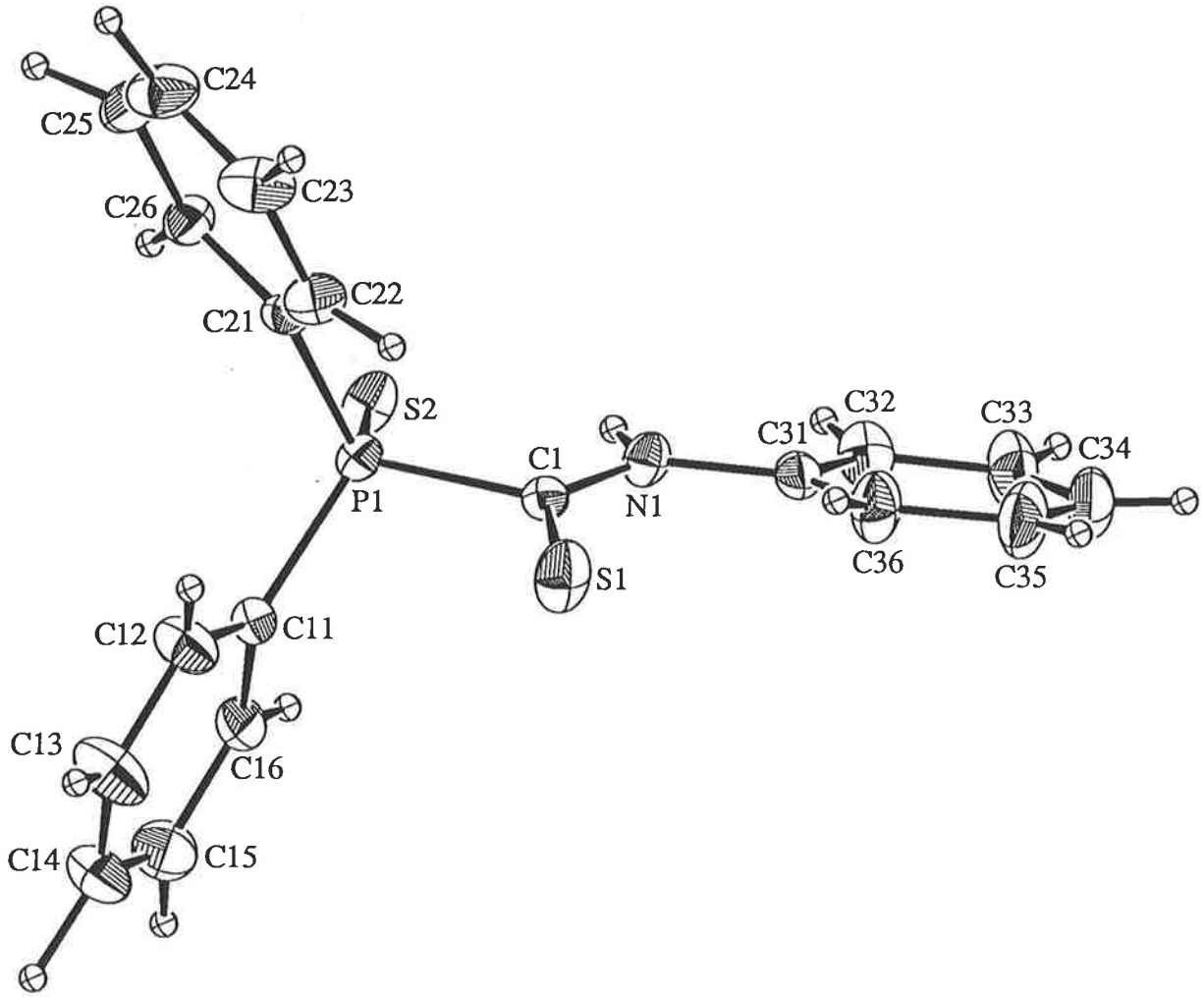

Fig. 3.2.1a The molecular structure of $[Ph_2P(S)C(S)N(H)Ph]$

(symmetry operation: 1.5-x, 0.5+y, +z). There was no intramolecular S(2)...H(1) interaction present. The unit cell contents are shown in Fig. 3.2.1b.

Two complexes have been structurally characterised containing the deprotonated form of [$Ph_2P(S)C(S)N(H)Ph$]. The first, {$Mn(CO)_4$[$Ph_2P(S)C(S)NPh$]} [18] features S-, S-chelation to the six-coordinate manganese atom with the formation of a puckered MnSPCS five-membered ring. Significant changes have occurred to the P(S)C(S)N moiety, which except for the S(2) atom, is essentially planar. The P(1)=S(2), P(1)-C(1), C(1)-S(1) and N(1)-C(31) bond distances are 1.996(1), 1.826(3), 1.733(3) and 1.266(4) Å, respectively; the changes in bond distances are consistent with a formal C(1)-N(1) double bond. Significantly the P(1)-C(1) separation is substantially shorter than that observed in the acid [$Ph_2P(S)C(S)N(H)Ph$] (i.e. 1.855(5) Å). The second complex, {(η^5-C_5H_5)$Mo(CO)_2$-[$Ph_2P(S)C(S)NPh$]} [24], features a S-, N- coordination mode for the [$Ph_2P(S)C(S)NPh$]$^-$ anion in which the phosphorus-bound sulfur atom does not participate in bonding to the metal centre. In this example the P(1)=S(2), P(1)-C(1), C(1)-S(1) and N(1)-C(31) bond distances are 1.942(2), 1.838(6), 1.709(7) and 1.321(5) Å, respectively. Both structures, although having different coordination modes for the [$Ph_2P(S)C(S)NPh$]$^-$ anion, serve to emphasise that in the free [$Ph_2P(S)C(S)N(H)Ph$] ligand, the P(1)-C(1) bond is comparatively weak.

3.2.2 The Structure of [$Ph_2P(S)C(S)N(H)Me$]

The yellow crystals of *P*, *P*-diphenyl-*N*-methyl-thiophosphinylthioformamide, [$Ph_2P(S)C(S)N(H)Me$], were obtained from the slow evaporation of an isopropanol solution of the compound which was layered with hexane. Crystals are monoclinic, space group $P2_1/n$ with unit cell dimensions a = 12.903(1), b = 7.9719(7), c = 14.493(1) Å, β = 96.380(7)°, V = 1481.6(2) Å^3, Z = 4 and D_x = 1.306 g cm^{-3}. The structure was refined to final R = 0.046, R_w = 0.055 for 1853 reflections with $I \geq 3.0\sigma(I)$.

The molecular structure of [$Ph_2P(S)C(S)N(H)Me$] is shown in Fig. 3.2.2a ([14]; 20% thermal ellipsoids). The structure is molecular, there being no significant intermolecular contacts in the lattice; the closest non-hydrogen contact of 3.437(4) Å occurs between the

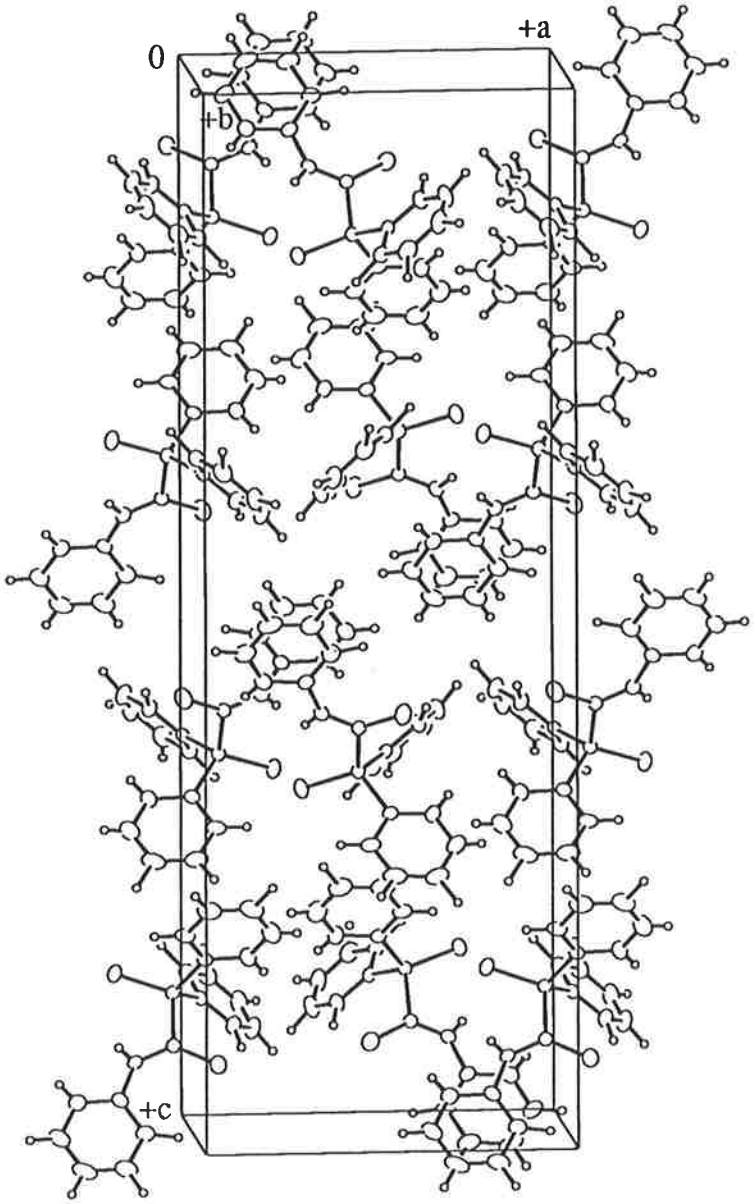

Fig. 3.2.1b The unit cell contents for [$Ph_2P(S)C(S)N(H)Ph$]

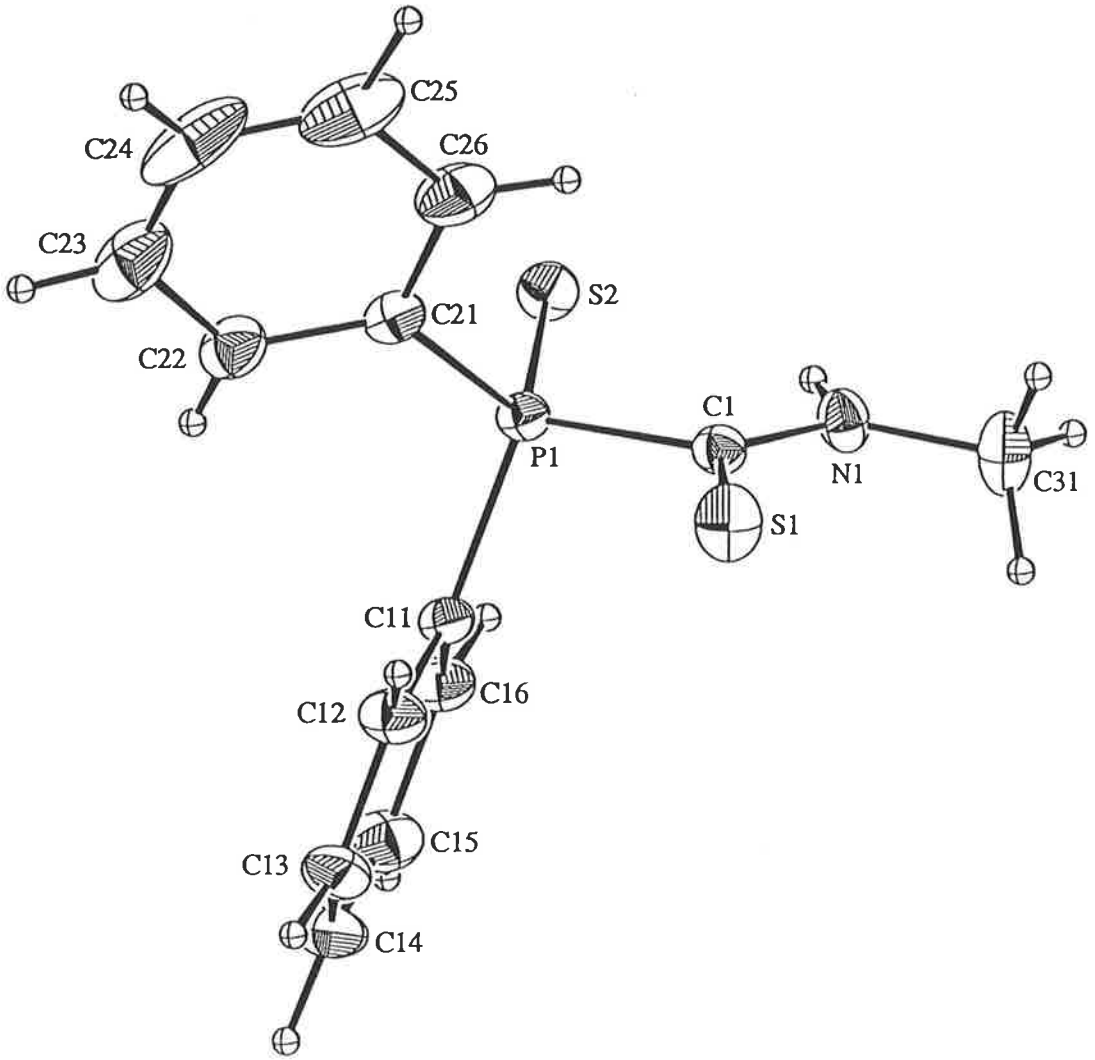

Fig. 3.2.2a The molecular structure of $[Ph_2P(S)C(S)N(H)Me]$

S(2) and N(1)' atoms (symmetry operation: 1-*x*, -*y*, 2-*z*) and the closest contact involving a hydrogen atom is between S(2) and H(1)' of 2.84(4) Å (symmetry operation: 1-*x*, -*y*, 2-*z*). A view of the unit cell contents is shown in Fig. 3.2.2b. The central P(S)C(S)N chromophore is not planar with deviations of the S(1), S(2), P(1), N(1) and C(1) atoms from their least-squares plane being 0.093(2), 0.063(1), -0.048(1), -0.351(4) and -0.078(4) Å, respectively; the C(31) atom lies -0.569(6) Å out of this plane. The lack of planarity is reflected in the torsion angles of 169.3(2) and -15.7(3)° for S(2)/P(1)/C(1)/S(1) and S(2)/P(1)/C(1)/N(1), respectively. The dihedral angles between the central chromophore and the two phenyl rings, C(11)-C(16) and C(21)-C(26), are 68.6 and 105.4°, respectively.

The P(1)=S(2) bond distance of 1.959(1) Å in the present compound is equal within experimental error to that found in [$Ph_2P(S)C(S)N(H)Ph$] (1.951(2) Å) and 1.956(3) Å in [$Ph_2P(S)C(SMe)NMe$] [52]. It is also comparable with the P(1)=S(2) distance found in [$Ph_2P(S)C(S)NMe_2$] [49] of 1.950(2) Å. The P(1)-C(1), C(1)=S(1), and N(1)-C(31) bond lengths of 1.847(4), 1.642(4) and 1.448(7) Å, respectively are shorter, longer and longer, respectively that the corresponding distances in the R' = Ph derivative of 1.855(5), 1.633(4) and 1.420(6) Å, respectively; the errors associated with the C(1)-N(1) distances are too large to make a valid comparison. Similar trends were found in the analogous Y = O species and were interpreted in terms of a relatively greater inductive effect of the nitrogen-bound phenyl group compared with the methyl substituent. The P-C(Ph) bond distances are equal within experimental error in the two $Ph_2P(S)C(S)N(H)R'$ structures, again consistent with the $Ph_2P(O)C(S)N(H)R'$ compounds.

3.2.3 The Structure of [$Cy_2P(S)C(S)N(H)Ph$]

Yellow crystals of *P, P*-diphenyl-*N*-phenyl-thiophosphinylthioformamide, [$Cy_2P(S)C(S)N(H)Ph$], were obtained from the slow evaporation of a dichloromethane solution of the compound. Crystals are triclinic, space group $P\bar{1}$, with dimensions a = 9.766(2), b = 11.111(2), c = 9.388(2) Å, α = 100.54(2), β = 104.66(1) and γ = 83.86(1)°, V = 966.9(3) Å^3, Z = 2 and D_x = 1.249 g cm^{-3}. The structure was refined to final R = 0.038, R_w = 0.039 for 2758 reflections with $I \geq 3.0\sigma(I)$.

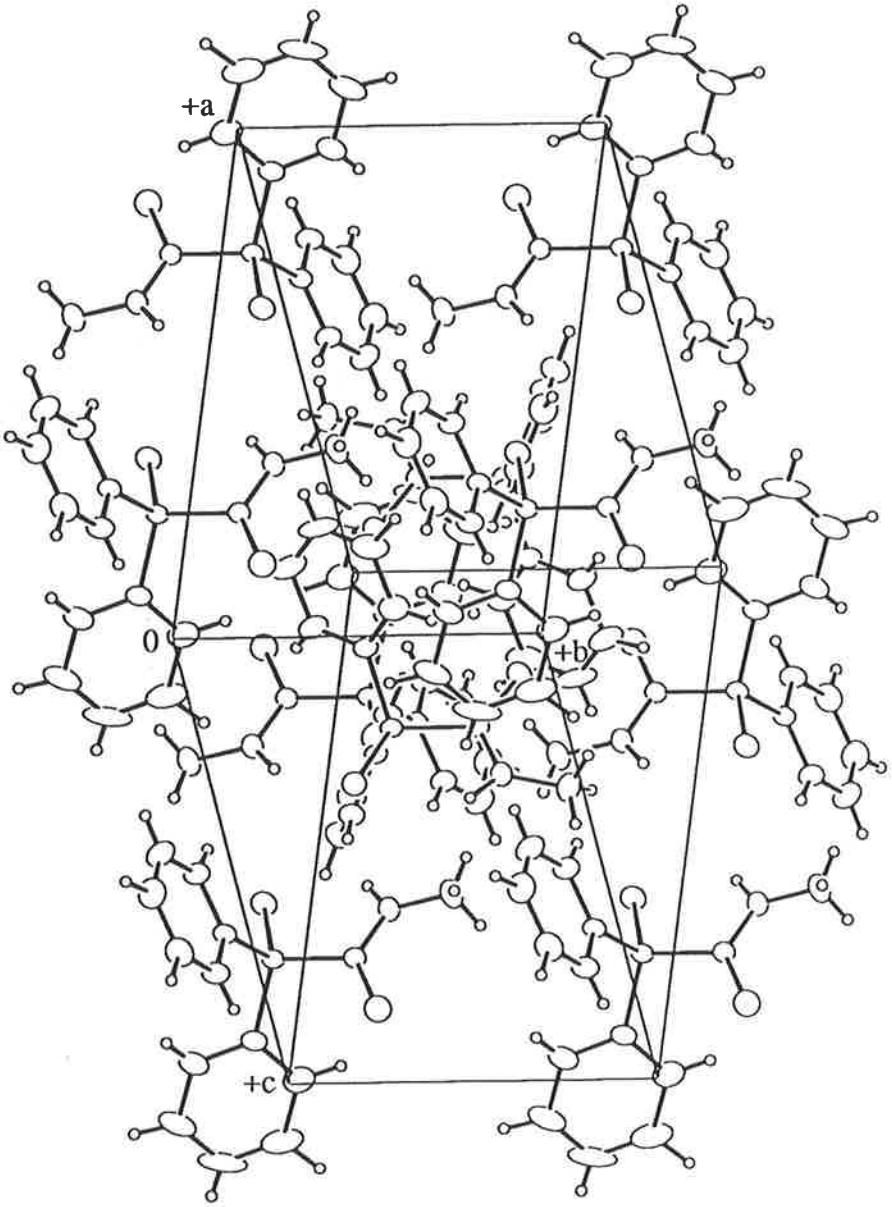

Fig. 3.2.2b The unit cell contents for $[Ph_2P(S)C(S)N(H)Me]$

The molecular structure of [$Cy_2P(S)C(S)N(H)Ph$] is represented in Fig. 3.2.3a ([14]; 30% thermal ellipsoids). The structure is as described for the above compounds except that the central portion of the molecule is more planar. The central S(1), S(2), P(1), N(1) and C(1) atoms lie 0.0264(8), 0.0275(8), -0.0233(7), -0.124(2) and -0.055(2) Å, respectively out of the least-squares plane through these atoms (the C(11) atom lies -1.523(4) Å out of this plane) and the S(2)/P(1)/C(1)/S(1) and S(1)/C(1)/N(1)/C(31) torsion angles are -4.1(2) and -1.0(5)°, respectively. The nitrogen-bound phenyl substituent is almost coplanar with the central chromophore as seen in the C(1)/N(1)/C(31)/C(32) torsion angle of -172.0(3)° and is reflected in the relatively short N(1)-C(31) bond distance of 1.401(3) Å. The P(1)=S(2) bond distance (1.9495(9) Å) lies within experimental error to that found in the related derivatives described above. Notable in this structure is the length of the P(1)-C(1) bond, i.e. 1.846(3) Å, which, thus far, is the longest seen in compounds of this type, i.e. for $Cy_2P(Y)C(S)N(H)R'$, Y = O or S, R' = Ph or Me. There are some interesting variations within the C(=S)N(H)C portion of the molecule between the $Cy_2P(Y)C(S)N(H)R'$, Y = O or S, structures.

The relatively low errors associated with the $Cy_2P(Y)C(S)N(H)R'$ structures enables a determination of the influence of the Y substituent on the central chromophore. In the [$Cy_2P(S)C(S)N(H)Ph$] compound, the C(1)=S(1) 1.624(2) Å, N(1)-C(1) 1.317(3) Å and N(1)-C(31) 1.401(3) Å bond distances are, respectively longer, shorter and shorter than those found in the Y = O analogue. These observations may be rationalised in terms of a comparatively weaker P(1)-C(1) bond in the Y = S compounds. As the bond order of the P(1)-C(1) bond decreases there is a concomitant increase in the C(1)-N(1) and N(1)-C(31) bond orders and a slight decrease in the C=S bond order.

The unit cell of [$Cy_2P(S)C(S)N(H)Ph$] is shown in Fig. 3.2.3b, and is comprised of discrete molecules of the compound. The closest non-hydrogen contact in the lattice is 3.527(2) Å and occurs between centrosymmetrically related S(1) atoms (symmetry operation: 1-x, -y, -z) while the closest hydrogen contact occurs between the S(1) and H(13a)' atoms of 2.93(3) Å (symmetry operation: 1-x, -y, -z).

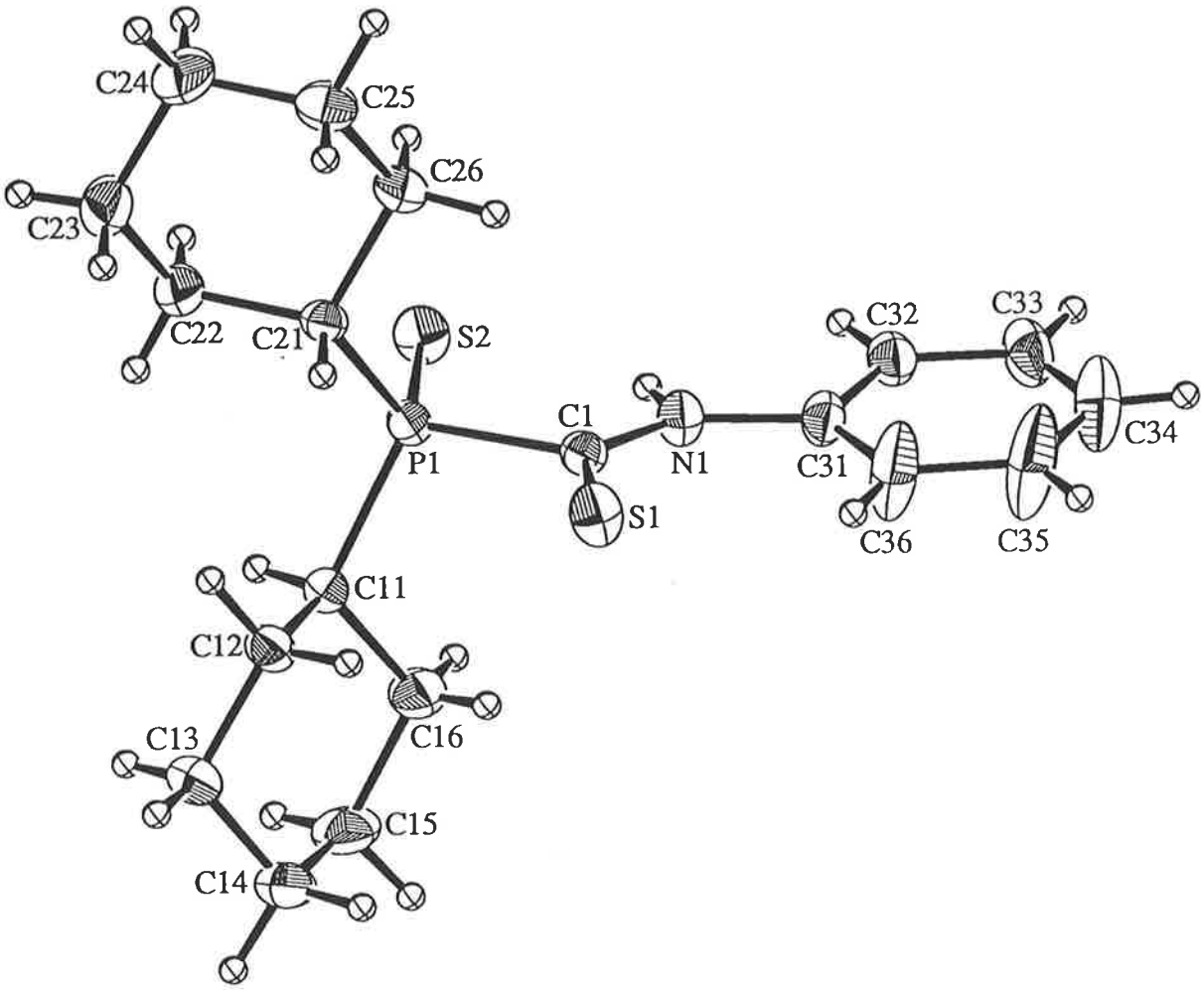

Fig. 3.2.3a The molecular structure of $[Cy_2P(S)C(S)N(H)Ph]$

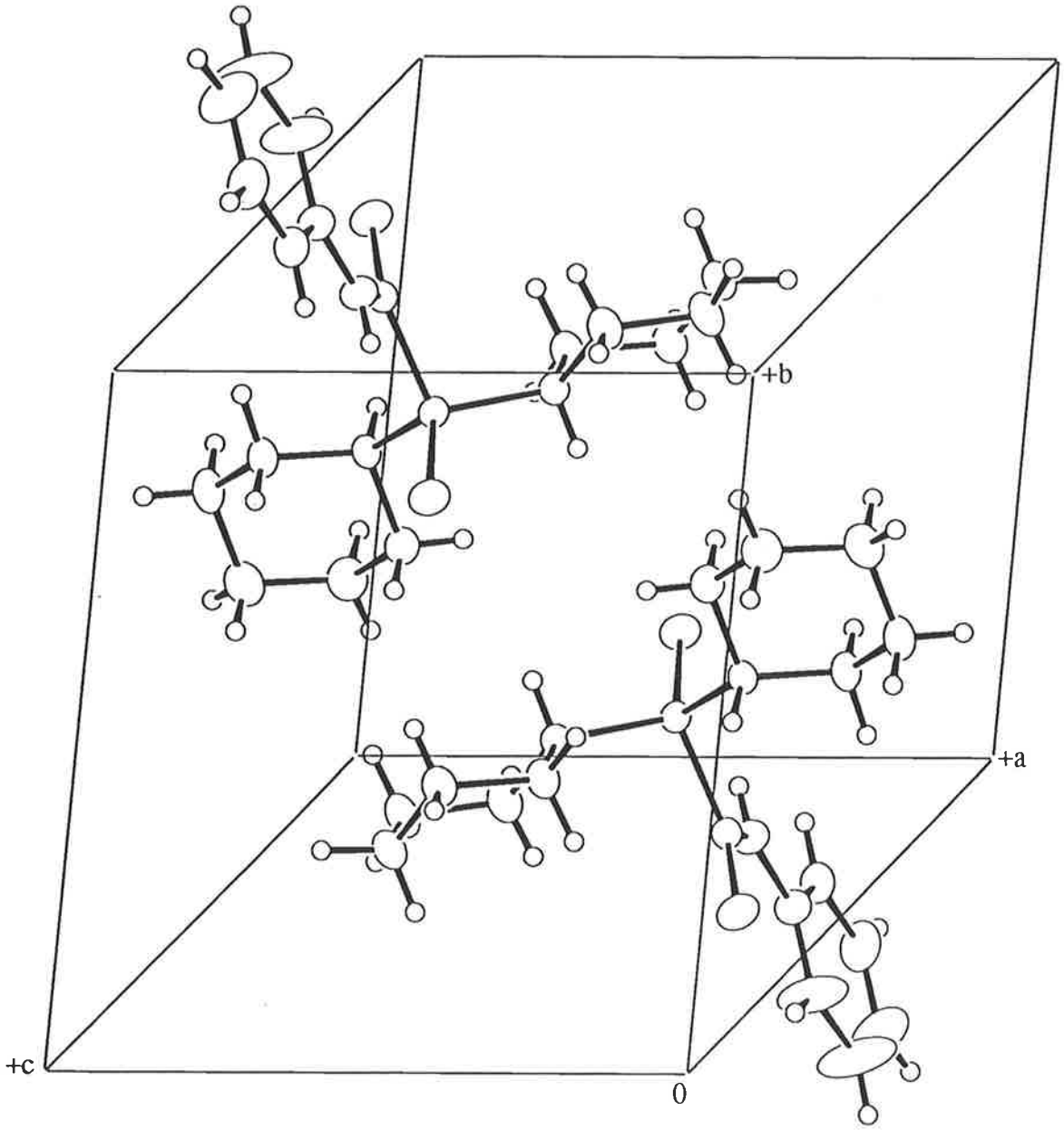

Fig. 3.2.3b The unit cell contents for [$Cy_2P(S)C(S)N(H)Ph$]

3.2.4 The Structure of [$Cy_2P(S)C(S)N(H)Me$]

Yellow crystals of *P, P*-diphenyl-*N*-methyl-thiophosphinylthioformamide, [$Cy_2P(S)C(S)N(H)Me$], were grown from the vapour diffusion of ether into an acetonitrile solution of the compound. Crystals are orthorhombic, space group *Pnma*, with dimensions a = 10.2600(9), b = 15.447(2), c = 10.141(3) Å, V = 1607.3(5) Å^3, Z = 4 and D_x = 1.254 g cm^{-3}. The structure was refined to final R = 0.040, R_w = 0.041 for 1362 reflections with $I \geq 3.0\sigma(I)$.

A molecule of [$Cy_2P(S)C(S)N(H)Me$], depicted in Fig. 3.2.4a ([14]; 30% thermal ellipsoids), is situated about a crystallographic mirror plane located at y = 1/4 with the two cyclohexyl groups related to each other across this plane. The structure is in essential agreement to that found for the Y = S compounds described above except that the central chromophore comprising the S(2), P(1), C(1), S(1) and N(1) atoms is constrained to planarity owing to the crystallographic symmetry. The P(1)=S(2) bond distance of 1.942(1) Å is equal within 5σ to 1.951(2) Å, the P=S distance found in the structure of [$Ph_2P(S)C(S)N(H)Ph$] and 1.951(1) Å found in the closely related [$Cy_2P(S)C(S)SMe$] structure [53]. The P-C(Cy) bond distances are equal within experimental error to those found in the Y = O analogue, however, there is some evidence that the P(1)-C(1) bond distance is slightly longer, i.e. weaker in the Y = S derivative. This elongation is more pronounced for the R' = Ph compound (see above).

The trends associated with the C(=S)N(H)C chromophore described in Section 3.2.3 for the R' = Ph compound are found also in the R' = Me compound. Similarly, the systematic changes in the interatomic parameters found when the nitrogen-bound phenyl substituent is replaced by the methyl group in the Y = O compounds is repeated in the Y = S analogues. A difference between the two Y = S molecules is found in the relative disposition of the cyclohexyl groups in that in the R' = Ph derivative the methine hydrogen atoms lie on opposite sides of the molecule whereas in the R' = Me compound the two methine hydrogen atoms are constrained by the crystallographic mirror symmetry to lie on

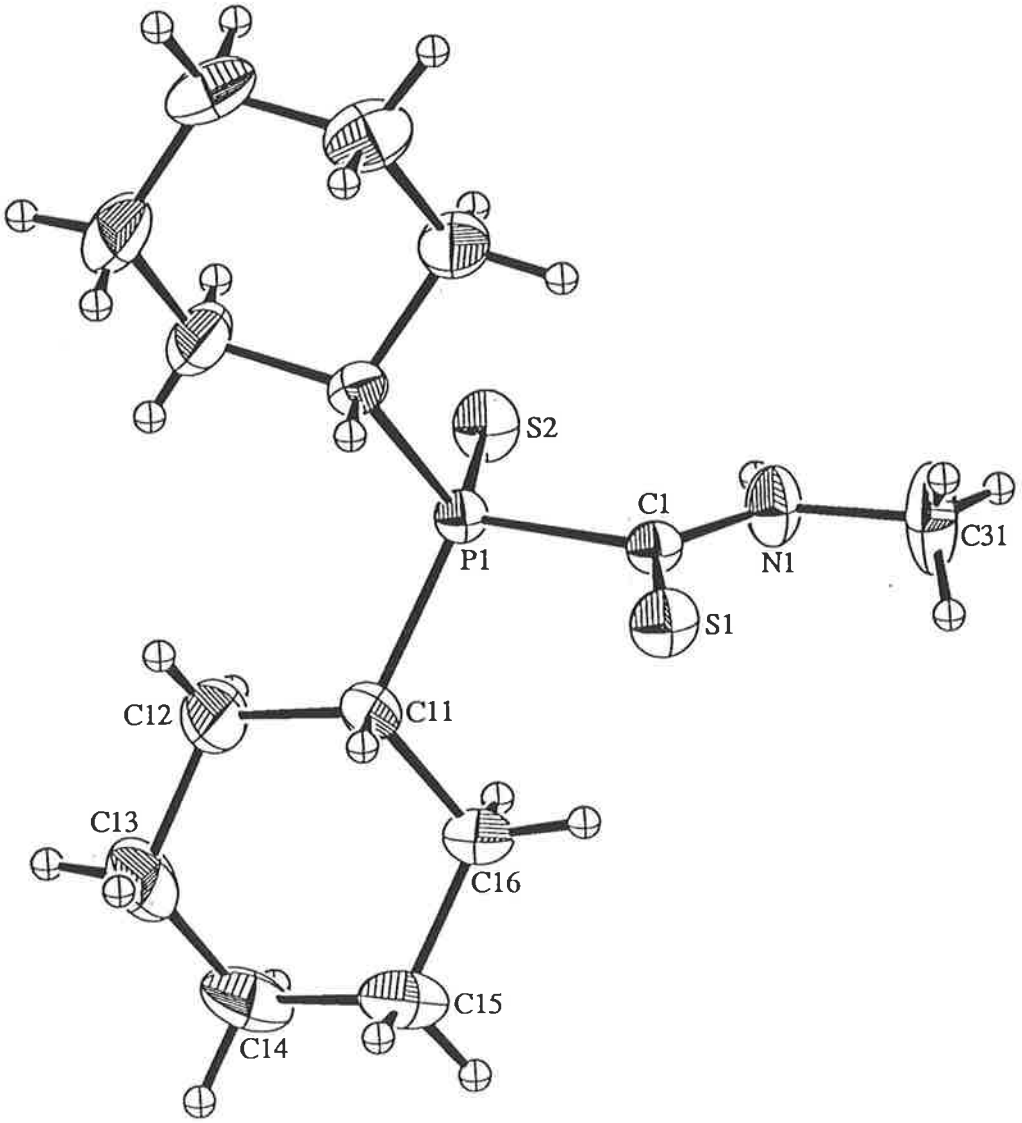

Fig. 3.2.4a The molecular structure of $[Cy_2P(S)C(S)N(H)Me]$

the same side of the molecule. It is noted that the opposite pattern was observed for the analogous Y = O compounds.

The unit cell contents for [$Cy_2P(S)C(S)N(H)Me$] are shown in Fig. 3.2.4b. The lattice is comprised of discrete molecular entities with the closest non-hydrogen contact occurring between the S(2) and C(31)' atoms of 3.495(6) Å (symmetry operation: -0.5+*x*, 0.5-*y*, -0.5-*z*). As was seen above for the R' = Ph analogue the closest hydrogen interaction involved the S(1) atom, the distance of 2.82(5) Å made with a H(31)' atom (symmetry operation: 0.5+*x*, 0.5-*y*, -0.5-*z*) is not considered a significant interaction.

3.3 The Structures of $R_2P(Se)C(S)N(H)R'$

Eight compounds of the type $R_2P(Se)C(S)N(H)R'$ have been structurally characterised for R = Ph or Cy, R' = Ph, Me, Et or Cy. The compounds will be discussed in the following order: R = Ph, R' = Ph (3.3.1), Me (3.3.2), Et (3.3.3) or Cy (3.3.4), and in the same R' order for the R = Cy systems (3.3.5-3.3.8). Consistent with the $R_2P(Y)C(S)N(H)R'$, Y = O or S, systems the conformation about the C(1)-N(1) bond is *Z*. Selected interatomic parameters are listed in Table 3.3. Four of the compounds i.e. $R_2P(Se)C(S)N(H)R'$ R = Ph or Cy, R' = Et or Cy, were supplied by Professor R. Kramolowsky.

3.3.1 The Structure of [$Ph_2P(Se)C(S)N(H)Ph$]

The green crystals of *P, P*-diphenyl-*N*-phenyl-selenophosphinylthioformamide, [$Ph_2P(Se)C(S)N(H)Ph$], were obtained by cooling the mother liquor of the compound from a benzene solution. Crystals are orthorhombic, space group *Pbca* with unit cell dimensions a = 11.978(1), b = 8.772(5), c = 34.241(4) Å, V = 3597(1) Å^3, Z = 8 and D_x = 1.478 g cm^{-3}. The structure was refined to final R = 0.045, R_w = 0.043 for 3167 reflections with $I \geq 3.0\sigma(I)$.

The structure of [$Ph_2P(Se)C(S)N(H)Ph$] is shown in Fig. 3.3.1a ([14]; 15% thermal ellipsoids) and is molecular, there being no significant intermolecular contacts in the crystal lattice. The closest hydrogen contact occurs between S(1) and H(24)' of 3.06(7) Å

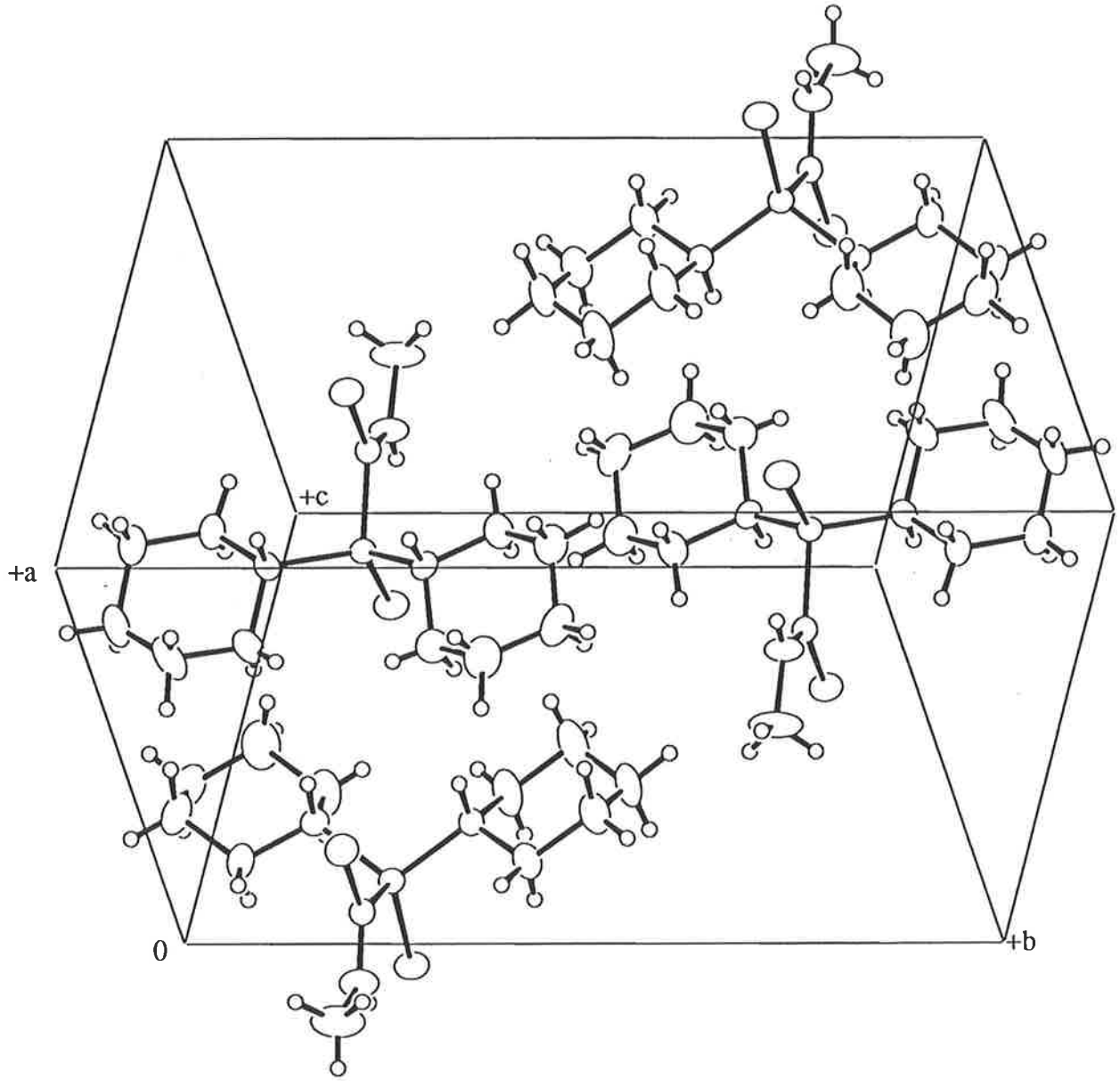

Fig. 3.2.4b The unit cell contents for [$Cy_2P(S)C(S)N(H)Me$]

Table 3.3 Selected bond distances (Å) and angles (deg.) for $R_2P(Se)C(S)N(H)R'$, R = Ph or Cy and R' = Ph, Me, Et or Cy

Parameter	R = Ph R' = Ph	R = Ph R' = Me	R = Ph R' = Et	R = Ph R' = Cy	R = Cy R' = Ph	R = Cy R' = Me	R = Cy R' = Et	R = Cy R' = Cy
P(1)-Se(2)	2.107(2)	2.083(2), 2.088(2)	2.084(1)	2.110(3)	2.098(1)	2.090(1)	2.112(1)	2.117(2)
P(1)-C(1)	1.868(7)	1.834(7), 1.849(8)	1.854(4)	1.84(1)	1.847(4)	1.842(5)	1.859(5)	1.833(8)
P(1)-C(11)	1.804(8)	1.788(7), 1.784(8)	1.782(4)	1.793(9)	1.806(4)	1.807(3)	1.835(5)	1.795(8)
P(1)-C(21)	1.821(7)	1.783(7), 1.776(7)	1.783(4)	1.77(1)	1.815(4)	1.807(3)*	1.836(5)	1.817(7)
C(1)-S(1)	1.632(8)	1.623(7), 1.623(8)	1.623(4)	1.62(1)	1.617(4)	1.627(4)	1.651(5)	1.623(8)
C(1)-N(1)	1.312(9)	1.279(9), 1.28(1)	1.287(5)	1.29(1)	1.322(5)	1.289(6)	1.314(6)	1.31(1)
N(1)-C(31)	1.41(1)	1.46(1), 1.45(1)	1.453(7)	1.48(1)	1.411(5)	1.447(8)	1.466(7)	1.51(1)
Se(2)-P(1)-C(1)	110.6(3)	111.5(2), 110.8(3)	111.7(1)	112.8(3)	110.8(1)	111.0(2)	111.7(2)	109.8(3)
Se(2)-P(1)-C(11)	114.6(3)	114.3(3), 114.8(3)	113.4(1)	111.9(3)	113.9(1)	114.0(1)	114.4(2)	113.6(3)
Se(2)-P(1)-C(21)	112.8(3)	114.3(2), 112.2(2)	113.9(2)	114.5(4)	111.6(1)	114.0(1)*	113.4(2)	110.9(3)
C(1)-P(1)-C(11)	105.0(3)	103.7(3), 107.4(4)	104.8(2)	105.2(4)	104.5(2)	103.4(1)	101.6(2)	106.5(4)
C(1)-P(1)-C(21)	106.4(3)	105.5(3), 105.1(4)	104.3(2)	106.1(5)	106.5(2)	103.4(1)*	103.3(2)	106.5(3)
C(11)-P(1)-C(21)	106.8(4)	106.7(3), 105.9(4)	108.0(2)	105.7(4)	109.2(2)	110.0(2)	111.4(2)	109.4(4)
S(1)-C(1)-P(1)	120.0(5)	121.2(4), 120.1(5)	120.4(3)	120.6(6)	118.4(2)	119.5(3)	120.1(3)	117.8(5)
S(1)-C(1)-N(1)	128.4(6)	125.2(6), 126.0(7)	125.9(4)	127.1(8)	130.2(3)	126.5(4)	126.1(4)	130.3(7)
P(1)-C(1)-N(1)	111.6(6)	113.6(6), 113.9(6)	113.7(3)	112.1(8)	111.4(3)	114.0(3)	113.8(4)	111.9(6)
C(1)-N(1)-C(31)	133.7(8)	125(1), 127(1)	124.2(5)	128(1)	131.6(4)	124.6(5)	125.1(5)	122.7(7)

* the C(21) atom is related across a crystallographic mirror plane

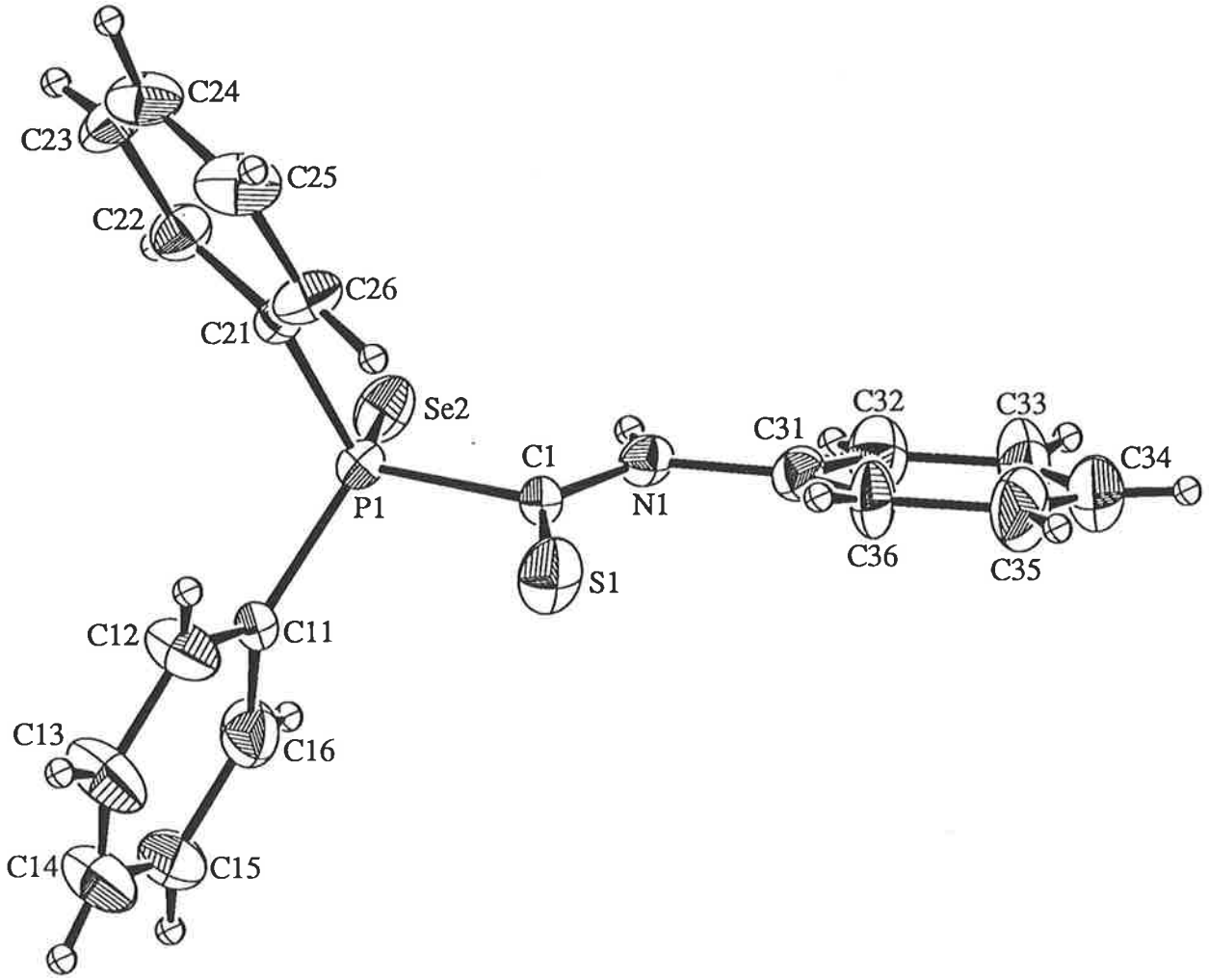

Fig. 3.3.1a The molecular structure of $[Ph_2P(Se)C(S)N(H)Ph]$

(symmetry operation: $+x$, $1+y$, $+z$), the closest non-hydrogen contact is 3.56(1) Å and occurs between the C(21) and C(32)' atoms (symmetry operation: $0.5-x$, $-0.5+y$, $+z$); the unit cell diagram appears in Fig. 3.3.1b. The structure determination of $[Ph_2P(Se)C(S)N(H)Ph]$ completes the series of compounds with the general formula $[Ph_2P(Y)C(S)N(H)Ph]$ where Y = 0 [15], Y = O (Section 3.1.1), Y = S (Section 3.2.1) and Y = Se. The atoms defining the P(Se)C(S)N chromophore deviate significantly from coplanarity, i.e. -0.069(2), 0.012(1), -0.116(7), 0.111(3) and -0.334(6) Å for the P(1), Se(2), C(1), S(1) and N(1) atoms, respectively, suggesting little conjugation over this moiety; the two torsion angles Se(2)/P(1)/C(1)/S(1) and Se(2)/P(1)/C(1)/N(1) are 168.1(4) and -11.5(6)°, respectively and emphasise the lack of coplanarity. The phenyl rings, C(11)-C(16), C(21)-C(26) and C(31)-C(36), form dihedral angles of 102.5, 125.9 and 173.5°, respectively with the least-squares plane through the P(Se)C(S)N atoms. The angles around P(1) range from 105.0(3) to 114.6(3)° and are very similar to those found for $[Ph_2P(S)C(S)N(H)Ph]$ as are the angles about the C(1) atom, 111.6(6)-128.4(6)°. These are different to those found in $[Ph_2P(O)C(S)N(H)Ph]$ for the reasons as discussed in Section 3.2.1.

The P(1)=Se(2) bond distance of 2.107(2) Å is experimentally equivalent to the distances of 2.106(1) Å found in the structure of $[Ph_3PSe]$ [54] and 2.103(1) Å found in $[Ph_2P(Se)CH_2PPh_2]$ [55]. Particular interest in this structure determination focuses on the parameters associated with the PC(S)N atoms where, despite the relatively high errors associated with these parameters, general conclusions may be made.

The P(1)-C(1), C(1)-S(1) and C(1)-N(1) separations of 1.868(7), 1.632(8) and 1.312(9) Å are longer, shorter and shorter, respectively than the comparable bond distances in the phosphorus(III) 'parent' acid $[Ph_2PC(S)N(H)Ph]$ [15], i.e. 1.862(3), 1.650(3) and 1.334(3) Å, respectively. These trends follow closely those observed previously for the $[Ph_2P(Y)C(S)N(H)Ph]$ compounds, Y = O (Section 3.1.1) or S (Section 3.2.1) which were interpreted as indicating the presence of comparatively weak P(1)-C(1) bonds.

The P(1)-C(1) bond distances for the $[Ph_2P(Y)C(S)N(H)Ph]$ Y = O, S or Se compounds are 1.852(4), 1.855(5) and 1.868(7) Å, respectively. Comparison of other

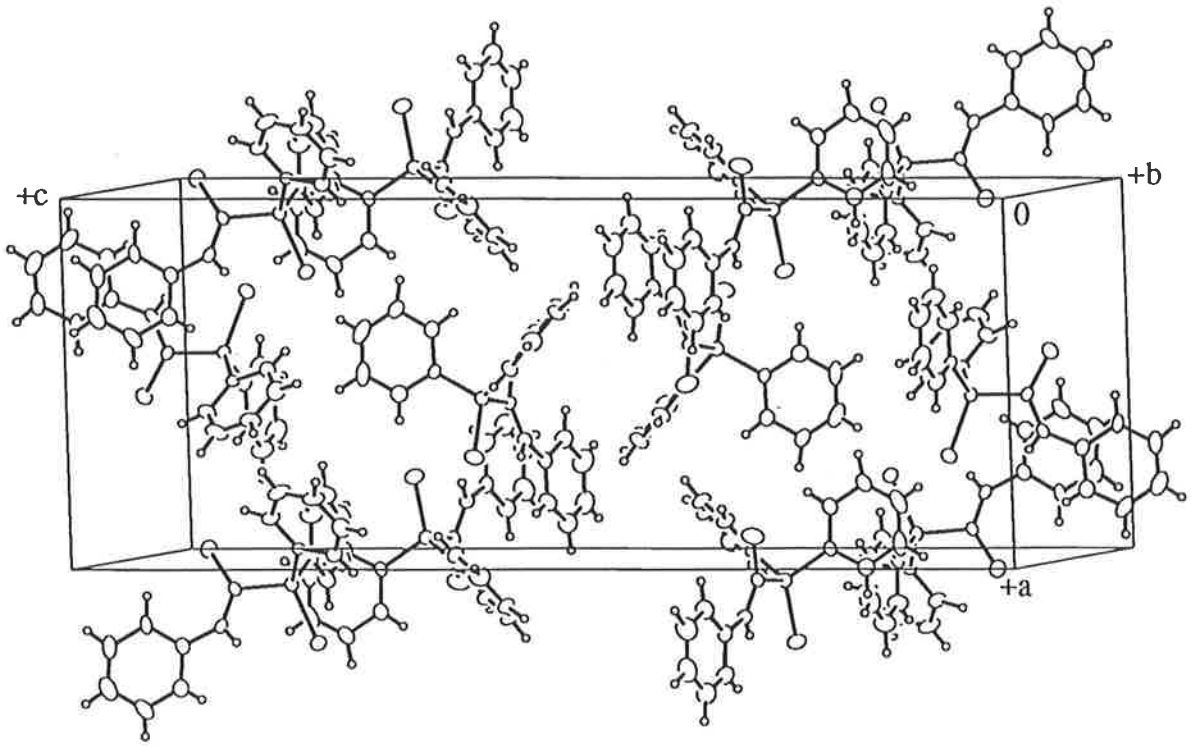

Fig. 3.3.1b The unit cell contents for $[Ph_2P(Se)C(S)N(H)Ph]$

parameters between the Y = S and Se derivatives reveals a close coincidence in the values of bond distances and angles in these two isomorphous compounds.

3.3.2 The Structure of [$Ph_2P(Se)C(S)N(H)Me$]

The green crystals of *P, P*-diphenyl-*N*-methyl-selenophosphinylthioformamide, [$Ph_2P(Se)C(S)N(H)Me$], were obtained from the evaporation of an ethyl acetate solution layered with petroleum spirit (40/60°C). Crystals are triclinic, space group $P\bar{1}$ with unit cell dimensions a = 12.511(3), b = 13.298(3), c = 10.178(3) Å, α = 109.28(2), β = 103.25(2), γ = 66.94(2)°, V = 1460.8(7) $Å^3$, Z = 4 and D_x = 1.538 g cm^{-3}. The structure was refined to final R = 0.038, R_w = 0.033 for 2097 reflections with $I \geq 3.0\sigma(I)$.

Two independent molecules of [$Ph_2P(Se)C(S)N(H)Me$], labeled *a* and *b*, comprise the asymmetric unit and are shown in Figs 3.3.2a and 3.3.2b ([14]; 30% thermal ellipsoids). The closest intermolecular contact occurs between the selenium atom and a symmetry related H(25) atom such that Se(2a)-H(25b)' is 2.94(7) Å (symmetry operation: 1-x, 1-y, 1-z) and Se(2b)-H(25a)' is 2.8(1) Å (symmetry operation: -x, 1-y, -z). These short distances are within the sum of the van der Waals radii for these atoms of 3.10 Å [21]. A similar close Se...H interaction was reported recently in diselenocin for the chair (Fig. 3.3.2c) and boat forms of the compound with intermolecular selenium "hydrogen bonds" of 2.92 and 2.86 Å [56]. The angles of 147(6) and 174(6)° for C(25a, b)-H(25a, b)...Se(2b, a) are wider than those reported for diselenocin which were 101.7° (chair form) and 107.0° (boat form). The closest non-hydrogen contact in the unit cell is 3.48(1) Å for the S(1a) and C(13a)' atoms (symmetry operation: -x, 2-y, -z). The unit cell contents are shown in Fig. 3.3.2d.

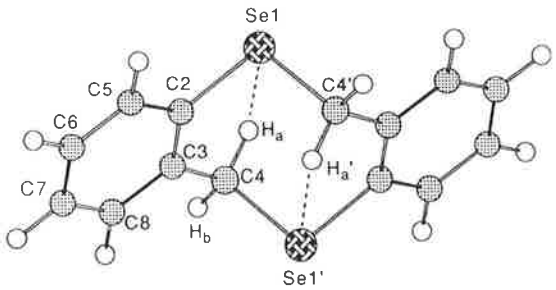

Fig. 3.3.2c The molecular structure of chair diselenocin

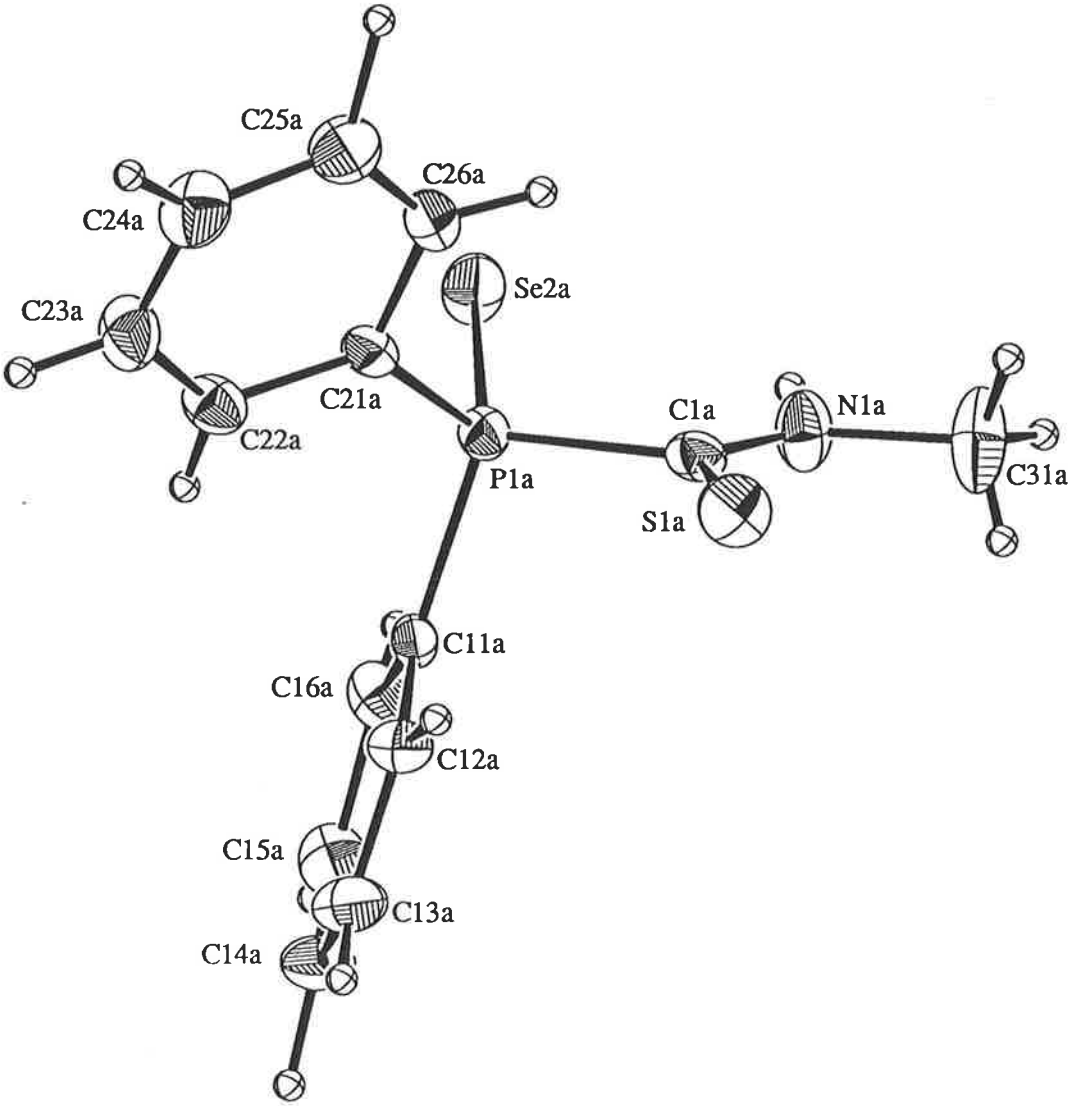

Fig. 3.3.2a The molecular structure of molecule *a* of $[Ph_2P(Se)C(S)N(H)Me]$

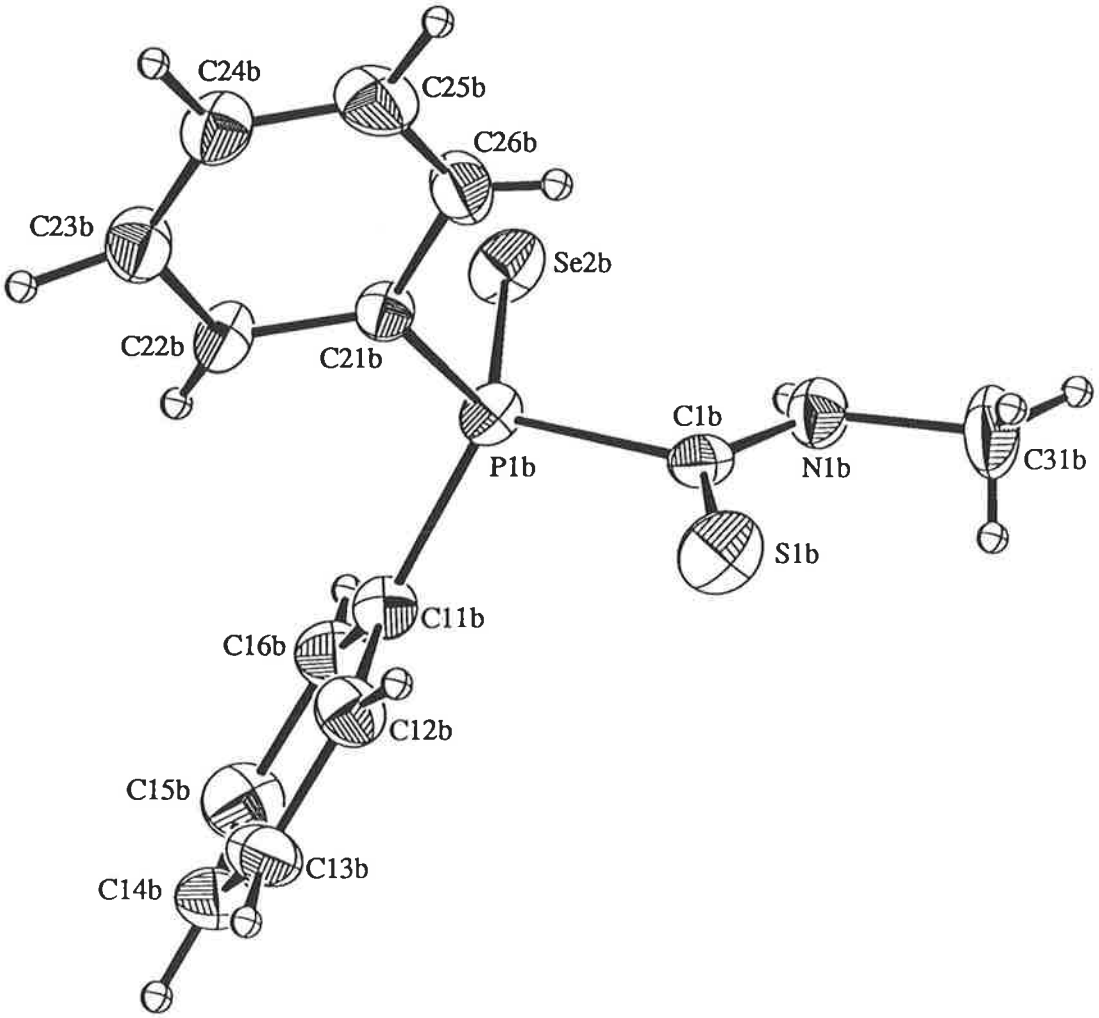

Fig. 3.3.2b The molecular structure of molecule *b* of $[Ph_2P(Se)C(S)N(H)Me]$

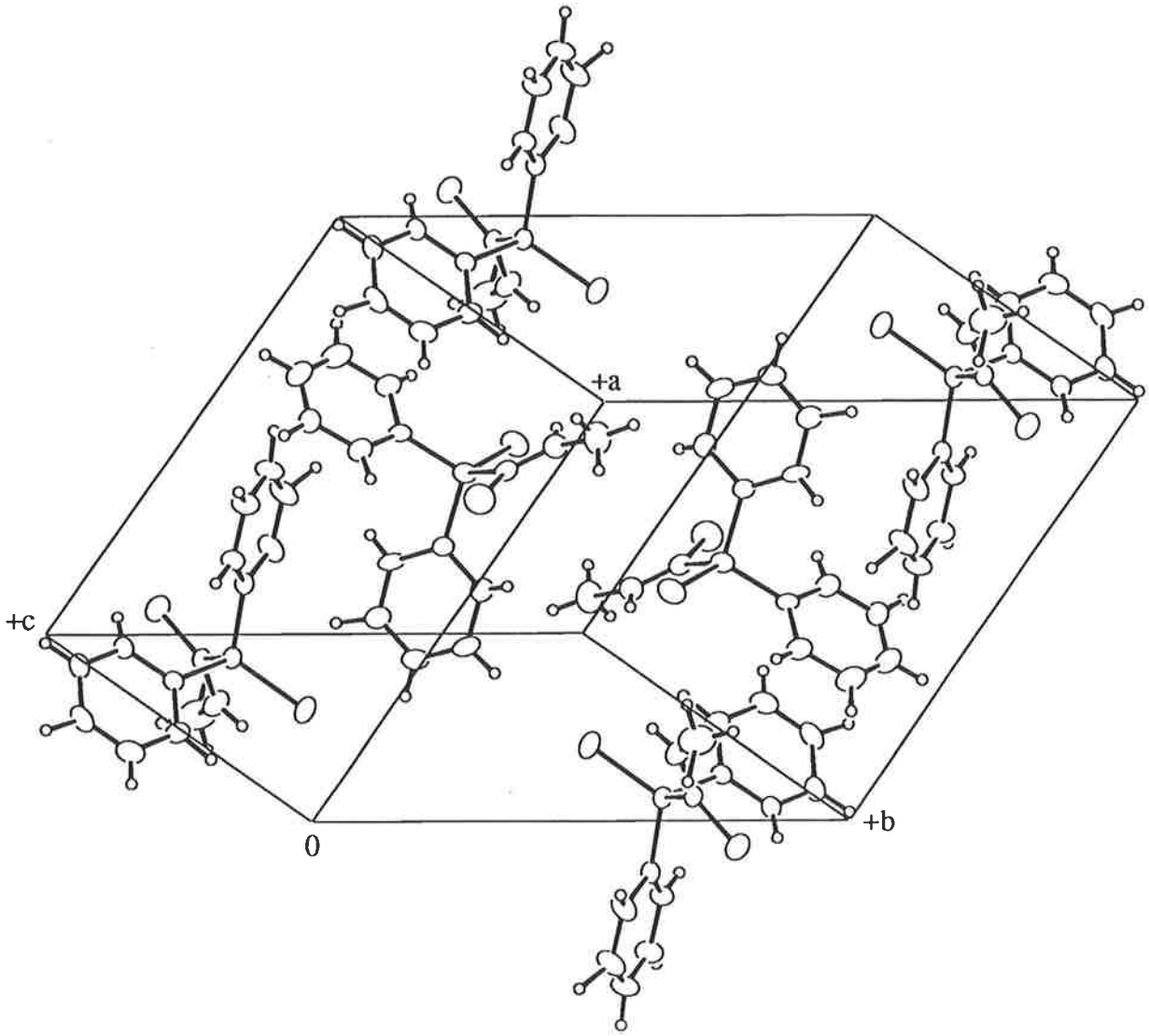

Fig. 3.3.2d The unit cell contents for [$Ph_2P(Se)C(S)N(H)Me$]

The parameters observed for the two molecules, *a* and *b*, are equal within experimental error given that there are relatively large errors associated with these parameters. The central SePC(1)SN moiety deviates from planarity with a mean deviation from the plane of 0.235 Å for molecule *a* and 0.010 Å for molecule *b*. The two torsion angles Se(2)/P(1)/C(1)/S(1) and Se(2)/P(1)/C(1)/N(1) of 160.5(3) *a*, 171.5(4) *b* and -21.7(7) *a*, -7.5(7)° *b*, respectively reflect this distortion. The phenyl rings C(11)-C(16) and C(21)-C(26) make dihedral angles of 62.39 and 73.66° for molecule *a* and 56.33 and 78.63° for molecule *b*, respectively with the central SePC(1)SN chromophore. It can be seen from these parameters that the central chromophore in molecule *b* is slightly more planar than the corresponding atoms in molecule *a* and that there are only minor conformational differences between the two molecules that comprise the asymmetric unit.

The P(1)=Se(2) distances of 2.083(2) and 2.088(2) Å for molecule *a* and *b*, respectively are marginally shorter to the distance found for the R' = Ph derivative of 2.107(2) Å. The C(1)=S(1) bond distances of 1.623(7) and 1.623(8) Å, respectively are comparable to 1.632(8) Å found in [Ph_2P(Se)C(S)N(H)Ph]. The C(1)-N(1) and N(1)-C(31) bond distances are shorter and longer, respectively than those in the R' = Ph derivative, i.e. 1.279(9) and 1.28(1), 1.46(1) and 1.45(1) compared to 1.312(9) and 1.41(1) Å, respectively. The biggest difference, however, is found for the P(1)-C(1) bond length which at 1.868(7) Å in [Ph_2P(Se)C(S)N(H)Ph] is longer than 1.834(7) and 1.849(8) Å found in the two molecules of [Ph_2P(Se)C(S)N(H)Me]. The most notable difference in the angles between the R' = Me and Ph compounds is found in the C(1)-N(1)-C(31) angle which is approximately 7° greater in the R' = Ph analogue owing to the additional steric pressure exerted by the phenyl group compared with the less bulky methyl substituent.

The comparison of selected parameters for [Ph_2P(Se)C(S)N(H)Me] with those of the parent compound [Ph_2PC(S)N(H)Me] [25], which also had two molecules in the asymmetric unit, showed that the C(1)-S(1), C(1)-N(1) and N(1)-C(31) bond distances are shorter, shorter and equivalent, respectively on going from the phosphorus(III) to the phosphorus(V) compound. The P(1)-C(1) distances, 1.834(7) Å for molecule *a* and 1.849(8) Å for molecule *b* in [Ph_2P(Se)C(S)N(H)Me] are equal within experimental error to

the average distance of 1.849(4) Å in the parent molecule, whereas the P-C(Ph) distances have contracted by approximately 0.03 Å in the [$Ph_2P(Se)C(S)N(H)Me$] compound as expected. These data further support the earlier conclusion which stated that the P(1)-C(1) bond distance is relatively weak in the phosphorus(V) derivatives.

3.3.3 The Structure of [$Ph_2P(Se)C(S)N(H)Et$]

The yellow crystals of *P, P*-diphenyl-*N*-ethyl-selenophosphinylthioformamide, [$Ph_2P(Se)C(S)N(H)Et$], were grown from the diffusion of petroleum spirit (40/60°) into an acetone solution of the compound. Crystals are monoclinic, space group $P2_1/c$ with unit cell dimensions a = 11.944(3), b = 8.999(7), c = 14.882(3) Å, β = 100.71(2), V = 1571(1) Å^3, Z = 4 and D_x = 1.489 g cm^{-3}. The structure was refined to final R = 0.036, R_w = 0.034 for 1761 reflections with $I \geq 3.0\sigma(I)$.

The molecular structure of [$Ph_2P(Se)C(S)N(H)Et$] is depicted in Fig. 3.3.3a ([14]; 30% thermal ellipsoids). The atoms that comprise the central chromophore, SePC(1)SN, lie 0.001(1), -0.004(1), -0.017(4), 0.007(2) and -0.027(5) Å, respectively out of the least-squares plane through these atoms. The planarity is reflected in the torsion angles for Se(2)/P(1)/C(1)/S(1) of 178.8(6)° and Se(2)/P(1)/C(1)/N(1) of -0.3(4)°. The dihedral angles of the phenyl rings with the central chromophore are approximately equal at 72.9 and 72.5° for the C(11)-C(16) and C(21)-C(26) rings, respectively.

The P(1)=Se(2) distance of 2.084(1) Å is identical to that found for the R' = Me compound described above as are the S(1)=C(1), P(1)-C(1), C(1)-N(1) and N(1)-C(31) distances. Further, the angles are similar in both structures and will not be discussed in detail. The derived parameters for [$Ph_2P(Se)C(S)N(H)Et$] suggest that the substitution of the methyl substituent for an ethyl group has little discernible effect on the central Se(2)P(1)C(1)S(1)N(1) chromophore.

The unit cell contents are shown in Fig. 3.3.3b. The closest non-hydrogen contact was between the C(23) and C(23)' atoms of 3.39(1) Å (symmetry operation: 2-x, -y, 1-z) and the closest contact involving a hydrogen atom occurs between Se(2) and H(26)' of 3.07(4) Å (symmetry operation: 1-x, -y, 1-z).

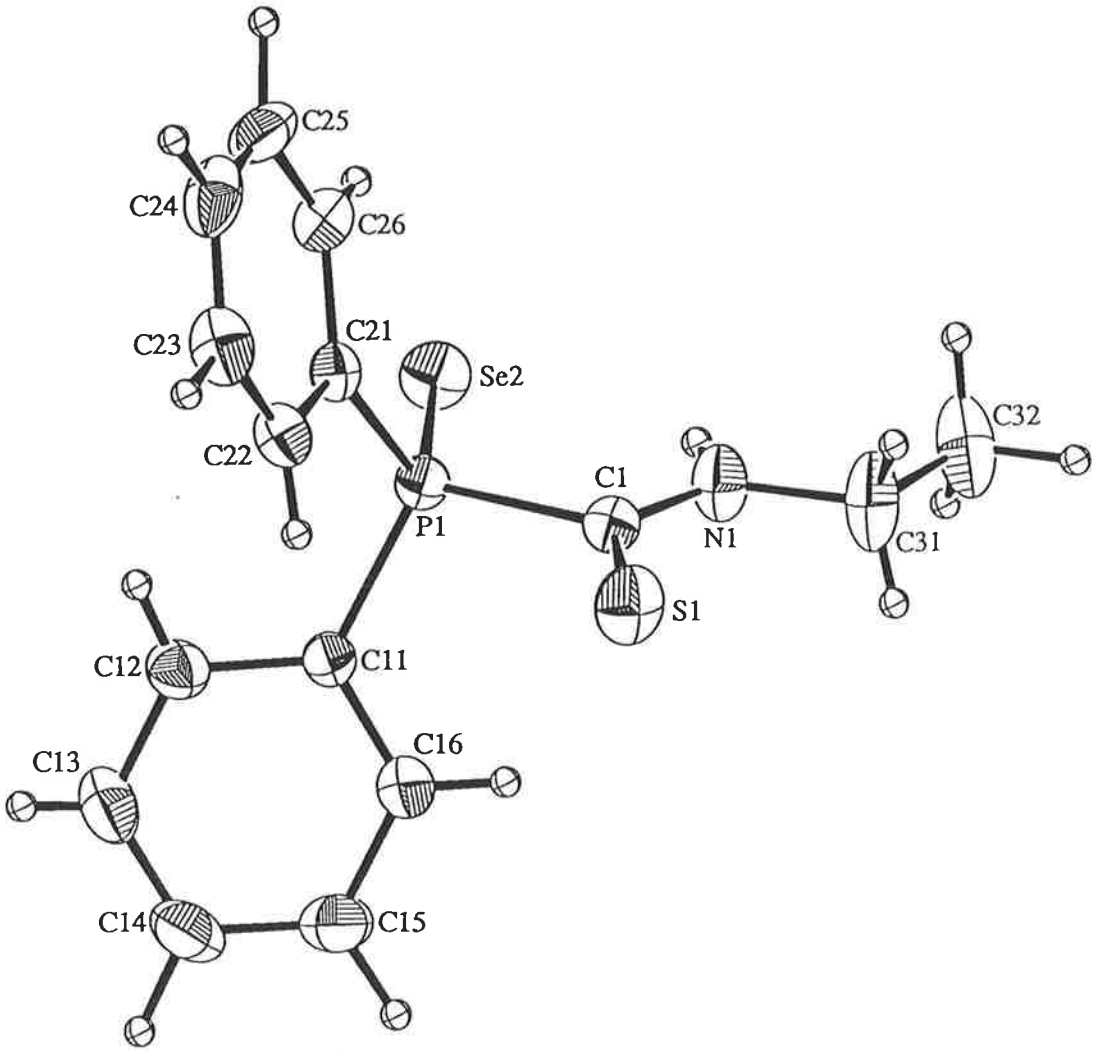

Fig. 3.3.3a The molecular structure of $[Ph_2P(Se)C(S)N(H)Et]$

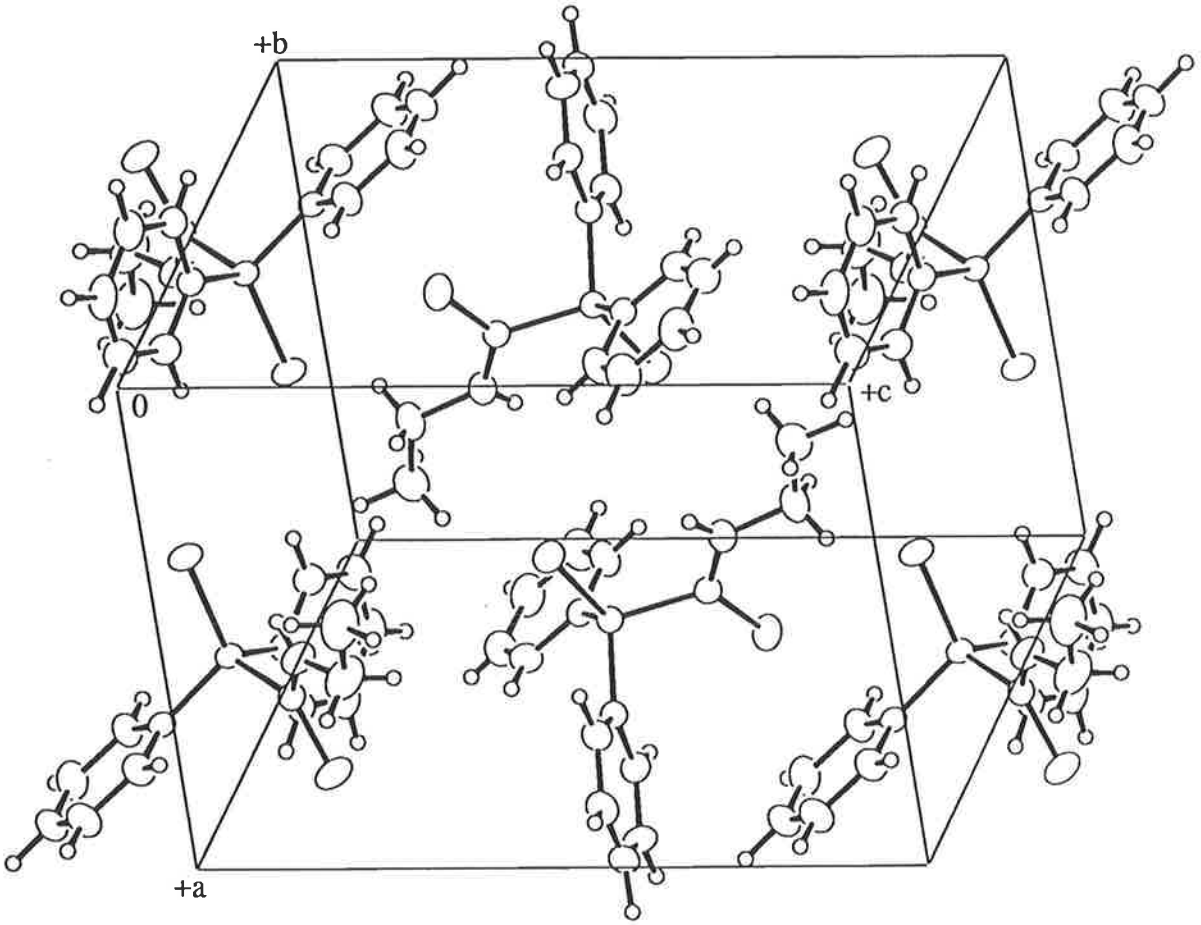

Fig. 3.3.3b The unit cell contents for [$Ph_2P(Se)C(S)N(H)Et$]

3.3.4 The Structure of [$Ph_2P(Se)C(S)N(H)Cy$]

Bright green crystals of *P, P*-diphenyl-*N*-cyclohexyl-selenophosphinylthioformamide, [$Ph_2P(Se)C(S)N(H)Cy$], were obtained from the diffusion of petroleum spirit (40/60°) into an acetone solution of the compound. Crystals are triclinic, space group $P\bar{1}$ with unit cell dimensions a = 8.638(4), b = 8.764(2), c = 7.488(2) Å, α = 114.72(1), β = 113.03(2), γ = 88.78(3)°, V = 467.0(3) Å^3, Z = 1 and D_x = 1.445 g cm^{-3}. The structure (preferred hand) was refined to final R = 0.046, R_w = 0.054 for 1411 reflections with $I \geq 3.0\sigma(I)$.

The molecular structure of the compound is represented in Fig. 3.3.4a ([14]; 30% thermal ellipsoids). The central chromophore deviates significantly from coplanarity with the mean deviation of the atoms being 0.137 Å. The phosphorus-bound phenyl rings form dihedral angles of 77.1 and 62.8° with the central plane. The P(1)=Se(2) distance of 2.110(3) Å is identical to the equivalent separation found for [$Ph_2P(Se)C(S)N(H)Ph$] (2.107(2) Å) whereas the P(1)-C(1) distance (1.84(1) Å) appears to be shorter (1.868(7) Å). A notable difference is the length of 1.48(1) Å for the N(1)-C(31) bond which is by far the longest found in the Y = Se derivatives.

No significant interactions were found in the lattice, the shortest distance involving a hydrogen atom was 2.88(1) Å which occurs between the S(1) and H(13)' atoms (symmetry operation: 1+x, +y, +z) and the closest non-hydrogen contact of 3.58(2) Å occurs between the C(14) and C(34)' atoms (symmetry operation: -1+x, -1+y, -1+z); the unit cell contents are shown in Fig. 3.3.4b.

3.3.5 The Structure of [$Cy_2P(Se)C(S)N(H)Ph$]

The yellow crystals of *P, P*-dicyclohexyl-*N*-phenyl-selenophosphinylthioformamide, [$Cy_2P(Se)C(S)N(H)Ph$], were obtained from the vapour diffusion of diethyl ether into a chloroform solution of the compound. Crystals are triclinic, space group $P\bar{1}$ with unit cell dimensions a = 9.738(2), b = 11.248(2), c = 9.406(1) Å, α = 100.72(1), β = 104.84(1), γ = 83.58(1)°, V = 976.3(3) Å^3, Z = 2 and D_x = 1.403 g cm^{-3}. The structure was refined to final R = 0.033, R_w = 0.037 for 2508 reflections with $I \geq 3.0\sigma(I)$.

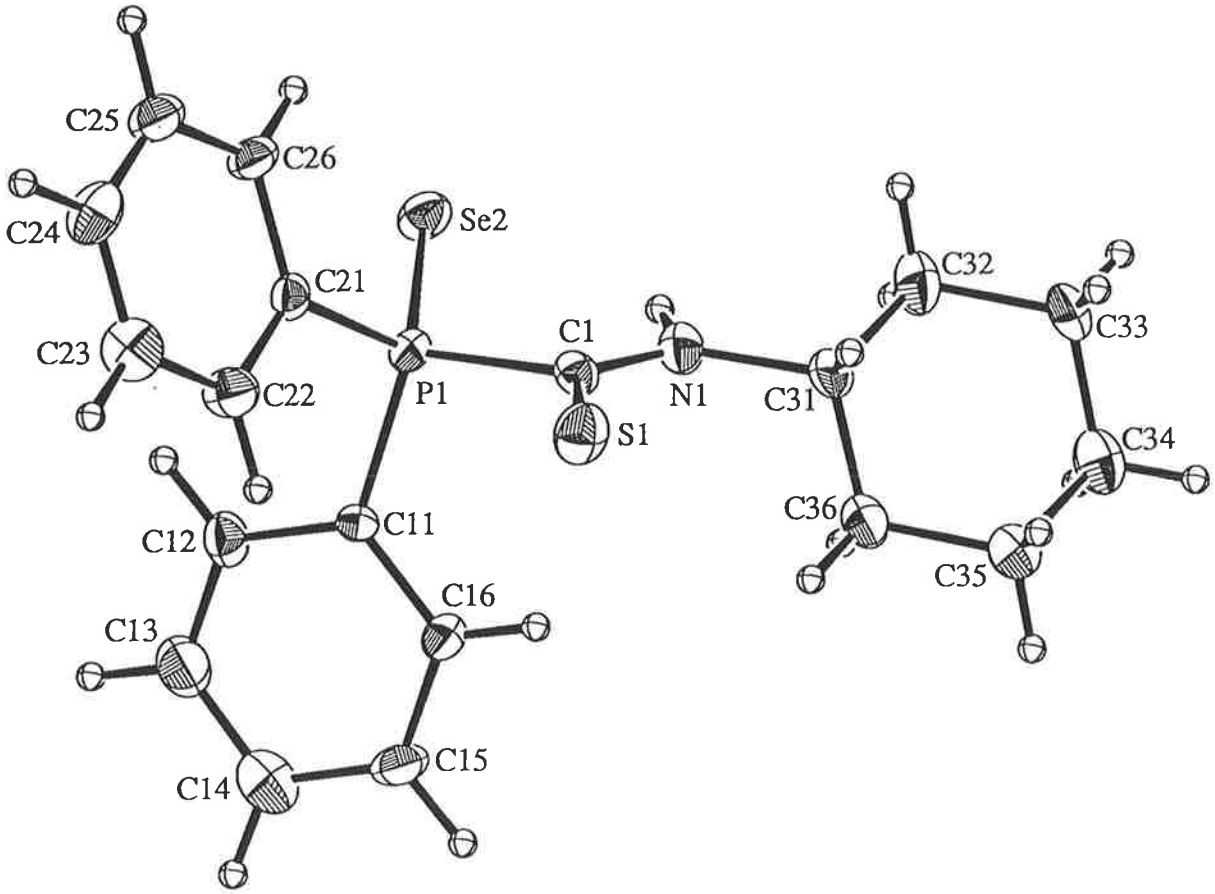

Fig. 3.3.4a The molecular structure of $[Ph_2P(Se)C(S)N(H)Cy]$

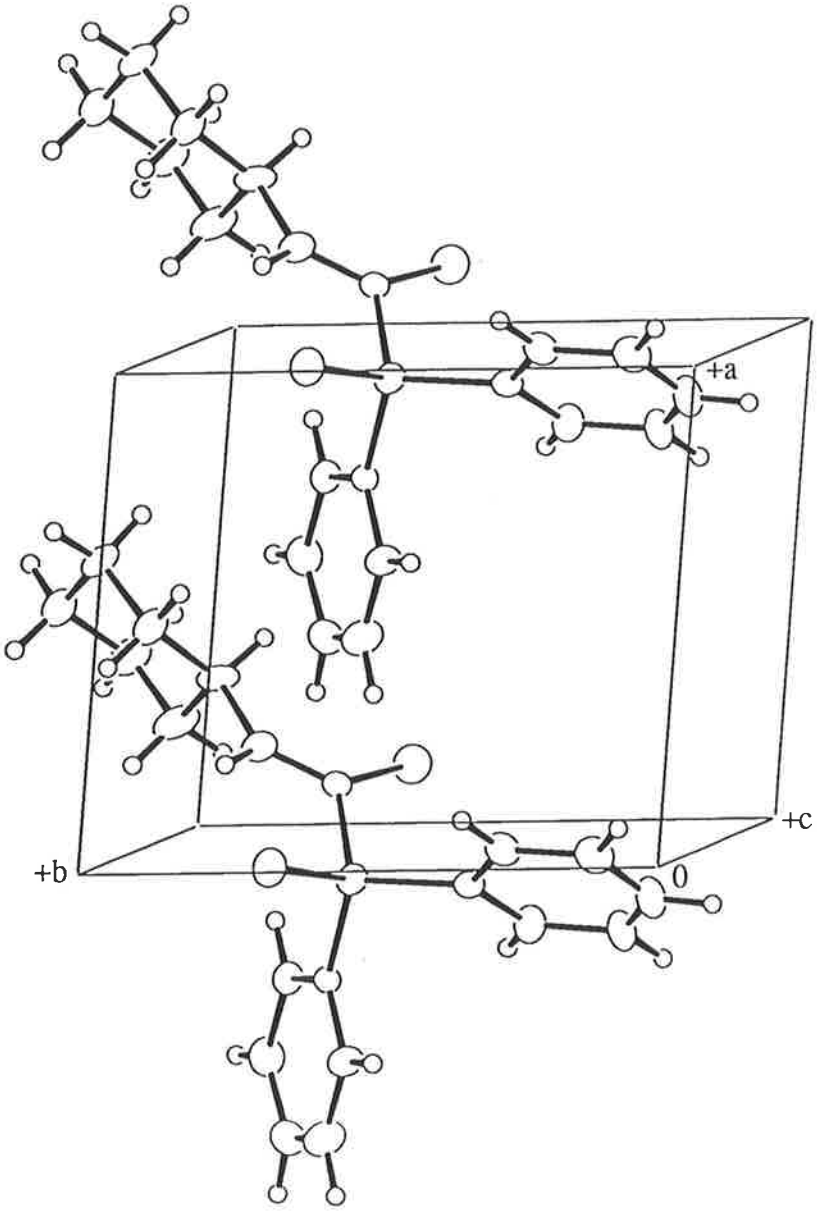

Fig. 3.3.4b The unit cell contents for [$Ph_2P(Se)C(S)N(H)Cy$]

The molecular structure of [$Cy_2P(Se)C(S)N(H)Ph$] is depicted in Fig. 3.3.5a ([14]; 30% thermal ellipsoids). The deviations of the atoms from the least-squares plane through the central SePC(1)SN moiety are -0.007(1), -0.039(1), 0.029(1), 0.160(4) and 0.063(4) Å, respectively and is indicative of a non-planar grouping. The torsion angles Se(2)/P(1)/C(1)/S(1) -174.7(2)° and Se(2)/P(1)/C(1)/N(1) 4.8(3)° provide additional evidence for the lack of planarity of the central chromophore. The nitrogen-bound phenyl group forms a dihedral angle of 4.1° with the central chromophore.

The P(1)=Se(2) separation of 2.098(1) Å is similar to the equivalent values found for the related Y = Se derivatives mentioned above. All the bond distances and angles associated with the P, C(1), S and N atoms are equal within experimental error to those parameters found in [$Ph_2P(Se)C(S)N(H)Ph$] except for the P(1)-C(1) distance. The P(1)-C(1) separation of 1.847(4) Å is 0.021 Å shorter in [$Cy_2P(Se)C(S)N(H)Ph$] and therefore this bond is stronger in this compound compared to [$Ph_2P(Se)C(S)N(H)Ph$] (1.868(7) Å). The P(1)-C(1) distance has contracted approximately 0.02 Å from the equivalent distance in the parent compound, [$Cy_2PC(S)N(H)Ph$] [15], which has an average value of 1.868(5) Å for the two independent molecules comprising the asymmetric unit. By contrast, the contraction of the P-C(Cy) distances was approximately 0.04 Å; clearly a uniform contraction is not observed. The angle subtended by the two cyclohexyl groups at phosphorus, C(11)-P(1)-C(21), is approximately 2.5° larger in the [$Cy_2P(Se)C(S)N(H)Ph$] compound, 109.2(2)°, as compared with the analogous angle in [$Ph_2P(Se)C(S)N(H)Ph$] of 106.8(4)°. The reason for this difference can be attributed to the presence of the bulky cyclohexyl rings in [$Cy_2P(Se)C(S)N(H)Ph$].

The [$Cy_2P(Se)C(S)N(H)Ph$] crystals are isomorphous with [$Cy_2P(S)C(S)N(H)Ph$]. Except for the obvious difference in the P=Y bond lengths, the other comparable parameters are virtually identical in the two structures. The methine hydrogen atoms of the cyclohexyl groups are on opposite sides of the molecule. In the lattice, the closest non-hydrogen contact occurs between centrosymmetrically related sulfur atoms of 3.504(3) Å (symmetry operation: 1-x, 1-y, 1-z), as was the case for the Y = S derivative. The S(1) and H(23a)'

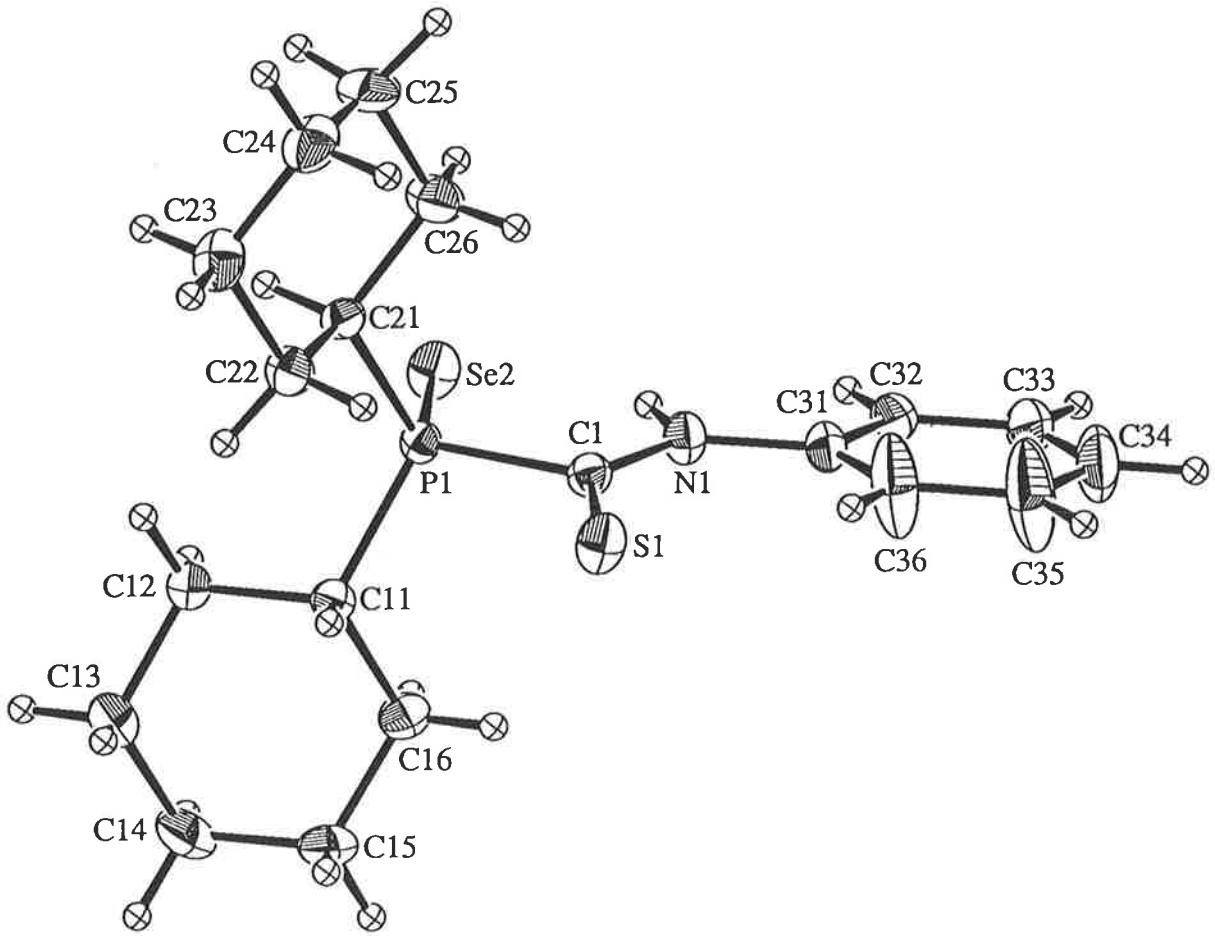

Fig. 3.3.5a The molecular structure of $[Cy_2P(Se)C(S)N(H)Ph]$

separation of 2.925 Å (symmetry operation: 1-x, 1-y, +z) was the closest contact involving a hydrogen atom; the unit cell contents are shown in Fig. 3.3.5b.

3.3.6 The Structure of [Cy_2P(Se)C(S)N(H)Me]

Yellow crystals of *P, P*-dicyclohexyl-*N*-methyl-selenophosphinylthioformamide, [Cy_2P(Se)C(S)N(H)Me], were obtained from the slow evaporation of a dichloromethane solution of the compound. Crystals are orthorhombic, space group *Pnma*, with dimensions a = 10.299(2), b = 15.384(3), c = 10.344(2) Å, V = 1638.9(5) Å^3, Z = 4 and D_x = 1.420 g cm^{-3}. The structure was refined to final R = 0.034, R_w = 0.027 for 1180 reflections with $I \geq 3.0\sigma(I)$. Owing to the crystallographically imposed symmetry, the central moiety comprising the Se(2), P(1), C(1), S(1) and N(1) atoms is constrained to planarity being situated on the crystallographic mirror plane located at y = 1/4. The molecular structure of [Cy_2P(S)C(S)N(H)Me] is shown in Fig. 3.3.6a ([14]; 30% thermal ellipsoids).

The P(1)=Se(2) distance of 2.090(1) Å was similar to the distances found in the closely related [Ph_2P(Se)C(S)N(H)Me] compound of 2.083(2) and 2.088(2) Å (for which there were two independent molecules in the asymmetric unit, Section 3.3.2). All other bond distances were equal within experimental for the two R' = Me compounds. The P(1)-C(1) separation of 1.842(5) Å is experimentally equivalent to the one found in [Cy_2P(Se)C(S)N(H)Ph] while the S(1)=C(1) 1.627(4) Å, C(1)-N(1) 1.289(6) Å and N(1)-C(31) 1.447(8) Å distances are longer, shorter and longer, respectively when compared with the latter compound. These observed changes can be attributed to the greater inductive effect of the nitrogen-bound phenyl group over that of the methyl group. As a result, more π-electron density is concentrated between the N(1) and C(31) atoms in the R' = Ph compound, so that the resulting C(1)-N(1) and S(1)-C(1) distances become longer and shorter, respectively.

The P(1)-C(1) separation is approximately 0.02 Å shorter than the distance found in the Y = S analogue suggesting that the P(1)-C(1) bond is stronger in the [Cy_2P(S)C(S)N(H)Me] compound compared to [Cy_2P(Se)C(S)N(H)Me]. The methine hydrogen atoms lie on the same side of the molecule (constrained by the crystallographic

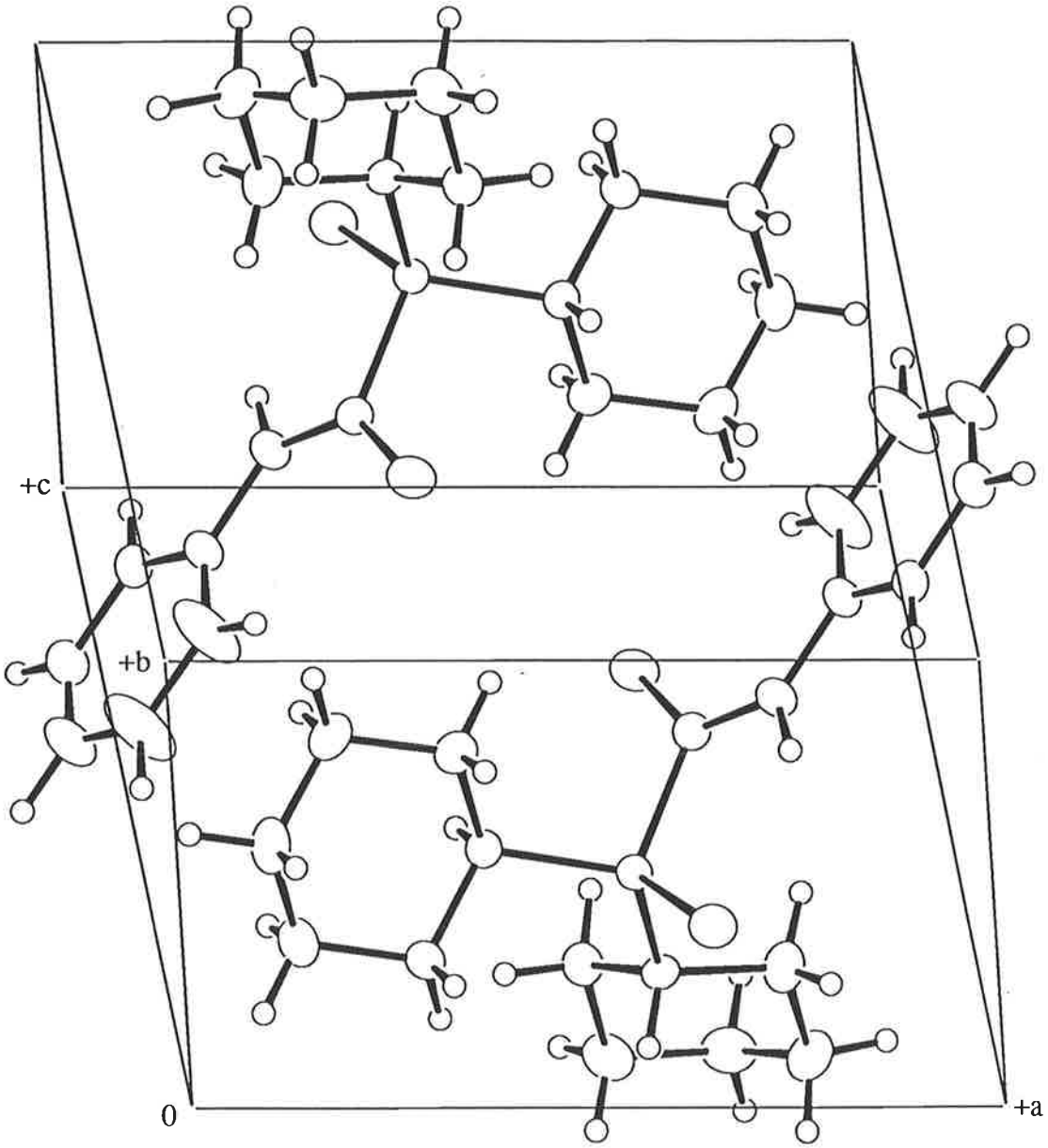

Fig. 3.3.5b The unit cell contents for [$Cy_2P(Se)C(S)N(H)Ph$]

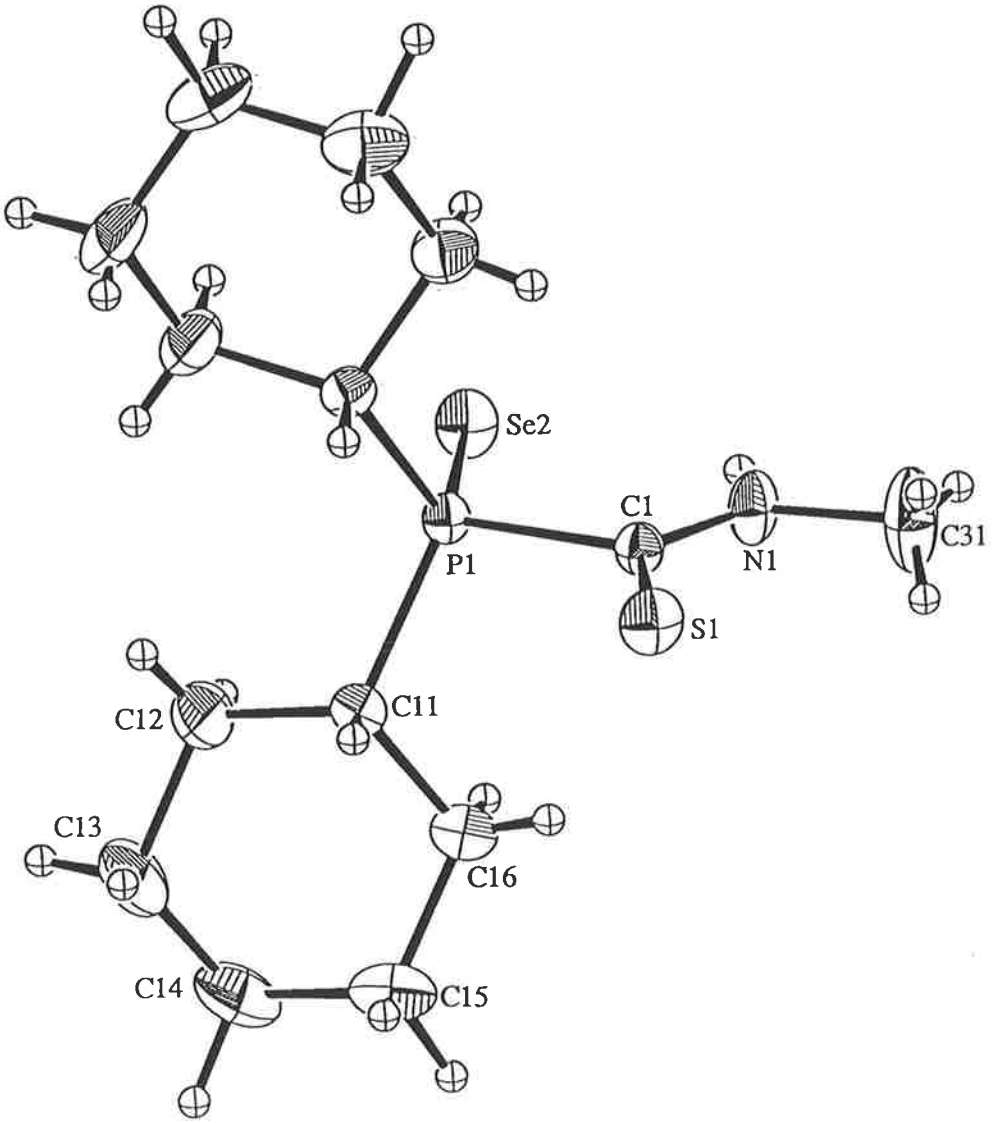

Fig. 3.3.6a The molecular structure of $[Cy_2P(Se)C(S)N(H)Me]$

symmetry) as observed in the structure of [$Cy_2P(S)C(S)N(H)Me$] but opposite to that found for [$Cy_2P(Se)C(S)N(H)Ph$].

In the lattice of [$Cy_2P(Se)C(S)N(H)Me$] (the unit cell is shown in Fig. 3.3.6b) the closest non-hydrogen contact of 3.533(7) Å occurs between the Se(2) and C(31)' atoms (symmetry operation: 0.5+x, 0.5-y, 0.5-z). The S(1) atom was involved in a short intermolecular interaction with a H(31)' atom of 2.86(5) Å (symmetry operation: -0.5+x, 0.5-y, 0.5-z).

3.3.7 The Structure of [$Cy_2P(Se)C(S)N(H)Et$]

The yellow crystals of *P, P*-dicyclohexyl-*N*-ethyl-selenophosphinylthioformamide, [$Cy_2P(Se)C(S)N(H)Et$], were obtained from the slow evaporation of an acetone solution of the compound. Crystals are triclinic, space group $P\bar{1}$ with unit cell dimensions a = 10.063(1), b = 10.864(1), c = 9.710(1) Å, α = 102.904(9), β = 114.275(8), γ = 101.962(9)°, V = 888.2(2) Å^3, Z = 2 and D_x = 1.359 g cm^{-3}. The structure was refined to final R = 0.044, R_w = 0.050 for 2097 reflections with $I \geq 3.0\sigma(I)$.

The molecular structure of [$Cy_2P(Se)C(S)N(H)Et$] is depicted in Fig. 3.3.7a ([14]; 25% thermal ellipsoids). The mean deviation of 0.023 Å from the least-squares plane through the Se(2), P, C(1), S and N atoms suggests that this central chromophore is planar and this is confirmed in the torsion angles of -178.0(2) and -1.6(5)° for Se(2)/P(1)/C(1)/S(1) and Se(2)/P(1)/C(1)/S(1), respectively.

The P(1)=Se(2) bond distance is longer than the corresponding distance found for the related [$Ph_2P(Se)C(S)N(H)Et$] compound, i.e. 2.112(1) compared to 2.084(1) Å. Notable differences between these two selenium analogues occurs in the length of the S(1)-C(1) and P-C(Cy) distances. The S(1)=C(1) separation of 1.651(5) Å found in [$Cy_2P(Se)C(S)N(H)Et$] is the longest distance seen for any of the $R_2P(Y)C(S)N(H)R'$ compounds characterised structurally in this thesis, the equivalent distance in [$Ph_2P(Se)C(S)N(H)Et$] is 1.623(4) Å. The P-C(Cy) distances in [$Cy_2P(Se)C(S)N(H)Et$], i.e. 1.835(5) and 1.836(5) Å, are approximately 0.05 Å longer than the distances in [$Ph_2P(Se)C(S)N(H)Et$], 1.782(4) and 1.783(4) Å, and are the longest distances observed

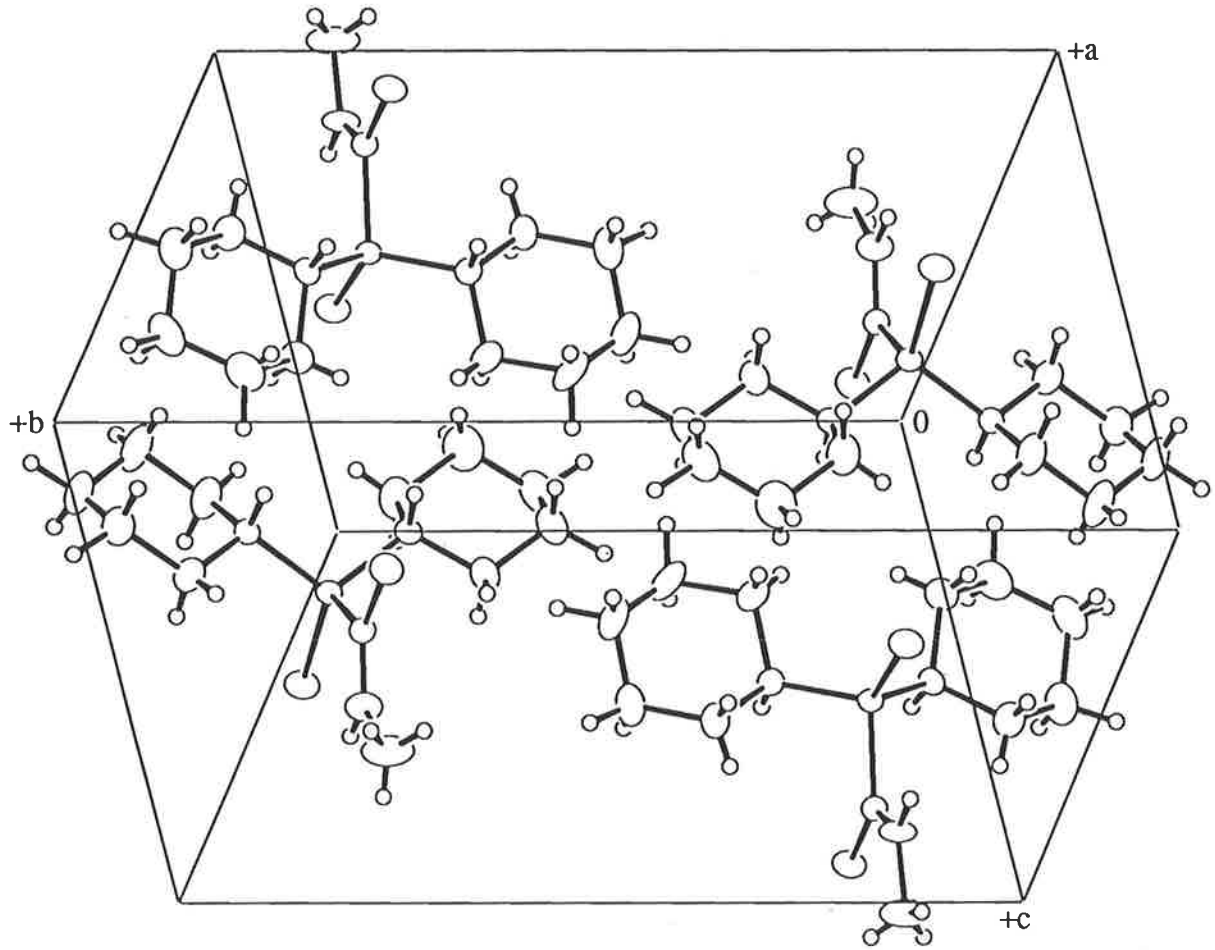

Fig. 3.3.6b The unit cell contents for [$Cy_2P(Se)C(S)N(H)Me$]

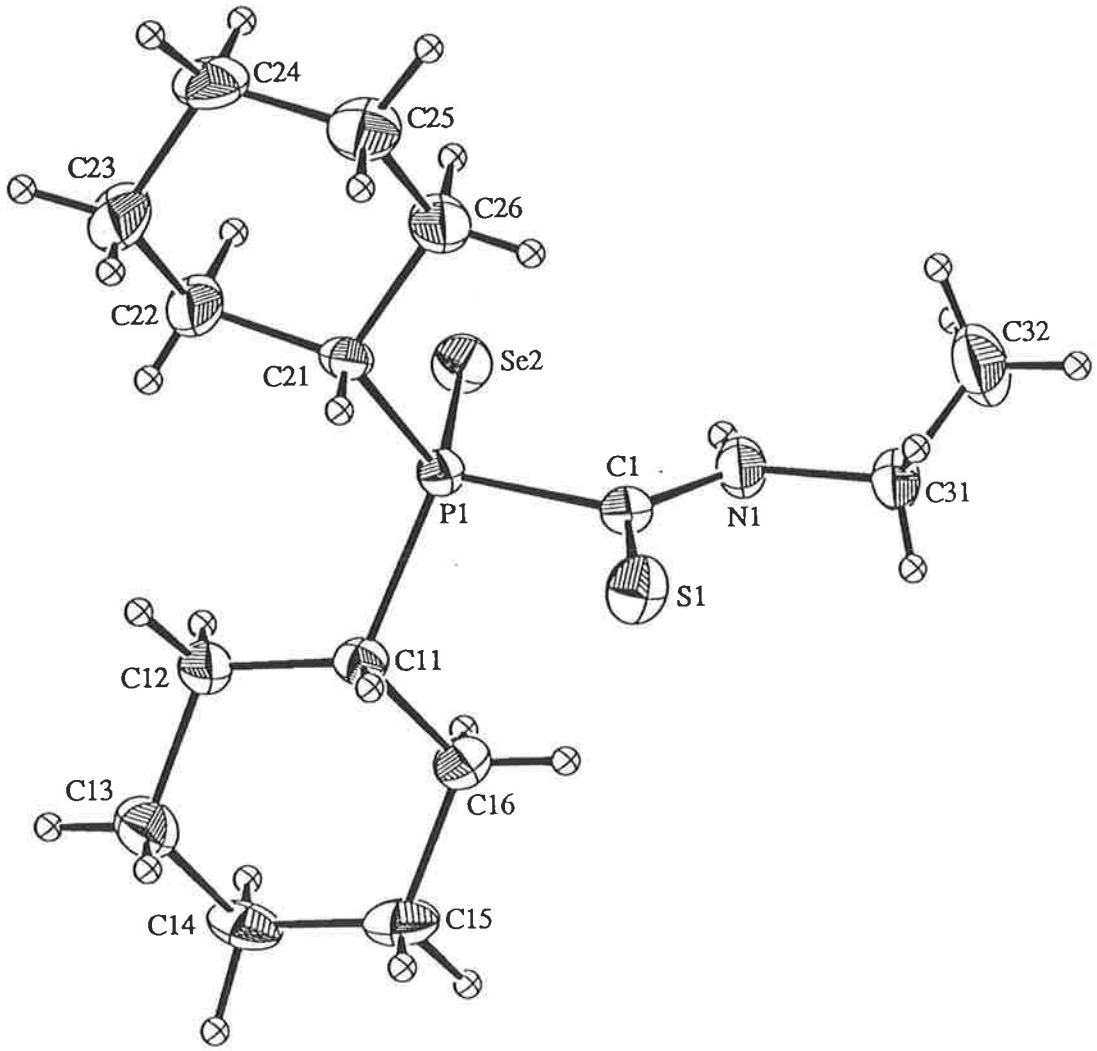

Fig. 3.3.7a The molecular structure of $[Cy_2P(Se)C(S)N(H)Et]$

for any of the R = Cy derivatives. The absence of the parameters for the parent structure, [Cy_2PC(S)N(H)Et], for comparison, does not enable further definitive conclusions to be made. The bond distances associated with the P, C(1), S and N atoms are marginally longer for the [Cy_2P(Se)C(S)N(H)Et] compound when compared to the closely related [Cy_2P(Se)C(S)N(H)Me] derivative while the bond angles about these atoms are equal within 4σ for the two compounds, Table 3.3.

There were no significant non-hydrogen contacts between atoms of less than 3.6 Å. The closest hydrogen contact of 3.08(7) Å was between atoms S(1) and H(32a)' (symmetry operation: 2-*x*, 1-*y*, 1-*z*). The unit cell contents for [Cy_2P(Se)C(S)N(H)Et] are shown in Fig. 3.3.7b.

3.3.8 The Structure of [Cy_2P(Se)C(S)N(H)Cy]

The green crystals of *P, P*-dicyclohexyl-*N*-cyclohexyl-selenophosphinylthioformamide, [Ph_2P(Se)C(S)N(H)Cy], were grown from the slow evaporation of an acetone solution of the compound. Crystals are monoclinic, space group $P2_1/c$ with unit cell dimensions a = 12.591(4), b = 12.868(4), c = 12.888(3) Å, β = 98.79(2), V = 2063(1) Å^3, Z = 4 and D_x = 1.347 g cm^{-3}. The structure was refined to final R = 0.058, R_w = 0.051 for 1955 reflections with $I \geq 3.0\sigma(I)$.

The molecular structure of [Cy_2P(Se)C(S)N(H)Cy] is represented in Fig. 3.3.8a ([14]; 30% thermal ellipsoids). The central chromophore is not planar with the deviations from the least-squares plane of the atoms being Se(2) -0.009(1) Å, P(1) 0.051(2) Å, C(1) 0.106(8) Å, S(1) -0.044(2) Å and N(1) 0.224(7) Å. The torsion angles reflect this lack of coplanarity in the angles of -172.0(4) and 6.0(7)° for the Se(2)/P(1)/C(1)/S(1) and Se(2)/P(1)/C(1)/S(1) atoms, respectively.

The errors associated with the derived interatomic parameters for this compound are fairly high but certain trends can be established. The P(1)=Se(2) distance, 2.117(2) Å, is equal within 4σ to the equivalent distance found in the R = Ph derivative, 2.110(3) Å, while the other distances are equal within experimental error for the two compounds. The N(1)-C(31) separation of 1.51(1) Å is the longest distance found in any of the

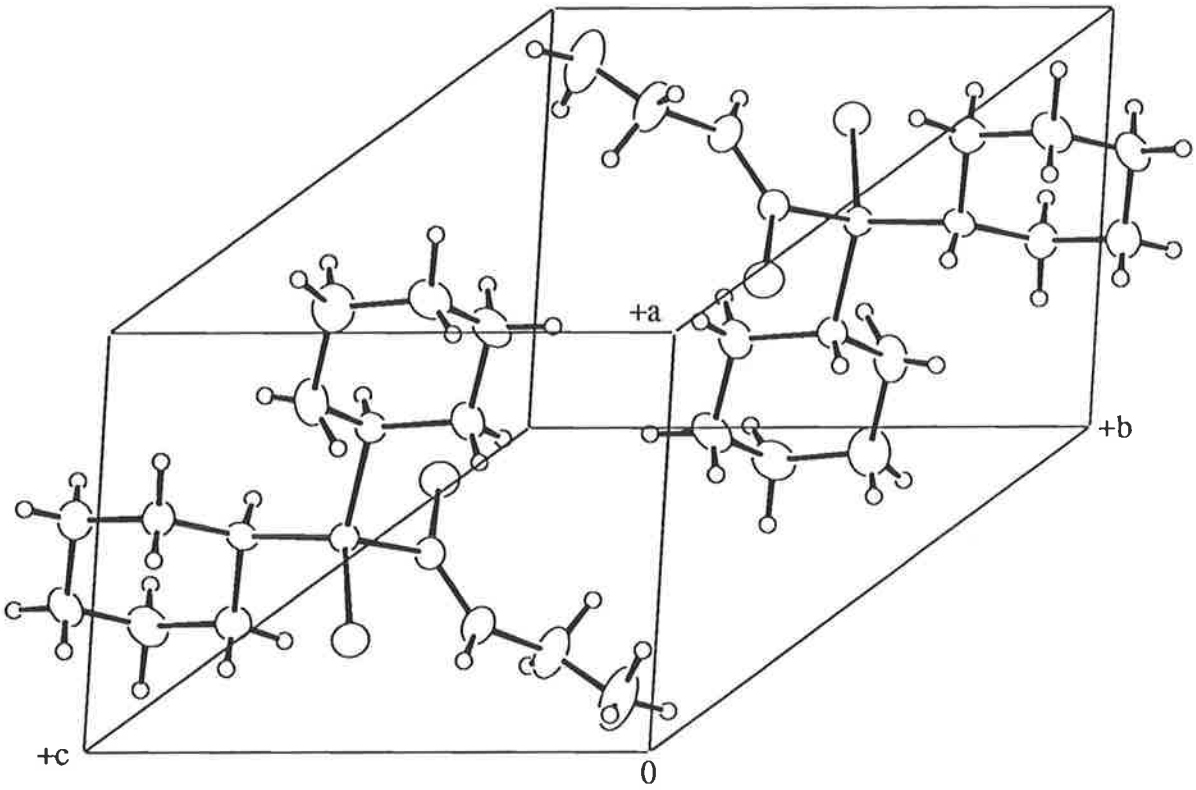

Fig. 3.3.7b The unit cell contents for $[Cy_2P(Se)C(S)N(H)Et]$

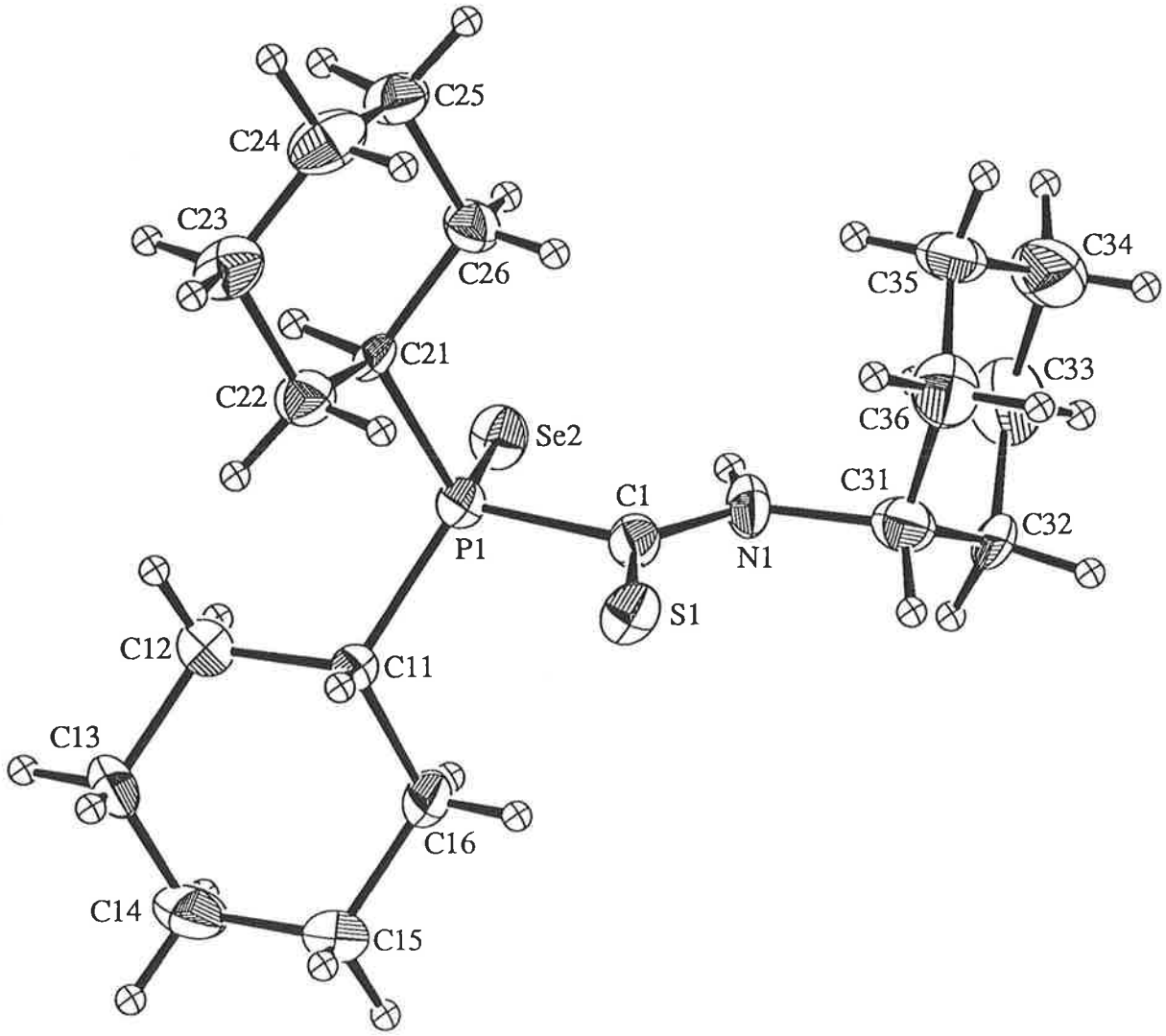

Fig. 3.3.8a The molecular structure of $[Cy_2P(Se)C(S)N(H)Cy]$

$R_2P(Y)C(S)N(H)R'$ compounds. The C(11)-P(1)-C(21) and C(1)-N(1)-C(31) angles are approximately 4 and 5° wider in [$Cy_2P(Se)C(S)N(H)Cy$] compared with the [$Ph_2P(Se)C(S)N(H)Cy$] compound, this being the most notable difference between these two. The parent [$Cy_2PC(S)N(H)Cy$] compound is unavailable for any comparison to be made with the selenium derivative.

The methine hydrogen atoms of the phosphorus-bound cyclohexyl rings are on opposite sides of the molecule which was also the case in each of [$Cy_2P(Se)C(S)N(H)Ph$] and [$Cy_2P(Se)C(S)N(H)Et$]. The unit cell contents for [$Cy_2P(Se)C(S)N(H)Cy$] are shown in Fig. 3.3.8b. The closest contact involving a hydrogen atom was 3.114 Å which occurs between the Se(2) and H(25b)' atoms (symmetry operation: $+x$, $-0.5-y$, $0.5+z$) whereas there were no intermolecular contacts less than 3.6 Å between non-hydrogen atoms.

3.4 Conclusions

As mentioned in the *Introduction* (Chapter 1), the chemistry of compounds of the general formula $R_2P(Y)C(S)N(H)R'$ is often dependent on the nature of the phosphine-bound substituents. The availability of a number of structures enabled a systematic comparison of the derived interatomic parameters and this analysis may provide an explanation for the disparate chemical behaviour exhibited by these compounds.

The first conclusion is based on the following observations. When the P-C bond distances of phosphorus(V) compounds are compared with those of the parent phosphorus(III) compounds (where available) a systematic contraction is observed, as expected. What was not anticipated was observation that the P-C bond distances contracted by differing amounts. For example, when [$Ph_2P(O)C(S)N(H)Ph$] is compared to [$Ph_2PC(S)N(H)Ph$], it is noted that the P-C(Ph) bond distances are contracted by approximately 0.04 Å and by contrast the P(1)-C(1) bond distance is contracted by only 0.01 Å. The analogous contractions in the [$Cy_2P(O)C(S)N(H)Ph$] compounds are approximately 0.06 and 0.05 Å for the P-C(Cy) and P(1)-C(1) distances, respectively, i.e. there is a more uniform contraction in these parameters. Hence, while there is evidence for a general weakening in the P(1)-C(1) bonds in the phosphorus(V) compounds, the weakening

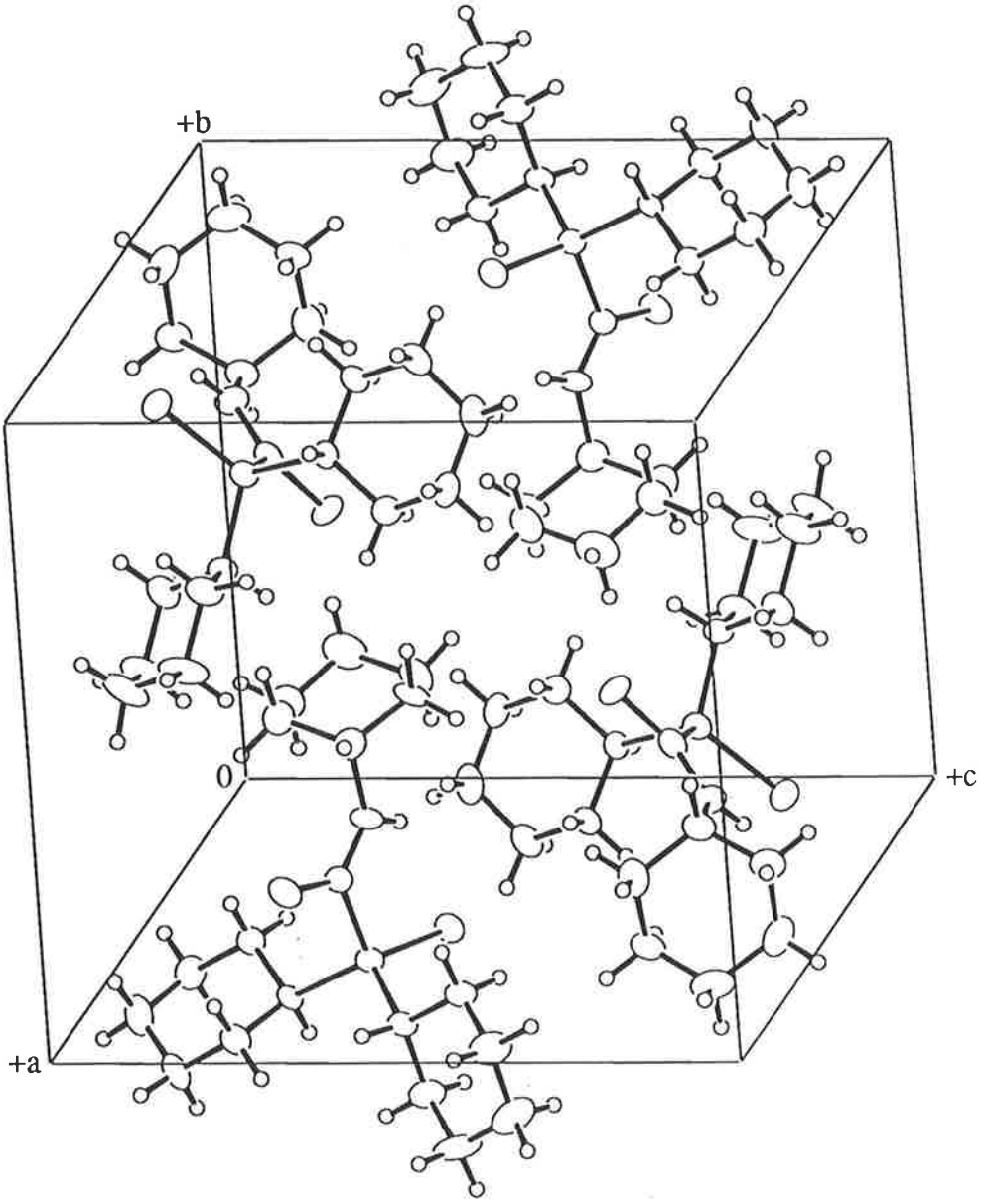

Fig. 3.3.8b The unit cell contents for $[Cy_2P(Se)C(S)N(H)Cy]$

is more pronounced in the Ph_2P(Y)C(S)N(H)R' derivatives. It is noteworthy that the remaining geometric parameters pertaining to the thioamide grouping in the compounds appear to be independent of the nature of the phosphine-bound organo groups. Hence, the crystallographic evidence suggests that the central P(1)-C(1) bonds in the Ph_2P(O)C(S)N(H)R' derivatives are significantly weaker than the comparable bonds in the Cy_2P(O)C(S)N(H)R' compounds; a similar conclusion is true also for the R_2P(S)C(S)N(H)R' and R_2P(Se)C(S)N(H)R' analogues. This observation points to the reduced stability of the Ph_2P(Y)C(S)N(H)R' compounds compared with the Cy_2P(Y)C(S)N(H)R' compounds and may be related to the greater electron withdrawing ability, i.e. greater inductive effect, of the phenyl substituents over that of the cyclohexyl groups.

The structural study of the R_2P(Y)C(S)N(H)R' compounds reported here coupled with those of the parent R_2PC(S)N(H)R' compounds [14, 25] showed that the P(1)-C(1) bond strength decreased for each series of compounds in the following order R_2PC(S)N(H)R' > R_2P(O)C(S)N(H)R' > R_2P(S)C(S)N(H)R' > R_2P(Se)C(S)N(H)R'. This trend may be correlated with the diminishing delocalisation of π-electron density over the P(1)Y(2)C(1)S(1)N(1) moieties in the order Y = 0 > O > S > Se.

It is noteworthy that the P-C(Ph or Cy) bond distances are equal within experimental error in the structures of each of the Y = O, S, and Se series. This observation is also consistent with the interpretation that the central P(1)-C(1) bond in the R = Ph derivatives is relatively weaker than the corresponding P(1)-C(1) bonds in the R = Cy compounds. Further, the elongation of the P(1)-C(1) bond in the Y = O compounds was in the order: [Ph_2P(O)C(S)N(H)Ph] > [Ph_2P(O)C(S)N(H)Me] > [Cy_2P(O)C(S)N(H)Ph] > [Cy_2P(O)C(S)N(H)Me], an order that is consistent with the inductive effect of the various substituents. The Y = S and Se derivatives adopted the same trend.

In the R_2P(Y)C(S)N(H)*Me* compounds, the C(1)=S(1), N(1)-C(1) and N(1)-C(31) bond distances are, respectively, longer, shorter and longer than those found in the corresponding R_2P(Y)C(S)N(H)*Ph* analogues; these differences became more evident as the Y atom was changed from oxygen to sulfur to selenium. These observations may be

rationalised in terms of the greater inductive effect of the nitrogen-bound phenyl substituents in the R' = Me compounds. The variation in these parameters suggest that the resonance structure in which π-electron density is localised in the C(1)-N(1) bond, leading to S^- and N^+ centres (as shown in 3.4), is of more significance in the R' = Me compounds. The identical resonance contributor can be drawn for the R' = Et and Cy compounds as well, however, these are of lesser significance.

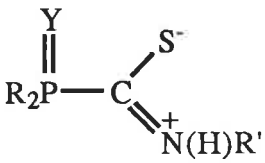

3.4

The ranges found for the P=Y separation in each series of compounds were as follows:- $R_2P(O)C(S)N(H)R'$ 1.476(3) to 1.487(2) Å, $R_2P(S)C(S)N(H)R'$ 1.942(1) to 1.959(1) Å and $R_2P(Se)C(S)N(H)R'$ 2.083(2) to 2.117(2) Å. These ranges suggest that the P=Y bond distances vary most for the Y = Se derivatives. However, no definite correlation could be made between the magnitude of the P=Y distance and the nature of R and R'.

In summary, the crystallographic analysis of the $R_2P(Y)C(S)N(H)R'$ compounds shows that the P(1)-C(1) bond is comparatively weaker in the R = Ph derivatives. Systematic variations in the geometric parameters associated with the N-C-S chromophore are related to the inductive effects of the nitrogen-bound R' substituents. For a given series of $R_2P(Y)C(S)N(H)R'$ compounds, the magnitude of the P=Y bond distance is not affected systematically by the nature of R and R'.

Chapter 4

SPECTROSCOPIC ANALYSIS OF DIORGANO-PHOSPHINYL-, DIORGANOTHIOPHOSPHINYL- AND DIORGANOSELENOPHOSPHINYL-THIOFORMAMIDES

4.1 The Preparation of the Diorganophosphinothioformamides

The $R_2PC(S)N(H)R'$ compounds were synthesised from the insertion reaction of the isothiocyanate, SCNR', R' = Ph and Me, into the P-H bond of the appropriate secondary phosphine, R_2PH, R = Ph and Cy. The compounds were never obtained from the reaction mixture in the pure form, i.e. $R_2PC(S)N(H)R'$, but invariably contained a small percentage of the oxo-derivative, $R_2P(O)C(S)N(H)R'$. The oxo impurity was far more pronounced in the R = Cy compounds and especially so for $[Cy_2PC(S)N(H)Me]$. Attempts to remove the oxidised species was never one hundred percent effective. Fractional crystallisation was not successful. The chromatographic techniques of passing the compound through either a column or on a chromatatron, appeared to oxidise the $R_2PC(S)N(H)R'$ compounds further. An attempt to selectively remove the oxygen atom from phosphorus with trichlorosilane was also unsuccessful, a procedure known to be effective for other types of P=O containing systems [57]. It is noted that the commercially available precursor secondary phosphines contained small amounts of the $R_2P(O)H$ impurity, as determined by ^{31}P NMR analyses. The spectra thus obtained for $[Cy_2PC(S)N(H)Me]$ were contaminated with a significant proportion of the $[Cy_2P(O)C(S)N(H)Me]$ derivative (estimated at 40%) and the spectroscopic parameters for the $[Cy_2PC(S)N(H)Me]$ species were determined by comparing these spectra with the spectra of a pure sample of $[Cy_2P(O)C(S)N(H)Me]$ and extracting the appropriate values. In the remaining spectra, the $R_2P(O)C(S)N(H)R'$ impurity was present in amounts less than five percent.

4.2 The Preparation of the Diorganophosphinyl-, Diorganothiophosphinyl- and Diorgano-selenophosphinyl-thioformamides

The phosphorus(V), $R_2P(Y)C(S)N(H)R'$, compounds could be synthesised by either of two methods. In the first method, the oxygen, sulfur and selenium phosphorus(V) derivatives were readily obtained by the oxidation of the phosphorus(III) precursor with the appropriate oxidant.

For the $R_2P(O)C(S)N(H)R'$ compounds, oxygen gas was passed into a stirred ethanolic solution of the parent compound, $R_2PC(S)N(H)R'$, for at least two hours. The product was passed through a flash column which also helped to oxidise any unreacted $R_2PC(S)N(H)R'$ (see above).

The sulfido derivatives were prepared by refluxing elemental sulfur with the phosphorus(III) precursor for at least two hours, in an inert atmosphere. The products were purified by passing a dichloromethane solution of each compound through a flash column to separate it from starting material and the unwanted oxo-analogue.

Purification by flash chromatography was successful in producing pure $R_2P(S)C(S)N(H)R'$ compounds as the Y = O impurity had a much slower retention time.

The selenium analogues were obtained by stirring the $R_2PC(S)N(H)R'$ compound with red selenium in an inert atmosphere at room-temperature for one hour. Then the solution was refluxed for a further three hours. If the reflux procedure was used exclusively, i.e. without prior reaction at room-temperature, the red selenium reverted to the less reactive grey/black form and the yield of compound obtained was comparatively low. The crude products were purified by passing a dichloromethane solution of each compound through a flash column.

The second method of preparation of the $R_2P(Y)C(S)N(H)R'$ compounds involved the direct reaction of the appropriate $R_2P(Y)H$ (Y = O [58], S [58] and Se [59]) compound with the appropriate SCNR' compound in benzene, but this procedure resulted in significantly lower yields.

Spectroscopic Characterisation

Despite the fact that several of the ligands have been reported previously, either in the coordinated or uncoordinated form, no systematic analysis of their spectroscopic characteristics have been reported (see *Introduction*). It was thought worthwhile to collect the infrared (IR) data (Section 4.3), the ^{1}H, ^{13}C and ^{31}P nuclear magnetic resonance (NMR) data (Section 4.4) as well as the electron impact (EI) mass spectroscopic data (Section 4.5) for these potential ligands. This information serves to facilitate the analysis of the

spectroscopic properties of the metal complexes reported in the latter portion of this thesis. Further, the spectroscopic data enables an examination of the correlation between the IR and NMR data with the crystallographic results described in Chapter 3.

4.3 IR Spectroscopy

The main regions of interest in the IR spectra of the $R_2P(Y)C(S)N(H)R'$ compounds involves the bands that can be attributed to the υ(N-H) and υ(NCS) stretches. Major absorptions with their assignments are listed in Table 4.3. The υ(N-H) absorptions are found in the region above 3000 cm^{-1}. Two bands are found for the υ(NCS) vibrations, one in the region 1400-1600 cm^{-1} and the other at around 1350 cm^{-1}, these bands will be denoted υ(thioamide I) and υ(thioamide II), respectively [10, 47, 60]. It has been suggested that the band attributed to υ(thioamide I) contains more C-N character whereas the υ(thioamide II) band contains more C=S character [61].

The frequency for the υ(thioamide II) band is considerably lower for the R' = Me compounds compared to the equivalent compounds for which R' = Ph. The difference in the frequency for the υ(thioamide II) band was as large as 76 cm^{-1} for the pair of compounds $[Ph_2P(S)C(S)N(H)Ph]$ (1388 cm^{-1}) and $[Ph_2P(S)C(S)N(H)Me]$ (1312 cm^{-1}) and the smallest difference was 21 cm^{-1} for the $[Ph_2P(O)C(S)N(H)Ph]$ (1370 cm^{-1}) and $[Ph_2P(O)C(S)N(H)Me]$ (1349 cm^{-1}) compounds. This observation correlates well with the X-ray crystallographic analyses in Chapter 3 in that for the R' = Ph compounds, the C-S bond has more double bond character. With the above observation in mind, it would be expected that the υ(thioamide I) band, i.e. predominantly due to C-N, would be at a lower frequency in the R' = Ph compounds compared with the R' = Me compounds. This was not the case as there were only small differences between the position of the absorptions. In fact, the υ(thioamide I) band occurred at a slightly higher frequency for the R' = Ph compounds compared with the R' = Me compounds. This suggests that the υ(C-N) stretch is in fact only a minor contributor to the υ(thioamide I) band.

In the phosphorus(V) derivatives, $R_2P(Y)C(S)N(H)R'$, an additional band, due to the υ(P=Y) (Y = O, S or Se) stretch, was observed. The υ(P=O), υ(P=S) and υ(P=Se)

Table 4.3: Selected infrared absorptions (cm^{-1}) for $R_2P(Y)C(S)N(H)R'$, Y = 0, O, S or Se, R = Ph or Cy and R' = Ph or Me

	υ(N-H)	υ(thioamide I)	υ(thioamide II)	υ(P-Y)
$[Ph_2PC(S)N(H)Ph]$	3318	1528	1388	-
$[Ph_2PC(S)N(H)Me]$	3326	1506	1338	-
$[Cy_2PC(S)N(H)Ph]$	3201	1502	1330	-
$[Cy_2PC(S)N(H)Me]$	3209	1521	1345	-
$[Ph_2P(O)C(S)N(H)Ph]$	3085, 3063	1528	1370	1184
$[Ph_2P(O)C(S)N(H)Me]$	3169	1520	1349	1191
$[Cy_2P(O)C(S)N(H)Ph]$	3080	1531	1373	1161
$[Cy_2P(O)C(S)N(H)Me]$	3119, 3004	1524	1344	1148
$[Ph_2P(S)C(S)N(H)Ph]$	3054	1543	1388	748, 640
$[Ph_2P(S)C(S)N(H)Me]$	3224, 3187	1524	1312	748, 660
$[Cy_2P(S)C(S)N(H)Ph]$	3107, 3026	1539	1378	759, 623
$[Cy_2P(S)C(S)N(H)Me]$	3192	1524	1338	764, 655
$[Ph_2P(Se)C(S)N(H)Ph]$	3157, 3004	1543	1389	554
$[Ph_2P(Se)C(S)N(H)Me]$	3194	1524	1363	550
$[Cy_2P(Se)C(S)N(H)Ph]$	3099	1536	1376	532
$[Cy_2P(Se)C(S)N(H)Me]$	3160	1525	1338	526

absorptions are normally found to occur in the ranges of 1200-1150 [2, 3], 760-750 [2, 3] and 652-618 [10] and 525-561 [62-64] cm^{-1}, respectively in compounds which contain these atoms. The absorptions for υ(P=Y) are very close to or fall neatly into these ranges. The υ(P=Y) absorptions tend to occur at lower frequencies for the R = Cy compounds as compared with the analogous R = Ph compounds. In the previous chapter describing the crystallographic analyses of these compounds it was noted that the P=Y bond separations were equal within experimental error and independent of the nature of the R group and so the reason for this trend remains unclear.

The υ(N-H) bands for the phosphorus(V) derivatives occur at a lower frequencies compared with the values for the phosphorus(III) compounds. This is especially so for the Y = O compounds where the values occur about 150-200 cm^{-1} to lower frequency. The reason for such a difference in these derivatives can be attributed to the intermolecular hydrogen bonding, as revealed by the structural characterisation (Chapter 3). The υ(N-H) bands for the Y = S and Se compounds also occur at lower frequencies even though significant intermolecular S (or Se)...H interactions were not noted in the crystallographic analyses.

4.4 NMR Spectroscopy

4.4.1 ^{1}H NMR Spectroscopy

Table 4.4.1 lists the assignments for the protons in each compound, including the multiplicity and coupling constants when determined. The resonances for aromatic protons occur as complex multiplets due to the many proton-proton and phosphorus-proton coupling combinations, so only a range is given. This range is typical of phenylphosphine absorptions, e.g. as in Ph_3P [65]. As expected, the positions of the resonances due to the aromatic protons are invariant in all spectra. A similar, but broader, complex multiplet occurs for the cyclohexyl protons, also due to complex coupling patterns (not resolved), upfield owing to their alkyl nature. For both the phenyl and/or cyclohexyl protons (where appropriate) the integration of the broad multiplets were consistent with what was expected from the molecular formula.

Table 4.4.1: ^{1}H NMR data for $R_2P(Y)C(S)N(H)R'$, Y = 0, O, S or Se, R = Ph or Cy and R' = Ph or Me

	N-H	N-Ph	N-Me	R_2P
$[Ph_2PC(S)N(H)Ph]$	8.73, br	7.22-7.64, m		7.22-7.64, m
$[Ph_2PC(S)N(H)Me]$	8.84, s		3.20, d, (4.85^a)	7.37-7.50, m
$[Cy_2PC(S)N(H)Ph]$	9.46, br	7.24-8.04, m		1.18-2.58, m
$[Cy_2PC(S)N(H)Me]$	8.62, br		3.24, d, (4.80^a)	1.15-2.54, m
$[Ph_2P(O)C(S)N(H)Ph]$	11.20, d (7.47)	7.30-8.12, m		7.30-8.12, m
$[Ph_2P(O)C(S)N(H)Me]$	10.67, br		3.26, dd, (4.95^a, 1.62^b)	7.43-8.00, m
$[Cy_2P(O)C(S)N(H)Ph]$	10.92, d (6.96)	7.27-8.07, m		1.18-2.40, m
$[Cy_2P(O)C(S)N(H)Me]$	9.97, br		3.21, dd, (3.21^a, 3.21^b)	1.14-2.56, m
$[Ph_2P(S)C(S)N(H)Ph]$	11.92, d (9.18)	7.31-8.11, m		7.31-8.11, m
$[Ph_2P(S)C(S)N(H)Me]$	10.25, br		3.29, dd, (5.10^a, 1.77^b)	7.42-8.02, m
$[Cy_2P(S)C(S)N(H)Ph]$	11.53, d (7.59)	7.27-8.07, m		1.15-2.65, m
$[Cy_2P(S)C(S)N(H)Me]$	9.91, br		3.26, dd, (5.06^a, 1.58^b)	1.14-2.56, m
$[Ph_2P(Se)C(S)N(H)Ph]$	12.01, d (8.38)	7.28-8.07, m		7.31-8.12, m
$[Ph_2P(Se)C(S)N(H)Me]$	10.35, br		3.29, dd, (5.13^a, 1.80^b)	7.41-7.99, m
$[Cy_2P(Se)C(S)N(H)Ph]$	11.60, d (7.44)	7.28-8.07, m		1.16-2.65, m
$[Cy_2P(Se)C(S)N(H)Me]$	9.98, br		3.26, dd, (5.15^a, 1.65^b)	1.14-2.60, m

coupling constants are in parentheses: a $^{3}J(HH)$, b $^{4}J(PH)$

br = broad, d = doublet, dd = doublet of doublets, m = multiplet, s = singlet, t = triplet

The N-H resonance occurs at the most downfield position with respect to the other protons found in the compounds. For the $R_2PC(S)N(H)R'$ compounds this resonance appeared as a broad peak in the range δ 8.62-9.46 ppm. In the $R_2P(Y)C(S)N(H)R'$ compounds the resonances were observed even more downfield ranging from *ca* δ 10 to 12 ppm. For the $R_2P(Y)C(S)N(H)R'$ compounds with R' = Me, the N-H resonance was broad but when R' = Ph the N-H resonance was split into a doublet with coupling constants in the range 7 to 9 Hz, the exact values can be found in Table 4.4.1. The broadness and subsequent splitting in the R' = Ph derivatives could be due to the presence of *E* and *Z* isomers of the compound with the two peaks due to the different N-H resonances.

Since there is some partial double bond character associated with the C(1)-N(1) bond, see Chapter 3, there exists the possibility of *E/Z* isomerism. For some secondary thioamide, thioimide and thioimidate groups *E* and *Z* isomers have been found to exist [66-69]. For the phosphorus(III) compounds, $R_2PC(S)N(H)R'$, the two forms which could be adopted appear below:

R = Ph or Cy; R' = Ph or Me

The three crystal structures reported for the $R_2PC(S)N(H)R'$ compounds showed that these compounds adopted the *Z* configuration only [15, 25]. For the phosphorus(V) compounds, $R_2P(Y)C(S)N(H)R'$, the possible conformations that may exist are shown overleaf.

A study which incorporated a variable temperature NMR study on some of the $Ph_2P(Y)C(S)N(H)R'$, Y = O or S; R' = Ph or Me, derivatives found no evidence for the existence of both *E* and *Z* isomers for these compounds in solution [70]. From the four possible conformations shown above the *E* isomer was determined to be sterically unfavourable, however, the endo *Z* configuration was preferred as the possibility of additional stabilisation owing to an intramolecular hydrogen bond with the Y atom, shown dashed in the figure above, exists. When the R' group is replaced with a Me_3Si group, the *E* isomer is preferred. Of the sixteen crystal structure determinations for the phosphorus(V)

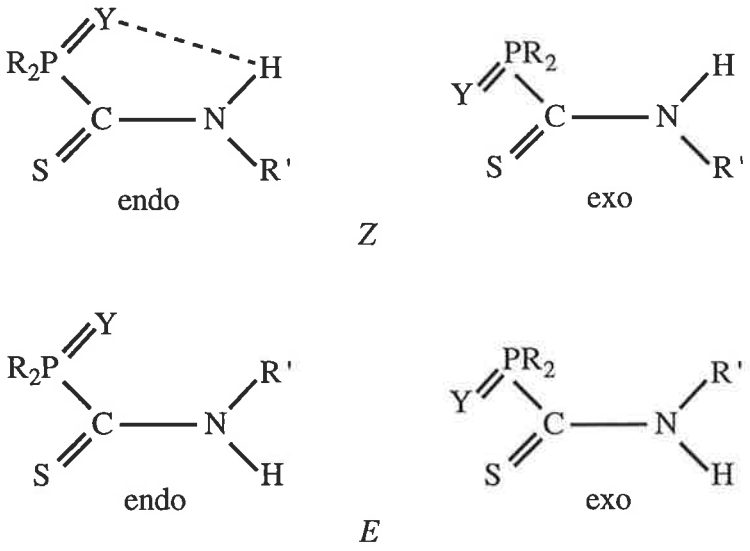

Y = O, S or Se; R = Ph or Cy; R' = Ph or Me

derivatives described in Chapter 3, it was shown that all structures adopted the *Z* conformation. There was no observation of a significant intramolecular hydrogen bonding contact between the Y atom and the amide hydrogen atom as suggested by Kunze et al [70] but there was evidence for significant intermolecular hydrogen bonding in the Y = O compounds which would favour the *Z* configuration.

No evidence for the *E* conformation for any of the compounds in this thesis has been found in either the solid or solution states. The use of variable temperature NMR could be used as a tool to ascertain whether or not the splitting of the N-H resonance was due to the presence of two isomers in solution, but this was beyond the scope of this thesis.

Another possibility to account for the splitting of the N-H resonance could be the coupling of the amide proton with the phosphorus atom, however, a typical $^{3}J(PH)$ coupling constant is in the order of 18 Hz [71] and the lower value found in these compounds precluded this possibility. Similarly, the magnitude of the coupling constant precluded $^{4}J(HH)$ coupling of the amide proton and a proton on the nitrogen-bound phenyl ring.

It was noted that for the Y = S and Se compounds which contained the R' = Ph group the amide proton resonance was approximately 1.6 ppm downfield with respect to the analogous compounds with R' = Me, e.g. δ 12.01 ppm *cf.* δ 10.35 ppm for $[Ph_2P(Se)C(S)N(H)Ph]$ and $[Ph_2P(Se)C(S)N(H)Me]$, respectively. This difference was not as pronounced for the Y = O compounds, i.e. the shift was about 0.5 ppm downfield.

The downfield chemical shift for the N-H resonance in the R' = Ph species is consistent with deshielding of the amide proton in these compounds compared with the corresponding R' = Me derivatives.

For the R' = Me compounds the methyl resonance appeared between δ 3.20 and 3.30 ppm. Phosphorus-proton and proton-proton coupling was observed leading to the appearance a doublet of doublets; see Table 4.4.1.

4.4.2 ^{13}C NMR Spectroscopy

The proton decoupled ^{13}C NMR resonances in the spectra of all the $Ph_2P(Y)C(S)N(H)R'$ compounds were generally simple and therefore assignment was straightforward. Assignment of the resonances was also facilitated by the occurrence of ^{13}C-^{31}P spin-spin coupling. Similarly, ^{13}C-^{31}P spin-spin coupling was observed for the quaternary carbon atom, C_q, and the methine carbon atom, Cα, for the cyclohexyl groups. The assignment of the remaining carbon atoms, Cβ-Cδ, of the cyclohexyl rings was difficult, however, owing to overlapping of peaks and hence, only a range was quoted for these atoms. The chemical shifts and coupling constants are listed in Tables 4.4.2a-4.4.2d. The numbering scheme adopted for the carbon atoms is shown in Fig. 4.4.2.

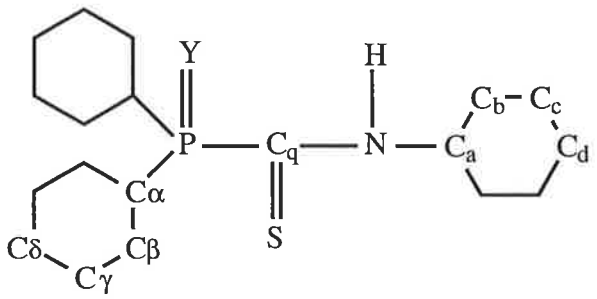

Fig. 4.4.2 Numbering scheme for the carbon atoms in the $R_2P(Y)C(S)N(H)R'$ species

The quaternary carbon atom, C_q, appeared as a doublet at the most downfield position in the spectra for all compounds. The resonance due to C_q was shifted significantly upfield in the $R_2P(Y)C(S)N(H)R'$ compounds compared with the respective phosphorus(III) precursors. This is consistent with the shielding of the C_q atom in the phosphorus(V) compounds. For a series of phosphorus(V) derivatives with R and R' held constant, the C_q

Table 4.4.2a: $^{13}C\{^{1}H\}$ NMR values for $R_2PC(S)N(H)R'$, R = Ph or Cy and R' = Ph or Me

	C_q	$C\alpha$	$C\beta$	$C\gamma$	$C\delta$	C_a	C_b	C_c	C_d
$[Ph_2PC(S)N(H)Ph]$	206.6	134.5	134.3	129.2	130.2	138.7	128.9	122.3	126.9
	$^{1}J(PC)$ 39.9		$^{2}J(PC)$ 20.5	$^{3}J(PC)$ 7.3					
$[Ph_2PC(S)N(H)Me]$	208.5	133.4	134.2	129.0	130.0	33.3			
	$^{1}J(PC)$ 37.9	$^{1}J(PC)$ 119.5	$^{2}J(PC)$ 20.6	$^{3}J(PC)$ 7.6					
$[Cy_2PC(S)N(H)Ph]$	210.3	35.6		26.2 - 29.5		138.9	128.3	123.1	126.7
	$^{1}J(PC)$ 34.4	$^{1}J(PC)$ 11.6				$^{3}J(PC)$ 11.6			
$[Cy_2PC(S)N(H)Me]$	210.8	35.0		26.1 - 29.3		33.0			
	$^{1}J(PC)$ 34.9	$^{1}J(PC)$ 11.1				$^{3}J(PC)$ 7.7			

Chemical shifts are in ppm and coupling constants, $^{x}J(PC)$ where x = 1-4, are in Hz

Table 4.4.2b: $^{13}C\{^{1}H\}$ NMR values for $R_2P(O)C(S)N(H)R'$, R = Ph or Cy, R' = Ph or Me

	C_q	$C\alpha$	$C\beta$	$C\gamma$	$C\delta$	C_a	C_b	C_c	C_d
$[Ph_2P(O)C(S)N(H)Ph]$	193.9	128.7	128.4	132.9	132.7	138.3	129.1	121.6	127.4
	$^{1}J(PC)$ 89.7	$^{1}J(PC)$ 108.1	$^{2}J(PC)$ 12.3	$^{3}J(PC)$ 9.6	$^{4}J(PC)$ 2.3	$^{3}J(PC)$ 11.2			
$[Ph_2P(O)C(S)N(H)Me]$	196.9	129.3	128.2	132.5	132.4	32.5			
	$^{1}J(PC)$ 90.2	$^{1}J(PC)$ 108.4	$^{2}J(PC)$ 12.4	$^{3}J(PC)$ 8.7		$^{3}J(PC)$ 6.2			
$[Cy_2P(O)C(S)N(H)Ph]$	194.4	35.9		24.9 - 26.2		138.1	128.9	121.8	127.2
	$^{1}J(PC)$ 69.1	$^{1}J(PC)$ 65.7				$^{3}J(PC)$ 9.7			
$[Cy_2P(O)C(S)N(H)Me]$	197.7			24.8 - 26.2		32.1			
	$^{1}J(PC)$ 70.4	$^{1}J(PC)$ 66.3				$^{3}J(PC)$ 5.4			

Chemical shifts are in ppm and coupling constants, $^{x}J(PC)$ where x = 1-4, are in Hz

Table 4.4.2c: $^{13}C\{^{1}H\}$ NMR values for $R_2P(S)C(S)N(H)R'$, R = Ph or Cy, R' = Ph or Me

	C_q	$C\alpha$	$C\beta$	$C\gamma$	$C\delta$	C_a	C_b	C_c	C_d
$[Ph_2P(S)C(S)N(H)Ph]$	188.9	130.0	128.4	133.0	132.3	138.5	129.1	121.2	127.6
	$^{1}J(PC)$ 67.4	$^{1}J(PC)$ 90.1	$^{2}J(PC)$ 12.8	$^{3}J(PC)$ 10.0	$^{4}J(PC)$ 3.5	$^{3}J(PC)$ 12.6			
$[Ph_2P(S)C(S)N(H)Me]$	193.3	130.0	128.2	132.8	132.1	33.4			
	$^{1}J(PC)$ 66.7	$^{1}J(PC)$ 89.5	$^{2}J(PC)$ 13.1	$^{3}J(PC)$ 10.1	$^{4}J(PC)$ 3.0	$^{3}J(PC)$ 6.7			
$[Cy_2P(S)C(S)N(H)Ph]$	190.2	38.2		25.6 - 26.3		138.3	129.0	121.4	127.4
	$^{1}J(PC)$ 51.3	$^{1}J(PC)$ 49.4				$^{3}J(PC)$ 10.8			
$[Cy_2P(S)C(S)N(H)Me]$	193.7	38.0		25.5 - 26.2		32.7			
	$^{1}J(PC)$ 51.3	$^{1}J(PC)$ 49.3				$^{3}J(PC)$ 5.6			

Chemical shifts are in ppm and coupling constants, $^{x}J(PC)$ where x = 1-4, are in Hz

Table 4.4.2d: $^{13}C\{^{1}H\}$ NMR values for $R_2P(Se)C(S)N(H)R'$, R = Ph or Cy, R' = Ph, Me, Et or Cy

	C_q	Cα	Cβ	Cγ	Cδ	C_a	C_b	C_c	C_d
$[Ph_2P(Se)C(S)N(H)Ph]$	186.3	129.5	128.4	133.3	132.3	138.5	129.1	121.0	127.6
	$^{1}J(PC)$ 58.9	$^{1}J(PC)$ 82.0	$^{2}J(PC)$ 12.7	$^{3}J(PC)$ 10.6	$^{4}J(PC)$ 3.3	$^{3}J(PC)$ 13.2			
$[Ph_2P(Se)C(S)N(H)Me]$	190.9	129.4	128.3	133.1	132.2	33.8			
	$^{1}J(PC)$ 58.6	$^{1}J(PC)$ 81.1	$^{2}J(PC)$ 13.0	$^{3}J(PC)$ 10.7	$^{4}J(PC)$ 3.0	$^{3}J(PC)$ 6.8			
$[Ph_2P(Se)C(S)N(H)Et]$	189.6	129.6	128.3	133.2	132.2	42.0	12.6		
	$^{1}J(PC)$ 56.8	$^{1}J(PC)$ 81.4	$^{2}J(PC)$ 12.6	$^{3}J(PC)$ 10.5	$^{4}J(PC)$ 3.2	$^{3}J(PC)$ 6.3			
$[Ph_2P(Se)C(S)N(H)Cy]$	188.0	129.7	128.3	133.2	132.1	54.9	30.6	25.4	24.1
	$^{1}J(PC)$ 56.1	$^{1}J(PC)$ 81.7	$^{2}J(PC)$ 13.3	$^{3}J(PC)$ 10.8	$^{4}J(PC)$ 3.3	$^{3}J(PC)$ 5.7			
$[Cy_2P(Se)C(S)N(H)Ph]$	187.4	38.4		25.6 - 26.7		138.3	129.0	121.3	127.5
	$^{1}J(PC)$ 44.2	$^{1}J(PC)$ 41.9				$^{3}J(PC)$ 11.5			
$[Cy_2P(Se)C(S)N(H)Me]$	191.0	38.1		25.5 - 26.4		33.0			
	$^{1}J(PC)$ 44.2	$^{1}J(PC)$ 42.1				$^{3}J(PC)$ 5.8			
$[Cy_2P(Se)C(S)N(H)Et]$	189.9	38.2		25.6 - 26.5		41.1	12.7		
	$^{1}J(PC)$ 43.0	$^{1}J(PC)$ 41.9				$^{3}J(PC)$ 5.2			
$[Cy_2P(Se)C(S)N(H)Cy]$	188.2	38.1		25.6 - 26.5		54.1	30.6	25.3	24.1
	$^{1}J(PC)$ 42.6	$^{1}J(PC)$ 42.3				$^{3}J(PC)$ 4.6			

Chemical shifts are in ppm and coupling constants, $^{x}J(PC)$ where x = 1-4, are in Hz

resonance in the $R_2P(O)C(S)N(H)R'$ compounds was downfield compared with the $R_2P(S)C(S)N(H)R'$ species which, in turn, was downfield compared with the $R_2P(Se)C(S)N(H)R'$ derivatives. This observation is correlated with the order of decreasing electronegativity associated with the oxygen, sulfur and selenium atoms. For a given $R_2P(Y)C(S)N(H)R'$ series of compounds with the same R group but different R', i.e. Ph or Me, the C_q resonance was shifted downfield for the R' = Me compounds. The largest difference of 4.6 ppm was found for the $[Ph_2P(Se)C(S)N(H)Ph]$ (δ 186.3 ppm) and $[Ph_2P(Se)C(S)N(H)Me]$ (δ 190.9 ppm) compounds whilst the smallest difference was found for $[Ph_2P(O)C(S)N(H)Ph]$ (δ 193.9 ppm) and $[Ph_2P(O)C(S)N(H)Me]$ (δ 196.9 ppm) of 3.0 ppm. This result is entirely consistent with the crystallographic studies which showed that for the R' = Me compounds additional electron density resided in the NCS chromophore owing to the smaller inductive effect of the methyl substituent. Some interesting observations were also noted with the coupling constants involving the quaternary atom, C_q.

Within a series of $R_2P(Y)C(S)N(H)R'$ compounds, i.e. with fixed R and R' groups but different Y (O, S or Se), the ^{13}C-^{31}P coupling constant decreased in the following order O > S > Se. This trend can be related to the length of the P(1)-C(1) bond in these compounds as determined from the X-ray structural analyses described in the Chapter 3, i.e. the longer the bond, the smaller the coupling constant.

The assignment for the Ph_2P carbon resonances was achieved by the analysis of the ^{13}C-^{31}P coupling constants. All the carbon atoms were found to be coupled with the phosphorus atom and hence doublets were observed for each carbon atom. The Cy_2P carbon resonances were difficult to assign except for the methine carbon atom, Cα, which was the most shielded and occurred downfield, separated from the other resonances. The remaining carbon atoms, Cβ-Cδ, gave various splitting patterns and it was difficult to assign the resonances.

4.4.3 ^{31}P NMR Spectroscopy

The proton decoupled ^{31}P NMR spectra of all the compounds with the general formula

$R_2P(Y)C(S)N(H)R'$, R = Ph or Cy, R' = Ph or Me, Y = 0, O, S or Se, were recorded in $CHCl_3$ solution and the results are presented in Table 4.4.3.

For the phosphorus(III) compounds, $R_2PC(S)N(H)R'$, a sharp signal was observed in all cases. In addition, there was another (sometimes significant) peak in these spectra which was assigned to the corresponding Y = O derivative. For the R = Ph compounds the Y = O resonance was between 5-10% of the major peak while in the R = Cy compounds the proportion of the oxo derivative was more pronounced, i.e. up to 40%. By contrast, the spectra for the Y = O, S and Se compounds contained a single sharp peak only. There was an additional feature in the Y = Se compounds in that there were two satellite peaks. These satellites were attributed to ^{31}P-^{77}Se coupling; the natural abundance of ^{77}Se with spin I = 1/2 is 7.6%. The $^1J(^{31}P$-$^{77}Se)$ coupling constants ranged from 692-725 Hz for the four selenium derivatives and this is in the range for couplings observed in other tertiary phosphine-selenium compounds [72-74]. Fig. 4.3 shows the spectra of two compounds in the region of interest containing the selenium satellites. It was noted that the $^1J(^{31}P$-$^{77}Se)$ coupling constants were larger for the R = Ph compounds (R' = Ph or Me) as opposed to the R = Cy compounds (R' = Ph or Me). This is consistent with the literature in that it has been shown that the respective coupling constants increase as the groups attached to the phosphorus atom become more electron-withdrawing in accordance with Bent's rule [75]. The ^{31}P NMR shifts for the Y = O derivatives occurred some 20-25 ppm upfield compared to the values found for the Y = S and Se derivatives. This result is rationalised in terms of the greater electronegativity of the oxygen atom compared with the sulfur or selenium atoms. The resonances for the Y = S and Se derivatives occur in the same region, i.e. within about 2-5 ppm away from each other, as they have similar electronegativities [76].

4.5 Mass Spectroscopy

Major fragments for the electron impact mass spectra of the $R_2P(Y)C(S)N(H)R'$ compounds are summarised in Tables 4.5a-4.5d. The molecular ion $[M]^+$ appeared for each of the compounds at varying intensities and for only two compounds was this ion the most abundant, i.e. $[Cy_2P(Se)C(S)N(H)Et]$ and $[Cy_2P(Se)C(S)N(H)Cy]$. The $[R_2P(Y)H]^+$ ion

Table 4.4.3: $^{31}P\{^{1}H\}$ NMR Data for $R_2P(Y)C(S)N(H)R'$, Y = 0, O, S or Se, R = Ph or Cy, R' = Ph or Me

$[Ph_2PC(S)N(H)Ph]$	19.2	$[Ph_2PC(S)N(H)Me]$	14.7
$[Ph_2P(O)C(S)N(H)Ph]$	20.9	$[Ph_2P(O)C(S)N(H)Me]$	20.5
$[Ph_2P(S)C(S)N(H)Ph]$	47.4	$[Ph_2P(S)C(S)N(H)Me]$	42.7
$[Ph_2P(Se)C(S)N(H)Ph]$	45.3 (722)	$[Ph_2P(Se)C(S)N(H)Me]$	40.5 (725)
$[Cy_2PC(S)N(H)Ph]$	43.9	$[Cy_2PC(S)N(H)Me]$	48.4
$[Cy_2P(O)C(S)N(H)Ph]$	50.1	$[Cy_2P(O)C(S)N(H)Me]$	49.2
$[Cy_2P(S)C(S)N(H)Ph]$	74.1	$[Cy_2P(S)C(S)N(H)Me]$	71.2
$[Cy_2P(Se)C(S)N(H)Ph]$	75.4 (692)	$[Cy_2P(Se)C(S)N(H)Me]$	71.1 (697)

Chemical shifts are in ppm and coupling constants, $^{1}J(^{31}P\text{-}^{77}Se)$, in parentheses, are in Hz

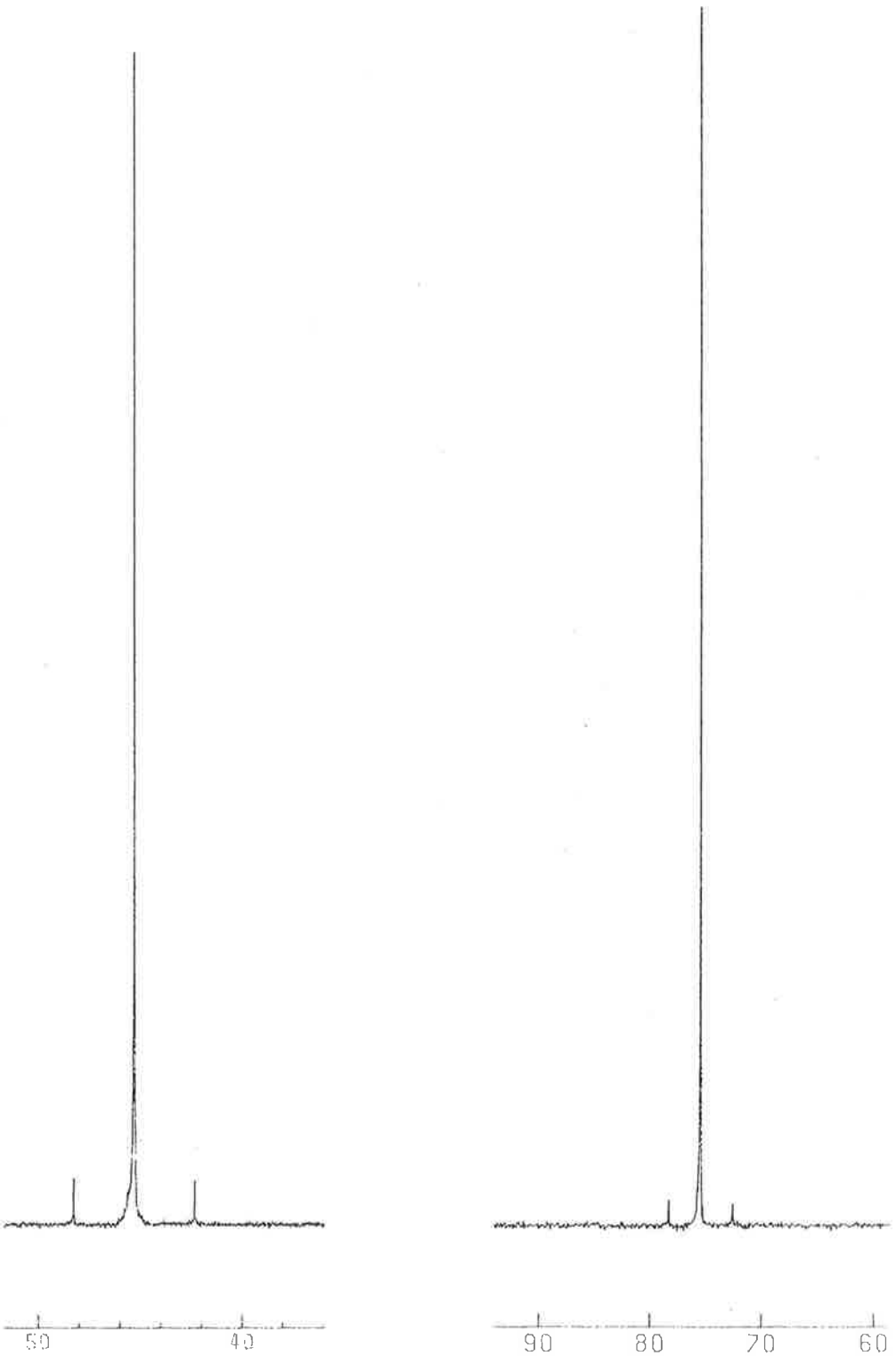

Fig. 4.3 $^{31}P\{H\}$ NMR spectra for (a) $[Ph_2P(Se)C(S)N(H)Ph]$ and (b) $[Cy_2P(Se)C(S)N(H)Ph]$ recorded in $CHCl_3$ solution showing the $^{1}J(PSe)$ coupling

Table 4.5a: Fragment ions for $R_2P(O)C(S)N(H)R'$, R = Ph or Cy, R' = Ph or Me[a]

Ion	R = Ph R' = Ph	R = Ph R' = Me	R = Cy R' = Ph	R = Cy R' = Me
$[M]^+$	337(20)	275(14)	350(17)	287(39)
$[R_2P(O)H]^+$	202(100)	202(100)	214(100)	214(100)
$[R_2PH]^+$	186(11)	-	198(28)	198(16)
$[R_2P]^+$	185(24)	-	197(24)	-
$[RPCS]^+$	154(10)	154(27)	159(49)	159(19)
$[R'N(H)CS]^+$	136(37)	74(73)	136(55)	74(14)
$[R'NCS]^+$	135(98)	73(29)	135(52)	-
$[RP(O)]^+$	124(12)	124(24)	130(88)	130(60)
$[Cy]^+$	-	-	83(72)	83(34)
$[Ph]^+$	77(52)	77(64)	77(93)	-
$[PO]^+$	47(9)	47(18)	47(40)	-

[a] Represented as molecular weight followed by relative abundance in parentheses

Table 4.5b: Fragment ions for $R_2P(S)C(S)N(H)R'$, R = Ph or Cy, R' = Ph or Me[a]

Ion	R = Ph R' = Ph	R = Ph R' = Me	R = Cy R' = Ph	R = Cy R' = Me
$[M]^+$	353(8)	292(10)	365(33)	303(38)
$[R_2P(S)H]^+$	218(100)	218(55)	230(26)	230(84)
$[R_2PH]^+$	186(38)	186(18)	-	-
$[R_2P]^+$	185(38)	185(70)	-	-
$[R'N(H)CS]^+$	136(48)	74(100)	136(28)	74(78)
$[RP(S)]^+$	140(36)	140(95)	147(100)	147(83)
$[RP]^+$	108(30)	108(16)	114(15)	114(24)
$[Cy]^+$	-	-	83(80)	83(100)
$[Ph]^+$	77(56)	77(36)	77(45)	-
$[PS]^+$	63(22)	63(27)	63(8)	-

[a] Represented as molecular weight followed by relative abundance in parentheses

Table 4.5c: Fragment ions for $Ph_2P(Se)C(S)N(H)R'$, R' = Ph, Me, Et or Cy[a]

Ion	R' = Ph	R' = Me	R' = Et	R' = Cy
$[M]^+$	400(11)	339(22)	353(17)	406(34)
$[Ph_2P(Se)H]^+$	266(65)	266(42)	266(46)	266(100)
$[Ph_2PH]^+$	186(51)	186(23)	186(37)	186(50)
$[Ph_2P]^+$	185(100)	185(100)	185(94)	185(97)
$[(C_6H_4)_2P]^+$	183(59)	183(55)	183(58)	183(78)
$[PhP]^+$	108(65)	108(27)	108(36)	108(38)
$[C_6H_4P]^+$	107(32)	107(30)	107(24)	107(30)
$[Ph]^+$	77(68)	77(13)	77(36)	77(15)
$[R'NCS]^+$	135(88)	74(27)	-	141(12)
$[PCNC]^+$	69(22)	-	69(100)	69(21)
$[Cy]^+$				83(37)

[a] Represented as molecular weight followed by relative abundance in parentheses

Table 4.5d: Fragment ions for $Cy_2P(Se)C(S)N(H)R'$, R' = Ph, Me, Et or Cy[a]

Ion	R' = Ph	R' = Me	R' = Et	R' = Cy
$[M]^+$	412(26)	350(40)	365(100)	419(100)
$[M\text{-}Se]^+$	332(7)	271(23)	285(13)	338(15)
[M-Se and Cy]$^+$	250(22)	188(71)	202(81)	256(92)
$[Cy_2P(Se)H]^+$	277(33)	277(22)	277(60)	277(76)
$[CyP(Se)H]^+$	196(51)	196(55)	196(91)	196(93)
$[CyPH]^+$	115(16)	115(17)	115(11)	115(27)
$[C_6H_{10}P]^+$	112(16)	112(28)	113(13)	112(44)
$[Cy]^+$	83(100)	83(100)	83(37)	83(100)
$[R'N(H)CS]^+$	136(25)	74(74)	88(17)	-
$[PCNC]^+$	69(33)	-	69(48)	-

[a] Represented as molecular weight followed by relative abundance in parentheses

occurred for all the compounds as did the $[Ph]^+$ and $[Cy]^+$ ions, when appropriate. In the literature only a few metal complexes containing diorganophosphinothioformamides have had their electron impact mass spectra recorded making a systematic comparison difficult [77-78].

In the $R_2P(O)C(S)N(H)R'$ compounds the $[R_2P(O)H]^+$ ion was the most abundant. The protonated form of the isothiocyanate, i.e. $[R'N(H)CS]^+$, was evident in all spectra and corresponds to the cleavage of the P-C bond. Other common fragment ions were those that contained the PO grouping e.g. $[RP(O)]^+$ and $[PO]^+$.

In the mass spectra of the $R_2P(S)C(S)N(H)R'$ derivatives there was no common abundant ion. The most abundant ion in $[Ph_2P(S)C(S)N(H)Ph]$, $[Ph_2P(S)C(S)N(H)Me]$, $[Cy_2P(S)C(S)N(H)Ph]$ and $[Cy_2P(S)C(S)N(H)Me]$ was $[Ph_2P(S)H]^+$, $[MeN(H)CS]^+$, $[CyP(S)]^+$ and $[Cy]^+$, respectively. A common fragment was that of the $[RP(S)]^+$ ion which was always present at greater than 35% abundance.

For the Y = Se analogues the common fragment was assigned to the $[R_2P(Se)H]^+$ ion which was fairly abundant although there was no evidence for the $[RP(Y)]^+$ or $[PY]^+$ ions (Y = Se) as was the case for the Y = O and S compounds described above. Fragments that contained selenium had a characteristic isotopic pattern, as below, and this made the assignment of selenium-containing ions possible. For the $[Ph_2P(Se)C(S)N(H)R']$ species,

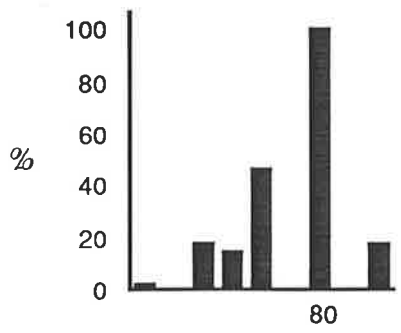

the $[Ph_2PH]^+$ ion was in very high abundance, over 90% in each case. With the exception of the $[M]^+$ and $[Ph_2P(Se)H]^+$ ions there were no other fragments that contained selenium for $Ph_2P(Se)C(S)N(H)R'$. In the spectra of the $Cy_2P(Se)C(S)N(H)R'$ compounds, however, there was an additional ion that contained selenium, namely $[CyP(Se)H]^+$ which

was present at 50% abundance or more. The $[Cy]^+$ ion was a common feature in these spectra as well. The loss of the selenium atom lead to the observation of the respective phosphorus(III) parent ions, $[Cy_2PC(S)N(H)R']^+$. Loss of a further cyclohexyl group from the parent ion resulted in the formation of the relatively abundant $[CyPC(S)N(H)R']^+$ ion.

4.6 Conclusions

The infrared and multinuclear magnetic resonance spectroscopic studies are entirely consistent with the solid state structures of the $R_2P(Y)C(S)N(H)R'$ compounds as revealed by the X-ray crystallographic study; see Chapter 3. In particular, the systematic variation in the P(1)-C(1) bond distances with the nature of R, the changes in the C(1)-S(1) and C(1)-N(1) bond distances with the nature of R' and the effect of substitution at Y were evident.

Chapter 5

THE COORDINATION CHEMISTRY OF DIORGANO-PHOSPHINO-, DIORGANOPHOSPHINYL-, DIORGANO-THIOPHOSPHINYL- AND DIORGANOSELENO-PHOSPHINYL-THIOFORMAMIDES TOWARDS GOLD

5.1 Introduction

Metal-based drugs have been used for medicinal purposes for many centuries. Gold compounds and their applications have a long history in medicine; dating back to as early as 2500 BC [79, 80]. The publication of the results in 1890 of Koch, which showed the inhibition of the growth of tubercle bacilli (*in vitro*) with gold cyanide compounds, is often cited as the beginning of gold pharmacology [81]. Diseases such as tuberculosis, lupus vulgarus, syphilis and rheumatoid arthritis have been treated, with different levels of success, with gold complexes [82, 83].

Chrysotherapy, the use of gold compounds in medicine, is largely restricted to the use of gold compounds in the treatment of rheumatoid arthritis. It is appropriate at this point to discuss the disease rheumatoid arthritis briefly. Arthritis, also known as rheumatic disease or rheumatism, is derived from 'arth' (Greek word for joint) and 'itis' (Greek word for inflammation). It is a crippling disease of the joint connective tissue which afflicts people of all ages. It is not normally a fatal disease but may be severely debilitating. Of the 150 different forms of arthritis, one of the more common manifestations is rheumatoid arthritis.

Rheumatoid arthritis is characterised by the inflammation of the synovial lining of the joint, Fig. 5.1, and is often associated with inflammation of other body tissues. Most commonly, the joints of the fingers, wrists, shoulders, knees and feet are affected.

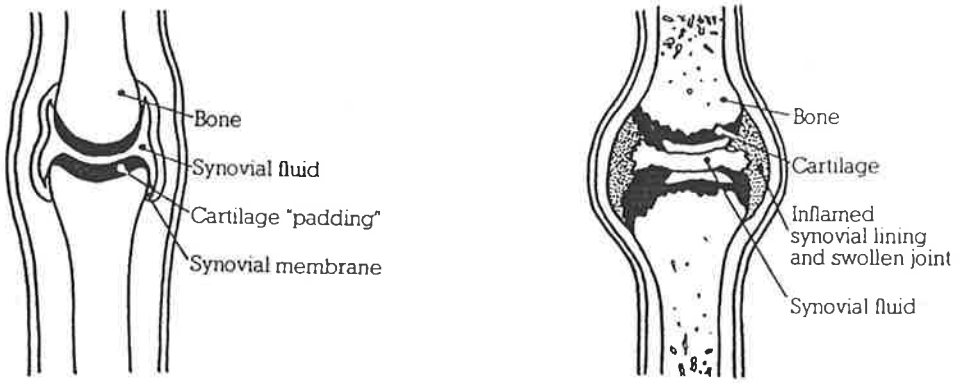

(a) Normal joint (b) Joint with rheumatoid arthritis

Fig. 5.1

Prominent in the treatment of rheumatoid arthritis are gold(I) compounds, especially gold(I) thiolates. These compounds fall into two categories: i) self-associating monomers, i.e. gold sodium thiomalate (Myochrysine, **A**), gold thioglucose (Solganol, **B**), gold sodium thiosulphate (Sanocrisin, **C**) and gold sodium thiopropanol sulphonate (Allochrysine, **D**) and ii) monomeric species i.e. *S*-2,3,4,5-tetra acetyl-1-β-D-thioglucose triethylphosphinegold(I) (Auranofin, **E**). Compounds **A-D** are polymeric, hydrophilic (due to their residual charges and/or to the presence of water solubilising substituents) and must be administered by either an intravenous or intramuscular injection, a process which is both expensive and unpleasant. By contrast to **A-D**, the other anti-arthritic drug in current clinical use, i.e. auranofin, is administered orally. The presence of the phosphine group and the tetra-acetylated thioglucose group in this complex impart lipophilic properties which are compatible with the lipophilic media found in cell membranes and, hence, the complex can be absorbed into the intestine. This oral method of administration is much easier and the more preferred. There are problems, however, with the clinically available gold drugs. Compounds **A-D** are readily excreted from the body owing to their water solubility and for compound **E** only 25% of the gold is absorbed. There are additional problems associated with these compounds in that adverse side-effects such as dermatitis, nephritis and bone marrow depletion occur in some patients [84].

The mode of action of the clinically used gold thiolates is unclear but several theories exist [85-90]. The possible mechanisms of action for myochrysine and auranofin, being representative of the two classes of drug employed in the treatment of rheumatoid arthritis, will be used to illustrate the possible modes of action.

Once administered to the vascular fluids myochrysine associates with the extracellular receptors until some of the Au-S bonds are cleaved and new Au-S bonds are formed with the major plasma protein albumin, Alb-SH, (I); see Scheme 5.1.1. The gold atom coordinates at the cysteine-34 site to form an auro-albumin monomer (II). Further reaction with more albumin leads to the formation of the auro-albumin complex (III). Both of the latter complexes, (II) and (III), are "recognised" as foreign by white blood cells, particularly macrophages, and consequently are ingested by these cells.

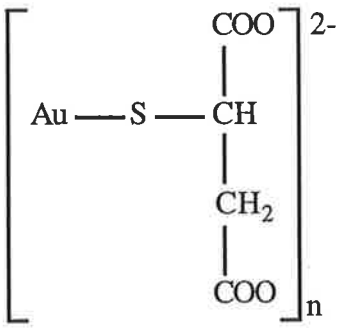

Myochrysine, **A**

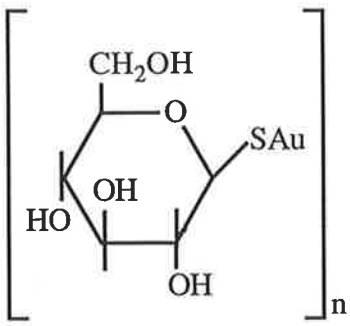

Solganol, **B**

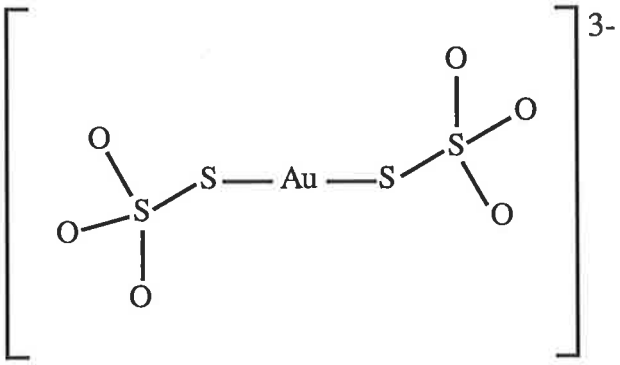

Sanocrisin, **C**

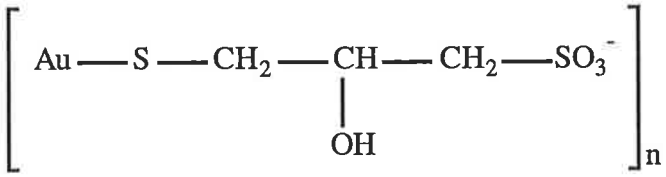

Allochrysine, **D**

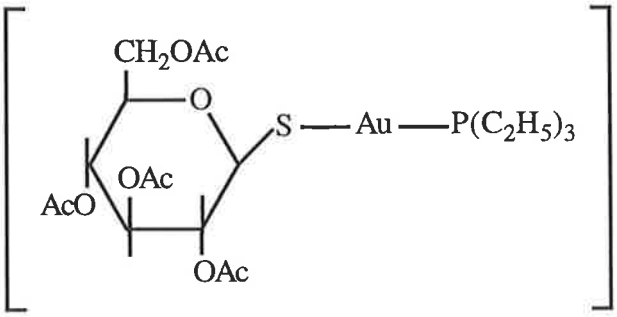

Auranofin, **E**

$$(\text{Au-SR'})_n + \text{Alb-SH} \longrightarrow \underset{\text{(I)}}{\text{Alb-S-Au-SR'}} \longrightarrow \underset{\text{(II)}}{\text{Alb-S-Au-S-Alb}} + \underset{\text{(III)}}{\text{SR'}}$$

SR' = thiomalate

Scheme 5.1.1

It is possible that these interactions with the leukocytes facilitate the targeting of the drugs to the inflamed lesion. Certainly, some directing of these gold drugs occurs, as evidenced by their effectiveness against arthritis.

The mode of action of the monomeric species auranofin would be expected to be different to that found for the polymeric gold(I) thiolate, myochrysine, owing to its different mode of administration. Model studies [89] have demonstrated that once in the vascular system, it is likely that the thiolate group of auranofin is replaced by the cysteine-34 group of albumin. The triethylphosphine group may be displaced subsequently by either another albumin cysteine-34 group or by a small thiol group, such as glutathione (Glut). Oxidation of the phosphine group, i.e. $Et_3P \longrightarrow Et_3PO$, precludes rebinding to the gold atom; see Scheme 5.1.2. The doubly coordinated gold species can thus be transported by the 'ball of protein' to the site of inflammation.

$$Et_3P\text{-Au-S-R'} \longrightarrow Et_3P\text{-Au-S-Alb} \longrightarrow \text{Glut-S-Au-S-Alb} + Et_3P{=}O$$

Scheme 5.1.2

A more recent development in chrysotherapy concerns the anti-tumour activity of gold compounds. Since the discovery of the anti-tumour activity of cisplatin, *cis* -$[(NH_3)_2PtCl_2]$, in 1969 [91], the most widely used anti-tumour drug in the Western world, many metal complexes have been investigated for any potential anti-tumour activity [91-93].

The gold(III) centre is isoelectronic with the platinum(II) centre found in cisplatin, and also forms square planar complexes. The disadvantage of the gold(III) species is that the gold centre is highly oxidising and in the reducing mammalian environment, readily disproportionates to yield metallic gold. By contrast, some gold(I) compounds have been shown to exhibit promising biological activity [94, 95]. Auranofin was tested for anti-tumour activity and was active *in vitro* and *in vivo*, against fifteen tumour models. More recently, the bis-chelated diphosphine gold(I) complex, $[Au(Ph_2P(CH_2)_2PPh_2)_2]^+$, which features an uncommon tetrahedral gold(I) centre [96], exhibited good activity but subsequent

trials have shown that it caused fatal cardiovascular breakdowns and, hence, further testing was discontinued [97]. Other phosphine gold(I) thiolates modeled on the linear P-Au-S arrangement have shown promising activity in this context. In particular, the triorganophosphine gold(I) complexes of thionucleobases are known to display good activity and reduced toxicity against a variety of cell lines both *in vitro* and *in vivo* [98]. These results confirm that the phosphinegold(I) species form a potent combination for biological activity.

Diorganophosphinothioformamides incorporate both phosphorus and sulfur atoms in the one ligand. It was thought of interest to examine what type of gold complexes could be formed with these ligands in both their protonated and deprotonated forms and to examine their biological activity; this thesis focuses only on the chemical aspects. It was also of interest to explore the interaction of the diorgano-phosphinylthioformamides, -thiophosphinylthioformamides and -selenophosphinylthioformamides with gold. Of particular interest would be the possible interaction of the $R_2P(Se)C(S)N(H)R'$ compounds with gold to examine whether a gold-selenium interaction is present as (i) there are very few such examples reported in the literature [99, 100] and (ii) selenium containing complexes are of increasing interest in terms of their biological activity [101].

Two different types of reactions were attempted with the $R_2P(Y)C(S)N(H)R'$, Y = O, S or Se, R = Ph or Cy, R' = Ph or Me, ligands. In one case, $HAuCl_4$, which has the gold atom in the +III oxidation state, was reduced to a gold(I) species and the ligand added. In the other method, the direct reaction of each ligand with the gold(I) species in the form of Ph_3PAuCl, in the presence of base to initiate the reaction, was attempted.

5.2 Reaction of Diorganophosphinothioformamides with Gold(I) Salts

5.2.1 Reaction of $R_2PC(S)N(H)R'$ with $HAuCl_4$

After the reduction of $HAuCl_4$ with thiodiglycol to a gold(I) species the phosphorus(III) ligands of the form $R_2PC(S)N(H)R'$, R = Ph or Cy and R' = Ph or Me, were added. This resulted in the formation of complexes which incorporated a central eight-membered ring system except for the R = Cy, R' = Me compound. The ligands were deprotonated and

coordinated to the gold atoms in a bidentate bridging mode *via* the phosphorus and sulfur atoms as shown in Fig. 5.2.1.

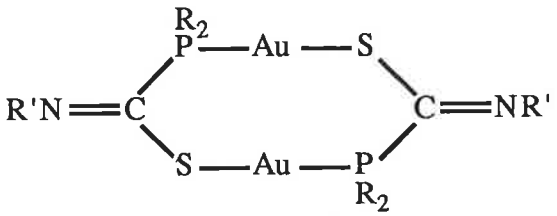

Fig. 5.2.1

The [$Cy_2PC(S)N(H)Me$] compound did not form the same cyclic eight-membered ring system in its reaction with $HAuCl_4$. As has been mentioned earlier, Chapter 4, this compound had an impurity of [$Cy_2P(O)C(S)N(H)Me$], which influenced the reaction.

5.2.2 Reaction of $R_2PC(S)N(H)R'$ with Ph_3PAuCl

The reaction between the phosphorus(III) ligands, $R_2PC(S)N(H)R'$, and Ph_3PAuCl yielded products as in 5.2.1; the reaction needed the presence of the base to initiate the process. In contrast to its reaction with $HAuCl_4$, the impure [$Cy_2PC(S)N(H)Me$] compound reacted with Ph_3AuCl to produce the $\{Au[Cy_2PC(S)NMe]\}_2$ complex which adopted the same conformation as the other cyclic bidentate bridging complexes mentioned above. The [$Cy_2P(O)C(S)N(H)Me$] impurity did not react with the gold(I) species and was removed by washing the reaction product with warm ethanol followed by ether.

5.2.3 The Spectroscopic Characterisation of $\{Au[R_2PC(S)NR']\}_2$

The spectroscopic characterisation for the four gold(I) complexes are similar and, hence, a general description will be given. The IR spectra of the cyclic complexes showed the absence of the υ(N-H) absorptions that were found in the free ligands. The absorptions of interest were due to the thioamide(I) band that occurs at about 1500 cm^{-1} in the free ligands. In the complexes these bands were found to move to higher frequencies. The thioamide(II) band found at approximately 1350 cm^{-1} in the IR spectrum of each parent ligand, was not

evident, however, a peak at about 950 cm^{-1} became apparent and was assigned to υ(C-S). The IR spectroscopic results appear below in Table 5.2.3a.

The IR spectral data indicate that the υ(C=N) bands are at higher frequencies for the R' = Me complexes by approximately 10 cm^{-1} compared with the corresponding R' = Ph complexes. By contrast the υ(C-S) absorptions for the R' = Me complexes are at lower frequencies than those for the corresponding R' = Ph complexes.

Table 5.2.3a: Selected infrared absorptions (cm^{-1}) for $\{Au[R_2PC(S)NR']\}_2$, R = Ph or Cy, R' = Ph or Me

	υ(C=N)	υ(C-S)	thioamide(I)*
$\{Au[Ph_2PC(S)NPh]\}_2$	1550	946	1528
$\{Au[Ph_2PC(S)NMe]\}_2$	1561	913	1506
$\{Au[Cy_2PC(S)NPh]\}_2$	1548	945	1502
$\{Au[Cy_2PC(S)NMe]\}_2$	1558	924	1521

* thioamide(I) band in parent ligand $R_2PC(S)N(H)R'$

These observations are consistent with a significant contribution to the overall structure of canonical form 5.2.3B for the R' = Ph complexes in addition to 5.2.3A. A similar conclusion was made for the R' = Ph and Me phosphorus(V) compounds for the same R group, Chapter 3.

5.2.3A 5.2.3B

The ^1H NMR spectrum displayed the expected resonances in the alkyl/aryl regions with the absence of the N-H resonance. For the R' = Me complexes the methyl resonance shifted downfield marginally upon coordination of the ligand. The ^{13}C NMR spectra showed the alkyl/aryl peaks in the expected regions with the C_q signals moving upfield by approximately 40 ppm with respect to the respective free ligands and there was also an increase in the magnitude of the ^1J(PC) coupling constant by a factor of approximately two. For complexes

with the same R group, it was found that the C_q resonance for the R' = Ph complexes was consistently 2.5 ppm downfield than the chemical shift found for the R' = Me complexes. This observation can be attributed to the significant contribution of canonical form 5.2.3B (see above). The $^1J(PC)$ coupling constant was invariably larger by 5.5 Hz for the R' = Me complexes. The C_a atom of the nitrogen-bound R' group moved downfield by at least 10 ppm upon coordination and there was an increase in $^3J(PC)$ coupling constant by about fifty percent with respect to the value found in the free ligand consistent with the greater π-electron density in the C(1)-N(1) bond. The ^{31}P NMR spectra showed one peak with the signal in the complex having moved downfield with respect to the free ligand, indicating coordination of the phosphorus atom to the gold centre.

The FAB mass spectra showed the presence of the molecular ion $[M]^+$ (M = $\{Au[R_2PC(S)NR']\}_2$); this was never the most abundant ion. Other peaks were fragments or aggregates of varying size, which contained gold. The ion $[M\text{-}SCNR']^+$ appeared for all complexes whereas the fragment $[Au_2S_2]^+$ appeared in three of the spectra. The major ion in each FAB spectrum was: $\{Au[Ph_2PC(S)NPh]\}_2$: $[Au(Ph_2PC(S)NPh)_2]^+$ (m/z 838); $\{Au[Ph_2PC(S)NMe]\}_2$: $[Au_2S_2]^+$ (m/z 460); $\{Au[Cy_2PC(S)NPh]\}_2$: $[M\text{-}(SCNR', Cy)]^+$ (m/z 641) and $\{Au[Cy_2PC(S)NMe]\}_2$: $[Cy_3PAu]^+$ (m/z 476). Spectroscopic results for the complexes are summarised in Table 5.2.3b.

From the spectroscopic characterisation of the complexes, it is concluded that the coordination of the ligands to the gold(I) centres is through the phosphorus and sulfur atoms. The absence of the N-H signal in the IR and ^1H NMR spectra and the relatively high value of υ(C=N) indicates deprotonation at the nitrogen atom and the presence of significant π-electron density in the CN bond. The upfield shift of the quaternary carbon compared to the free ligand and the appearance of the υ(C-S) band in the IR spectra confirm the predicted coordination mode. The spectroscopic characterisation of $\{Au[Cy_2PC(S)NMe]\}_2$ provides unequivocal evidence for the formation of this gold(I) complex with the $[Cy_2PC(S)NMe]^-$ anion and, hence, confirms the preparation of the $[Cy_2PC(S)N(H)Me]$ ligand and thereby completes the series for the four diorganophosphinothioformamides used in this thesis. The availability of suitable crystals afforded the opportunity for a structure determination of one

Table 5.2.3b: Spectroscopic data for $\{Au[R_2PC(S)NR']\}_2$, R = Ph or Cy, R' = Ph or Me

$\{Au[Ph_2PC(S)NPh]\}_2$

IR: υ(C=N) 1550 cm^{-1}; υ(C-S) 946 cm^{-1}

NMR: (chemical shifts, δ, are in ppm)

^1H: Ph_2P and PhN δ 6.90-8.08

^{13}C: Ph_2P Cα-Cδ δ 120.2-135.0; PhN C_a δ 150.8 $^3J(PC)$ 20.4 Hz, C_b-C_d δ 120.2-135.0; C_q δ 169.2 $^1J(PC)$ 65.3 Hz

^{31}P: δ 52.4

FAB*: 1340, $[M(AuPPh)]^+$ 10%; 1035, $[M]^+$ 18%; 900, $[M-(SCNPh)]^+$ 38%; 838, $[Au(Ph_2PC(S)NPh)_2]^+$ 100%; 762, [M-(Au, Ph)]$^+$ 35%; 702, $[Ph_2PAu(Ph_2PC(S)NPh)]^+$ 68%; 580, $[Au_2PPh_2]^+$ 60%; 518, $[Au(Ph_2PC(S)NPh)]^+$ 42%; 459, $[Au_2S_2]^+$ 23%; 382, $[Ph_2PAu]^+$ 95%; 320, $[(Ph_2PC(S)NPh)]^+$ 25%

$\{Au[Ph_2PC(S)NMe]\}_2$

IR: υ(C=N) 1561 cm^{-1}; υ(C-S) 913 cm^{-1}

NMR: (chemical shifts, δ, are in ppm)

^1H: Ph_2P δ 7.37-7.59; MeN δ 3.56 $^4J(PH)$ 2.63 Hz

^{13}C: Ph_2P Cα-Cδ δ 128.6-135.0; MeN C_a δ 43.6 $^3J(PC)$ 17.9 Hz; C_q δ 167.6 $^1J(PC)$ 70.8 Hz

^{31}P: δ 48.4

FAB: 1410, $[(Ph_3PAu)S]^+$ 31%; 1148, $[(Ph_3PAu)_2SAu]^+$ 14%; 911, $[M]^+$ 14%; 837, [M-(SCNMe)]$^+$ 20%; 763, $[(Ph_2PAu)_2]^+$ 10%; 722, $[(Ph_3P)_2Au]^+$ 33%; 580, $[Au_2PPh_2]^+$ 30%; 459, $[Au_2S_2]^+$ 100%; 382, $[Ph_2PAu]^+$ 40%; 258, $[(Ph_2PC(S)NMe)]^+$ 15%

$\{Au[Cy_2PC(S)NPh]\}_2$

IR: υ(C=N) 1548 cm^{-1}; υ(C-S) 945 cm^{-1}

Table 5.2.3b continued

NMR: (chemical shifts, δ, are in ppm)

^{1}H: Cy_2P δ 1.20-2.70; PhN δ 6.89-7.40

^{13}C: Cy_2P Cα δ 34.9 $^{1}J(PC)$ 25.4 Hz, Cβ-Cδ δ 26.0-29.7; PhN C_a δ 151.6 $^{3}J(PC)$ 17.8 Hz, δ C_b 128.8, C_c δ 119.8, C_d δ 124.1; C_q δ 168.3 $^{1}J(PC)$ 55.1 Hz

^{31}P: δ 76.4

FAB: 1059, $[M]^+$ 24%; 924, $[M-(SCNPh)]^+$ 22%; 821, $[M-(Cy, 2Ph)]^+$ 25%; 789, $[821-(S)]^+$ 22%; 760, $[(Cy_3P)_2Au]^+$ 37%; 726, $[Cy_2PAu(Cy_2PC(S)NPh)]^+$ 15%; 658, $[M-(3Cy, 2Ph)]^+$ 52%; 641, $[CyPAu(Cy_2PC(S)NPh)]^+$ 100%; 591, $[Cy_2PAu_2]^+$ 40%; 459, $[Au_2S_2]^+$ 28%; 426, $[Cy_2PAuS]^+$ 33%; 412, $[Au(CyPCNPh)]^+$ 84%

$\{Au[Cy_2PC(S)NMe]\}_2$

IR: υ(C=N) 1558 cm^{-1}; υ(C-S) 924 cm^{-1}

NMR: (chemical shifts, δ, are in ppm)

^{1}H: Cy_2P, δ 1.26-1.97; MeN δ 3.49, $^{4}J(PH)$ 2.76 Hz

^{13}C: Cy_2P, Cα δ 34.6 $^{1}J(PC)$ 26.0 Hz, Cβ-Cδ δ 29.6-25.5; MeN C_a δ 43.1 $^{1}J(PC)$ 15.2 Hz; C_q δ 165.8 $^{1}J(PC)$ 60.7 Hz

FAB: 935, $[M]^+$ 2%; 823, $[M-(Cy, NMe)]^+$ 4%; 820, $[(Cy_2PAu)_2S]^+$ 10%; 807, $[M-(Cy, NMe, Me)]^+$ 19%; 796, $[M-(Cy, CNMe, Me)]^+$ 20%; 578, $[Cy_2PAu(Cy_2PC(S)NMe)]^+$ 2%; 476, $[Cy_3PAu]^+$ 100%; 394, $[Cy_2PAu]^+$ 2%

---

*[m/e, assignment (intensity)]

$[M]^+$ = molecular ion $[\{Au(R_2PC(S)NR')\}_2]^+$

of these gold(I) complexes, i.e. $\{Au[Ph_2PC(S)NPh]\}_2$, which confirmed the spectroscopic analysis.

5.2.4 The Molecular Structure of $\{Au[Ph_2PC(S)NPh]\}_2$

The yellow crystals of *bis* μ–[*P*, *P*-diphenyl-*N*-phenyl-phosphinothioformamido] digold(I), $\{Au[Ph_2PC(S)NPh]\}_2$, were obtained from the slow evaporation of a chloroform solution of the compound which had been layered with ethanol. Crystals are monoclinic, space group $P2_1/n$ with unit cell dimensions a = 16.500(4), b = 13.862(1), c = 24.771(8) Å, β = 92.58(5)°, V = 5659(1) Å^3, Z = 4 and D_X = 1.871 g cm^{-3}. The structure was refined to final R = 0.040, R_w = 0.043 for 5123 reflections with $I \geq 3.0\sigma(I)$. The molecular structure of the two independent molecules, *a* and *b*, of $\{Au[Ph_2PC(S)NPh]\}_2$, are shown in Figs 5.2.4a and 5.2.4b, respectively ([14]; 20% thermal ellipsoids). Selected interatomic parameters are listed in Table 5.2.4.

The conformation of the central eight-membered rings in the two molecules, *a* and *b*, are different. In molecule *a* the structure is centrosymmetric whilst in molecule *b* two crystallographic independent ligands, b and c, which have only minor conformational differences, chelate the gold atoms. This has the consequence that 1.5 dinuclear molecules comprise the crystallographic asymmetric unit, i.e. there are three independent gold atoms and half a molecule of dichloromethane of solvation. In molecule *a* the central eight-membered ring is approximately planar while in molecule *b* the ring has a twist conformation. For molecule *a* the torsion angles S(1a)/Au(1)/Au(1)'/S(1a)' and P(1a)/Au(1)/Au(1)'/P(1a)' both of 180° and the S(1a)/Au(1)/Au(1)'/P(1a) torsion angle of 5.7° reflect the planarity of the central eight-membered ring, while the equivalent torsion angles found in molecule *b*, i.e. S(1b)/Au(2)/Au(3)/S(1c), S(1b)/Au(2)/Au(3)/P(1b), S(1c)/Au(2)/Au(3)/P(1c) and P(1b)/Au(2)/Au(3)/P(1c) of -153.5(2), 29.7(1), 23.4(2) and 153.5(1)°, respectively serve to emphasise the skewed positions of the atoms that comprise this ring. Each of the three independent gold atoms is bound by a phosphorus atom of one ligand and the sulfur atom derived from another ligand indicating the presence of bidentate

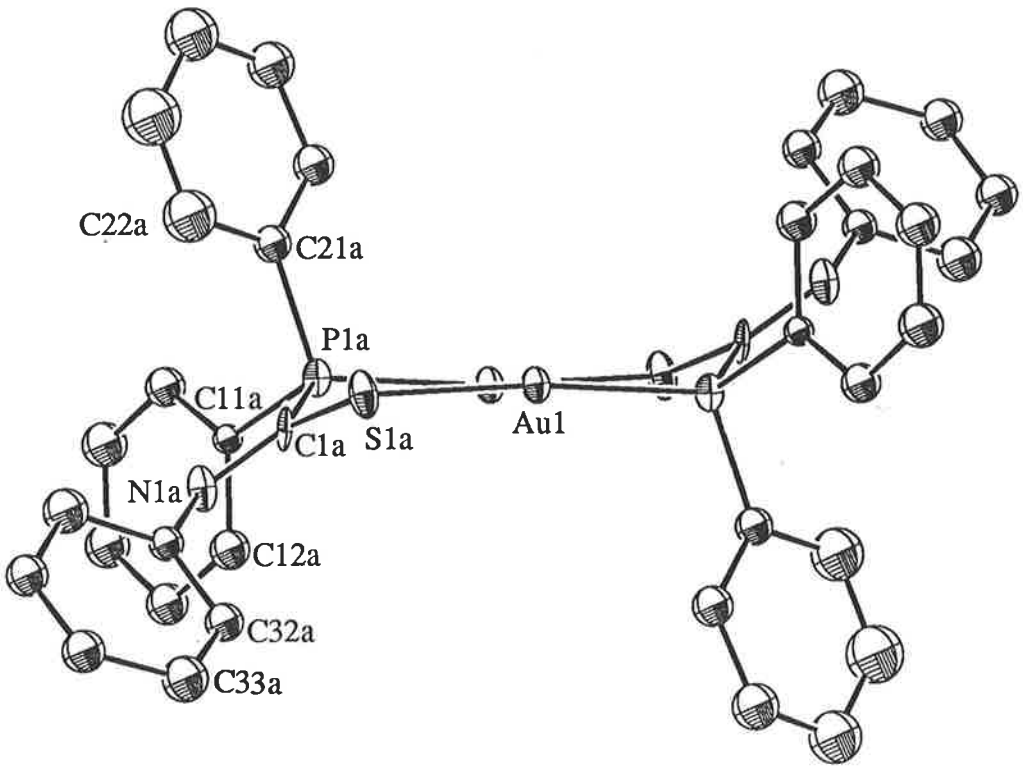

Fig. 5.2.4a The molecular structure of molecule *a* of $\{Au[Ph_2PC(S)NPh]\}_2$

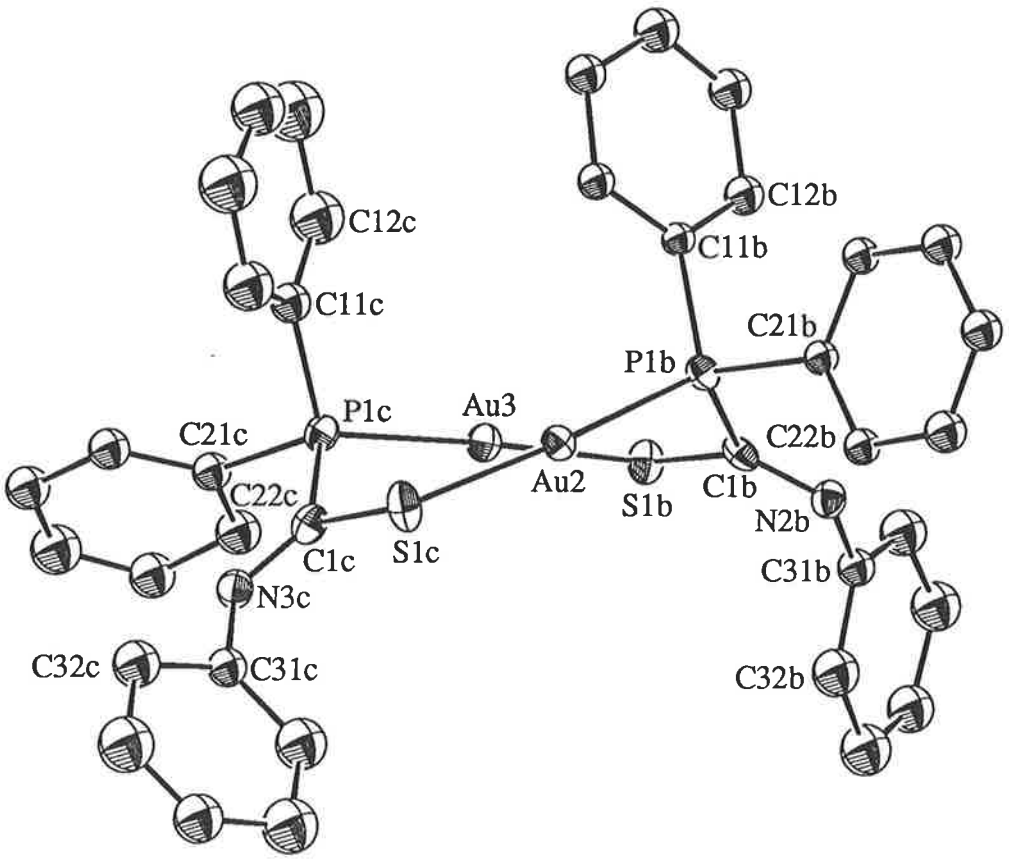

Fig. 5.2.4b The molecular structure of molecule *b* of $\{Au[Ph_2PC(S)NPh]\}_2$

Table 5.2.4: Selected bond distances (Å) and angles (deg.) for $\{Au[Ph_2PC(S)NPh]_2\}$

Au(1)-S(1a)	2.316(3)	Au(2)-S(1c)	2.305(5)
Au(3)-S(1b)	2.305(5)	Au(1)-P(1a)	2.270(4)
Au(2)-P(1b)	2.268(4)	Au(3)-P(1c)	2.272(5)
S(1a)-C(1a)	1.73(1)	S(1b)-C(1b)	1.76(1)
S(1c)-C(1c)	1.74(1)	P(1a)-C(1a)	1.84(1)
P(1b)-C(1b)	1.83(1)	P(1c)-C(1c)	1.86(2)
N(1a)-C(1a)	1.29(1)	N(1b)-C(1b)	1.28(2)
N(1c)-C(1c)	1.27(2)	N(1a)-C(31a)	1.46(2)
N(1b)-C(31b)	1.43(2)	N(1c)-C(31c)	1.42(2)
S(1a)-Au(1)-P(1a)'*	173.3(2)	S(1b)-Au(3)-P(1c)	176.4(1)
S(1c)-Au(2)-P(1b)	175.3(1)	Au(1)-S(1a)-C(1a)	107.6(4)
Au(2)-S(1c)-C(1c)	108.2(6)	Au(3)-S(1b)-C(1b)	104.4(6)
Au(1)-P(1a)-C(1a)	116.3(4)	Au(2)-P(1b)-C(1b)	110.0(5)
Au(3)-P(1c)-C(1c)	111.1(5)	S(1a)-C(1a)-P(1a)	119.4(7)
S(1b)-C(1b)-P(1b)	117.5(9)	S(1c)-C(1c)-P(1c)	117(1)
S(1a)-C(1a)-N(1a)	127(1)	S(1b)-C(1b)-N(1b)	125(1)
S(1c)-C(1c)-N(1c)	127(1)	P(1a)-C(1a)-N(1a)	113.9(9)
P(1b)-C(1b)-N(1b)	117(1)	P(1c)-C(1c)-N(1c)	116(1)
C(1a)-N(1a)-C(31a)	123(1)	C(1b)-N(1b)-C(31b)	120(1)
C(1c)-N(1c)-C(31c)	121(1)	C(11a)-P(1a)-C(21a)	103.7(8)
C(11b)-P(1b)-C(21b)	103.6(6)	C(11c)-P(1c)-C(21c)	107.0(7)

* Primed atom related by crystallographic centre of inversion

bridging ligands. The range of the P-Au-S angles of 173.3(2) to 176.4(1)° indicate almost linear coordination geometries at the gold atoms as expected.

As has been noted for other gold(I) complexes [102-106], the usual short Au-Au separations of approximately 3 Å are also observed in $\{Au[Ph_2PC(S)NPh]\}_2$. In molecule *a*, the centrosymmetrically related gold atoms have an intramolecular separation of 2.925(2) Å while in molecule *b* the distance between the two gold atoms of the eight-membered ring is 2.919(2) Å. These separations compare fairly well with those found in closely related cyclic gold(I) compounds that feature SAuP arrangements. In the nine-membered ring system of $\{Au_2$ μ-[i-MNT] μ-[dppee]} (i-MNT is 1,1-dicyanoethene-2,2 dithiolate and dppee is bis(diphenylphosphinoethylene) [107], the intramolecular separation is 2.867(1) Å and in the ten-membered ring system $\{AuS(CH)_2PEt_2\}_2$, [108], the intramolecular separation is 3.104(1) Å. In $\{Au[Ph_2PC(S)NPh]\}_2$ there is also an intermolecular separation of 3.145(1) Å between the Au(1) and Au(2) atoms. The Au...Au separations in $\{Au[Ph_2PC(S)NPh]\}_2$ are marginally longer than the value for metallic gold of 2.884 Å and these types of interactions have been attributed to relativistic effects [109]. The closest contact between non-hydrogen atoms (and not involving gold atoms) is between the C(22c) and C(36a)' atoms of 3.32(2) Å (symmetry operation: $-x$, $1-y$, $-z$) while the closest contact involving a hydrogen atom is 2.490 Å between atoms N(1b) and H(142) (symmetry operation: $+x$, $+y$, $+z$). This distance is very short and indicative of some kind of weak interaction between the main molecule and the solvent dichloromethane from which the hydrogen atom is derived. The unit cell contents are shown in Fig. 5.2.4c.

The Au-S bond distances lie in a narrow range, i.e. 2.305(5)-2.316(3) Å, and indeed are equal within experimental error. A similar observation was noted for the Au-P separations which lie in the range of 2.268(4)-2.272(5) Å. The Au-S distances lie in the range of 2.301(1)-2.339(6) Å, i.e. for Au-S interactions found in other phosphine-gold(I) complexes containing thiolate functions [110-112] and similarly, the Au-P separations occur in the range 2.226(3)-2.277(2) Å [110-112]. Clearly, the incorporation of the PAuS grouping into a cyclic system such as found for $\{Au[Ph_2PC(S)NPh]\}_2$ does not have a great influence on the magnitude of the Au-S and Au-P separations.

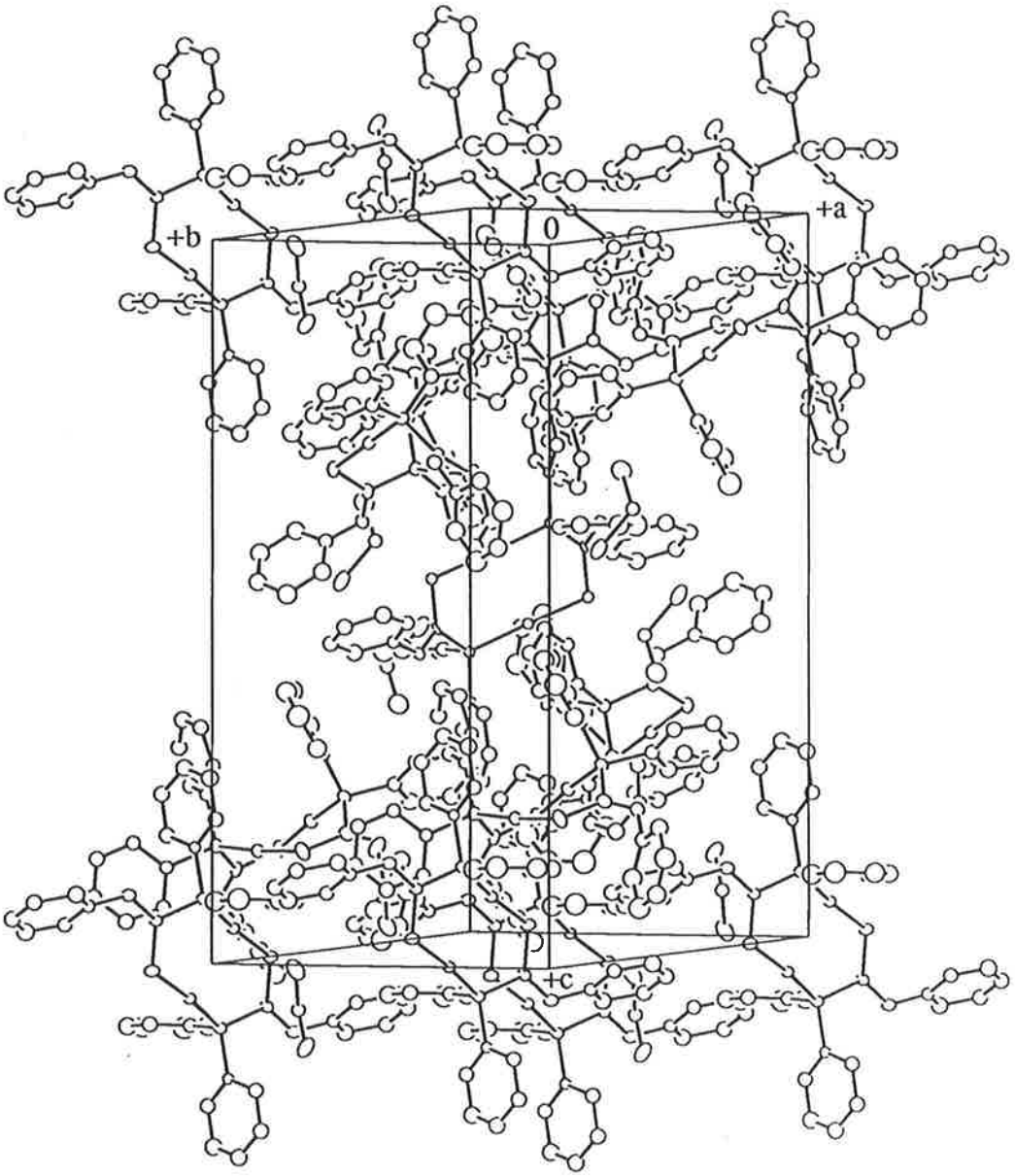

Fig. 5.2.4c The unit cell contents for $\{Au[Ph_2PC(S)NPh]\}_2$

The S(1)-C(1), P(1)-C(1) and N(1)-C(31) separations are indicative of single bond character for these bonds while the C(1)-N(1) separation is suggestive of a formal double bond between these atoms. The atoms of the central chromophore of the ligand, i.e. P(1)/C(1)/S(1)/N(1)/C(31) are approximately planar as can be seen in the following torsion angles: ligand a: S/C(1)/N/C(31) -4(2)° and P/C(1)/N/C(31) 177(1)°, ligand b: S/C(1)/N/C(31) -1(2)° and P/C(1)/N/C(31) 177(1)° and ligand c: S/C(1)/N/C(31) -7(2)° and P/C(1)/N/C(31) 175(1)°. The greatest difference between the two independent molecules are found in the Au-P(1)-C(1) and S(1)-C(1)-N(1) angles. In molecule *a* the Au-P(1)-C(1) angle is approximately 5 and 6° larger than the equivalent angles found for ligands b and c of molecule *b*, respectively. The angles about the C(1) atom are comparable to those found in the free ligand except for the S(1)-C(1)-N(1) angle in ligand a, which is approximately 10° less than that found for the free ligand.

At the completion of this work, Professor R. Kramolowsky (University of Hamburg) indicated that the crystal structure of the closely related derivative $\{Au[Ph_2PC(S)NMe]\}_2$ had been determined independently in his laboratories. These results have not appeared in the open literature. Indeed, similar overlap occurred with the structures of *trans*-$\{Ni[Cy_2PC(S)NPh]_2\}$ (Section 6.1.4b) and $\{Cd[Cy_2P(Se)C(S)NPh]_2\}$ (Section 6.4.2b). These, too, have not been published in the literature.

The molecular geometry of $\{Au[Ph_2PC(S)NMe]\}_2$ is virtually the same as reported above for $\{Au[Ph_2PC(S)NPh]\}_2$, however, the relatively high errors associated with the light atom parameters preclude a detailed comparison of the structures.

5.3 Reaction of Diorganophosphinylthioformamides with Gold(I) Salts

5.3.1 Reaction of $R_2P(O)C(S)N(H)R'$ with $HAuCl_4$

Reaction of the $Ph_2P(O)C(S)N(H)R'$, R' = Ph or Me, and $[Cy_2P(O)C(S)N(H)Ph]$ compounds with the $HAuCl_4$ species (after reduction with thiodiglycol) did not produce any type of gold complexes containing these ligands. As has been mentioned earlier, the $[Cy_2PC(S)N(H)Me]$ ligand was not isolated in pure form and contained some of the oxygen analogue, i.e.$[Cy_2P(O)C(S)N(H)Me]$. The complex that was isolated from the reaction

between the reduced $HAuCl_4$ species and impure $[Cy_2PC(S)N(H)Me]$ was $\{Au[Cy_2P(O)C(S)N(H)Me]Cl\}$, so in actual fact the $[Cy_2P(O)C(S)N(H)Me]$ ligand reacted with the gold(I) species.

5.3.2 Reaction of $R_2P(O)C(S)N(H)R'$ with Ph_3PAuCl

Under the reaction conditions employed, the $R_2P(O)C(S)N(H)R'$ derivatives did not react with the gold(I) species, Ph_3PAuCl (in the presence of Et_3N). Characterisation of the species recovered from the reaction mixtures revealed that they were the initial reactants, hence, no new gold complexes had formed.

5.3.3 The Spectroscopic Characterisation of $\{Au[Cy_2P(O)C(S)N(H)Me]Cl\}$

The IR spectrum of $\{Au[Cy_2P(O)C(S)N(H)Me]Cl\}$ shows two absorptions at 3114 and 3041 cm^{-1}, assigned to υ(N-H), compared to 3065 and 3025 cm^{-1} for the free ligand. The absorption due to υ(C=N), i.e. 1561 cm^{-1}, was found to shift to higher frequency in the complex compared to that of the free ligand (1526 cm^{-1}). The υ(P=O) absorptions were found at 1176, 1165 and 1150 cm^{-1} compared to 1180 cm^{-1} in the free ligand. In the FAB mass spectrum the molecular ion was observed ($[M]^+$, m/z 520, relative abundance 32%, M = $\{Au[Cy_2P(O)C(S)N(H)Me]Cl\}$), and the major fragment in the low molecular weight region was assigned to $[M-Cl]^+$ (484, 79%). The most abundant fragment in the spectrum was found in the high molecular weight region at m/z 771 and was assigned to $[Au(Cy_2P(O)C(S)N(H)Me)_2H]^+$. In the ^1H NMR spectrum the expected resonances and integrations were observed and no evidence was found for the N-H proton. Similarly, the ^{13}C NMR spectrum showed the expected resonances with the quaternary carbon atom occurring as a doublet centred at δ 195.3 ppm with ^1J(P-C) 51.0 Hz; this has shifted 2.5 ppm upfield compared to the free ligand. In the ^{31}P NMR spectrum there is one resonance at δ 57.8 ppm which is shifted downfield by approximately 9 ppm compared to the free ligand. A summary of the spectroscopic results can be found in Table 5.3.3. Whereas the

Table 5.3.3: Spectroscopic data for {Au[$Cy_2P(O)C(S)N(H)Me$]Cl}

IR: υ(C=N) 1561 cm^{-1}, υ(C-S) 946 cm^{-1}, υ(P=O) 1176, 1165 and 1150 cm^{-1}

NMR: (chemical shifts, δ, are in ppm)

^1H: Cy_2P δ 1.18-2.78; MeN δ 3.57 (broad)

^{13}C: Cy_2P: Cα δ 36.3 $^1J(PC)$ 64.3 Hz, Cβ-Cδ δ 25.5-26.1; MeN δ 34.8 (broad);

C_q δ 195.3 $^1J(PC)$ 51.0 Hz

^{31}P: δ 57.8

FAB*: 771, $[Au(Cy_2P(O)C(S)N(H)Me)_2H]^+$ 100%; 637, $[M(P(O)CSNC)]^+$ 42%; 520, $[M]^+$ 32%; 484, $[M\text{-}Cl]^+$ 79%; 468, [M-(Cl, O)]$^+$ 21%; 459, $[Au_2S_2]^+$ 47%; 411, $[Cy_2P(O)Au]^+$ 23%

*[m/e, assignment (intensity)]

$[M]^+$ = molecular ion $[Au(Cy_2P(O)C(S)N(H)Me)Cl]^+$

spectroscopic results indicate the coordination of the ligand the unambiguous structure determination was achieved by a single-crystal structure analysis.

5.3.4 The Molecular Structure of {Au[$Cy_2P(O)C(S)N(H)Me$]Cl}

The pale-green crystals of *P, P*-dicyclohexylphosphinyl-N-methyl-thioformamido gold(I) chloride, {Au[Cy_2P(O)C(S)N(H)Me]Cl}, were obtained from the slow evaporation of a dichloromethane solution of the compound. Crystals are monoclinic, space group $P2_1$ with unit cell dimensions a = 18.507(4), b = 12.204(2), c = 18.513(6) Å, β = 117.69(2)°, V = 3702(1) Å^3, Z = 8 and D_x = 1.865 g cm^{-3}. The structure was refined to final R = 0.042, R_w = 0.034 for 4106 reflections with $I \geq 3.0\sigma(I)$. The structure is unusual in that there are four molecules in the crystallographic asymmetric unit for the acentric space group $P2_1$; this choice was supported by the distribution of the E statistics. The centrosymmetric equivalent, i.e. $P2_1/m$, would require two molecules in the asymmetric unit, however, an analysis of the data did not show the presence of additional symmetry [39].

Non-hydrogen atoms were refined with anisotropic thermal parameters except for the cyclohexyl ring atoms C(21d) - C(26d), for which some disorder was noted, and several other carbon atoms which refined with non-positive definite values when treated anisotropically. The disordered ring was modeled such that there were two sites for the C(23d) to C(26d) atoms, each with a site occupancy factor 0.5. The hydrogen atoms were included in the model in their calculated positions (C-H 0.97 Å, N-H 0.95 Å) except those in the disordered group. The absolute configuration was determined on the basis of the refinement of the opposite hand which yielded markedly higher residuals.

The structure determination confirms the stoichiometry of the complex as {Au[Cy_2P(O)C(S)N(H)Me]Cl} and shows it to be an adduct of AuCl with the neutral [Cy_2P(O)C(S)N(H)Me] ligand. Although there are four independent molecules of {Au[Cy_2P(O)C(S)N(H)Me]Cl} in the asymmetric unit, there are only minor conformational differences between them. The molecular structures of the four independent molecules of {Au[Cy_2P(O)C(S)N(H)Me]Cl} showing the numbering scheme employed are shown in Figs 5.3.4a to 5.4.3d and selected interatomic parameters are listed in Table 5.3.4.

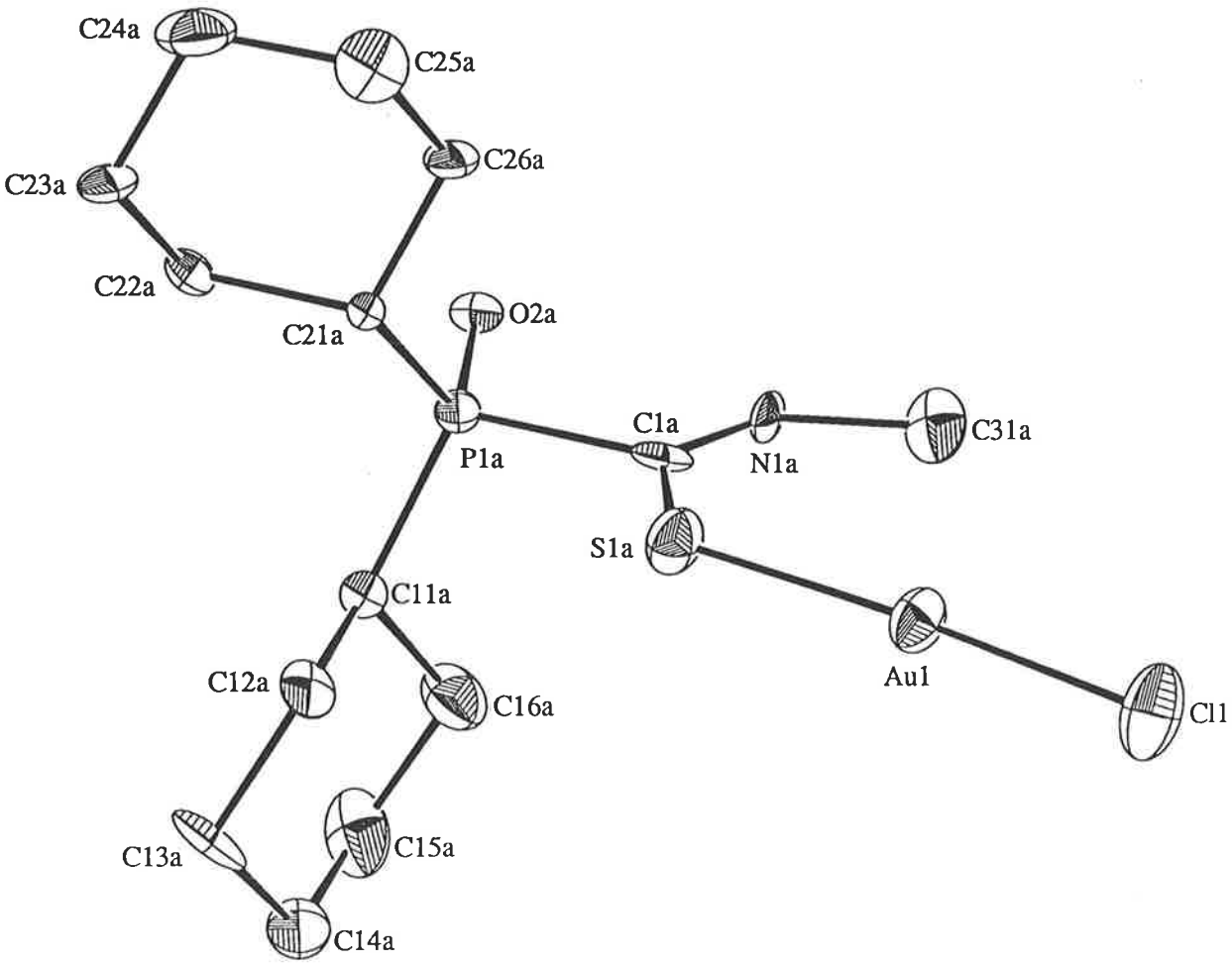

Fig. 5.3.4a The molecular structure of molecule *a* of {Au[$Cy_2P(O)C(S)N(H)Me$]Cl}

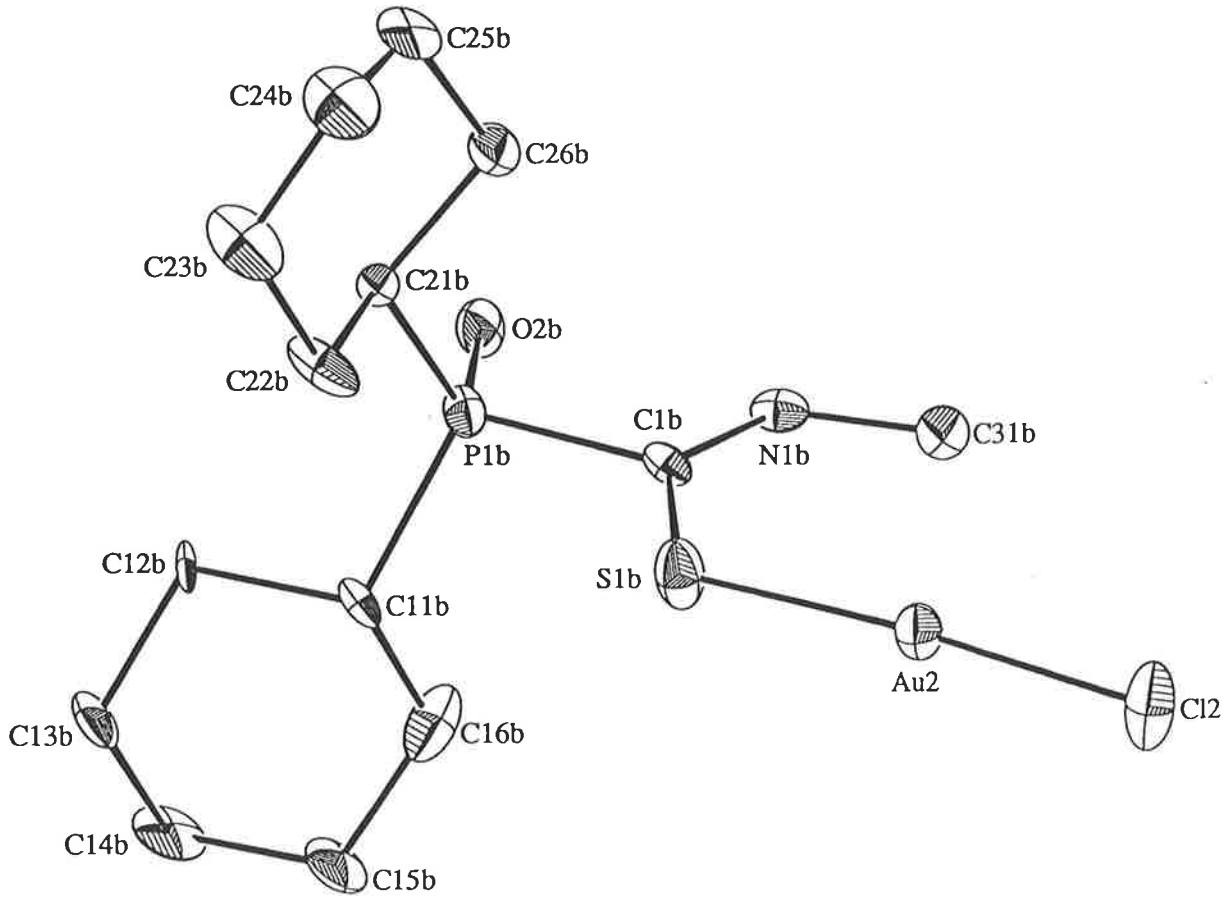

Fig. 5.3.4b The molecular structure of molecule *b* of {Au[Cy_2P(O)C(S)N(H)Me]Cl}

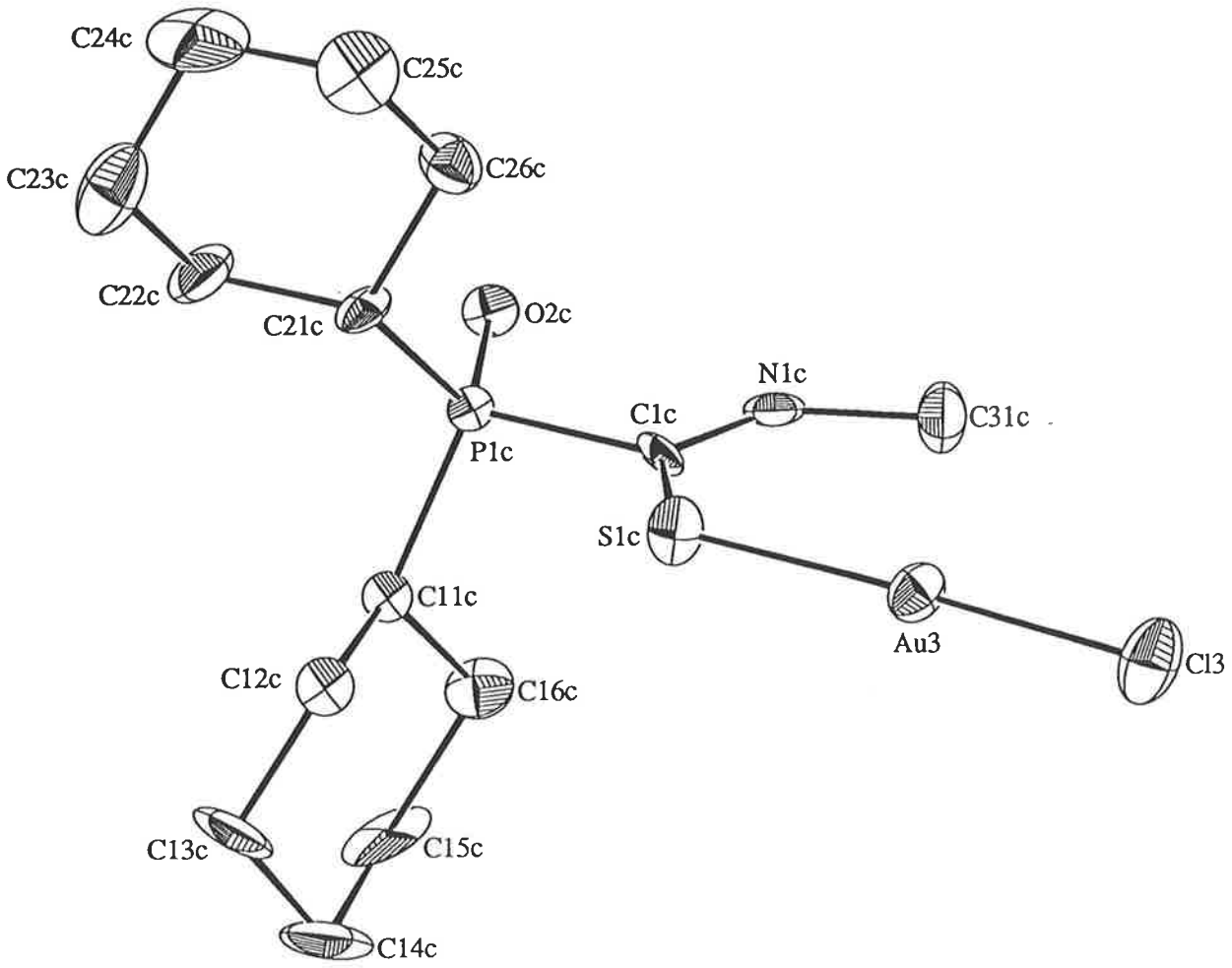

Fig. 5.3.4c The molecular structure of molecule *c* of {Au[Cy_2P(O)C(S)N(H)Me]Cl}

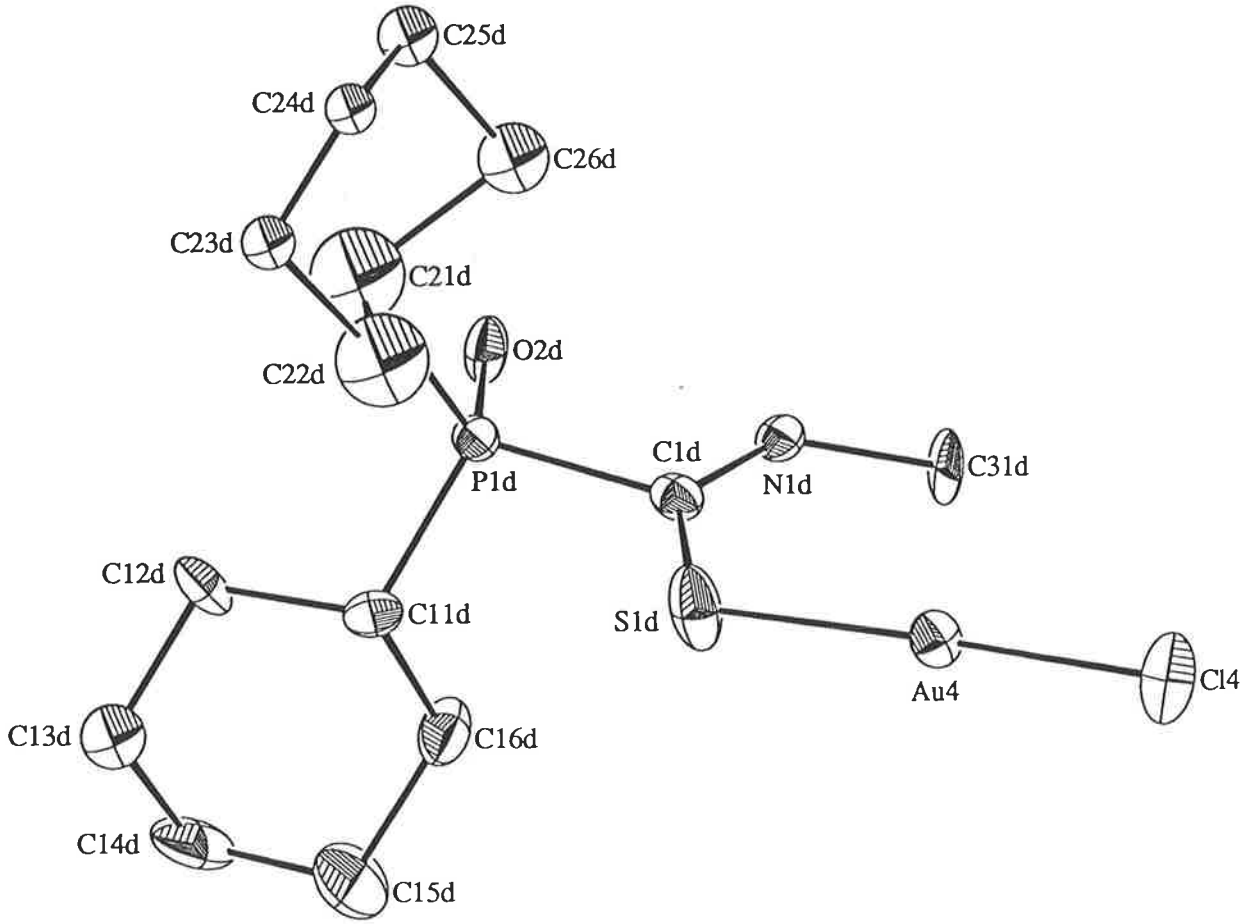

Fig. 5.3.4d The molecular structure of molecule *d* of {Au[Cy_2P(O)C(S)N(H)Me]Cl}

Table 5.3.4: Selected bond distances (Å), angles and torsion angles (deg.) for {Au[Cy_2P(O)C(S)N(H)Me]Cl}

Atoms	molecule *a*	molecule *b*	molecule *c*	molecule *d*
Au-Cl	2.242(7)	2.221(6)	2.231(6)	2.216(6)
Au-S(1)	2.227(6)	2.198(6)	2.218(6)	2.213(7)
S(1)-C(1)	1.68(2)	1.67(2)	1.66(2)	1.65(2)
P(1)-O(2)	1.50(1)	1.47(1)	1.49(1)	1.43(1)
P(1)-C(1)	1.84(2)	1.85(2)	1.79(2)	1.85(2)
N(1)-C(1)	1.28(3)	1.31(2)	1.30(2)	1.30(2)
Cl-Au-S(1)	175.6(3)	175.0(3)	176.9(3)	176.2(3)
Au-S(1)-C(1)	114.9(9)	115.4(8)	116.1(7)	115.2(8)
S(1)-C(1)-P(1)	116(1)	116(1)	119(1)	117(1)
S(1)-C(1)-N(1)	132(2)	130(2)	129(2)	132(2)
P(1)-C(1)-N(1)	112(2)	114(1)	112(2)	111(2)
C(1)-N(1)-C(31)	129(2)	128(2)	131(2)	125(2)
Au/S(1)/C(1)/P(1)	172.6(8)	-179.2(8)	176.8(9)	-169.8(9)
Au/S(1)/C(1)/N(1)	-6(3)	3(3)	-7(3)	9(3)
S(1)/C(1)/P(1)/O(2)	171(1)	-175(1)	168(1)	-177(1)

The [$Cy_2P(O)C(S)N(H)Me$] ligand coordinates the gold atom *via* the sulfur atom exclusively (Au-S range: 2.198(6) to 2.227(6) Å), there being no significant interactions between any of the remaining atoms of the ligand and the gold atom. Indeed, the conformation of the ligand is such as to place the N(H)Me portion of the molecule, rather than the $Cy_2P{=}O$ atoms, in close proximity to the gold atom; this orientation facilitates the formation of intermolecular hydrogen-bonding (see later). The central PC(1)SN chromophore and the gold atom form an essentially planar grouping in molecule *b* whereas there are significant deviations from planarity for molecules *a*, *c* and *d* as can be seen from the torsion angles involving these atoms, Table 5.3.4. The coordination about the gold atom is completed by the chloride atom (Au-Cl range: 2.216(6) to 2.242(7) Å) thereby defining a linear gold atom geometry (S-Au-Cl range: 175.0(3) to 176.9(3)°). The Au-S(1)-C(1) angles lie in the range 114.9(9) to 116.1(7)° which are approximately 10° greater than that found in related systems [96, 114-116] In the latter systems, there is either a close intramolecular Au...N or Au...S interaction in addition to the primary Au-S bond which results in the contraction of the Au-S(1)-C(1) angle. The expansion of the Au-S(1)-C(1) angle in the present structure is consistent with the absence of a significant interaction with the remaining portion of the ligand and the gold atom. Further, the widest angle subtended at the C(1) atom is the S(1)-C(1)-N(1) angle, presumably to minimise steric repulsions.

The S(1)-C(1)-N(1) angles are also wider than the comparable angle of 126.0(3)° found in the structure of the free ligand, Section 3.1.4. This expansion results in a contraction of the S(1)-C(1)-P(1) angles in the complex by approximately 5° compared to the free ligand. The overall planarity of the central SC(N)PO moiety in the free ligand is maintained in the complex and is consistent with the delocalisation of π-electron density over these atoms. Unfortunately, the relatively high errors associated with the derived parameters in the structure of {Au[$Cy_2P(O)C(S)N(H)Me$]Cl} precludes a detailed analysis of the electronic structures of the coordinated and uncoordinated ligands.

Molecules of {Au[$Cy_2P(O)C(S)N(H)Me$]Cl} associate in the lattice *via* hydrogen-bonding contacts. Pairs of molecules associate *via* the oxo functions and the amide protons as illustrated in Fig. 5.3.4e for molecules *a* and *d*; similar associations occur for molecules *b*

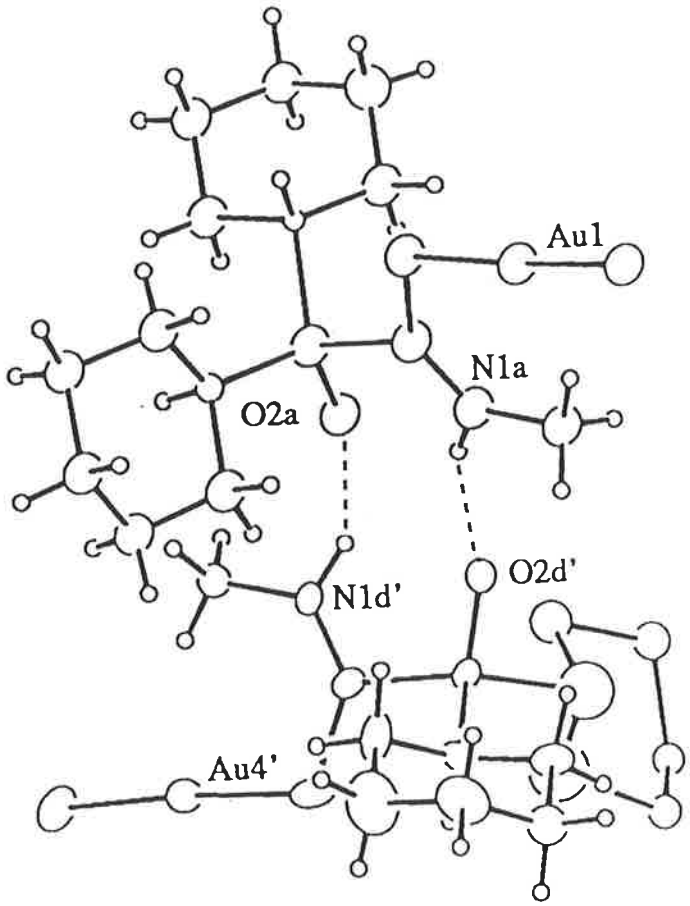

Fig. 5.3.4e Mode of association between symmetry related molecules *a* and *d* of {Au[Cy_2P(O)C(S)N(H)Me]Cl}

and *c*. The oxo function of one molecule is connected to the N-H atom of a symmetry related molecule such that O(2a)...H(4)^{I} is 1.81 Å (O(2a)...N(1d) 2.66(2) Å, the O(2a)...H(4)-N(1d) angle is 145°, symmetry operation: 1-*x*, -0.5+*y*, 2-*z*), O(2b)...H(3)^{II} is 1.85 Å (O(2b)...N(1c) 2.67(2) Å, O(2b)...H(3)-N(1c) is 140°, symmetry operation: +*x*, -1+*y*, +*z*), O(2c)...H(2)^{III} is 1.86 Å (O(2c)...N(1b) 2.73(2) Å, O(2c)...H(2)-N(1b) is 148°, symmetry operation: +*x*, 1+*y*, +*z*) and O(2d)...H(1)^{IV} is 1.86 Å (O(2a)...N(1a) 2.70(2) Å, O(2d)...H(1)-N(1a) is 143°, symmetry operation: 1-*x*, 0.5+*y*, 2-*z*). Similar associations between the molecules are found in the structure of the free ligand [$Cy_2P(O)C(S)N(H)Me$]. The unit cell contents for {Au[$Cy_2P(O)C(S)N(H)Me$]Cl} are shown in Fig. 5.3.4f.

5.4 Reaction of Diorganothiophosphinylthioformamides with Gold(I) Salts

5.4.1 Reaction of $R_2P(S)C(S)N(H)R'$ with $HAuCl_4$ and Spectroscopic Characterisation

$R_2P(S)C(S)N(H)R'$, R = Ph or Cy, R' = Ph or Me, were reacted with $HAuCl_4$ after it had been reduced with thiodiglycol. The $Cy_2P(S)C(S)N(H)R'$ compounds did not form any new products. The $Ph_2P(S)C(S)N(H)R'$ compounds, however, formed complexes which were air-stable and insoluble in most organic solvents and water. From the limited spectroscopic results obtained it was tentatively concluded that these latter complexes were polymeric species with the structural unit $\{Au[Ph_2P(S)C(S)NR']\}_\infty$. From the IR spectra of these complexes the absence of the υ(N-H) band suggests deprotonation of the nitrogen atom and the increased frequency for the thioamide(I) absorption band suggests that there is an increase in the bond order of the C(1)-N(1) bond. The thioamide(II) absorption is not evident in the 1350 cm^{-1} region but an absorption band attributed to υ(C-S) appeared and there is a slight decrease in frequency of the υ(P=S) band. The spectroscopic data suggests coordination of the thiocarbonyl sulfur atom to the gold(I) centre and perhaps an association of the thiophosphinyl sulfur atom with gold. No solution spectroscopy could be obtained due to the insolubility of the complexes. FAB mass spectra were recorded for these complexes which gave evidence for the basic {Au[$Ph_2P(S)C(S)NR'$]} unit. The presence of high molecular weight, high nuclearity clusters involving up to four gold atoms were also noted. The molecular fragment $[(Ph_3PAu)_3S]^+$ was seen in the complexes at various

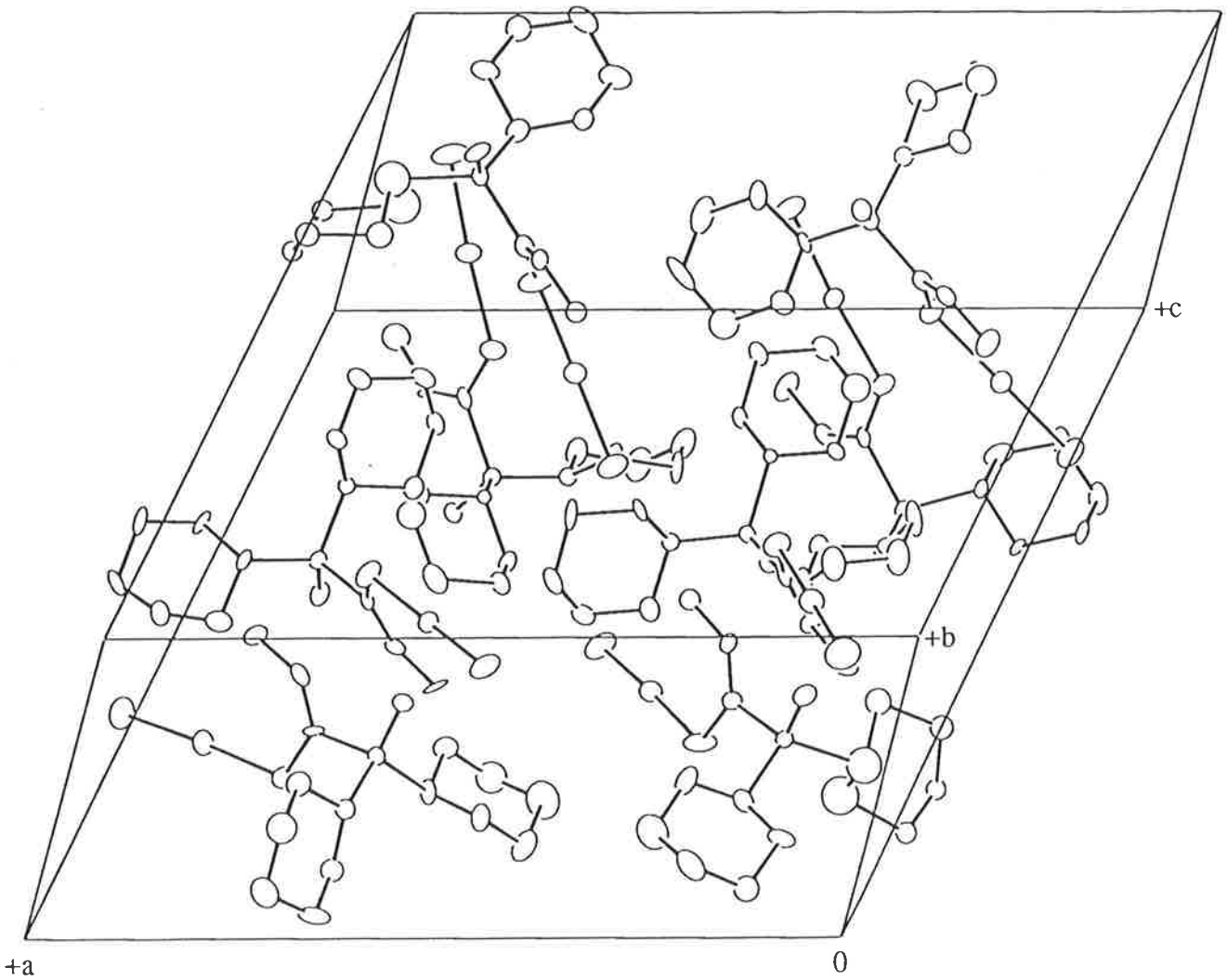

Fig. 5.3.4f The unit cell contents for {Au[Cy_2P(O)C(S)N(H)Me]Cl}

abundances and has been observed previously for similar systems [112]. This ion was the most abundant ion for $\{Au[Ph_2P(S)C(S)NMe]\}_\infty$. The most abundant ion in the FAB mass spectrum of $\{Au[Ph_2P(S)C(S)NPh]\}_\infty$ was assigned to the deprotonated ligand $[(Ph_2P(S)C(S)NPh)]^+$. Selected spectroscopic parameters are listed in Table 5.4.1.

5.4.2 Reaction of $R_2P(S)C(S)N(H)R'$ with Ph_3PAuCl and Spectroscopic Characterisation

The mixing of each $R_2P(S)C(S)N(H)R'$ derivative with Ph_3PAuCl did not result in an immediate reaction. When the base (Et_3N) was added the colour of the initial solution faded, indicating that some reaction had occurred. After filtration of the solution to remove Et_3NHCl, the solvent was removed until an oily residue remained which was solidified on addition of petroleum spirit. In the IR spectra of these complexes there was an indication that there was some kind of interaction of the thiocarbonyl sulfur atom with the gold atom as evidenced by the position of the thioamide(II) band which was not in the characteristic region found for the free ligands. Instead, a band attributed to υ(C-S) was identified occurring in the region 950 ± 20 cm^{-1}. The υ(N-H) absorption band was absent indicating that the ligand was deprotonated. Additional phenyl absorption bands derived from the triphenylphosphine moiety were observed located at 1591, 1480 and 1435 cm^{-1}.

Addition of any chlorinated solvent to the complexes thus formed, resulted in minute traces of elemental gold being precipitated and a dark orange solution. This observation indicated decomposition of the complex and, hence, solution spectroscopy could not be attempted. On standing of a chloroform solution of the product obtained from the reaction of Ph_3PAuCl and $[Ph_2P(S)C(S)N(H)Me]$, yellow crystals were obtained which were shown by X-ray structural analysis (unpublished results) to be $\{Au(S_2PPh_2)\}_2$, a gold(I) dithiophosphinate.

The FAB mass spectral results did not show the presence for the molecular ion. The main ions corresponded to certain fragments that contained mainly gold, sulfur and tri- or di-organophosphine, which are attributes of the decomposition product. Selected spectroscopic parameters are listed in Table 5.4.2. With these limited spectroscopic observations a

Table 5.4.1: Spectroscopic data for $\{Au[Ph_2P(S)C(S)NPh]\}_\infty$, R = Ph or Cy, R' = Ph or Me

$\{Au[Ph_2P(S)C(S)NPh]\}_\infty$

IR: υ(C=N) 1578 cm^{-1}; υ(C-S) 923 cm^{-1}; υ(P=S) 604 cm^{-1}

FAB*: 1439, $[(Ph_2P(S)Au)_3Au]^+$ 5%; 1025, $[M\text{-}Ph]^+$ 15%; 760, $[M\text{-}(AuS_2, Ph)]^+$ 22%; 657, $[M(PPh)]^+$ 12%; 550, $[Au(Ph_2P(S)C(S)NPh)]^+$ 7%; 459, $[Au_2S_2]^+$ 18%; 352, $[Ph_2P(S)C(S)NPh]^+$ 100%

$\{Au[Ph_2P(S)C(S)NMe]\}_\infty$

IR: υ(C=N) 1575 cm^{-1}; υ(C-S) 954 cm^{-1}; υ(P=S) 598 cm^{-1}

FAB: 1428, $[1.5(Au(Ph_2P(S)C(S)NMe)\text{-}S]^+$ 13%; 1410, $[(Ph_3PAu)_3S]^+$ 100%; 950, $[(Ph_3PAu)_2S]^+$ 7%; 777, $[Au(Ph_2P(S)C(S)NMe)_2]^+$ 2%; 721, $[(Ph_3P)_2Au]^+$ 14%

*[m/e, assignment (intensity)]

[M] = ion corresponds to $\{Au(Ph_2P(S)C(S)NPh)\}_2$

Table 5.4.2: Spectroscopic data for {$Ph_3PAu[R_2P(S)C(S)NR']$}, R = Ph or Cy, R' = Ph or Me

{$Ph_3PAu[Ph_2P(S)C(S)NPh]$}

IR: υ(C=N) 1533 cm^{-1}; υ(C-S) 941 cm^{-1}; υ(P=S) 637 cm^{-1}

FAB*: 811, $[M]^+$ 10%; 721, $[(Ph_3P)_2Au]^+$ 92%; 676, $[M-(SCNPh)]^+$ 36%; 594, $[M-(Ph_2PS)]^+$ 7%; 459, $[Au_2S_2]^+$ 100%; 382, $[Ph_2PAu]^+$ 3%.

{$Ph_3PAu[Ph_2P(S)C(S)NMe]$}

IR: υ(C=N) 1520 cm^{-1}; υ(C-S) 973 cm^{-1}; υ(P=S) 638 cm^{-1}

FAB: 890, $[Ph_3PAu(Ph_2P(S)C(S)NMe)(PhPS)]^+$ 10%; 459, $[Au_2S_2]^+$ 100%;

{$Ph_3PAu[Cy_2P(S)C(S)NPh]$}

IR: υ(C=N) 1524 cm^{-1}; υ(C-S) 960 cm^{-1}; υ(P=S) 617 cm^{-1}

FAB: 823, $[M]^+$ 10%; 721, $[(Ph_3P)_2Au]^+$ 23%; 688, $[M-(SCNPh)]^+$ 17%; 606, $[M-(Ph_2PS)]^+$ 11%; 459, $[Au_2S_2]^+$ 100%

{$Ph_3PAu[Cy_2P(S)C(S)NMe]$}

IR: υ(C=N) 1538 cm^{-1}, υ(C-S) 931 cm^{-1}, υ(P=S) 619 cm^{-1}

*[m/e, assignment (intensity)]

[M] = ion corresponds to $[Ph_3PAu(R_2P(S)C(S)NR')]$

tentative structure can be proposed with monodentate coordination of the thiocarbonyl sulfur atom to the gold centre, i.e. $Ph_3PAu\text{-}SC(NR')P(S)R_2$.

For the R, R' = Ph complex the absorption band attributed to C=N, i.e. thioamide(I), decreased in value compared to the parent ligand, which may be explained in terms of the close approach of the nitrogen atom to the gold atom as represented in 5.4.2A.

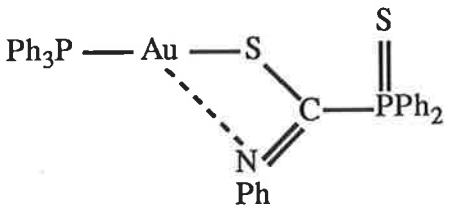

5.4.2A

Such a phenomenon with a secondary interaction between a gold atom and nitrogen atom has been reported in the literature before in phosphinegold(I) thionucleobases [114]. By contrast to the R' = Ph complex, the IR spectrum of the analogous R' = Me complex showed that the υ(C=N) band increased in frequency and the υ(P=S) band decreased in frequency by approximately 20 cm^{-1} giving rise to the possibility that in this case there is a secondary interaction between the phosphorus-bound sulfur atom and the gold centre as represented in 5.4.2B. A similar interaction involving the uncoordinated sulfur atom has been observed in gold(I) xanthates [117].

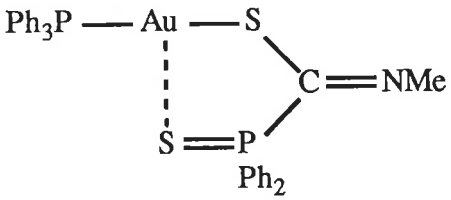

5.4.2B

It is stressed here, that the above assignments are tentative.

5.5 Reaction of Diorganoselenophosphinylthioformamides with Gold(I) Salts

5.5.1 Reaction of $R_2P(Se)C(S)N(H)R'$ with $HAuCl_4$ and Spectroscopic Characterisation

The complexes that formed were similar to those of the Y = S derivatives, i.e. $\{Au[R_2P(Se)C(S)NR']\}_\infty$. The addition of the $[Cy_2P(Se)C(S)N(H)R']$ ligands to the gold(I) species, obtained from the reduction of $HAuCl_4$ with thiodiglycol, resulted in no

detectable gold complex for the R' = Me ligand, however, the precipitation of elemental gold and selenium was observed. For the R' = Ph ligand a gold complex was formed. These complexes were also insoluble and thought to be polymeric species. From the IR spectra of these complexes the absence of the υ(N-H) and thioamide(II) absorption bands, coupled with the increase in the value of thioamide(I) band, i.e. υ(C=N), suggests that the sulfur atom is in some way coordinated. The slight decrease in the frequency of the υ(P=Se) band indicates that there is coordination or, more likely, a secondary interaction of the selenium atom to a gold centre. No solution spectroscopy could be obtained due to the very poor solubility of the compounds.

FAB mass spectra were recorded for these complexes and gave evidence for the basic $\{Au[R_2P(Se)C(S)NR']\}$ unit. The presence of high molecular weight, high nuclearity clusters involving up to four gold atoms was also noted. The $\{Au[R_2P(Se)C(S)NR']\}_2$ ion was observed for the R = Ph complexes but not for the R = Cy complex. The ion $[(Ph_3PAu)_3S]^+$ was observed for the Y = S complexes and similarly the analogous $[(Ph_3PAu)_3Se]^+$ ion was observed for the Y = Se compounds. The m/z values containing selenium were based on ^{80}Se and the fragments and aggregates which contained selenium exhibited the typical isotopic distribution for selenium. Selected spectroscopic parameters are listed in Table 5.5.1.

5.5.2 Reaction of $R_2P(Se)C(S)N(H)R'$ with Ph_3PAuCl

Reaction of the $R_2P(Se)C(S)N(H)R'$, R = Ph or Cy, R' = Ph or Me, compounds with triphenylphosphine gold chloride and base produced an unexpected finding. Spectroscopic characterisation of the resulting compounds and in some cases determination of the unit cell of representative crystals revealed that the compounds obtained were the cyclic gold(I) complexes reported in Section 5.2. Triphenylphosphine selenide was determined to be a by product of the reaction (IR, unit cell data) and a reaction scheme is proposed below:

$$Ph_3PAuCl + R_2P(Se)C(S)N(H)R' \xrightarrow{Et_3N} 0.5\{Au[R_2PC(S)NR']\}_2 + Ph_3PSe + Et_3NHCl$$

The spectroscopic parameters are as listed in Table 5.2.3b.

Table 5.5.1: Spectroscopic data for $\{Au[Ph_2P(Se)C(S)NPh]\}_\infty$, R = Ph or Cy, R' = Ph or Me

$\{Au[Ph_2P(Se)C(S)NPh]\}_\infty$

IR: υ(C=N) 1534 cm^{-1}; υ(C-S) 926 cm^{-1}; υ(P=Se) 523 cm^{-1}

FAB*: 1456, $[(Ph_3PAu)_3Se]^+$ 100%; 1427, $[M(Ph_2PSe)(-S)]^+$ 75%; 1409, $[(Ph_3PAu)S)]^+$ 63%; 1391, $[M(Au)]^+$ 67%; 1380, $[(Ph_3PAu)_2(Ph_2PAu)Se]^+$ 57%; 1194, $[M]^+$ 35%; 1162, $[M\text{-}S]^+$ 18%; 997, $[M\text{-}(Au)]^+$ 12%; 957, [M-(2Se, Ph)]$^+$ 30%; 837, [M-(Au, 2Se)]$^+$ 45%; 722, $[(Ph_3P)_2Au]^+$ 60%; 628, $[(Au(Ph_2P(Se)C(S)NPh)(S)]^+$ 64%

$\{Au[Ph_2P(Se)C(S)NMe]\}_\infty$

IR: υ(C=N) 1558 cm^{-1}; υ(C-S) 931 cm^{-1}; υ(P=Se) 528 cm^{-1}

FAB: 2096, $[(Ph_3PAu)_4S_2Au]^+$ 60%; 1794, $[(Ph_3PAu)_3(Ph_2PAu)S]^+$ 20%; 1530, $[(Ph_3PAu)_2(Ph_2PAu)SAu]^+$ 22%; 1456, $[(Ph_3PAu)_3Se]^+$ 80%; 1424, $[M(Ph_3PSe)Me]^+$ 90%; 1409, $[(Ph_3PAu)S)]^+$ 100%; 1380, $[(Ph_3PAu)_2(Ph_2PAu)Se]^+$ 91%; 1329, $[M(PAuS)]^+$ 94%; 1299, $[M(AuS)]^+$ 16%; 1194, [(MAu-(SCNMe)]$^+$ 35%; 1146, $[M(PCS)]^+$ 88%; 1100, $[M(P)]^+$ 70%; 1069, $[M]^+$ 20%

$\{Au[Cy_2P(Se)C(S)NPh]\}_\infty$

IR: υ(C=N) 1563 cm^{-1}; υ(C-S) 925 cm^{-1}; υ(P=Se) 526 cm^{-1}

FAB: 1412, $[MAu]^+$ 15%; 1019, $[M\text{-}(Au)]^+$ 5%; 936, [M-(Au, Cy)]$^+$ 10%; 837, $[(Au(Ph_2P(Se)C(S)NPh)(AuS)]^+$ 25%; 692, $[S_2Au_2Se_2P_2C]^+$ 10%; 618, $[S_2Au_2Se_2]^+$ 15%; 585, $[Au_2Se_2P]^+$ 20%; 554, $[Au_2Se_2]^+$ 4%; 459, $[Au_2S_2]^+$ 100%; 412, $[Cy_2P(Se)C(S)N(H)Ph]^+$ 11%

*[m/e, assignment (intensity)]

[M] = ion corresponds to $\{Au(Ph_2P(Se)C(S)NPh)\}_2$

5.6 Miscellaneous Reactions with Gold Salts

An alteration to the procedure reported in 2.10.1a was attempted. Selected phosphorus(V) compounds were added directly to the Au(III) species, i.e. $HAuCl_4$, before the addition of the thiodiglycol but the precipitation of elemental gold discouraged the continuation of this technique.

To the $\{Au\{Ph_2PC(S)NPh]\}_2$ complex in benzene solution was added either sulfur or selenium in an inert atmosphere. Refluxing the solution for three hours after an initial hour of stirring at room temperature resulted in the isolation of the two reactants in each case.

5.7 Summary of Reactions with Gold(I) Salts

From the reactions of the compounds with the gold(I) salts, i.e. reduced $HAuCl_4$ and Ph_3PAuCl, it was found that the diorganophosphinothioformamides reacted to form dinuclear gold(I) complexes. These species were also obtained from the reaction of the $R_2P(Se)C(S)N(H)R'$ compounds with Ph_3PAuCl.

The diorganophosphinylthioformamides were unreactive except for the reaction between $HAuCl_4$ and $[Cy_2P(O)C(S)N(H)Me]$ which yielded the $\{Au\{Cy_2P(O)C(S)N(H)Me]Cl\}$ complex.

Some diorganothiophosphinylthioformamide ligands reacted with $HAuCl_4$ and Ph_3PAuCl to produce either insoluble polymeric compounds formulated tentatively as $\{Au[Ph_2P(S)C(S)NR']\}_\infty$, or alternatively, reaction with Ph_3PAuCl yielded (tentatively) $Ph_3PAu[R_2P(S)C(S)NR']$, i.e. with the deprotonated ligand coordinated in a monodentate manner.

The diorganoselenophosphinylthioformamide ligands gave the analogous polymeric complexes as for the Y = S derivatives when reacted with reduced $HAuCl_4$ and the cyclic bidentate gold(I) complexes when reacted with Ph_3PAuCl. The flow charts below summarise the reactions and possible products obtained.

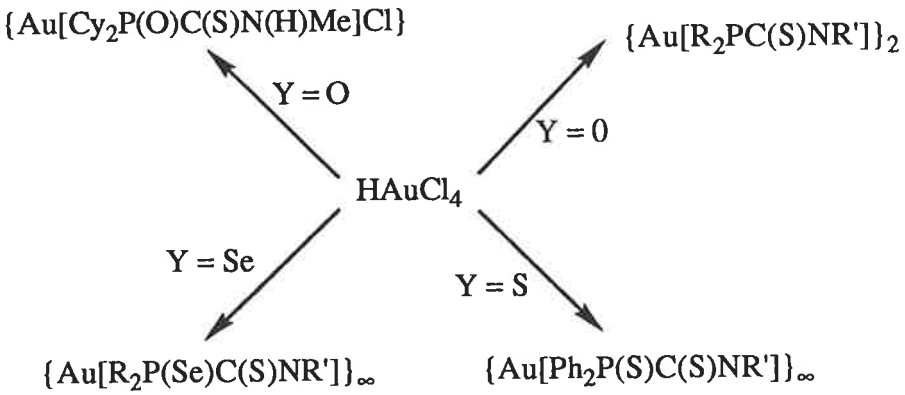

Flow Chart 5.7.1 The reaction of reduced $HAuCl_4$ with $R_2P(Y)C(S)N(H)R'$, Y = 0, O, S or Se, R = Ph or Cy, R' = Ph or Me.

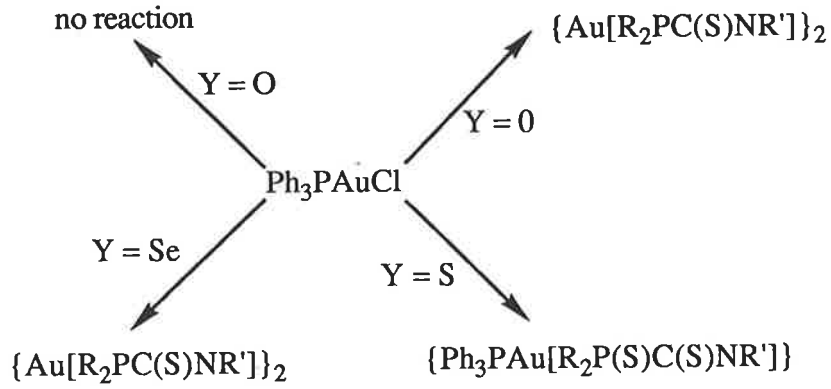

Flow Chart 5.7.2 The reaction of Ph_3PAuCl with $R_2P(Y)C(S)N(H)R'$, Y = 0, O, S or Se, R = Ph or Cy, R' = Ph or Me, in the presence of Et_3N.

5.8 The Structural Analysis of $\{Me_2Au[Cy_2PC(S)NCy]\}$

This chapter has focussed on gold(I) complexes with the diorganophosphinothioformamides and their derivatives. A gold(III) complex, $\{Me_2Au[Cy_2PC(S)NCy]\}$, containing the $[Cy_2PC(S)N(H)Cy]^-$ anion was made available to the author by Professor R. Kramolowsky. This afforded the opportunity to characterise crystallographically a complex with the gold atom in the +III oxidation state.

5.8.1 The Molecular Structure of {$Me_2Au[Cy_2PC(S)NCy]$}

White crystals of *P, P*-dicyclohexyl-*N*-cyclohexyl-phosphinothioformamido dimethyl gold(III), {$Me_2Au[Cy_2PC(S)NCy]$}, crystallise in the orthorhombic space group $P2_12_12_1$ with unit cell dimensions a = 12.860(1), b = 14.975(1), c = 12.230(4) Å, V = 2355.3(4) Å^3, Z = 4 and D_x = 1.595 g cm^{-3}. The structure was refined to final R = 0.039, R_w = 0.042 for 1453 reflections with $I \geq 3.0\sigma(I)$. The molecular structure of {$Me_2Au[Cy_2PC(S)NCy]$} is illustrated in Fig. 5.8.1a ([14]; 15% thermal ellipsoids) showing the numbering scheme employed and selected interatomic parameters are listed in Table 5.8.1.

The square planar geometry about the gold(III) centre can be seen from Fig. 5.8.1a. The $[Cy_2PC(S)N(H)Cy]^-$ anion functions as a P-, S- chelating ligand, Au-S(1) 2.400(5) Å and Au-P(1) 2.344(5) Å. The S(1), P(1), N(1) and C(1) atoms are planar with a mean deviation from the least-squares plane through these atoms of 0.018 Å. The gold atom lies 0.547(1) Å above this plane and thus the four-membered chelate ring, i.e. AuPC(1)S, is far from planar. This is reflected in the deviations of the Au, P(1), C(1) and S(1) atoms from their least-squares plane of 0.001(1), -0.019(6), 0.24(2) and -0.023(6) Å, respectively, indicating substantial puckering in the four-membered ring. The torsion angles Au/P(1)/C(1)/S(1) and Au/S(1)/C(1)/P(1) are -11.6(8) and 11.3(8)°, respectively. The angles about the gold centre are close to those expected for an ideal square planar system except for the chelate angle formed by the ligand which is 74.0(2)°, this can be attributed to the restricted bite angle of the ligand. Comparison of this structure to that of {$Au[Ph_2PC(S)NPh]$}$_2$, Section 5.2.4, which features a pseudo five-membered ring, reveals a number of differences. The Au-S(1) and Au-P(1) separations are approximately 0.10 and 0.07 Å longer, respectively in the {$Me_2Au[Cy_2PC(S)NCy]$} complex. The angles also differ between the two complexes, i.e. the Au-S(1)-C(1), Au-P(1)-C(1) and S(1)-C(1)-P(1) angles are considerably smaller in {$Me_2Au[Cy_2PC(S)NCy]$} while the S(1)-C(1)-P(1) and P(1)-C(1)-N(1) angles are wider. These differences can be attributed to the different coordination geometries about the gold centres. The P(1)-C(1)-N(1) angle is larger in the

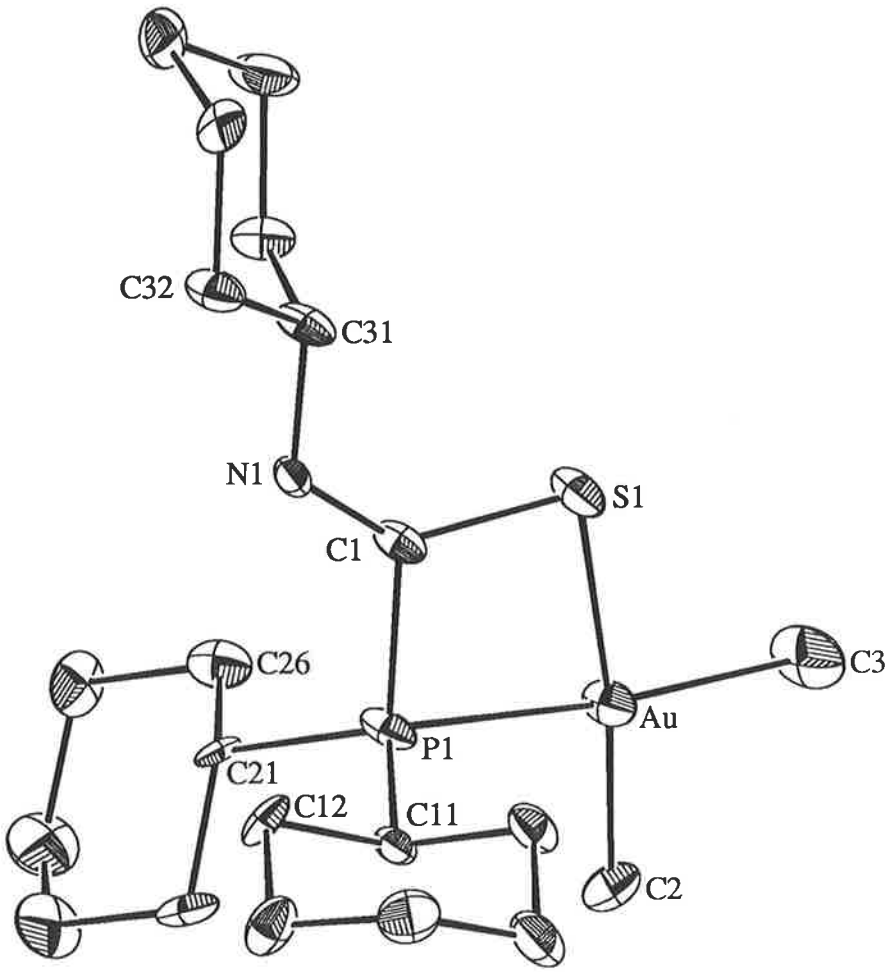

Fig. 5.8.1a The molecular structure of $\{Me_2Au[Cy_2PC(S)NCy]\}$

Table 5.8.1: Selected bond distances (Å) and angles (deg.) for $\{Me_2Au[Cy_2PC(S)NCy]\}$

Au-S(1)	2.400(5)	Au-P(1)	2.344(5)
Au-C(2)	2.08(2)	Au-C(3)	2.03(2)
S(1)-C(1)	1.77(2)	P(1)-C(1)	1.85(2)
P(1)-C(11)	1.84(2)	P(1)-C(21)	1.85(2)
N(1)-C(1)	1.25(2)	N(1)-C(31)	1.47(2)
S(1)-Au-P(1)	74.0(2)	S(1)-Au-C(2)	173.4(6)
S(1)-Au-C(3)	97.1(7)	P(1)-Au-C(2)	100.4(6)
P(1)-Au-C(3)	170.6(7)	C(2)-Au-C(3)	88.7(9)
Au-S(1)-C(1)	90.1(6)	Au-P(1)-C(1)	90.1(6)
Au-P(1)-C(11)	112.9(6)	Au-P(1)-C(21)	125.2(6)
C(1)-P(1)-C(11)	107.1(8)	C(1)-P(1)-C(21)	108.4(8)
C(11)-P(1)-C(21)	109.9(8)	C(1)-N(1)-C(31)	119(2)
S(1)-C(1)-P(1)	104(1)	S(1)-C(1)-N(1)	134(1)
P(1)-C(1)-N(1)	121(1)		

gold(III) complex, presumably to minimise the interaction between the bulky phosphine-bound and nitrogen-bound cyclohexyl groups.

The bond distances of the methyl groups to the gold centre, Au-C(2) and Au-C(3), are 2.08(2) and 2.03(2) Å, respectively. The C(1)-S(1) distance of 1.77(2) Å is indicative of a single bond, the C(1)-N(1) separation of 1.25(2) Å is suggestive of a formal double bond between these atoms and the P(1)-C(1) separation of 1.85(2) Å corresponds to that of a single bond. The crystal structure of the parent compound [$Cy_2PC(S)N(H)Cy$], is not available to make any comparisons with the deprotonated ligand in the complex.

Only one other gold(III) complex with a SPC_2 donor set has been reported in the literature, i.e. that of {$(C_6F_5)_2Au[PPh_2CHPPh_2S]$} [118]. The Au-P bond length of 2.331(1) Å is comparable with the distance found above while the Au-S separation of 2.345(2) Å is shorter. The Au-C distances are equivalent to the separations listed above. The bite angle of the ligand is much closer to 90°, i.e. S-Au-P is 89.6(1)°, and this is due to the additional atom in the chelate ring allowing for the greater flexibility of the ligand whereas in the structure of {$Me_2Au[Cy_2PC(S)NCy]$} the four-membered ring is strained.

There were no significant intermolecular contacts of note in the lattice; the unit cell contents are shown in Fig. 5.8.1b. The closest non-hydrogen contact occurs between atoms C(3) and C(34)' of 3.58(3) Å (symmetry operation: -1.5-*x*, 2-*y*, -0.5-*z*) and the closest contact involving a hydrogen atom of 3.188 Å occurs between the S(1) and H(11a)' atoms (symmetry operation: -0.5+*x*, -1.5-*y*, -*z*).

The crystal structure analysis confirms the stoichiometry of the compound and demonstrates the presence of a P-, S- chelating mode for the {$Me_2Au[Cy_2PC(S)NCy]$} complex and a strained four-membered AuPCS ring.

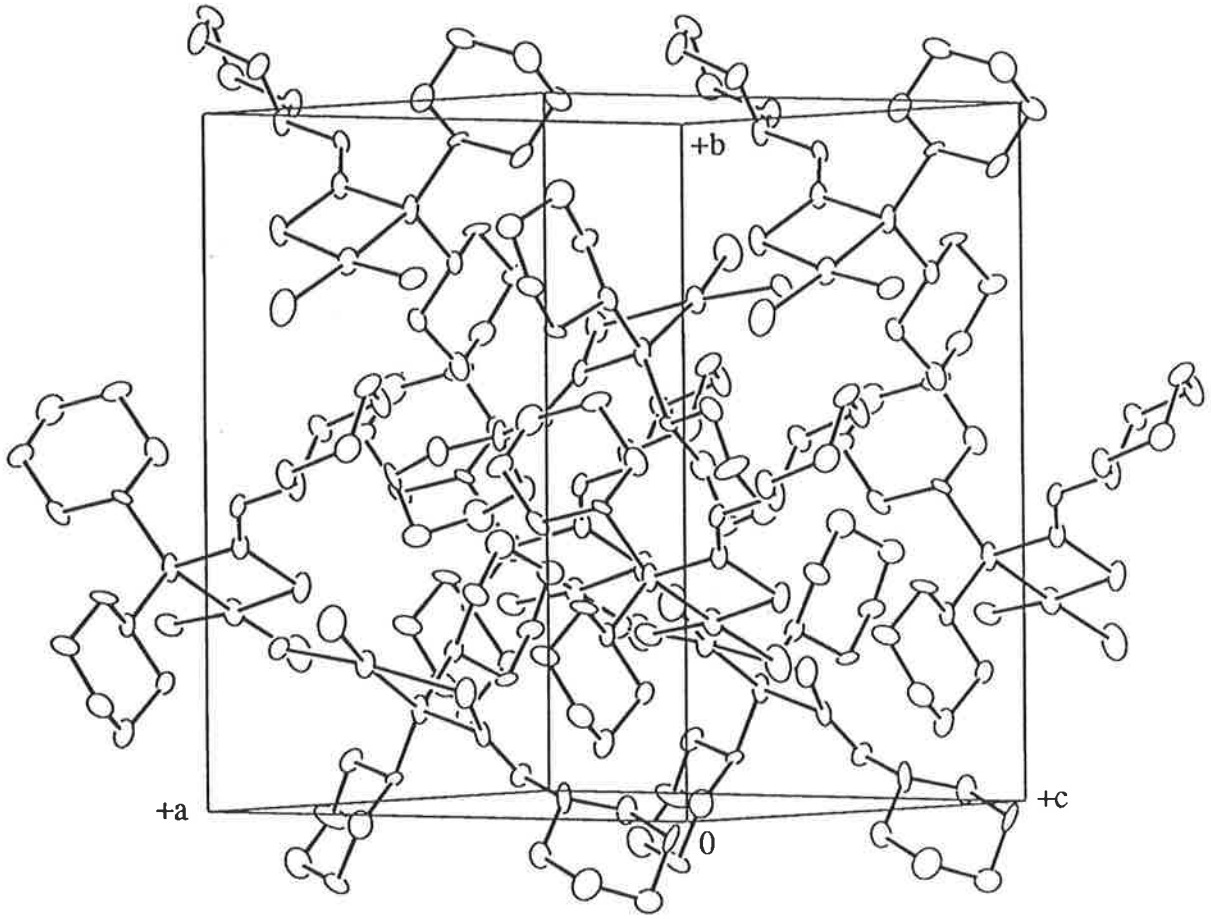

Fig. 5.8.1b The unit cell contents for {$Me_2Au[Cy_2PC(S)NCy]$}

Chapter 6

METAL COMPLEXES OF DIORGANOPHOSPHINO-, DIORGANOPHOSPHINYL-, DIORGANOTHIO-PHOSPHINYL- AND DIORGANOSELENOPHOSPHINYL-THIOFORMAMIDES

Introduction

In *the Introduction*, Chapter 1, the known coordination characteristics of neutral and deprotonated forms of $R_2PC(S)N(H)R'$, $R_2P(O)C(S)N(H)R'$ and $R_2P(S)C(S)N(H)R'$, R = Ph or Cy, R' = Ph or Me, as revealed by crystallographic techniques, were described. In this Chapter spectroscopic evidence (IR, NMR (the atom numbering scheme is as in Section 4.4.2) and FAB MS) and crystal structures (where possible) of a number of new coordination complexes are described. The complexes were either prepared by the author or kindly supplied by Professor R. Kramolowsky of the University of Hamburg, Germany. The coordination potential of several $[R_2PC(S)NR']^-$ anions is explored as well as a rare example of a complex containing the $[Cy_2PC(S)NMe]^-$ anion. Further, the coordination properties of several complexes of the anion derived from $R_2P(Se)C(S)N(H)Ph$ are reported for the first time.

6.1 Metal Complexes with Diorganophosphinothioformamides

The coordination chemistry of three different diorganophosphinothioformamide ligands are reported in this section, namely $[Ph_2PC(S)N(H)Ph]$, $[Cy_2PC(S)N(H)Ph]$ and $[Cy_2PC(S)N(H)Me]$ with the ligands in their deprotonated forms. There are several examples in the literature of metal complexes containing the $[R_2PC(S)NR']^-$ anions which have been described in Chapter 1. However, as mentioned earlier, it has not been possible to obtain the $[Cy_2PC(S)N(H)Me]$ ligand in pure form. Unequivocal evidence for its preparation is provided by the characterisation of the $\{Ni[Cy_2PC(S)NMe]_2\}$ complex, the crystal structure determination of which this is the first example of a complex containing the $[Cy_2PC(S)NMe]^-$ anion.

6.1.1 The Molecular Structure of $\{Co[Cy_2PC(S)NPh]_3\}$

The dark blue crystals of *tris*(*P, P*-dicyclohexyl-*N*-phenyl-phosphinothioformamido) cobalt(III), $\{Co[Cy_2PC(S)NPh]_3\}$, were grown from the slow evaporation of a chloroform solution of the compound; the complex was kindly supplied by Professor R. Kramolowsky.

Crystals are monoclinic, space group $P2_1/c$ with unit cell dimensions a = 16.053(2), b = 19.200(2), c = 18.257(3) Å, β = 101.59(1)°, V = 5512(1) Å^3, Z = 4 and D_x = 1.273 g cm^{-3}. The structure was refined to final R = 0.070, R_w = 0.066 for 3030 reflections with $I \geq 3.0\sigma(I)$. The molecular structure of the compound is shown in Fig. 6.1.1a ([14]; 20% thermal ellipsoids) and the unit cell contents are shown in Fig. 6.1.1b. Selected interatomic parameters are listed in Table 6.1.1.

The structure of {Co[Cy_2PC(S)NPh]$_3$} is molecular, there being no significant intermolecular contacts. The closest non-hydrogen contact of 3.53(3) Å occurs between atoms C(12c) and C(33c)' (symmetry operation: +x, 0.5-y, -0.5+z) and the separation of 2.85(4) Å was the closest contact involving a hydrogen atom and occurred between the atoms N(1b) and H(25c)' (symmetry operation: 1-x, -y, -z).

The molecule has no crystallographically imposed symmetry and consequently there are three independent [Cy_2PC(S)NPh]$^-$ anions labeled *a*, *b* and *c*. Each anion chelates the central cobalt(III) atom. Two of the ligands, i.e. *a* and *b*, chelate the cobalt atom *via* the phosphorus and sulfur atoms and form very different distances: Co-S(1) and Co-P(1) are 2.254(4) and 2.229(4) Å, respectively for ligand *a*, and 2.307(4) and 2.265(4) Å, respectively for ligand *b*. The third ligand, i.e. *c*, coordinates the central atom through the sulfur and nitrogen atoms such that the Co-S(1) and Co-N(1) distances are 2.311(4) and 2.02(1) Å, respectively. The sulfur atoms are in a meridional arrangement. The disparity in the Co-P distances may be traced to the different *trans* influences of the donor atoms opposite to the P(1a) and P(1b) atoms. Hence, the longer Co-P(1b) bond is *trans* to the Co-N(1c) bond and the shorter Co-P(1a) bond is *trans* to the Co-S(1b) separation. The reason for the different modes of coordination of the phosphinothioformamide ligands is possibly steric in origin. Molecular models show that either a facial or meridional arrangement of phosphorus donor atoms would lead to impossible steric strain in the molecule. Hence, a S_3P_2N donor set may be preferred for these steric considerations.

This is the first instance where a S_3P_2N donor set to a cobalt(III) centre has been reported, similarly, iridium and rhodium complexes with such a donor set also do not exist in the crystallographic literature. In the structure of {Co(S_2COEt)$_2$(dmpe)}[BPh_4] (where

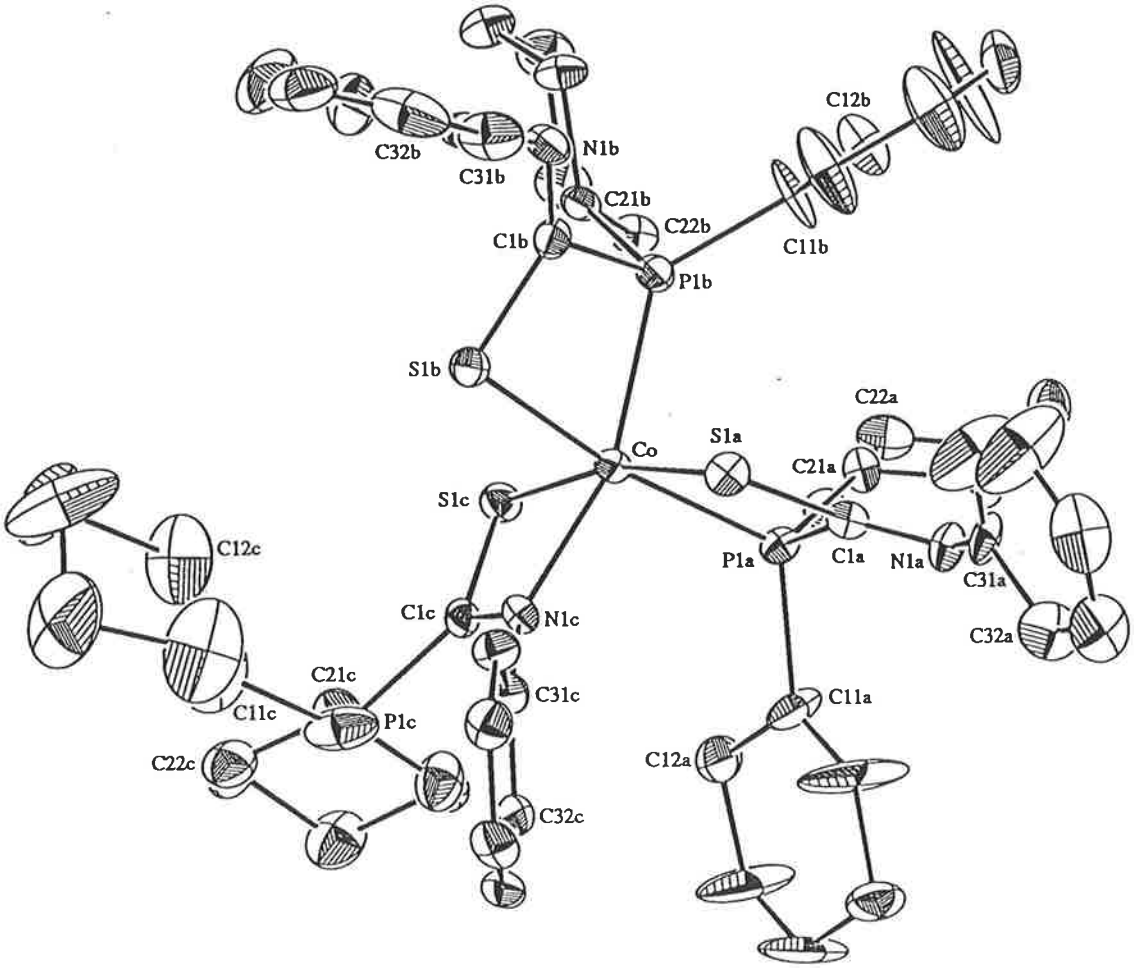

Fig. 6.1.1a The molecular structure of $\{Co[Cy_2PC(S)NPh]_3\}$

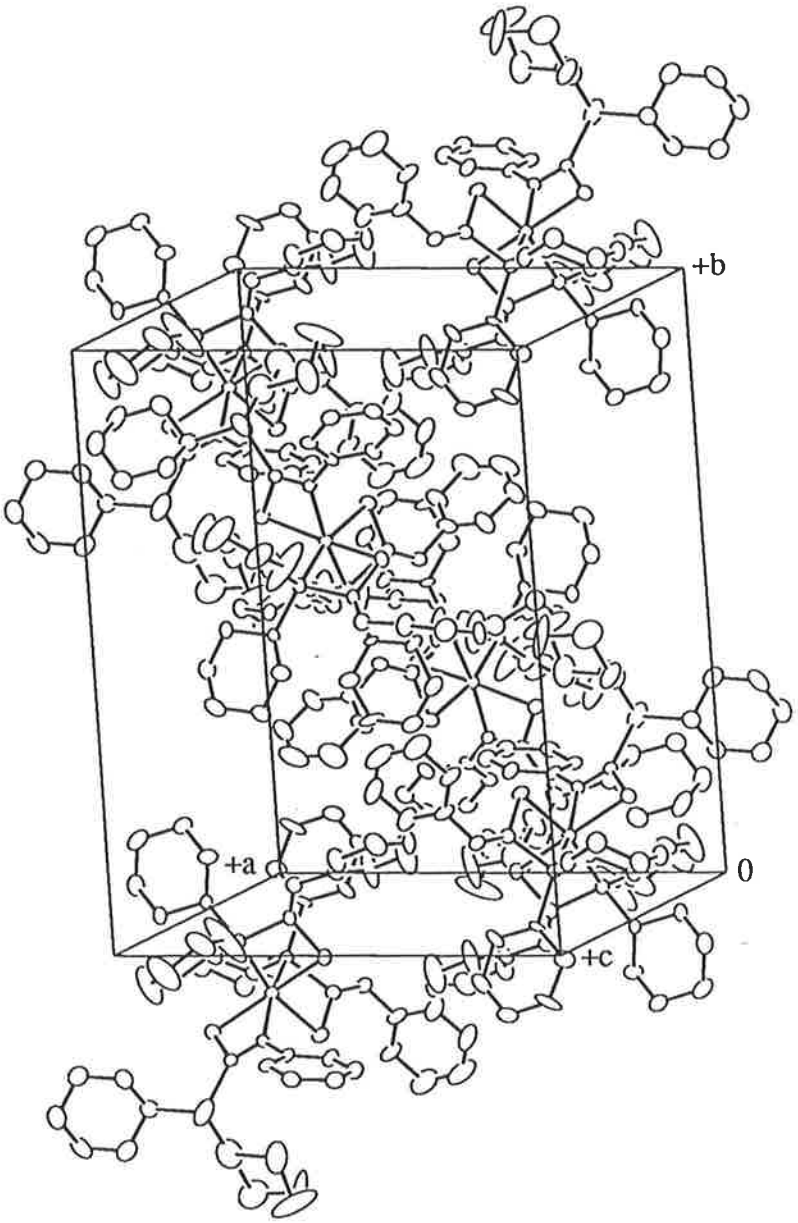

Fig. 6.1.1b The unit cell contents for $\{Co[Cy_2PC(S)NPh]_3\}$

Table 6.1.1: Selected bond distances (Å) and angles (deg.) for {Co[$Cy_2PC(S)NPh]_3$}

Atoms	ligand *a*	ligand *b*	ligand *c*
Co-S(1)	2.254(4)	2.307(4)	2.311(4)
Co-P(1)	2.229(4)	2.265(4)	—
Co-N(1)	—	—	2.02(1)
S(1)-C(1)	1.75(1)	1.74(1)	1.74(1)
P(1)-C(1)	1.84(1)	1.83(1)	1.94(1)
P(1)-C(11)	1.88(1)	1.86(1)	1.76(2)
P(1)-C(21)	1.87(1)	1.85(1)	1.88(1)
N(1)-C(1)	1.27(1)	1.26(1)	1.28(1)
N(1)-C(31)	1.42(1)	1.43(2)	1.42(1)

S(1a)-Co-S(1b)	91.6(1)	S(1a)-Co-S(1c)	167.1(1)
S(1a)-Co-P(1a)	75.3(1)	S(1a)-Co-P(1b)	90.4(1)
S(1a)-Co-N(1c)	99.4(3)	S(1b)-Co-S(1c)	95.7(1)
S(1b)-Co-P(1a)	166.0(1)	S(1b)-Co-P(1b)	74.0(1)
S(1b)-Co-N(1c)	88.9(3)	S(1c)-Co-P(1a)	98.1(1)
S(1c)-Co-P(1b)	101.9(1)	S(1c)-Co-N(1c)	70.1(3)
P(1a)-Co-P(1b)	100.7(1)	P(1a)-Co-N(1c)	98.0(3)
P(1b)-Co-N(1c)	160.6(3)	Co-S(1a)-C(1a)	92.9(4)
Co-S(1b)-C(1b)	90.6(4)	Co-S(1c)-C(1c)	78.1(4)
Co-P(1a)-C(1a)	91.2(4)	Co-P(1a)-C(11a)	121.4(5)
Co-P(1a)-C(21a)	118.4(4)	C(1a)-P(1a)-C(11a)	103.5(6)
C(1a)-P(1a)-C(21a)	109.8(6)	C(11a)-P(1a)-C(21a)	109.1(6)
Co-P(1b)-C(1b)	89.6(4)	Co-P(1b)-C(11b)	129.5(5)
Co-P(1b)-C(21b)	114.1(4)	C(1b)-P(1b)-C(11b)	108.1(6)
C(1b)-P(1b)-C(21b)	101.1(5)	C(11b)-P(1b)-C(21b)	108.4(6)
C(1c)-P(1c)-C(11c)	106.6(8)	C(1c)-P(1c)-C(21c)	103.1(6)
C(11c)-P(1c)-C(21c)	104.7(9)	C(1a)-N(1a)-C(31a)	121(1)
C(1b)-N(1b)-C(31b)	120(1)	Co-N(1c)-C(1c)	101.1(8)
Co-N(1c)-C(31c)	132.4(8)	S(1a)-C(1a)-P(1a)	99.6(7)
S(1a)-C(1a)-N(1a)	134(1)	P(1a)-C(1a)-N(1a)	126(1)
S(1b)-C(1b)-P(1b)	100.8(7)	S(1b)-C(1b)-N(1b)	133(1)
P(1b)-C(1b)-N(1b)	126(1)	S(1c)-C(1c)-P(1c)	120.9(7)
S(1c)-C(1c)-N(1c)	110.5(9)	P(1c)-C(1c)-N(1c)	129(1)

dmpe is bis(dimethylphosphino)ethane), which features a S_4P_2 donor set, the Co-S distances are in the range 2.255(1) to 2.290(2) Å and the Co-P separation is 2.205(1) Å [119] (the molecule has two-fold symmetry). The Co-N and Co-P separations have been found in the ranges 1.861(8)-1.965(9) and 2.236(3)-2.303(3) Å, respectively in the structure of $\{(PMe_3)_3Co(SCN)_3\}$ (two independent molecules in the unit cell) which features a P_3N_3 donor set to the cobalt atom [120]. In the structure of $\{Co(pyS)_3\}$, pyS = pyridine-2(1H)-thione, which contains a S_3N_3 donor set the Co-N and Co-S bond lengths are in the ranges 1.903(3)-1.938(3) and 2.286(1)-2.306(1) Å, respectively [121], while average values for these distances have been found in another related structure, i.e. $\{Co[Co(SCH_2CH_2NH_2)_3]_2\}_2(SO_4)Cl_4$, of 1.996(8) and 2.238(7) Å, respectively [122]. The value of 2.02(1) Å for Co-N(1c) is fractionally longer than similar distances found above and this could be possibly due to the nitrogen atom being *trans* to a phosphorus atom.

The cobalt atom exists in a distorted octahedral geometry with the major distortions attributed to the restricted bite angles of the ligands, i.e. S(1a)-Co-P(1a) 75.3(1)°, S(1b)-Co-P(1b) 74.0(1)° and S(1c)-Co-N(1c) 70.1(3)°. The mode of attachment of each of the three anions leads to the formation of a four-membered ring. The lack of planarity in the CoPC(1)S rings of ligands *a* and *b* is emphasised in the torsion angles Co/S(1)/C(1)/P(1) of -8.4(5) and 18.6(5)°, respectively and Co/P(1)/C(1)/S(1) of 8.5(5) and -19.0(5)°, respectively. The four-membered ring of ligand *c*, i.e. CoSC(1)N, is quite planar, however, as seen in the torsion angles Co/S(1)/C(1)/N(1) and Co/N(1)/C(1)/S(1) of -2.7(8) and 3.0(9)°, respectively.

The atoms comprising the central chromophore of ligands *b* and *c*, i.e. P(1), C(1), S(1) and N(1), are essentially coplanar with deviations from the least-squares plane through these atoms being -0.000(1), 0.01(1), -0.000(3) and -0.01(1) Å, respectively for ligand *b* and 0.001(5), -0.02(1), 0.001(3) and 0.006(9) Å, respectively for ligand *c*. (By contrast, the atoms of the central chromophore in ligand *a* are not as planar, with deviations in the same order as above, of -0.001(3), 0.06(1), -0.002(3) and -0.03(1) Å, respectively.) The C(1)-S(1), C(1)-N(1) and N(1)-C(31) separations are equal within experimental for the three ligands and consequently no trends in these parameters are discernible. Ligand *c*, which

coordinates the cobalt atom *via* the nitrogen atom still has considerable double bond character in the C(1)-N(1) bond as can be seen by the short C(1)-N(1) distance of 1.28(1) Å. There are, however, significant differences in the bond lengths associated with the phosphorus atom. The P(1)-C(1) distances of 1.84(1) Å for ligand *a* and 1.83(1) Å for ligand *b* are identical but the distance found in ligand *c* was considerably longer at 1.94(1) Å. Comparison of these distances with the average P(1)-C(1) distance in the parent ligand [$Cy_2PC(S)N(H)Ph$] [15], for which two independent molecules are found in the crystallographic asymmetric unit, of 1.868(5) Å, showed that the P(1)-C(1) separation decreased in ligands *a* and *b* while in ligand *c* the distance has elongated by approximately 0.07 Å. These observations indicate that the P(1)-C(1) bond is comparatively weak in ligand *c* and accounts, in part, for the relatively short C(1)-N(1) separation. The P-C(Cy) distances in the cobalt complex are equal within experimental error to the average distance found in [$Cy_2PC(S)N(H)Ph$] of 1.856(3) Å. Some disorder is noted in the cyclohexyl ring C(11b)-C(16b) as seen in the rather elongated thermal parameters of some of the atoms; only single sites could be discerned for these atoms, however.

The angles about the C(1) atom for ligands *a* and *b* are equivalent within experimental error, i.e. S(1)-C(1)-P(1) is 99.6(7)° and S(1)-C(1)-N(1) is 134(1)° for ligand *a* and 100.8(7) and 133(1)°, respectively for ligand *b* whereas for ligand *c*, the comparable angles are 120.9(7) and 110.5(9)°, respectively. The difference in these angles of approximately 20° and 22° for the S(1)-C(1)-P(1) and S(1)-C(1)-N(1) angles, respectively can be correlated with the different modes of coordination of the ligands.

The crystal structure determination of {$Co[Cy_2PC(S)NPh]_3$} demonstrates the flexible mode of coordination of phosphinothioformamide ligands with two distinct coordination modes being found in the same complex.

6.1.2 The Preparation and Characterisation of trans-{Ni[$Ph_2PC(S)NPh]_2$}

6.1.2a The Spectroscopic Characterisation of *trans*-{$Ni[Ph_2PC(S)NPh]_2$}

The reaction of $NiNO_3$ with two mole equivalents of $[Ph_2PC(S)N(H)Ph]$ in the presence of excess Et_3N affords the complex {$Ni[Ph_2PC(S)NPh]_2$} as an air-stable, crystalline solid in high yield. Spectroscopic data is given in Table 6.1.2a.

The IR spectrum of this complex shows strong bands at 1555 cm^{-1} and 924 cm^{-1}. The thioamide(I) band has increased in frequency (from 1528 cm^{-1} in $[Ph_2PC(S)N(H)Ph]$) indicating more double bond character in the C(1)-N(1) bond. The thioamide(II) band is no longer at 1388 cm^{-1}, as found in the free ligand $[Ph_2PC(S)N(H)Ph]$, but a band attributed to υ(C-S) has appeared at 924 cm^{-1}. The υ(C-S) absorption has been observed in the region of 930 ± 30 cm^{-1} for complexes involving phosphinothioformamide ligands that form four-membered chelate rings [123-126]. The above shifts and the absence of the υ(N-H) absorption band indicates coordination *via* the phosphorus and sulfur atoms to the metal atom [127]. The υ(Ni-S) and υ(Ni-P) absorption bands occur below 400 cm^{-1} [128], however, this range was not accessible on the laboratory spectrophotometer. Kunze et al have made a number of metal complexes coordinated with diorganophosphinothioformamides of which the IR data exhibit similar trends to those found for {$Ni[Ph_2PC(S)NPh]_2$} and for the subsequent nickel complexes [129-132].

The ^1H NMR spectrum of the complex in $CDCl_3$ solution was unremarkable with the phenyl resonances appearing in the expected region. The N-H peak was absent suggesting that the ligand was deprotonated. Two resonances in the ^{13}C NMR spectrum, Cβ and Cγ, were observed to be split into three resonances in the ratio 1:2:1. This situation could be due to two possibilities:- either i) the two ligands are in different environments, this was not evidenced by the X-ray crystallographic analysis (see later) or ii) that the complex is interchanging between the *cis* and *trans* isomers in solution (this could be verified by variable temperature ^{31}P NMR spectroscopy). It is suggested that a *cis* isomer is unlikely as this configuration would result in impossible steric interactions between the phosphorus-bound substituents [134]. The quaternary carbon signal, C_q, shifted upfield to δ 173.4 ppm

Table 6.1.2a: Spectroscopic data for *trans*-{Ni[$R_2PC(S)NR']_2$}, R = Ph or Cy, R' = Me or Ph

IR (frequencies given are in cm^{-1})

		υ(thioamide I)	υ(C-S)	υ(thioamide II)
{Ni[$Ph_2PC(S)NPh]_2$}		1555	924	
{Ni[$Ph_2PC(S)NMe]_2$}	ligand *a*	1599	902	
	ligand *b*	1479		1387
{Ni[$Cy_2PC(S)NPh]_2$}		1573	943	
{Ni[$Cy_2PC(S)NMe]_2$}		1591	914	

^1H NMR (chemical shifts, δ, are in ppm)

{Ni[$Ph_2PC(S)NPh]_2$}: PPh_2 7.11-8.03, NPh 7.11-8.03

{Ni[$Ph_2PC(S)NMe]_2$}: PPh_2 7.44-7.95, NMe 3.35 (broad)

{Ni[$Cy_2PC(S)NPh]_2$}: PCy_2 1.29-2.21, NPh 7.08-7.38

{Ni[$Cy_2PC(S)NMe]_2$}: PCy_2 1.18-2.23, NMe 3.58 $^3J(HH)$ 5.28 Hz

^{13}C NMR (chemical shifts, δ, are in ppm, n.o. = not observed)

{Ni[$Ph_2PC(S)NPh]_2$}: PPh_2 Cα 132.7 $^1J(PC)$ 10.1 Hz, Cβ 133.3 $^2J(PC)$ 6.2 Hz, Cγ 128.9 $^3J(PC)$ 4.9 Hz, Cδ 131.3, NPh C_a 151.6, C_b 128.4, C_c and C_d (n.o.), C_q 173.4

{Ni[$Ph_2PC(S)NMe]_2$}: PPh_2 Cα 132.7 $^1J(PC)$ 9.6 Hz, Cβ 133.3 $^2J(PC)$ 6.2 Hz, Cγ 128.9 $^3J(PC)$ 5.3 Hz, Cδ 131.4, NMe C_a 39.3 $^3J(PC)$ 9.8 Hz, C_q 173.3 and 201.5

{Ni[$Cy_2PC(S)NPh]_2$}: PCy_2 Cα 32.6 $^1J(PC)$ 7.5 Hz, Cβ-Cδ 28.7-25.9, NPh C_a 148.2 $^1J(PC)$ 9.2 Hz, C_b 128.8, C_c 121.6, C_d 124.5, C_q 175.6 $^1J(PC)$ 26.4 Hz

{Ni[$Cy_2PC(S)NMe]_2$}: PCy_2 Cα 34.9, Cβ-Cδ 26.3-24.7, NMe C_a 46.5, C_q 163.4 $^1J(PC)$ 33.0 Hz

FAB (m/z, [assignment] intensity)

{Ni[$Ph_2PC(S)NPh]_2$}: 699, $[M]^+$ 7%; 595, $[M-(CNPh)]^+$ 10%; 564, $[M-(SCNPh)]^+$ 16%; 461, $[(Ph_2P)_2NiS]^+$ 18%; 378, $[(Ph_2PC(S)NPh)Ni]^+$ 12%; 320, $[Ph_2PC(S)NPh]^+$ 15%; 307, $[Ph_2PNiS_2]^+$ 100%; 288, $[Ph_2PCNPh]^+$ 82%

{Ni[$Ph_2PC(S)NMe]_2$}: 575, $[M]^+$ 49%; 534, $[M-(CNMe)]^+$ 10%; 502, $[M-(SCNMe)]^+$ 100%; 461, $[(Ph_2P)_2NiS]^+$ 92%; 428, $[(Ph_2P)_2Ni]^+$ 22%; 391, $[M-(PPh_2)]^+$ 16%; 317, $[(Ph_2PC(S)NMe)Ni]^+$ 42%; 307, $[Ph_2PNiS_2]^+$ 94%; 260, $[Ph_2PC(S)N(H)Me]^+$ 79%: 260, $[Ph_2PCN(H)Me]^+$ 59%

{Ni[$Cy_2PC(S)NPh]_2$}: 723, $[M]^+$ 12%; 620, $[M-(CNPh)]^+$ 5%; 588, $[M-(SCNPh)]^+$ 5%; 516, $[(Cy_2PC(S)NPh)Ni(CyPC)]^+$ 16%; 391, $[(Cy_2PC(S)NPh)Ni]^+$ 6%; 334, $[Cy_2PC(S)N(H)Ph]^+$ 10%; 308, $[(CyPC(S)NPh)Ni]^+$ 24%; 300, $[Cy_2PCN(H)Ph]^+$ 31%; 288, $[Cy_2PNiS]^+$ 19%; 279, $[(CyPCNPh)Ni]^+$ 67%; 213, $[Cy_2PO]^+$ 100%

{Ni[$Cy_2PC(S)NMe]_2$}: 599, $[M]^+$ 4%; 620, $[M-(Cy)]^+$ 3%; 461, $[M+(SCN), -(PCy_2)]^+$ 9%; 403, $[M-(PCy_2)]^+$ 1%; 288, $[Cy_2PNiS]^+$ 13%; 231, $[Cy_2PC(S)(H)]^+$ 100%

whereas the C_a resonance (nitrogen-bound phenyl ring) moved downfield to δ 151.6 ppm with respect to the values of δ 206.6 ppm, $^1J(PC)$ 39.9 Hz and δ 138.7 ppm found for uncoordinated [$Ph_2PC(S)N(H)Ph$]; there was no sign of any phosphorus-carbon coupling found in the complex for the C_q carbon atom. The Cα resonance (phosphorus-bound phenyl ring) shifted upfield by 1.8 ppm (δ 132.7 ppm, $^1J(PC)$ 10.1 Hz).

In the FAB mass spectrum of the complex the molecular ion, $[M]^+$, was apparent in low abundance, 8%, and there were no ions that occurred at m/z greater than $[M]^+$. The most abundant fragment, m/z 307, and was assigned to $[Ph_2PNiS_2]^+$. Other fragments can be found in Table 6.1.2a.

6.1.2b The Molecular Structure of *trans*-{$Ni[Ph_2PC(S)NPh]_2$}

The orange crystals of *trans-bis*(*P, P*-diphenyl-*N*-phenyl-phosphinothioformamido) nickel(II), *trans*-{$Ni[Ph_2PC(S)NPh]_2$}, were obtained from the slow evaporation of a chloroform solution of the compound. Crystals are triclinic, space group $P\bar{1}$ with unit cell dimensions a = 10.357(1), b = 18.309(2), c = 8.9393(8) Å, α = 96.125(9), β = 99.152(7), γ = 80.479(9)°, V = 1644.8(3) Å^3, Z = 2 and D_x = 1.412 g cm^{-3}. The structure was refined to final R = 0.039, R_w = 0.041 for 2903 reflections with $I \geq 3.0\sigma(I)$.

An unsuccessful attempt to solve this structure has been reported previously [133] but disorder prevented an acceptable result, R = 0.1612. The crystallographic parameters given for the earlier attempt were: triclinic, space group $P\bar{1}$, a = 8.950(6), b = 9.745(4), c = 10.366(7) Å, α = 112.28(4), β = 99.09(5), γ = 90.88(4)° and Z = 1 (i.e. the molecule was constrained to be centrosymmetric).

In the present analysis, there is no crystallographically imposed symmetry in the {$Ni[Ph_2PC(S)NPh]_2$} molecule. Therefore, two crystallographically independent [$Ph_2PC(S)NPh]^-$ anions, i.e. *a* and *b*, chelate the central nickel atom which exists in a distorted square planar geometry defined by the phosphorus and sulfur atoms derived from each of the chelating [$Ph_2PC(S)NPh]^-$ ligands; Ni-S 2.188(2) Å for ligand *a* and 2.163(2) Å for ligand *b*, and Ni-P 2.171(2) Å for ligand *a* and 2.182(2) Å for ligand *b*. The molecular structure of the compound appears in Fig. 6.1.2a ([14]; 25% thermal ellipsoids) and selected

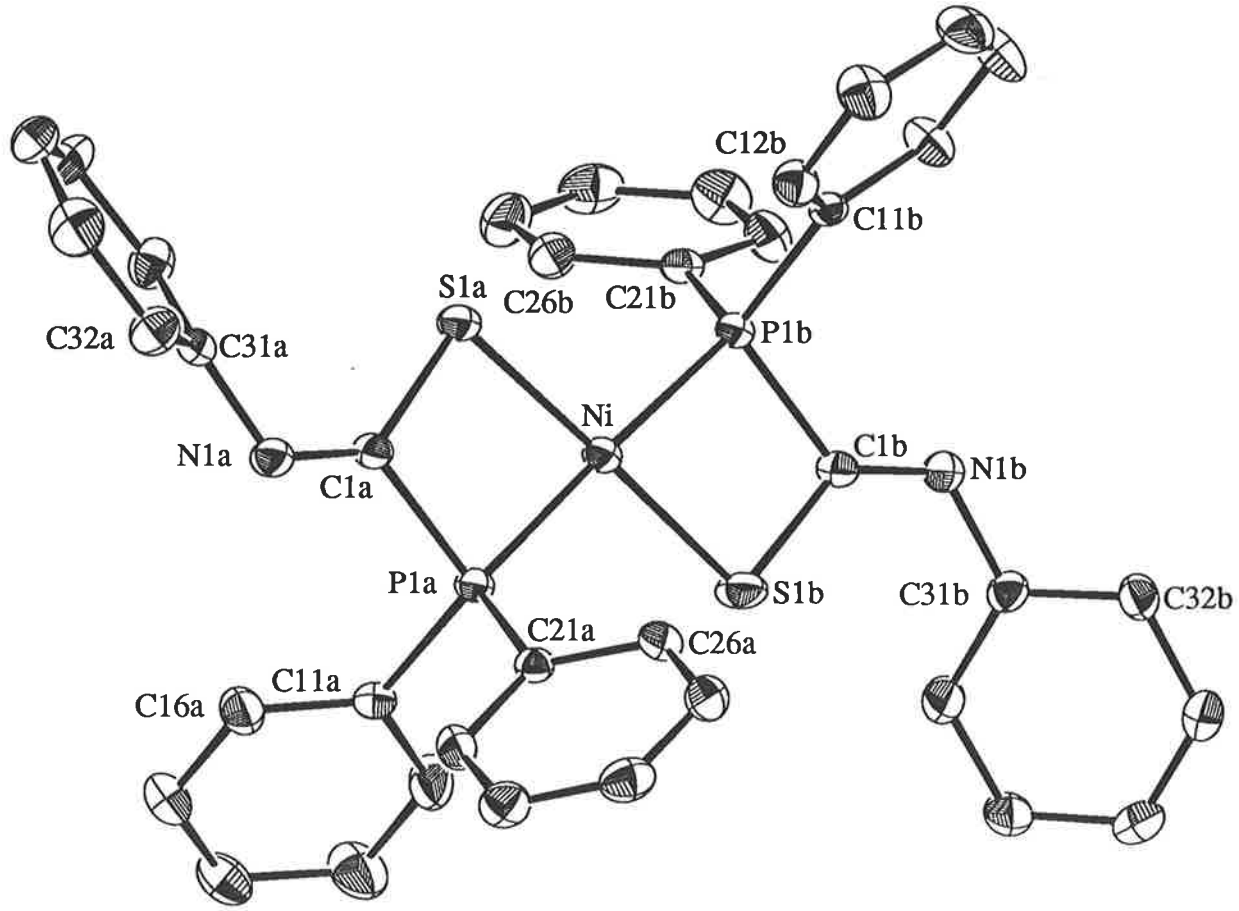

Fig. 6.1.2a The molecular structure of *trans*-{Ni[$Ph_2PC(S)NPh]_2$}

interatomic parameters can be found in Table 6.1.2b. The restricted bite angles, i.e. 77.58(5) and 77.40(6)° for S(1a)-Ni-P(1a) and S(1b)-Ni-P(1b), respectively, of the chelating ligands are responsible for the distortion from the ideal square planar geometry. The Ni-S and Ni-P separations compare favourably with the values found in the structure of $[Ni(Cy_2PCS_2)_2]$ which also features a *trans* P_2S_2 donor set; Ni-P, Ni-S and S-Ni-P were 2.185(2) Å, 2.167(3) Å and 77.2(2)°, respectively [134]. The atoms that define each four-membered ring i.e. Ni, P, C(1) and S, are planar as seen in the Ni/P(1)/C(1)/S(1) torsion angles of 0.4(2) and -3.3(2)° for ligands *a* and *b*, respectively.

A comparison of the interatomic parameters for the parent ligand, $[Ph_2PC(S)N(H)Ph]$, with those for the coordinated (and deprotonated) anions in the nickel complex revealed numerous variations in the parameters associated with the central PCSN chromophore. The values for ligand *b* will follow those for ligand *a* in curly brackets. The C(1)-S(1), P(1)-C(1) and C(1)=N(1) separations of 1.757(5) {1.763(5)}, 1.825(5) {1.829(5)} and 1.276(5) {1.265(5)} Å, respectively have elongated, contracted and contracted compared with the equivalent values in $[Ph_2PC(S)N(H)Ph]$ of 1.650(3), 1.862(3) and 1.334(3) Å, respectively. The respective parameters for the two ligands are equal within experimental error. The C(1)-S(1) distances in the complex approaches single bond character whilst the C(1)=N(1) bond lengths are indicative of considerable double bond character. The P(1)-C(1) distance is approximately 0.35 Å less than that of the parent ligand. Clearly, additional π-electron density is localised in the P(1)-C(1) bond in the complex. The angles around the C(1) atom, i.e. S(1)-C(1)-P(1), S(1)-C(1)-N(1) and P(1)-C(1)-N(1), have contracted, expanded and expanded by approximately 15, 4 and 10°, respectively compared to those in $[Ph_2PC(S)N(H)Ph]$. These changes are due to the strain at the C(1) atom when coordination of the ligand occurs to form a four-membered ring. The S(1)-C(1)-P(1) angle contracts to accommodate the bite of the ligand which results in a concomitant increase in the other two angles. The central PSCN chromophores in the complex are, however, planar as evidenced by the respective torsion angles S(1)/C(1)/N(1)/C(31) of -177.0(4)° {-177.5(4)°} and P(1)/C(1)/N(1)/C(31) of 6.4(8)° {2.6(8)°} which allows for delocalisation of π-electron density over these atoms.

Table 6.1.2b: Selected bond distances (Å) and angles (deg.) for *trans*-{Ni[$R_2PC(S)NR']_2$}

Atoms	R = Ph, R' = Ph		R = Cy, R' = Ph*	R = Cy, R' = Me*
	ligand *a*	ligand *b*		
Ni-S(1)	2.188(2)	2.163(2)	2.1773(9)	2.184(1)
Ni-P(1)	2.171(2)	2.182(2)	2.1766(9)	2.1739(9)
S(1)-C(1)	1.757(5)	1.763(5)	1.754(3)	1.777(4)
P(1)-C(1)	1.825(5)	1.829(5)	1.817(3)	1.824(4)
P(1)-C(11)	1.807(5)	1.810(5)	1.835(4)	1.834(4)
P(1)-C(21)	1.816(5)	1.813(5)	1.828(4)	1.837(3)
N(1)-C(1)	1.276(5)	1.265(5)	1.274(4)	1.254(4)
N(1)-C(31)	1.415(6)	1.441(6)	1.436(4)	1.470(5)
S(1a)-Ni-S(1b)	177.73(7)		180(-)	180(-)
S(1a)-Ni-P(1a)	77.58(5)		78.09(3)	78.23(4)
S(1a)-Ni-P(1b)	104.78(6)		101.91(3)	101.77(4)
S(1b)-Ni-P(1a)	100.24(6)			
S(1b)-Ni-P(1b)	77.40(6)			
P(1a)-Ni-P(1b)	177.62(7)		180(-)	180(-)
Ni-S(1)-C(1)	92.2(2)	93.3(2)	91.5(1)	91.5(1)
Ni-P(1)-C(1)	90.9(2)	90.9(2)	89.9(1)	90.5(1)
Ni-P(1)-C(11)	120.8(2)	119.7(2)	118.2(1)	121.5(1)
Ni-P(1)-C(21)	118.4(2)	118.0(2)	121.1(1)	119.1(1)
C(1)-P(1)-C(11)	108.6(2)	110.0(2)	108.8(2)	106.3(2)
C(1)-P(1)-C(21)	107.8(2)	105.3(2)	108.9(2)	108.9(2)
C(11)-P(1)-C(21)	107.9(2)	109.9(2)	107.7(2)	107.6(2)
S(1)-C(1)-P(1)	99.3(2)	98.3(2)	100.4(2)	99.5(2)
S(1)-C(1)-N(1)	134.3(4)	132.5(4)	131.1(3)	133.0(3)
P(1)-C(1)-N(1)	126.4(4)	129.3(4)	128.5(3)	127.5(3)
C(1)-N(1)-C(31)	121.3(4)	121.2(4)	117.7(3)	118.1(3)

* atoms designated by *a* and *b* are related by a crystallographic centre of inversion for the two R = Cy complexes

The structure of the complex is molecular with the closest non-hydrogen contact occurring between the C(24a) and C(26a)' atoms of 3.430(8) Å (symmetry operation: -1-*x*, 1-*y*, -*z*). The closest contact involving a hydrogen atom was 3.444 Å and occurs between Ni and H(33b)' (symmetry operation: 1+*x*, +*y*, +*z*). The unit cell contents are depicted in Fig. 6.1.2b.

6.1.3 The Characterisation of {Ni[$Ph_2PC(S)NMe]_2$}

6.1.3a The Spectroscopic Characterisation of {$Ni[Ph_2PC(S)NMe]_2$}

Reacting $NiNO_3$ with two mole equivalents of $[Ph_2PC(S)N(H)Me]$ with excess Et_3N gave a compound which did not behave like the {$Ni[Ph_2PC(S)NPh]_2$} complex. Major absorptions in the IR spectrum were found at 1599, 1479, 1387 and 902 cm^{-1}. There was no sign of the υ(N-H) band suggesting that the ligand was deprotonated. The bands at 1599 and 902 cm^{-1} are consistent with P-, S- chelation as discussed above for {$Ni[Ph_2PC(S)NPh]_2$}. The frequency of the υ(C-N) band of the complex with R' = Ph is lower than that of the analogous complex with R' = Me owing to the electron-withdrawing effect of the phenyl group. A similar situation was observed for related rhodium, molybdenum and tungsten complexes [124, 135]. The bands at 1479 and 1387 cm^{-1} however, correspond to a situation where the $[Ph_2PC(S)NMe]^-$ anion coordinates *via* the phosphorus and nitrogen atoms. The absorption band at 1479 cm^{-1} has shifted to lower frequency from the value found for the free ligand, whereas the 1387 cm^{-1} band has increased in frequency, indicative of more C=S character. These results are interpreted as indicating two different modes of coordination of the $[Ph_2PC(S)NMe]^-$ anion. One ligand chelates *via* the sulfur and phosphorus atoms and the other anion chelates as a phosphorus and nitrogen donor (as seen in the structure {$Co[Cy_2PC(S)NPh]_3$} of described above); see 6.1A and 6.1B (R and R' groups omitted for clarity). The postulated structures in 6.1A and

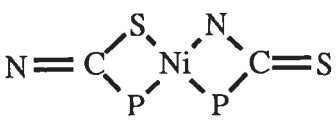

6.1A

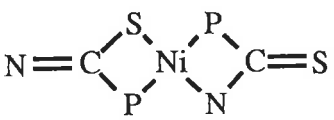

6.1B

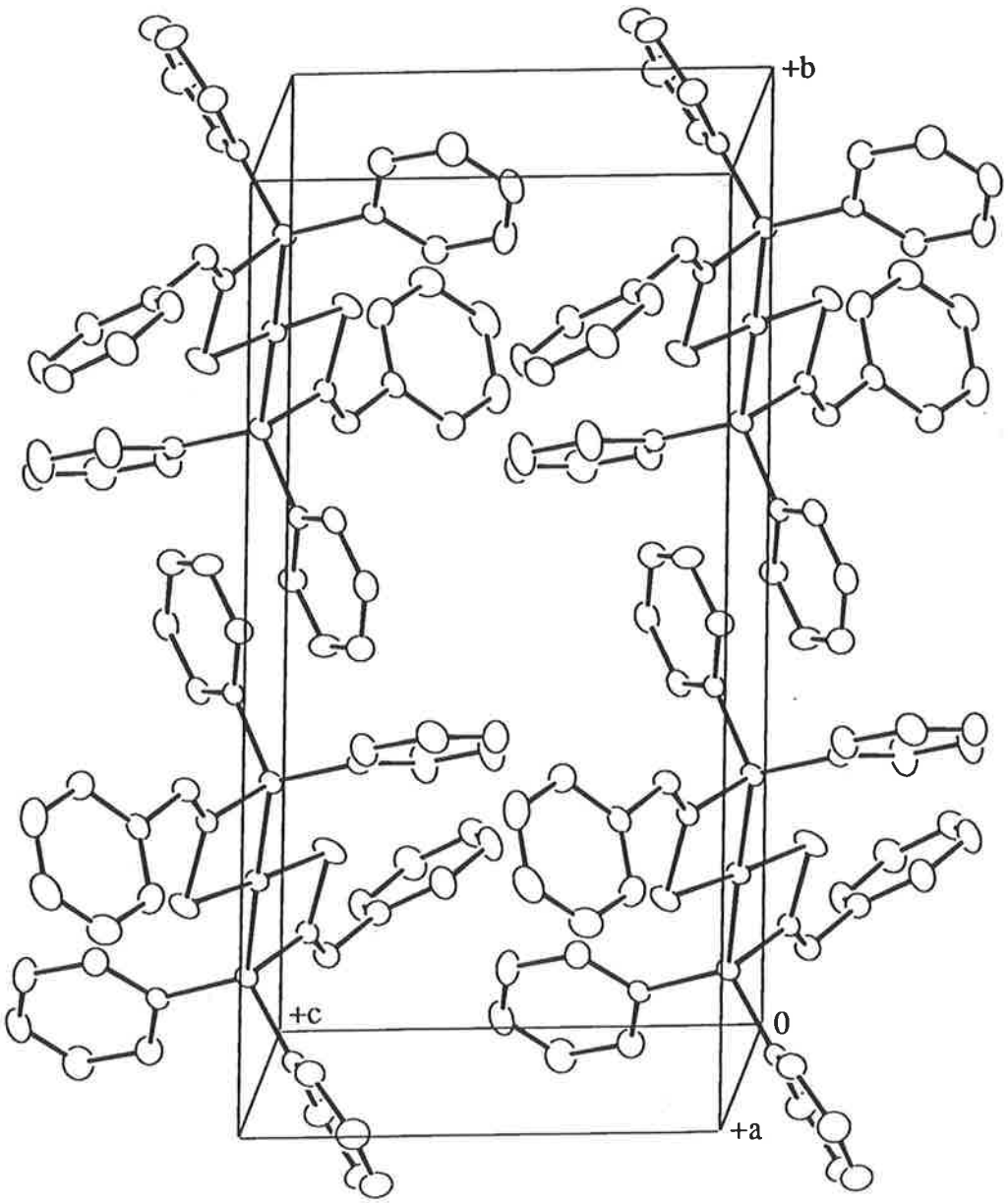

Fig. 6.1.2b The unit cell contents for *trans*-{Ni[$Ph_2PC(S)NPh]_2$}

6.1B differ in a *cis*- (6.1A) or *trans*- (6.1B) disposition of the phosphorus atoms. A similar coordination pattern has been observed before in a molybdenum complex, i.e. $\{Mo(CO)_2[Ph_2PC(S)NMe][\mu\text{-}Ph_2PC(S)NMe]\}_2$ [28, 29], where each ligand is attached in a bidentate manner to two molybdenum atoms, as described in Chapter 1. Crystals of the $\{Ni[Ph_2PC(S)NMe]_2\}$ complex were not obtained to confirm this assignment.

In the ^1H NMR spectrum the absence of the N-H resonance suggested that the ligand was deprotonated. The integration was consistent with what was expected for two phenyl groups and a methyl group. In the ^{13}C NMR spectrum a 1:2:1 ratio was seen for the Cβ, Cγ and C_a carbon atoms which indicated some in equivalence in the phenyl groups or the conversion between *cis* and *trans* isomers as described above. There were two values seen for the quaternary carbon atom C_q, one at δ 173.3 ppm which is similar in value to the one obtained above for $\{Ni[Ph_2PC(S)NPh]_2\}$ and suggests a P-, S- coordination mode while the other peak was at δ 201.5 ppm and could be due to a ligand with a P-, N- coordination mode. Both of these resonances were singlets.

In the FAB mass spectrum the molecular ion, $[M]^+$ appeared at 49% abundance. Two of the most intense ions were assigned to $[M\text{-}(SCNMe)]^+$, m/z 502, 100% and $[Ph_2PNiS]^+$, m/z 460, 93%. Other fragment ions are shown in Table 6.1.2a and reflect some similarity to the ions found for $\{Ni[Ph_2PC(S)NPh]_2\}$.

6.1.4 The Characterisation of trans-{Ni[Cy$_2$PC(S)NPh]$_2$}

6.1.4a The Spectroscopic Characterisation of *trans*-$\{Ni[Cy_2PC(S)NPh]_2\}$

Reaction of $NiNO_3$ with two mole equivalents of $[Cy_2PC(S)N(H)Ph]$ in the presence of excess Et_3N lead to the formation of $\{Ni[Cy_2PC(S)NPh]_2\}$ in high yield. The complex is an air-stable crystalline solid. Spectroscopic data is given in Table 6.1.2a.

The IR spectrum of this complex exhibited the same characteristic shifts as was seen for the $\{Ni[Ph_2PC(S)NPh]_2\}$ complex described above. Strong bands at 1573 cm^{-1} and 943 cm^{-1} are due to the ν(C=N) and ν(C-S) absorptions, respectively. In $[Cy_2PC(S)N(H)Ph]$ the thioamide(I) band occurred at 1502 cm^{-1} and the thioamide(II) band was observed at 1378 cm^{-1} (which is not evident in the complex). Clearly, this information coupled with the

absence of the υ(N-H) band indicates a coordination mode through the phosphorus and sulfur atoms.

The ^{1}H NMR spectrum of the complex was unremarkable with the phenyl ring protons in the expected region, i.e. δ 7.08 to 7.38 ppm, and the cyclohexyl protons in the range δ 1.18 to 2.45 ppm. As was seen from the IR analysis, the N-H resonance was also absent. An interesting resonance pattern was observed for the C_q, Cα and C_a carbon atoms in the ^{13}C NMR spectrum of the complex. The ^{13}C NMR spectrum had some resonances occurring as triplets in a 1:2:1 ratio, as has been mentioned above for the R = Ph complexes. The quaternary carbon signal shifted upfield to δ 175.6 ppm, ^{1}J(PC) 26.4 Hz, with respect to the value of δ 210.3 ppm, ^{1}J(PC) 34.4 Hz, found for [Cy_2PC(S)N(H)Ph]. The C_a resonance (nitrogen-bound phenyl ring) moved downfield to δ 148.2 ppm, ^{3}J(PC) 9.2 Hz, with respect to the value of δ 138.9 ppm, ^{3}J(PC) 11.6 Hz, found for the parent compound [Cy_2PC(S)N(H)Ph]. The Cα resonance (phosphorus-bound cyclohexyl ring) shifted upfield by approximately 3 ppm (δ 32.6 ppm, ^{1}J(PC) 7.5 Hz).

The molecular ion, $[M]^+$, was by no means the most abundant ion in the FAB mass spectrum with an intensity of 14%. The most abundant ion was assigned to $[Cy_2P(O)]^+$ with m/z of 213. Other ions are listed in Table 6.1.2a.

6.1.4b The Molecular Structure of *trans*-{Ni[Cy_2PC(S)NPh]$_2$}

The orange crystals of *trans-bis*(*P*, *P*-dicyclohexyl-*N*-phenyl-phosphinothioformamido) nickel(II), *trans*-{Ni[Cy_2PC(S)NPh]$_2$}, were obtained from the slow evaporation of a chloroform solution of the compound. Crystals are triclinic, space group $P\bar{1}$ with unit cell dimensions a = 10.591(1), b = 10.887(1), c = 10.385(1) Å, α = 112.699(9), β = 119.034(7), γ = 74.75(1)°, V = 961.6(2) Å^3, Z = 1 and D_x = 1.249 g cm^{-3}. The structure was refined to final R = 0.038, R_w = 0.043 for 1964 reflections with $I \geq 3.0\sigma(I)$. The molecular structure of the compound is shown in Fig. 6.1.4a ([14], 25% thermal ellipsoids) and selected interatomic parameters are listed in Table 6.1.2b.

The structure of *trans*-{Ni[Cy_2PC(S)NPh]$_2$} is as described above for *trans*-{Ni[Ph_2PC(S)NPh]$_2$} with only minor variations between the two molecules. The nickel

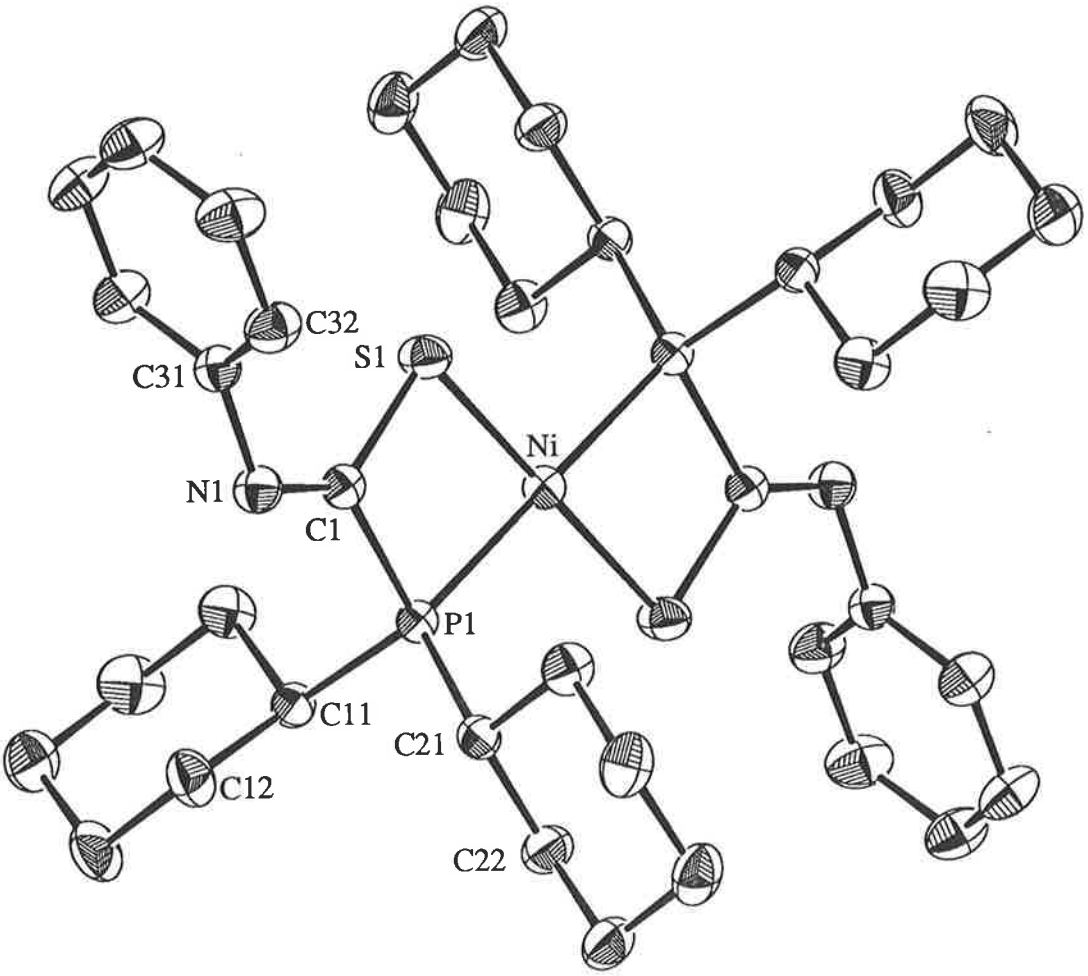

Fig. 6.1.4a The molecular structure of *trans*-{Ni[$Cy_2PC(S)NPh]_2$}

atom is disposed about a crystallographic centre of inversion located at (0, 0, 0). The atoms that comprise the central moiety of the ligand i.e. P(1), C(1), S(1) and N(1), are coplanar with deviations of 0.000(1), 0.006(3), 0.000(1) and -0.012(3) Å, respectively out of the least-squares plane through these atoms. The NiPC(1)S ring is essentially planar as can be seen in the torsion angles of -3.4(1)° for Ni/S(1)/C(1)/P(1) and 3.4(1)° for Ni/P(1)/C(1)/S(1). The chelation of the ligand occurs *via* the phosphorus and the thiocarbonyl sulfur atom, Ni-P(1) 2.1766(9) Å and Ni-S(1) 2.1773(9) Å, which define a chelate angle S(1)-Ni-P(1) of 78.09(3)°, these parameters being very similar to those found in the related {Ni[Ph_2PC(S)NPh]$_2$} complex. With respect to the parent ligand, [Cy_2PC(S)N(H)Ph], the distances C(1)-S(1), P(1)-C(1) and C(1)=N(1) have increased, decreased and decreased as expected with P-, S- coordination. The angles S(1)-C(1)-P(1), S(1)-C(1)-N(1) and P(1)-C(1)-N(1) followed the same trend as was observed above for the *trans*-{Ni[Ph_2PC(S)NPh]$_2$} complex.

The structure is molecular with no significant contacts between the atoms. The closest contact involving a hydrogen atom was 2.976 Å involving the N(1) and H(12a)' atoms (symmetry operation: 1-*x*, -*y*, -*z*) while there were no close contacts between non-hydrogen atoms less than 3.60 Å. The unit cell contents are shown in Fig. 6.1.4b.

6.1.5 The Characterisation of trans-{Ni[Cy_2PC(S)NMe]$_2$}

6.1.5a The Spectroscopic Characterisation of *trans*-{Ni[Cy_2PC(S)NMe]$_2$}

An ethanolic solution of $NiNO_3$ was reacted with two mole equivalents of impure [Cy_2PC(S)N(H)Me] with excess Et_3N (see Chapter 2). From this reaction, brick red crystals of {Ni[Cy_2PC(S)NMe]$_2$} were obtained. The complex is air-stable in the solid state and stable in solution. Spectroscopic data is given in Table 6.1.2a.

The IR spectrum of the complex shows bands at 1555 and 922 cm^{-1} attributable to the υ(C=N) stretching vibration and the υ(C-S) vibration, respectively. The υ(N-H) band was absent. As was seen for the R = Ph complexes, the υ(C=N) absorption is lower in frequency in the R' = Me complex with respect to the R' = Ph complex in {Ni[Cy_2PC(S)NR']$_2$}.

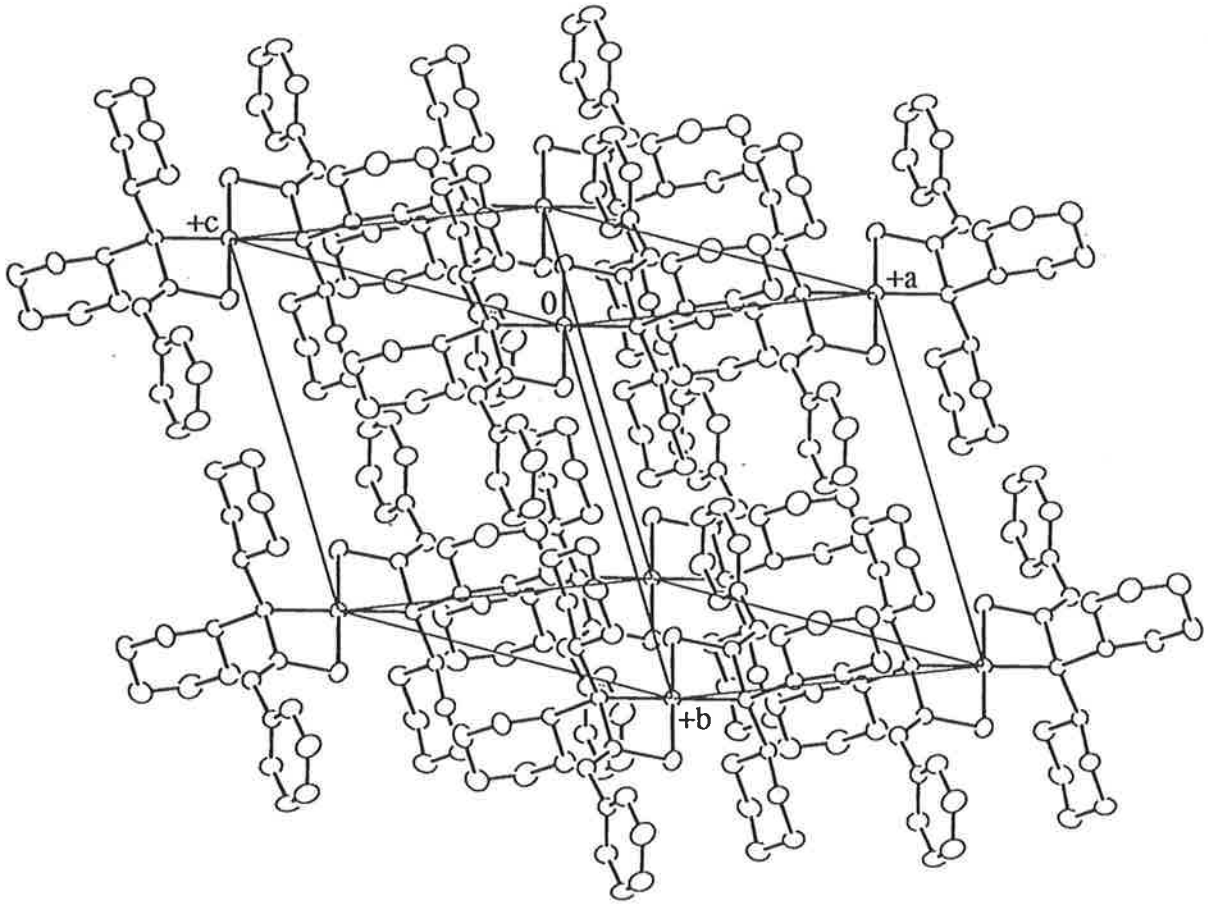

Fig. 6.1.4b The unit cell contents for *trans*-{Ni[$Cy_2PC(S)NPh]_2$}

The ^1H NMR spectrum was unremarkable and the important information derived was that the ligand was deprotonated and the cyclohexyl and methyl resonances were in their characteristic regions. In the ^{13}C NMR spectrum, the quaternary carbon resonance, C_q, occurred at δ 163.4 ppm, $^1J(PC)$ 33.0 Hz. The Cα and C_a resonances were not the expected doublets owing to P-C coupling but appeared as singlets. The chemical shift trends were consistent with the {Ni[$R_2PC(S)NR']_2$} structures described above and hence, a P-, S-coordination mode was concluded.

The FAB mass spectrum did not contain as many ions as was seen for the other three {Ni[$R_2PC(S)NR']_2$} complexes described above. The molecular ion, $[M]^+$, was present at 5% intensity and the most abundant ion was at m/z 231 and was assigned to $[Cy_2PC(S)H]^+$.

6.1.5b The Molecular Structure of *trans*-{Ni[$Cy_2PC(S)NMe]_2$}

The orange crystals of *trans-bis*(*P*, *P*-dicyclohexyl-*N*-methyl-phosphinothioformamido) nickel(II), *trans*-{Ni[$Cy_2PC(S)NMe]_2$}, were obtained from the slow evaporation of a chloroform solution of the compound layered with acetonitrile. Crystals are triclinic, space group $P\bar{1}$ with unit cell dimensions a = 9.068(2), b = 11.533(2), c = 8.704(1) Å, α = 92.23(1), β = 116.96(1), γ = 76.94(1)°, V = 788.3(2) Å^3, Z = 1 and D_x = 1.263 g cm^{-3}. The structure was refined to final R = 0.041, R_w = 0.044 for 2030 reflections with $I \geq 3.0\sigma(I)$. As mentioned earlier, the inclusion of this structure in this thesis is appropriate as it is the only complex which has been structurally characterised with the [$Cy_2PC(S)N(H)Me$] ligand in either the protonated or deprotonated form. The molecular structure is shown in Fig. 6.1.5a ([14], 35% thermal ellipsoids).

The parameters for the centrosymmetric molecule are equal within experimental error to those found in the two previous nickel complexes mentioned above except for the N(1)-C(31) separation of 1.470(5) Å which is longer than those found for {Ni[$Ph_2PC(S)NPh]_2$}, 1.415(6) and 1.441(6) Å, and {Ni[$Cy_2PC(S)NPh]_2$}, 1.436(4) Å. The coordination of the sulfur and phosphorus atoms to the nickel atom results in distances of Ni-S(1) 2.184(1) Å and Ni-P(1) of 2.1739(9) Å and a bite angle S(1)-Ni-P(1) of 78.23(4)°. A selection of bond distances and angles for {Ni[$Cy_2PC(S)NMe]_2$} can be found in Table 6.1.2b. The P(1),

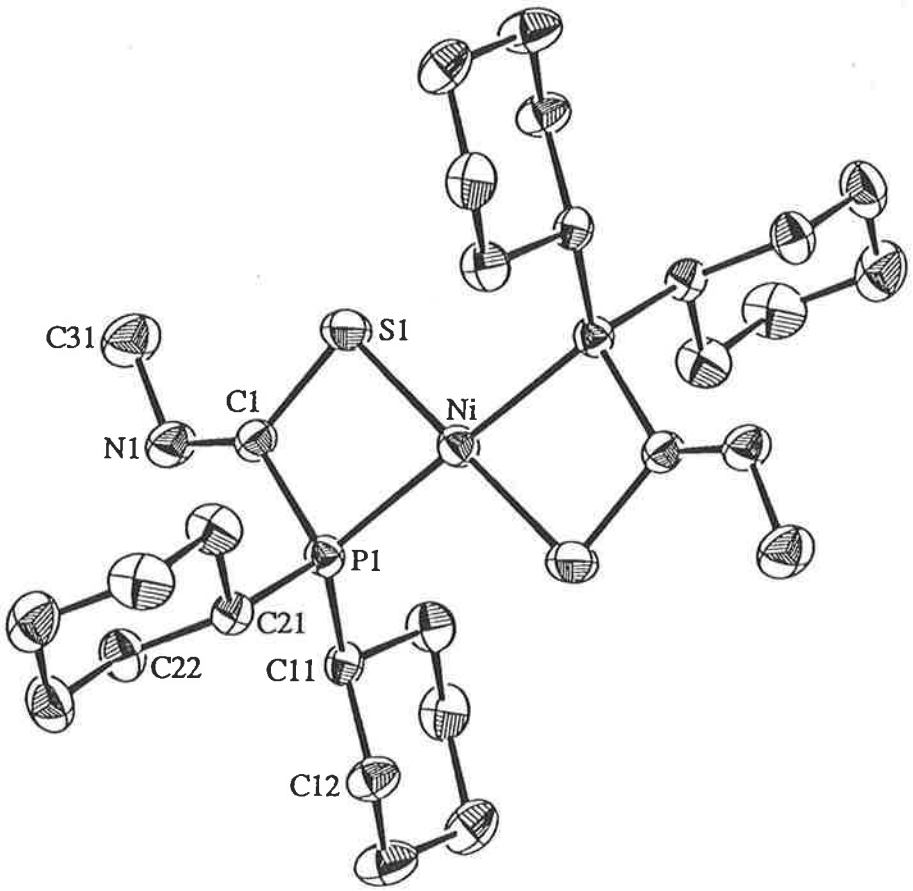

Fig. 6.1.5a The molecular structure of *trans*-{Ni[$Cy_2PC(S)NMe]_2$}

C(1), S(1) and N(1) atoms of the central chromophore of the ligand form a planar grouping with a mean deviation from the least-squares plane through these atoms being 0.004 Å (the nickel atom lying 0.177 Å above this plane) and this is consistent with significant π-electron density being delocalised over these atoms. The planarity of the four-membered ring comprising the Ni, S(1), C(1) and P(1) atoms is evident by the torsion angles of 4.2(1)° for Ni/S(1)/C(1)/P(1) and -4.2(1)° for Ni/P(1)/C(1)/S(1).

The S(1)-C(1) separation in {Ni[Cy_2PC(S)NMe]$_2$} of 1.777(4) Å is 0.023 Å longer than that found in {Ni[Cy_2PC(S)NPh]$_2$} and the N(1)=C(1) distance of 1.254(4) Å is 0.02 Å shorter than the comparable separation in {Ni[Cy_2PC(S)NPh]$_2$}. As noted above, the difference between the derived parameters are not great, however, some general conclusions may be made. The systematic variations suggests that the resonance contributor 6.1.5A is of more significance for the R' = Me complex whereas resonance form 6.1.5B is an important

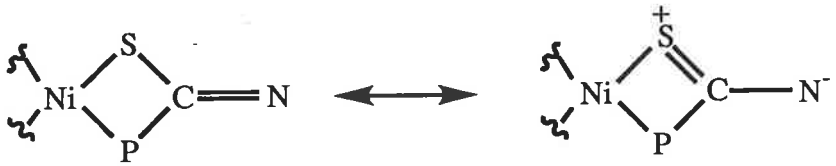

6.1.5A 6.1.5B

contributor for the R = Ph complex. These observations may be rationalised in terms of the greater inductive effect of the nitrogen-bound phenyl substituent. A similar situation was found for the free ligands when comparisons were made between the R' = Ph and Me derivatives with the R group kept constant. The angles for both {Ni[Cy_2PC(S)NR']$_2$} complexes are equal within experimental error.

In the lattice there were no significant inter- or intra-molecular interactions. The closest hydrogen contact was between atoms N(1) and H(14b)' of 2.888 Å (symmetry operation: -*x*, -1-*y*, -*z*) and there was no close contacts between non-hydrogen atoms less than 3.60 Å. The unit cell contents are shown in Fig. 6.1.5b.

6.1.6 The Molecular Structure of cis-{Pd[Cy_2PC(S)NPh]$_2$}

The yellow crystals of *cis-bis*(*P*, *P*-dicyclohexyl-*N*-phenyl-phosphinothioformamido) palladium(II), *cis*-{Pd[Cy_2PC(S)NPh]$_2$}, were obtained by the slow diffusion of ethanol

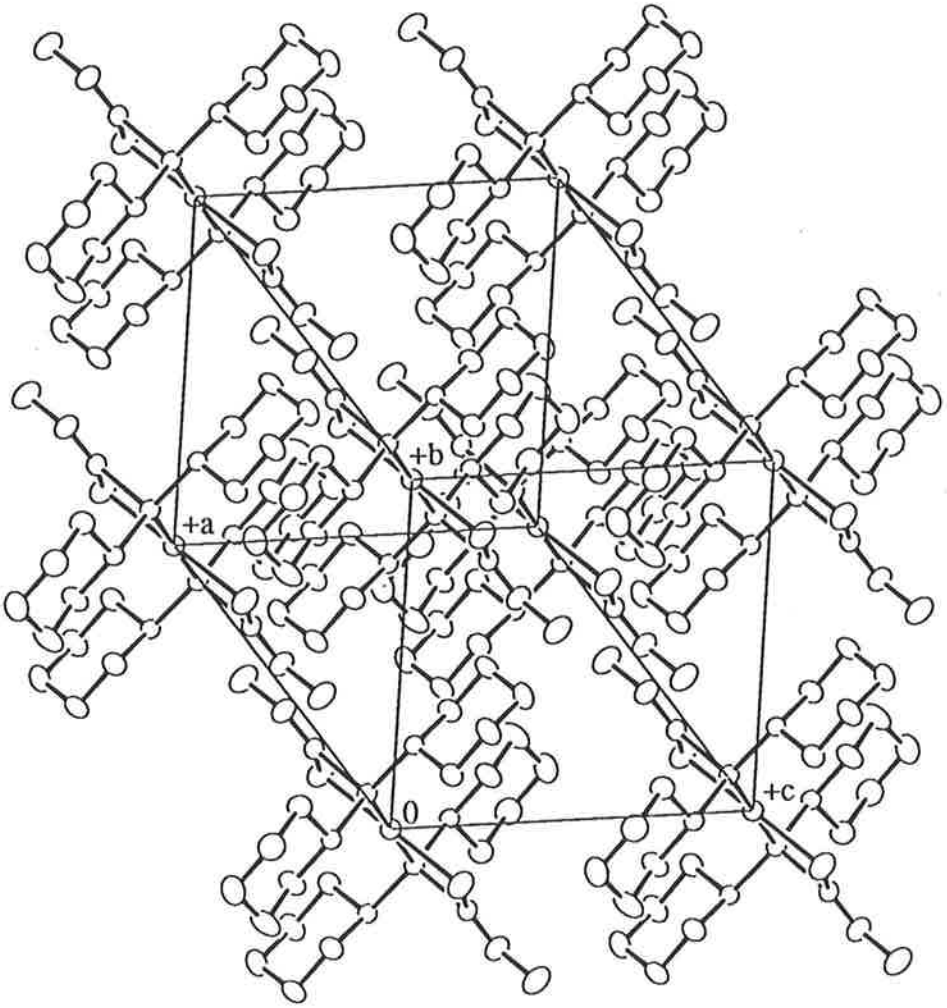

Fig. 6.1.5b The unit cell contents for *trans*-{Ni[$Cy_2PC(S)NMe]_2$}

into a chloroform solution of the compound which was kindly supplied by Professor R. Kramolowsky. Crystals are monoclinic, space group *C*2/*c* with unit cell dimensions a = 19.601(2), b = 8.2633(8), c = 23.627(1) Å, β = 94.218(6)°, V = 3816.5(6) Å^3, Z = 4 and D_x = 1.342 g cm^{-3}. The structure was refined to final R = 0.040, R_w = 0.049 for 2331 reflections with $I \geq 3.0\sigma(I)$. The molecular structure of *cis*-{Pd[$Cy_2PC(S)NPh]_2$} is shown in Fig. 6.1.6a ([14], 25% thermal ellipsoids) and selected interatomic parameters are listed in Table 6.1.6.

The structure is molecular there being no significant intermolecular contacts in the lattice. The closest non-hydrogen contact of 3.60(1) Å occurs between the C(32) and C(32)' atoms (symmetry operation: -0.5-*x*, 0.5-*y*, -*z*) and the closest contact involving a hydrogen atom is 2.867(2) Å between the S(1) and H(12a)' atoms (symmetry operation: +*x*, 1+*y*, +*z*); a view of the unit cell contents is shown in Fig. 6.1.6b. The ligands chelate the palladium atom *via* the sulfur and phosphorus atoms. The palladium atom is situated on a crystallographic two-fold axis, this results in a *cis*-S_2P_2 donor set and a square planar geometry about the palladium atom. The Pd-S(1) distance of 2.338(1) Å and the Pd-P(1) distance of 2.286(1) Å are comparable to the Pd-S and Pd-P distances found in other palladium complexes, i.e. Pd-S 2.368(2) and 2.415(2) Å in *cis*-{$Pd(C_6F_5)_2[S_2CPCy_3]$} [136] and Pd-S 2.362(2) and 2.366(2) Å and Pd-P 2.264(2) and 2.282(2) Å in {$Ph_2PCH_2PPh_2Pd(SCN)_2$} [137]. The maximum distortion from the ideal square planar geometry is found in the P(1)-Pd-P(1') angle of 111.44(6)° which has expanded presumably to minimise interactions between the phosphorus-bound cyclohexyl groups. The mean deviation of the atoms defining the square plane is 0.048(2) Å. The result of the S-, P-coordination mode of the ligand is the formation of a four-membered PdSCP ring which is essentially planar as seen in the Pd/S(1)/C(1)/P(1) and Pd/P(1)/C(1)/S(1) torsion angles of 3.0(2) and -3.1(2)°, respectively. Evidence that the [$Cy_2PC(S)NPh]^-$ anion functions as a thiolate ligand is found in the elongation of the S(1)-C(1) bond (1.749(5) Å) compared with the S(1)-C(1) bonds of 1.658(7) and 1.661(6) Å (two molecules in the asymmetric unit) found for the free protonated ligand [15]. Other significant changes between the free and coordinated ligands are evident in the derived bond distances and angles as discussed below.

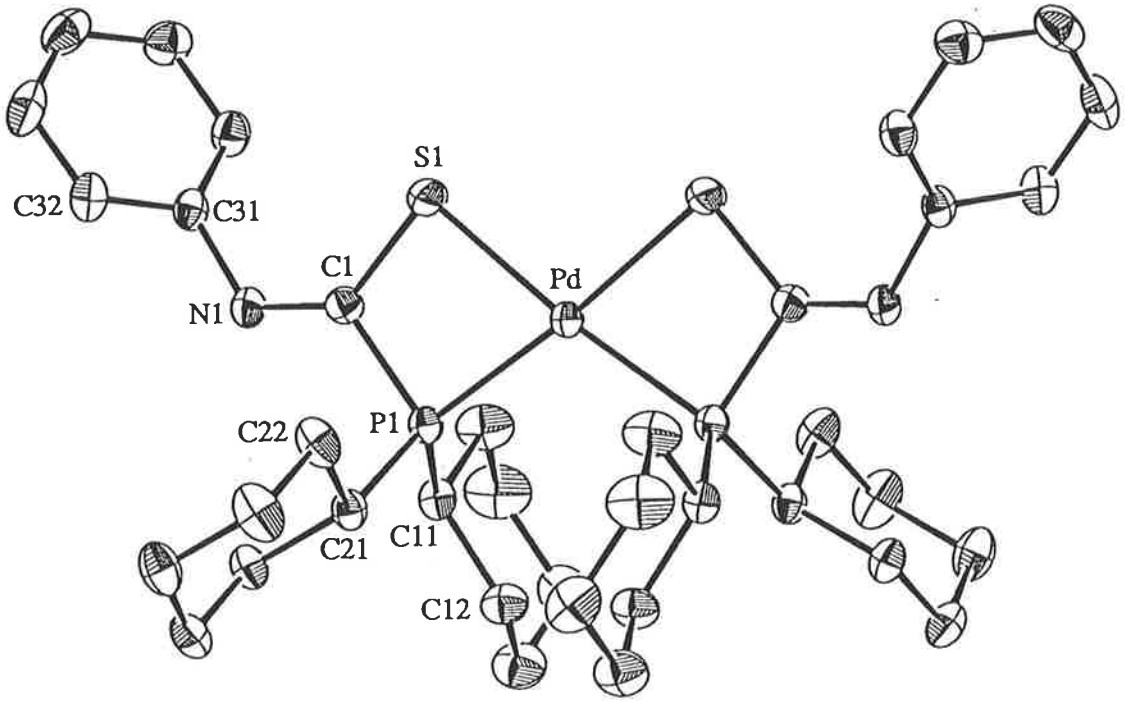

Fig. 6.1.6a The molecular structure of *cis*-{Pd[$Cy_2PC(S)NPh]_2$}

Table 6.1.6: Selected bond distances (Å) and angles (deg.) for *cis*-{Pd[$Cy_2PC(S)NPh]_2$}

Pd-S(1)	2.347(1)	Pd-P(1)	2.279(1)
S(1)-C(1)	1.749(5)	P(1)-C(1)	1.811(5)
P(1)-C(11)	1.826(5)	P(1)-C(21)	1.830(5)
N(1)-C(1)	1.285(6)	N(1)-C(31)	1.425(6)
S(1)-Pd-P(1)	74.19(4)	S(1)-Pd-S(1')*	100.27(7)
S(1)-Pd-P(1')	173.92(5)	P(1)-Pd-P(1')	111.44(6)
Pd-S(1)-C(1)	90.9(2)	Pd-P(1)-C(1)	91.5(2)
Pd-P(1)-C(11)	119.0(2)	Pd-P(1)-C(21)	121.1(2)
C(1)-P(1)-C(11)	106.1(2)	C(1)-P(1)-C(21)	107.3(2)
C(11)-P(1)-C(21)	108.5(2)	C(1)-N(1)-C(31)	121.5(4)
S(1)-C(1)-P(1)	103.3(2)	S(1)-C(1)-N(1)	132.0(4)
P(1)-C(1)-N(1)	124.7(4)		

* Primed atoms related by crystallographic two-fold axis

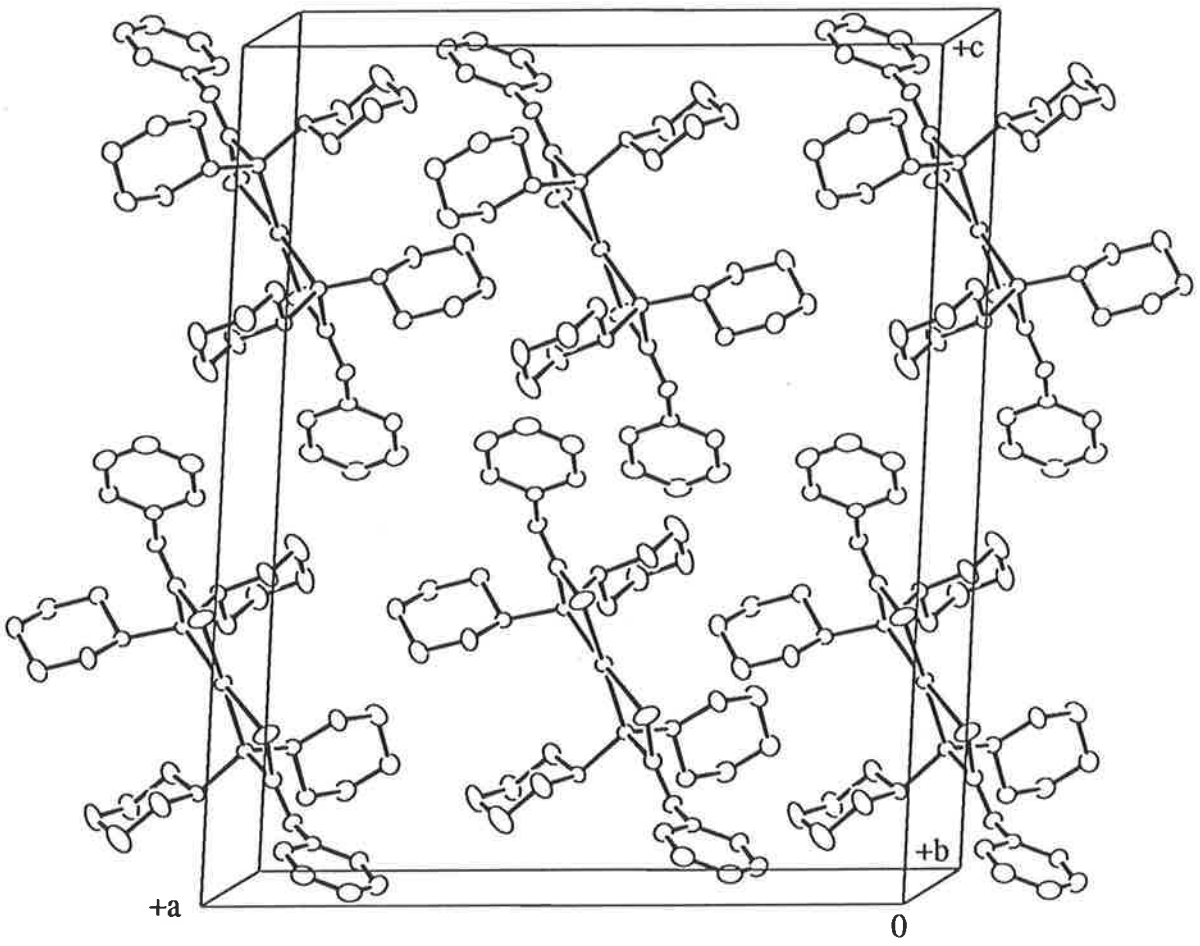

Fig. 6.1.6b The unit cell contents for *cis*-{Pd[$Cy_2PC(S)NPh]_2$}

On deprotonation of the [$Cy_2PC(S)N(H)Ph$] ligand and coordination of the resultant anion, there is a contraction of the P(1)-C(1) bond distance to 1.811(5) Å, *cf.* 1.859(7) and 1.877(7) Å in the free ligand [15], and a contraction in the C(1)-N(1) bond length to 1.285(6) Å (*cf.* 1.356(8) and 1.349(9) Å). These changes are consistent with those observations in the {$Ni[R_2PC(S)NR']_2$} complexes described above. Less significant, but notable, are the changes in the P-C(11) and P-C(21) bond distances, i.e. 1.826(5) and 1.830(5) Å, respectively which are shorter than the range of distances of 1.843(7) to 1.876(7) Å found for the comparable bonds in the free ligand [15]. The N(1)-C(31) separations are comparable in the two structures. The systematic variation of the S(1)-C(1) and N(1)-C(1) bond distances suggests that canonical structure (6.1.6A) is more important than canonical structure (6.1.6B) but the contraction in the P(1)-C(1) distance is unexpected. This observation, coupled with the planarity of the S(1), P(1), N(1) and C(1) chromophore (mean deviation from the least-squares plane: 0.002(2) Å), suggests the delocalisation of π-electron density over these atoms and provides evidence for a marked contribution of canonical form (6.1.6C) to the overall structure. Similar conclusions are valid for the {$Ni[R_2PC(S)NR']_2$} structures.

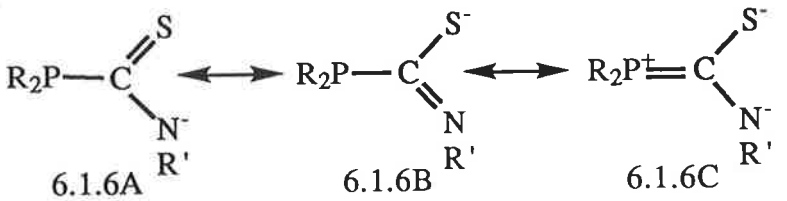

6.1.6A 6.1.6B 6.1.6C

Changes in bond angles that occur upon coordination are most apparent about the C(1) atom. Thus, the S(1)-C(1)-P(1) angle in the complex contracts and the S(1)-C(1)-N(1) and P(1)-C(1)-N(1) angles expand by approximately 21, 7 and 14°, respectively compared with those in the free ligand [15]. The contraction in the S(1)-C(1)-P(1) angle may be related to the formation of the four-membered ring and the other angles expand in order to compensate for this change. Owing to the presence of the palladium atom, the C-P-C angles open up by approximately 4-5° compared to the values in the free ligand to relieve the steric strain.

There is a palladium(II) structure available for comparison which contains the closely related dicyclohexylphosphinodithioformate anion, i.e. *cis*-{$Pd(Cy_2PC(S)S)_2$} [138]. The ligand chelates the palladium atom forming a *cis*-S_2P_2 donor set with Pd-S 2.338(1),

2.334(1) Å and Pd-P 2.286(1), 2.288(1) Å; the pendant sulfur atoms do not coordinate the palladium atom. These values are marginally shorter and longer, respectively than the comparable values in the structure of *cis*-{Pd[$Cy_2PC(S)NPh]_2$} suggesting that the two ligands have similar coordinating abilities towards palladium. It is also instructive to consider some of the ligand parameters in the dithioformato structure, in particular the S(1)-C(1) distances of 1.722(4) and 1.715(3) Å and the P(1)-C(1) distances of 1.830(4) and 1.844(4) Å (the atom labels in the original structure have been changed to be consistent with Fig. 6.1.6a). These parameters are shorter and longer, respectively than the S(1)-C(1) and P(1)-C(1) parameters found in *cis*-{Pd[$Cy_2PC(S)NPh]_2$}, consistent with the notion that the canonical structure analogous to 6.1.6C is not as important in the dithioformato complex owing to the diminished electronegativity of the non-coordinating sulfur atom compared with the NPh group in the thioformamido ligand.

The anionic $[Cy_2PC(S)NPh]^-$ ligand has been characterised crystallographically with the three nickel triad metals: *trans*-{Ni[$Cy_2PC(S)NPh]_2$} (above), *trans*-{Pt[$Cy_2PC(S)NPh]_2$} [139] and *cis*-{Pd[$Cy_2PC(S)NPh]_2$} (present study) in which a S-, P- coordination mode of the ligand was observed for the square-planar metal atom in each case. In the nickel and platinum structures the P_2S_2 donor set adopts the *trans* arrangement while in the palladium analogue the *cis* form was obtained from the reaction mixture. Variation of the metal centre does not alter the electronic character of the $[Cy_2PC(S)NPh]^-$ ligand significantly as all the parameters are equal within experimental error for the three structures.

6.2 Metal Complexes with Diorganophosphinylthioformamides

The two {Ni[$Ph_2P(O)C(S)NR']_2$}, R' = Ph and Me, complexes exhibited the same structural characteristics and, hence, a general description will be given for the {Ni[$Ph_2P(O)C(S)NPh]_2$} complex with details for {Ni[$Ph_2P(O)C(S)NMe]_2$} following in parentheses when relevant. The spectroscopic results for both complexes appear in Table 6.2.1.

Table 6.2.1: Spectroscopic data for $\{Ni[Ph_2P(O)C(S)NR']_2\}$, R' = Me or Ph

IR (frequencies given are in cm^{-1})

	υ(thioamide I)	υ(thioamide II)	υ(P=O)
{Ni[Ph₂P(O)C(S)NPh]₂}	1515	1384	1134
{Ni[Ph₂P(O)C(S)NMe]₂}	1495	1383	1136

^1H NMR (chemical shifts, δ, are in ppm)

{Ni[Ph₂P(O)C(S)NPh]₂}: PPh_2 δ 7.00-7.78 (broad), NPh δ 7.00-7.78 (broad)

{Ni[Ph₂P(O)C(S)NMe]₂}: PPh_2 δ 7.05-8.04 (broad), NMe δ 3.34 (broad)

^{13}C NMR (chemical shifts, δ, are in ppm)

{Ni[Ph₂P(O)C(S)NPh]₂}: PPh_2 Cα δ 141.0 (broad), Cβ-Cδ δ 133.7-122.4, NPh C_a δ 146.0 (broad), C_b δ 132.8, C_c δ 121.0, C_d δ 125.8, C_q δ 174.0 (broad)

{Ni[Ph₂P(O)C(S)NMe]₂}: PPh_2 Cα δ 143.0 (broad), Cβ-Cδ δ 132.6-123.3, NMe C_a δ 46.5, C_q δ 166.9 (broad)

FAB (m/z, [assignment] intensity)

{Ni[Ph₂P(O)C(S)NPh]₂}: 731, $[M]^+$ 2%; 578, $[M-(2xPh)]^+$ 10%; 550, $[(Ph_2P(O)C(S)NPh)Ni(PhPCS)]^+$ 5%; 514, $[M-(Ph_2P, S)]^+$ 4%; 501, $[M-(3xPh)]^+$ 2%; 338, $[Ph_2P(O)C(S)N(H)Ph]^+$ 59%; 320, $[Ph_2PC(S)N(H)Ph]^+$ 11%; 304, $[(Ph_2P(O)CS)Ni]^+$ 15%; 217, $[Ph_2P(O)OH]^+$ 12%; 201, $[Ph_2PO]^+$ 100%

{Ni[Ph₂P(O)C(S)NMe]₂}: 607, $[M]^+$ 6%; 562, $[M-(CNMe)]^+$ 2%; 534, $[M-(SCNMe)]^+$ 2%; 477, $[M-(2xCNMe, S)]^+$ 3%; 333, $[(Ph_2P(O)C(S)NMe)Ni]^+$ 3%; 276, $[Ph_2P(O)C(S)N(H)Me]^+$ 83%; 217, $[(Ph_2P(O)OH)]^+$ 19%; 201, $[(Ph_2PO)]^+$ 100%

6.2.1 The Spectroscopic Characterisation of {Ni[$Ph_2P(O)C(S)NPh]_2$}

The reaction between two mole equivalents of [$Ph_2P(O)C(S)N(H)Ph$] and nickel nitrate (with excess Et_3N) afforded the complex {$Ni[Ph_2P(O)C(S)NPh]_2$}. In the IR spectrum the υ(N-H) absorption band was not evident indicating that the ligand was deprotonated. The thioamide(I) band frequency decreased from the value found for the free ligand while the opposite was true for the thioamide(II) band which shifted to higher frequency, Table 6.2.1. These observations indicate that there was increased double bond character between the carbon and sulfur atoms and that the C(1)-N(1) bond approached a single bond. The change in the υ(P=O) absorption indicates that the oxygen atom participates in coordination to the nickel centre as evidenced by the lowering in the frequency of this band. Different metal complexes with the [$Ph_2P(O)C(S)N(H)R'$] ligands have been prepared previously. These studies have shown that these ligands may coordinate to such metal centres as manganese, iridium, rhodium and rhenium [140-142]. In these cases the coordination to the metal centre was *via* the oxygen atom (from IR spectroscopy) and chelation of the ligands involved the sulfur atom which lead to the formation of MOPCS five-membered rings. Support for this assignment was found in the appearance of a υ(C-S) absorption band at approximately 970 ± 20 cm^{-1} (when reported). If in each {$Ni[Ph_2P(O)C(S)NR']_2$} complex coordination to the nickel centre by sulfur was present, a υ(C-S) absorption band at approximately 970 cm^{-1} should be evident in each IR spectrum. No such band was observed in this region and, indeed, the thioamide(II) band shifted to higher frequency for both {$Ni[Ph_2P(O)C(S)NR']_2$} complexes, e.g. {$Ni[Ph_2P(O)C(S)NPh]_2$} υ(C-S) 1384 cm^{-1}. This suggests that the sulfur atom was exocyclic and did not participate in bonding to the nickel atom. With this information a plausible structure could be postulated where each ligand coordinates the nickel centre *via* the oxygen and nitrogen atoms as shown in 6.2A (the *trans* isomer is shown, however, the *cis* isomer may also exist).

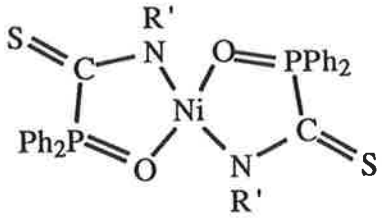

6.2A

Unfortunately, crystals of these complexes were not obtained and hence an X-ray analysis was precluded.

The ^{1}H NMR spectra were unremarkable and showed the phenyl and methyl resonances; the peaks in these regions were broad. The absence of the N-H resonance in each spectrum confirmed that the ligands are deprotonated. In the ^{13}C NMR spectra the expected resonances were observed; no coupling was observed. The C_q resonance did occur upfield with respect to the free ligand, i.e. δ 174.0 ppm for $\{Ni[Ph_2P(O)C(S)NPh]_2\}$ and δ 166.9 ppm for $\{Ni[Ph_2P(O)C(S)NMe]_2\}$. The other carbon atom resonances did not shift significantly from those found in the uncoordinated ligand.

The molecular ions, $[M]^+$, for the two complexes, i.e. $[\{Ni[Ph_2P(O)C(S)NPh]_2\}]^+$ and $[\{Ni[Ph_2P(O)C(S)NMe]_2\}]^+$, occurred at very small intensities, i.e. 2% and 5%, respectively, in their FAB mass spectra. Other ions that appeared resulted from cleavage of various functional groups were also of low abundance. The respective protonated ligands appeared at relatively high abundance and the $[Ph_2PO]^+$ ion was the most abundant ion for both complexes. FAB mass spectral results can be found in Table 6.2.1.

The reaction of the compounds $[Cy_2P(O)C(S)N(H)R']$, R' = Ph or Me, with the $NiNO_3$ species (in the presence of Et_3N) resulted in the formation of the $\{Ni[Cy_2PC(S)NR']_2\}$ complexes, as discussed earlier. Clearly, deprotonation of the nitrogen atom had occurred and there was the abstraction of the oxygen atom. This different reactivity of the $R_2P(O)C(S)N(H)R'$ ligands confirms that their chemistry depends on the nature of the phosphorus-bound R groups.

6.3 Metal Complex with Diorgano-N-phenyl-thiophosphinylthioformamide

6.3.1a The Spectroscopic Characterisation of *trans*-{Ni[$Ph_2P(S)C(S)NPh]_2$}

Reaction of two moles of [$Ph_2P(S)C(S)N(H)Ph$] with $NiNO_3$ and Et_3N produces a yellow/brown precipitate of {Ni[$Ph_2P(S)C(S)NPh]_2$}. Spectroscopic data is given in Table 6.3.1a.

There are three absorption bands of interest in the IR spectrum of {Ni[$Ph_2P(S)C(S)NPh]_2$} which are located at 1524, 948 and 605 cm^{-1} and are due primarily to υ(C=N), υ(C-S) and υ(P=S), respectively while the υ(N-H) band was absent. The υ(C=N) band has shifted to higher frequency by 19 cm^{-1} compared to the value of 1543 cm^{-1} found for the [$Ph_2P(S)C(S)N(H)Ph$] compound. The υ(P=S) band has shifted to lower frequency by 35 cm^{-1} suggesting that this sulfur atom is involved in coordination to the nickel centre. Previous studies of coordination complexes of this ligand in its deprotonated form with manganese and rhenium, showed values for υ(C=N) at 1550 and 1555 cm^{-1}, respectively and values for υ(P=S) are 615 and 610 cm^{-1}, respectively (no values were given for the υ(C-S) band). In these metal complexes, the coordination to the metal centre was reported to occur *via* the thiocarbonyl and phosphorus-bound sulfur atoms leading to the presence of MSPCS five-membered rings [142-144].

The ^1H NMR spectrum revealed that the ligand was deprotonated as the N-H resonance was not apparent. In the ^{13}C NMR spectrum the C_q and C_a resonances shifted significantly compared with the equivalent resonances in the free ligand. The C_q resonance moved upfield to δ 176.2 ppm, ^1J(PC) 109.3 Hz, and C_a shifted downfield to δ 149.2 ppm, ^3J(PC) 29.1 Hz.

The FAB mass spectrum showed the presence of the molecular ion, $[M]^+$, at 4% abundance. The most intense peak was assigned to $[Ph_2PNiS_3]^+$, the free ligand, i.e. $[Ph_2P(S)C(S)N(H)Ph]^+$, was also evident at 54% intensity.

Table 6.3.1a: Spectroscopic data for *trans*-{Ni[$Ph_2P(S)C(S)NPh]_2$}

IR (frequencies given are in cm^{-1})

	υ(thioamide I)	υ(C-S)	υ(P=S)
{Ni[$Ph_2P(S)C(S)NPh]_2$}	1524	948	605

^1H NMR (chemical shifts, δ, are in ppm)

PPh_2 7.03-7.96, NPh 7.03-7.96

^{13}C NMR (chemical shifts, δ, are in ppm)

PPh_2 Cα 127.8 $^1J(PC)$ 60.6 Hz, Cβ-Cδ 132.9-128.7, NPh C_a 149.2 $^3J(PC)$ 29.1 Hz, C_b 128.6, C_c 121.3, C_d 125.1, C_q 176.2 $^1J(PC)$ 109.3 Hz

FAB (m/z, [assignment] intensity)

763, $[M]^+$ 4%; 659, $[M-(CNPh)]^+$ 2%; 630, $[M-(SCNPh)]^+$ 3%; 523, $[(Ph_2PS)_2NiS]^+$ 7%; 354, $[Ph_2P(S)C(S)N(H)Ph]^+$ 54%; 338, $[Ph_2PNiS_3]^+$ 100%; 320, $[Ph_2PC(S)NPh]^+$ 6%; 306, $[Ph_2PNiS_2]^+$ 83%

6.3.1b The Molecular Structure of *trans*-{Ni[$Ph_2P(S)C(S)NPh]_2$}

The brown crystals of *trans-bis*(*P*, *P*-diphenyl-*N*-phenyl-thiophosphinylthioformamido) nickel(II), *trans*-{Ni[$Ph_2P(S)C(S)NPh]_2$}, were obtained by the vapour diffusion of acetonitrile into a chloroform solution of the compound. Crystals are monoclinic, space group $P2_1/c$ with unit cell dimensions a = 12.160(4), b = 8.909(2), c = 16.375(3) Å, β = 91.15(2)°, V = 1773.7(7) $Å^3$, Z = 2 and D_x = 1.430 g cm^{-3}. The structure was refined to final R = 0.049, R_w = 0.046 for 1336 reflections with $I \geq 3.0\sigma(I)$.

The nickel atom is centred about a crystallographic centre of inversion located at (0, 0, 0). The structure of the complex is depicted in Fig. 6.3.1a ([14], 25% thermal ellipsoids) and selected interatomic parameters are given in Table 6.3.1b. The $[Ph_2P(S)C(S)NPh]^-$ anion coordinates the nickel atom *via* the phosphinyl sulfur and the thioamide sulfur atoms leading to the formation of a NiSPCS five-membered ring. The two independent Ni-S distances are practically equal within experimental error, i.e. Ni-S(2) 2.197(2) Å and Ni-S(1) 2.184(2) Å, and the chelate angle S(1)-Ni-S(2) is 83.53(8)°. The Ni-S distances compare favourably to other dithiolate complexes with chelating ligands, e.g. 2.2035(5)-2.222(7) Å in {Ni{$S_2COR]_2$} [145] and 2.179(3)-2.208(3) Å in {Ni[$S_2CNR_2]_2$} [146-148]. The nickel atom exists in a slightly distorted square planar geometry, the major distortion arises as a result of the restricted bite angle of the ligand. The deviations from the least-squares plane through the central S(1), S(2), P(1) and C(1) atoms are 0.015(3), -0.009(2), 0.013(2) and -0.181(7) Å, respectively with the nickel atom lying 0.221(2) Å above this plane. The five-membered ring deviates significantly from planarity as reflected in the torsion angles Ni/S(2)/P(1)/C(1) of 6.8(4)° and Ni/S(1)/C(1)/P(1) of 13.0(3)°. The nickel atom geometry in {Ni[$Ph_2PC(S)NPh]_2$} exists in a more distorted environment owing to the presence of a four-membered ring. The additional strain of this ring is reflected in the bite angles of 77.58(5)° and 77.40(6)° (two independent $[Ph_2PC(S)NPh]^-$ anions). This contrasts that found in {Ni[$Ph_2P(S)C(S)NPh]_2$} where the five-membered ring accommodates the larger bite angle. i.e. 83.53(8)°. The C(1)-S(1) distances are approximately 0.05 Å longer in the {Ni[$Ph_2PC(S)NPh]_2$} complex compared to the

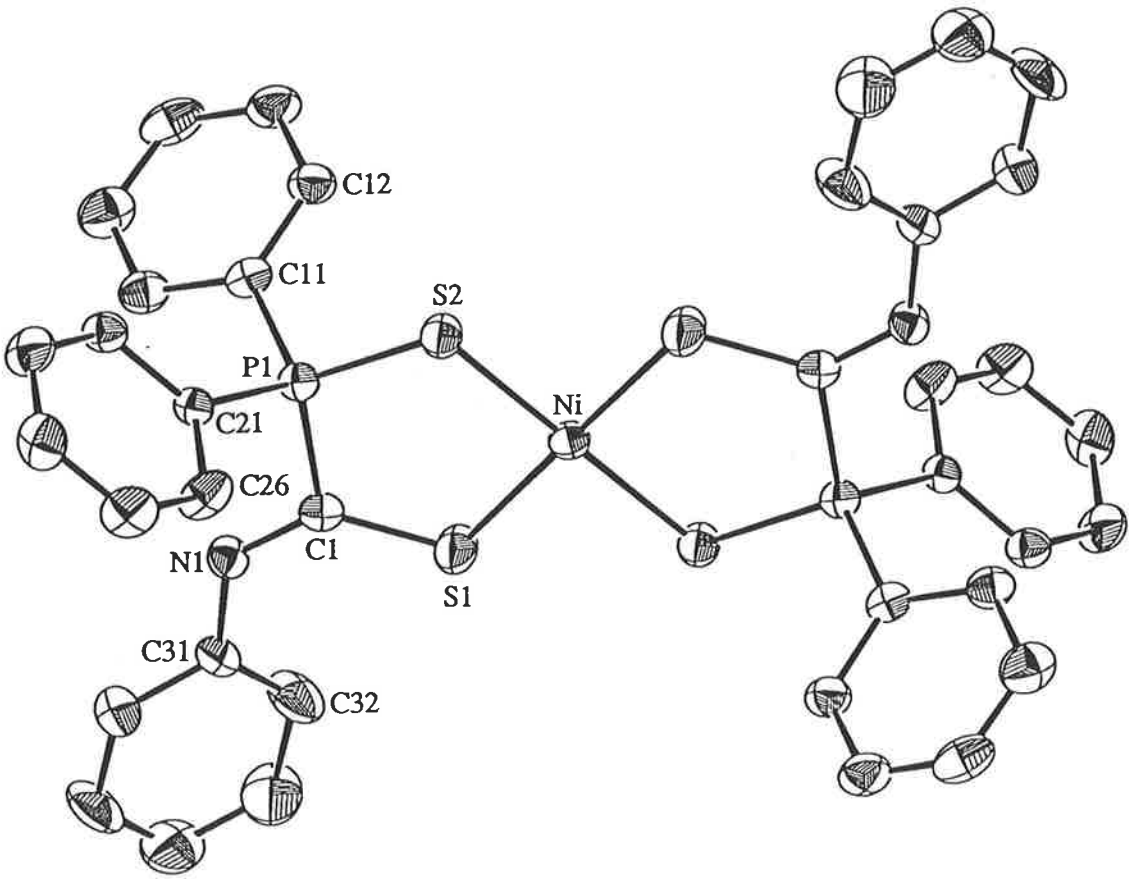

Fig. 6.3.1a The molecular structure of *trans*-{Ni[$Ph_2P(S)C(S)NPh]_2$}

Table 6.3.1b: Selected bond distances (Å) and angles (deg.) for *trans*-{Ni[$Ph_2P(S)C(S)NPh]_2$}

Ni-S(1)	2.184(2)	Ni-S(2)	2.197(2)
S(1)-C(1)	1.706(7)	S(2)-P(1)	2.001(3)
P(1)-C(1)	1.836(7)	P(1)-C(11)	1.820(7)
P(1)-C(21)	1.794(7)	N(1)-C(1)	1.290(8)
N(1)-C(31)	1.414(9)		
S(1)-Ni-S(2)	83.53(8)	S(1)-Ni-S(2)'*	96.47(8)
S(1)-Ni-S(1)'	180.00	S(2)-Ni-S(2')	180.00
Ni-S(1)-C(1)	111.8(3)	Ni-S(2)-P(1)	105.4(1)
S(2)-P(1)-C(1)	108.9(2)	S(2)-P(1)-C(11)	112.7(3)
S(2)-P(1)-C(21)	110.2(3)	C(1)-N(1)-C(31)	124.9(6)
S(1)-C(1)-P(1)	115.8(4)	S(1)-C(1)-N(1)	132.6(6)
P(1)-C(1)-N(1)	111.6(5)		

* Primed atoms related by crystallographic centre of inversion

equivalent separation in {Ni[$Ph_2P(S)C(S)NPh]_2$}. The reduced steric strain in the latter complex allows for an enhanced orbital overlap and hence a stronger interaction.

As expected, the S(1)-C(1) and S(2)=P(1) distances of 1.706(7) and 2.001(3) Å, respectively in {Ni[$Ph_2P(S)C(S)NPh]_2$} have been elongated significantly compared to the equivalent distances found for the uncoordinated ligand, i.e. [$Ph_2P(S)C(S)N(H)Ph$], of 1.634(6) and 1.954(2) Å, respectively. The P(1)-C(1), C(1)=N(1) and N(1)-C(31) separations have all contracted with respect to the corresponding distances in [$Ph_2P(S)C(S)N(H)Ph$]. The P(1)-C(1) distance is approximately 0.04 Å shorter in the complex and the C(1)=N(1) distance has attained additional double bond character. The torsion angles of -167.9(3) and 9.4(6)° for S(2)/P(1)/C(1)/S(1) and S(2)/P(1)/C(1)/N(1), respectively show that the possibility of delocalisation of π-electron density over these atoms is unlikely owing to this lack of planarity.

Two other metal complexes have been characterised structurally containing the $[Ph_2P(S)C(S)NPh]^-$ anion. In the structure of {$Mn(CO)_4$[$Ph_2P(S)C(S)NPh$]} the two sulfur atoms, i.e. S(1) and S(2), chelate the manganese atom forming disparate Mn-S bond distances of 2.390(1) Å and 2.410(1) Å, respectively [18]. In the structure of {$Mo(CO)_2(\eta^5\text{-}C_5H_5)$[$Ph_2P(S)C(S)NPh$]}, the molybdenum atom chelated by the S(1) and N(1) atoms (Mo-S(1) 2.490(2) Å and Mo-N(1) 2.175(5) Å) with the S(2) atom not participating in coordination to the central atom [24]. Details for the two complexes can be found in Section 1.6.

No significant interactions are found within the unit cell of {Ni[$Ph_2P(S)C(S)NPh]_2$}. The closest non-hydrogen contact occurs between two symmetry related C(32) atoms with a separation of 3.47(2) Å (symmetry operation: $-x$, $1-y$, $-z$). The closest contact involving an hydrogen atom of 3.074 Å occurs between the Ni and H(25)' atoms (symmetry operation: $-x$, $-0.5+y$, $-0.5-z$). The contents of the unit cell are shown in Fig. 6.3.1b.

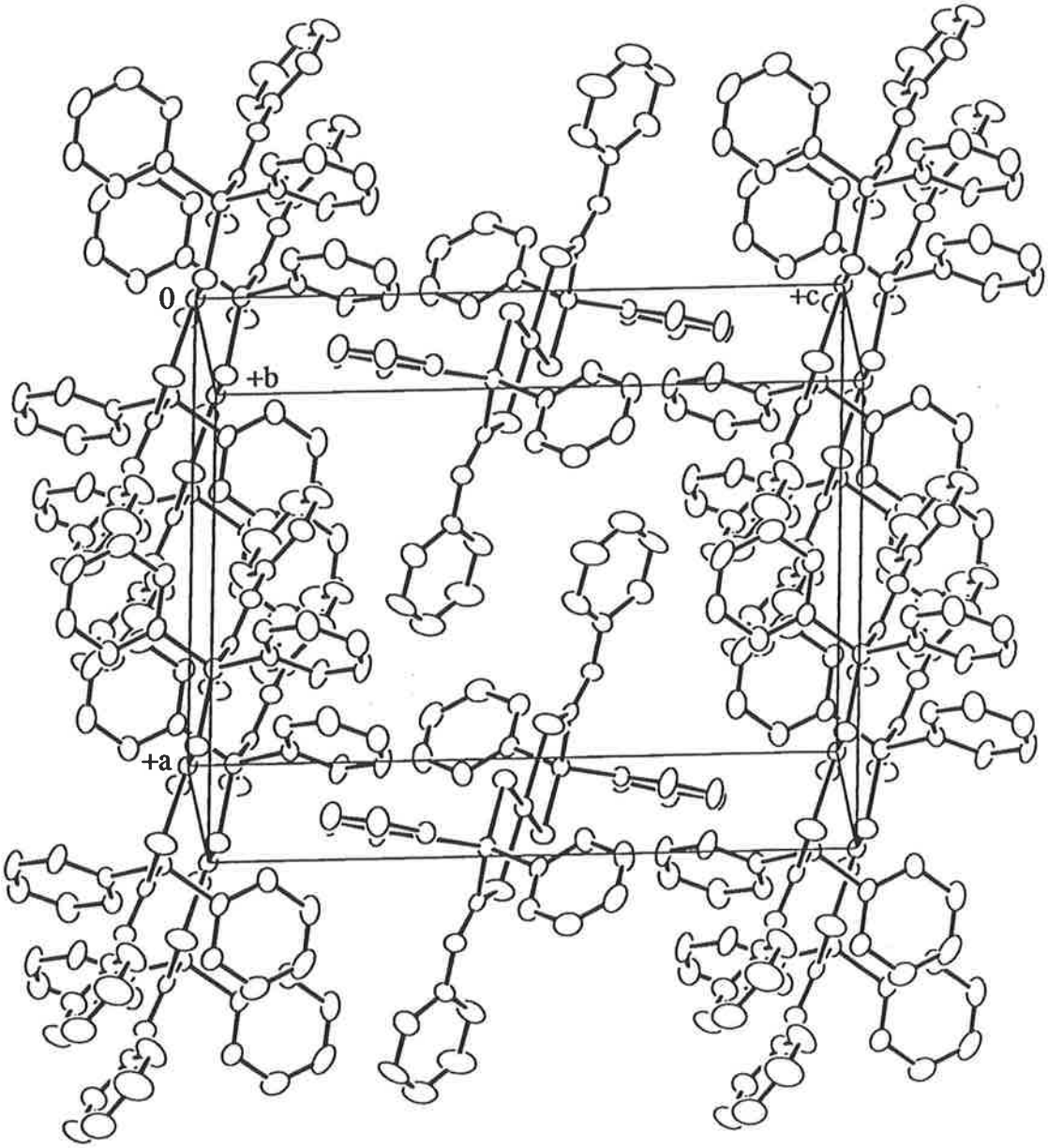

Fig. 6.3.1b The unit cell contents for *trans*-{Ni[$Ph_2P(S)C(S)NPh]_2$}

6.4 Metal Complexes with Diorgano-N-phenyl-selenophosphinylthioformamides

6.4.1 The Structure of trans-{Ni[$Ph_2P(Se)C(S)NPh]_2$}

6.4.1a The Spectroscopic Characterisation of *trans*-{$Ni[Ph_2P(Se)C(S)NPh]_2$}

By reaction of $[Ph_2P(Se)C(S)N(H)Ph]$ and $NiNO_3$ (2:1), with Et_3N, at room temperature, brown wedge-shaped crystals of {$Ni[Ph_2P(Se)C(S)NPh]_2$} are obtained. The complex is air-stable and soluble in chlorinated organic solvents. Spectroscopic data is given in Table 6.4.1a.

The IR spectrum is similar to the one obtained for the {$Ni[Ph_2P(S)C(S)NPh]_2$} complex described above. The υ(P=Se) band has shifted by 20 cm^{-1} to lower frequency, i.e. 529 cm^{-1}, compared with that in $[Ph_2P(Se)C(S)N(H)Ph]$ and is consistent with coordination of the selenium atom to nickel. The υ(C=N) and υ(C-S) bands occur at 1523 and 944 cm^{-1}, respectively. As expected there is no sign of any υ(N-H) absorption. The υ(Ni-Se) absorption band occurs at a frequency lower than 400 cm^{-1} and for similar reasons mentioned above for υ(Ni-S) and υ(Ni-P) bands, was not measured.

The ^1H NMR spectrum showed that the ligand was deprotonated as the N-H resonance was not apparent and revealed the expected resonances. The ^{13}C NMR spectrum showed that the C_q resonance shifted upfield to δ 177.8 ppm with a coupling constant $^1J(PC)$ of 98.9 Hz which has approximately doubled in magnitude to the value of 56.1 Hz found in $[Ph_2P(Se)C(S)N(H)Ph]$. The Cα resonance has shifted upfield by 2 ppm to δ 127.5 ppm and the coupling constant, $^1J(PC)$ 70.7 Hz, has decreased by approximately 10 Hz in the complex. The C_a resonance has shifted downfield to δ 149.2 ppm and the coupling constant, $^3J(PC)$ 29.1 Hz, has approximately doubled compared to 13.2 Hz in $[Ph_2P(Se)C(S)N(H)Ph]$. These shifts resemble closely those for {$Ni[Ph_2P(S)C(S)NPh]_2$}.

In the FAB mass spectrum no molecular ion, $[M]^+$, was observed. The most abundant peak was found at m/z 306 and assigned to $[Ph_2PNiS_2]^+$.

Table 6.4.1a: Spectroscopic data for *trans*-{Ni[$Ph_2P(Se)C(S)NPh]_2$}

IR (frequencies given are in cm^{-1})

	υ(thioamide I)	υ(C-S)	υ(P=Se)
{Ni[$Ph_2P(Se)C(S)NPh]_2$}	1523	944	529

^1H NMR (chemical shifts, δ, are in ppm)

PPh_2 7.05-7.93, NPh 7.05-7.93

^{13}C NMR (chemical shifts, δ, are in ppm)

PPh_2 Cα 127.5 $^1J(PC)$ 70.7 Hz, Cβ-Cδ 128.6-133.0, NPh C_a 149.2 $^3J(PC)$ 28.1 Hz, C_b 128.9, C_c 121.4, Cd 125.1, C_q 177.8 $^1J(PC)$ 98.9 Hz

*FAB (m/z, [assignment] intensity)

402, $[Ph_2P(Se)C(S)N(H)Ph]^+$ 14%; 338, $[Ph_2PNiS_3]^+$ 16%; 320, $[Ph_2PC(S)NPh]^+$ 8%; 306, $[Ph_2PNiS_2]^+$ 100%

* ions based on ^{80}Se

6.4.1b The Molecular Structure of *trans*-{Ni[$Ph_2P(Se)C(S)NPh]_2$}

The brown crystals of *trans-bis*(*P*, *P*-diphenyl-*N*-phenyl-selenophosphinylthioformamido) nickel(II), *trans*-{Ni[$Ph_2P(Se)C(S)NPh]_2$}, were obtained by the vapour diffusion of ethanol into a chloroform solution of the compound. Crystals are monoclinic, space group $P2_1/n$ with unit cell dimensions a = 9.74(1), b = 19.26(1), c = 10.39(2) Å, β = 115.22(9)°, V = 1763(3) $Å^3$, Z = 2 and D_x = 1.614 g cm^{-3}. The structure was refined to final R = 0.053, R_w = 0.059 for 1701 reflections with $I \geq 3.0\sigma(I)$. The molecular structure of {Ni[$Ph_2P(Se)C(S)NPh]_2$} is represented in Fig. 6.4.1a ([14], 30% thermal ellipsoids). This is the first complex containing either [$Ph_2P(Se)C(S)N(H)Ph$] or its anion to be characterised structurally in a metal complex. Selected bond distances and angles can be found in Table 6.4.1b.

The nickel atom is centred about a crystallographic centre of inversion at (0, 0.5, -0.5), a similar situation was seen earlier for the closely related {Ni[$Ph_2P(S)C(S)NPh]_2$} complex. The selenium and sulfur atoms of the deprotonated ligand chelate the metal atom such that the Ni-Se(2) and Ni-S(1) distances are 2.344(1) and 2.202(3) Å, respectively. A comparable Ni-Se distance of 2.330(2) Å was found in the structure of [$(n\text{-}C_4H_9)_4N$][$Ni(SSeC{=}C(CN)_2)_2$], which features a *trans* S_2Se_2 donor set about the central nickel atom, and the Ni-S distance of 2.292(3) Å is significantly longer [149]. The differences in these distances can be attributed to the fact that the complex used for comparison has only a four-membered chelate ring with a the bite angle of 82.02(9)°. The bite angle, Se(2)-Ni-S(1), of 83.8(1)° in *trans*-{Ni[$Ph_2P(Se)C(S)NPh]_2$} is identical to the one observed for the analogous Y = S complex of 83.53(8)°. The P(1)=Se(2) separation has increased to 2.145(3) Å compared to 2.106(3) Å which was the value found in the neutral [$Ph_2P(Se)C(S)N(H)Ph$] species. Other parameters which have changed from those of the parent ligand are the S(1)-C(1), P(1)-C(1) and C(1)=N(1) separations. The S(1)-C(1) distance in {Ni[$Ph_2P(Se)C(S)NPh]_2$} has elongated (1.751(8) *cf.* 1.629(9) Å) reflecting the diminished double bond character in this bond. The P(1)-C(1) bond distance has contracted by approximately 0.05 Å and represents a stronger interaction (1.821(8) *cf.* 1.875(8) Å).

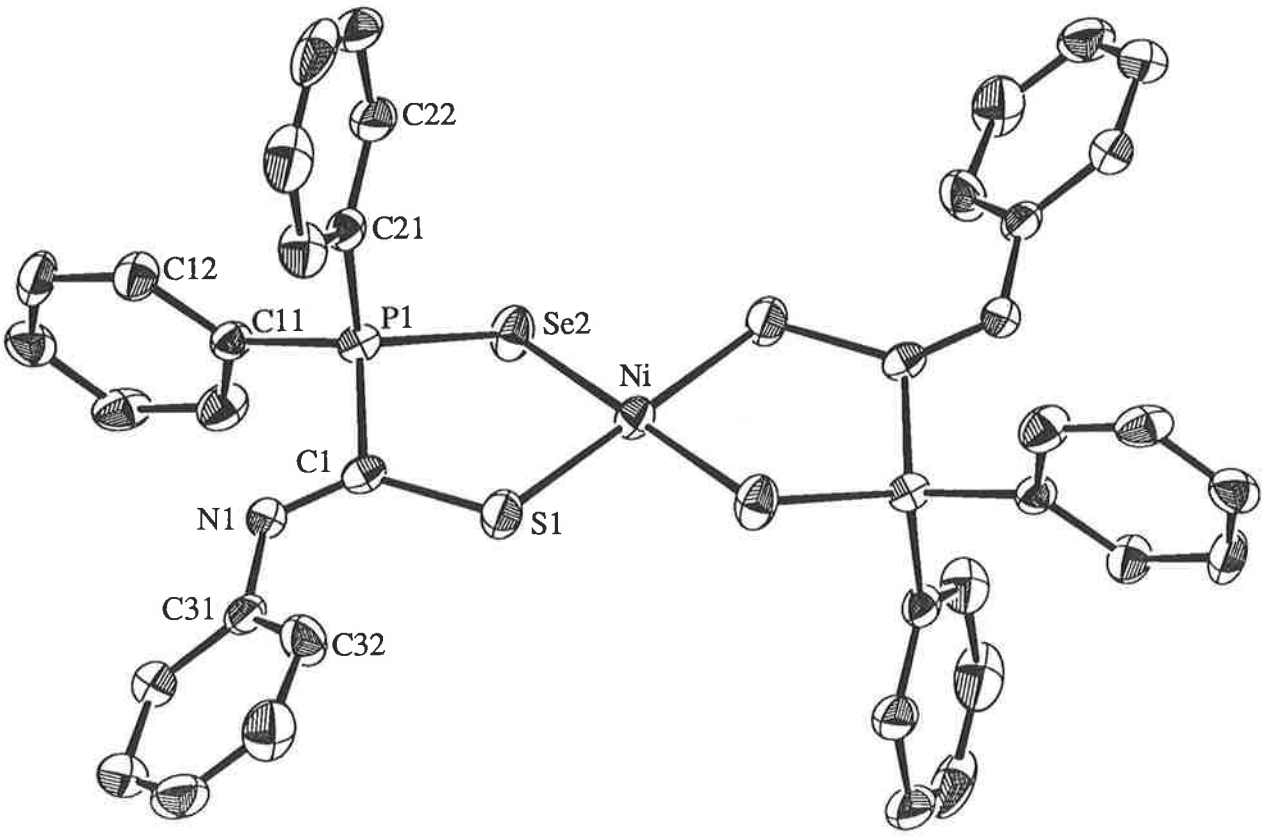

Fig. 6.4.1a The molecular structure of *trans*-{Ni[$Ph_2P(Se)C(S)NPh]_2$}

Table 6.4.1b: Selected bond distances (Å) and angles (deg.) for *trans*-{Ni[$Ph_2P(Se)C(S)NPh]_2$}

Ni-Se(2)	2.344(1)	Ni-S(1)	2.202(3)
Se(2)-P(1)	2.145(3)	S(1)-C(1)	1.751(8)
P(1)-C(1)	1.821(8)	P(1)-C(11)	1.794(7)
P(1)-C(21)	1.811(9)	N(1)-C(1)	1.260(9)
N(1)-C(31)	1.42(1)		
Se(2)-Ni-S(1)	83.8(1)	S(1)-Ni-Se(2)'*	96.2(1)
S(1)-Ni-S(1)'	180.00	Se(2)-Ni-Se(2')	180.00
Ni-Se(2)-P(1)	97.1(1)	Ni-S(1)-C(1)	112.2(3)
Se(2)-P(1)-C(1)	108.1(3)	Se(2)-P(1)-C(11)	112.9(3)
Se(2)-P(1)-C(21)	113.5(3)	C(1)-N(1)-C(31)	125.2(7)
S(1)-C(1)-P(1)	113.9(5)	S(1)-C(1)-N(1)	132.2(6)
P(1)-C(1)-N(1)	113.9(6)		

* Primed atoms related by crystallographic centre of inversion

The C(1)=N(1) separation has contracted reflecting the additional double bond character in this bond (1.260(9) *cf.* 1.31(1) Å). Similar changes were also observed in the *trans*-{Ni[$Ph_2P(S)C(S)NPh]_2$} complex. The central five-membered ring, NiSePC(1)S, has a mean deviation of the atoms from the least-squares plane of 0.193 Å. The central chromophore of the ligand, i.e. SePC(1)SN, deviates significantly from planarity as can be seen in the two torsion angles Se(2)/P(1)/C(1)/S(1) and Se(2)/P(1)/C(1)/N(1) of 33.0(5) and -148.0(6)°, respectively.

The unit cell of *trans*-{Ni[$Ph_2P(Se)C(S)NPh]_2$} is comprised of discrete molecules of the compound; see Fig. 6.4.1b. The closest non-hydrogen contact in the lattice is 3.29(2) Å and occurs between centrosymmetrically related C(23) atoms (symmetry operation: -1-*x*, 1-*y*, 1-*z*) while the closest contact involving a hydrogen atom is between atoms Se(2) and H(35)' of 3.102 Å (symmetry operation: 0.5-*x*, -0.5+*y*, 1.5-*z*).

6.4.2 The Structure of {Cd[$Cy_2P(Se)C(S)NPh]_2$}

6.4.2a The Spectroscopic Characterisation of {Cd[$Cy_2P(Se)C(S)NPh]_2$}

The reaction between $CdCl_2$ and [$Cy_2P(Se)C(S)N(H)Ph$] in ethanol solution (1:2) with excess Et_3N yields a complex of composition {Cd[$Cy_2P(Se)C(S)NPh]_2$}. The complex was a white solid which decomposed slowly over a period of time when kept in an open environment but was stable indefinitely when stored under an inert atmosphere. Spectroscopic data for {Cd[$Cy_2P(Se)C(S)NPh]_2$} is given in Table 6.4.2a.

The IR spectrum showed that the υ(P=Se) band decreased in frequency from that of the neutral [$Cy_2P(Se)C(S)N(H)Ph$] ligand by 9 cm^{-1} and the bands at 1516 and 949 cm^{-1} were assigned to υ(C=N) and υ(C-S), respectively. The nitrogen atom was deprotonated, based on the absence of the υ(N-H) absorption. The coordination of the [$Cy_2P(Se)C(S)NPh]^-$ anion was determined to involve the selenium and sulfur atoms by comparison with related systems.

The ^1H NMR spectrum of the complex showed that the phenyl and cyclohexyl resonances were in the expected regions and had the appropriate integrations. The N-H resonance was not evident. In the ^{13}C NMR spectrum the notable shifts, compared to those

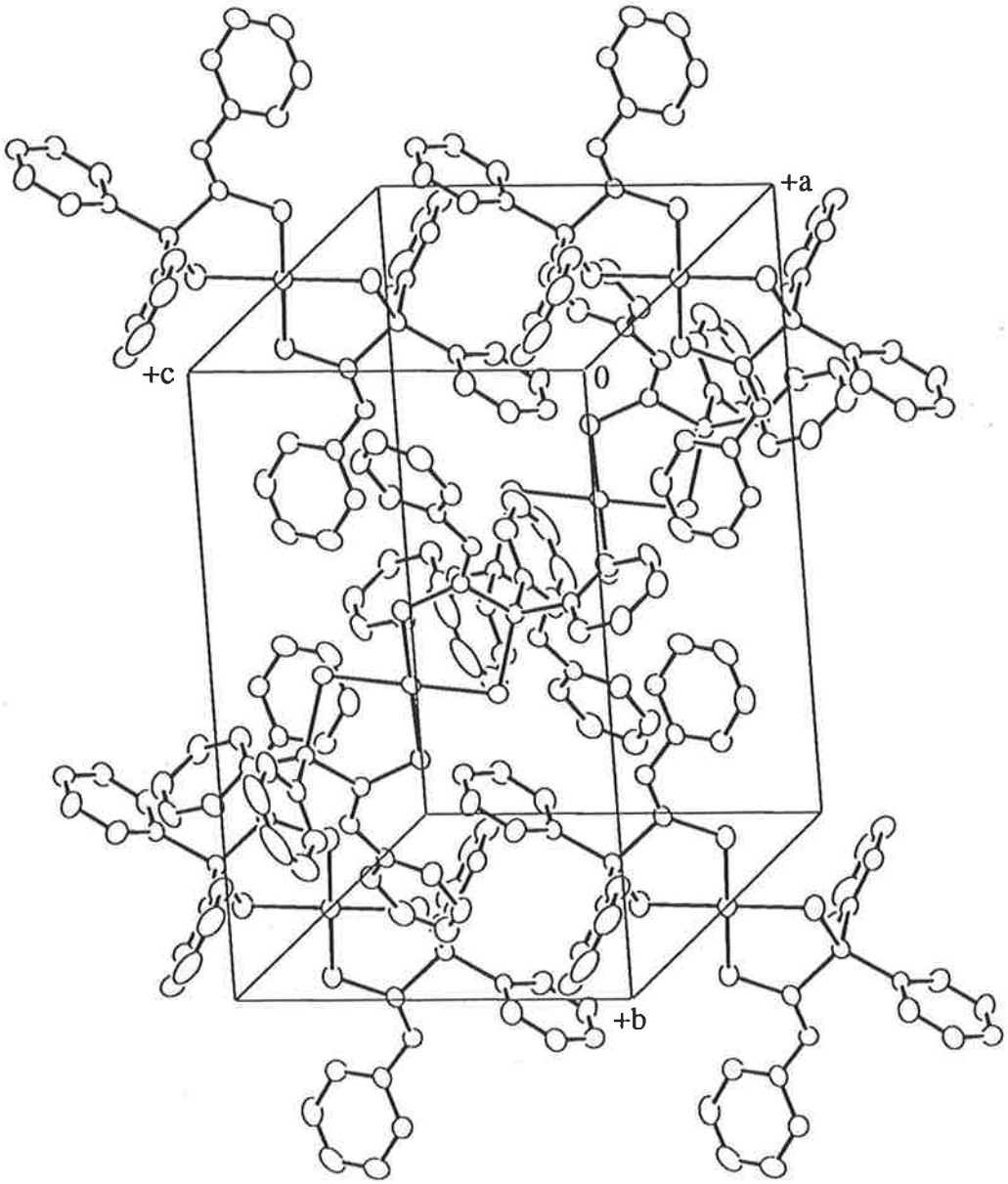

Fig. 6.4.1b The unit cell contents for *trans*-{Ni[$Ph_2P(Se)C(S)NPh]_2$}

Table 6.4.2a: Spectroscopic data for {Cd[$Cy_2P(Se)C(S)NPh]_2$}

IR (frequencies given are in cm^{-1})

	υ(thioamide I)	υ(C-S)	υ(P=Se)
{Cd[$Cy_2P(Se)C(S)NPh]_2$}	1516	949	523

^1H NMR (chemical shifts, δ, are in ppm)

PCy_2 1.20-2.56, NPh 7.04-7.40

^{13}C NMR (chemical shifts, δ, are in ppm)

PCy_2 Cα 37.9 $^1J(PC)$ 35.9 Hz, Cβ-Cδ 27.2-25.7, NPh C_a 151.8 $^3J(PC)$ 25.5 Hz, C_b 128.8, C_c 120.5, C_d 124.4, C_q 170.6 $^1J(PC)$ 74.2 Hz

FAB* (m/z, [assignment] intensity)

936, $[M]^+$ 4%; 854, $[M-(Cy)]^+$ 10%; 801, $[M-(SCNPh)]^+$ 16%; 770, $[M-(Cy_2)]^+$ 18%; 740, $[M-(PCy_2)]^+$ 12%; 696, [M-(2xPhNC, S)]$^+$ 15%; 664, [M-(2xPhNCS)]$^+$ 100%; 614, $[Cd(Cy_2P(Se)C(S)NPh)S_2CN]^+$ 82%; 580, $[(Cd(Cy_2P(Se)C(S)NPh)S_2CN)-(P)]^+$ 71%; 532, $[M-(2xPCy_2)]^+$ 84%; 498, $[(Cd(Cy_2P(Se)C(S)NPh)S_2CN)-(PCy)]^+$ 77%; 468, $[(Cy_2P(Se)C(S)NPh)SCN]^+$ 81%; 420, $[(Cd(Cy_2P(Se)C(S)NPh)S_2CN)-(PCy, Ph)]^+$ 62%; 388, $[(Cd(Cy_2P(Se)C(S)NPh)S_2CN)-(S, PCy, Ph)]^+$ 59%; 354, $[(Cy_2P(Se)C(S)NPh)-(SCN)]^+$ 68%; 332, $[Cy_2PC(S)N(H)Ph]^+$ 82%; 300, $[Cy_2PCN(H)Ph]^+$ 95%

* ions based on ^{114}Cd

of the parent ligand (which appear in parentheses), were associated with the quaternary carbon atom which moved upfield to δ 170.6 ppm (δ 187.4 ppm) with a coupling constant, $^1J(PC)$, of 74.2 Hz (44.2 Hz) and the C_a atom of the nitrogen-bound phenyl ring which moved downfield δ 151.8 ppm (δ 138.3 ppm), $^3J(PC)$ 25.5 Hz (11.5 Hz). These two coupling constants have approximately doubled in value in the complex compared to those found in [$Cy_2P(Se)C(S)N(H)Ph$]. The carbon atom, C_d, of the nitrogen-bound phenyl ring shifted upfield by approximately 3 ppm to δ 124.4 ppm (δ 127.5 ppm).

In the FAB mass spectrum the molecular ion, $[M]^+$, was observed in low abundance, i.e. 4%, and the most abundant ion was the molecular ion minus both of the SCNPh groups, i.e. $[M-2(SCNPh)]^+$.

6.4.2b The Molecular Structure of {$Cd[Cy_2P(Se)C(S)NPh]_2$}

The yellow crystals of *bis*(*P, P*-dicyclohexyl-*N*-phenyl-selenophosphinylthioformamido) cadmium(II), {$Cd[Cy_2P(Se)C(S)NPh]_2$}, were obtained from the slow evaporation of a chloroform solution of the compound. Crystals are triclinic, space group $P\bar{1}$ with unit cell dimensions a = 19.848(4), b = 20.485(3), c = 10.969(2) Å, α = 105.49(1), β = 102.37(1), γ = 101.06(1)°, V = 4048(1) Å^3, Z = 4 and D_x = 1.534 g cm^{-3}. The structure was refined to final R = 0.052, R_w = 0.048 for 7052 reflections with $I \geq 3.0\sigma(I)$.

Two independent molecules comprise the asymmetric unit and these are shown in Figs 6.4.2a and 6.4.2b ([14], 25% thermal ellipsoids). There are no major differences between the two independent molecules which differ from each other in minor conformational variations. Selected interatomic parameters are given in Table 6.4.2b. There are four independent [$Cy_2P(Se)C(S)NPh$] ligands, labeled *a*, *b*, *c* and *d*, two on each cadmium atom. The deprotonated form of the ligand is coordinated to the cadmium atoms *via* the selenium and sulfur atoms in each case. The Cd-Se distances lie in the range of 2.612(1)-2.624(1) Å and the Cd-S distances lie in the range 2.486(3)-2.521(3) Å. Only twelve complexes containing Cd-Se separations were found in the Cambridge Crystallographic Data Base and the Cd-Se bond distances in these structures lie in the range of 2.483(3) to 2.735(3) Å [150-161]. The Cd-Se distances in {$Cd[Cy_2P(Se)C(S)NPh]_2$} clearly lie within this range. Cd-

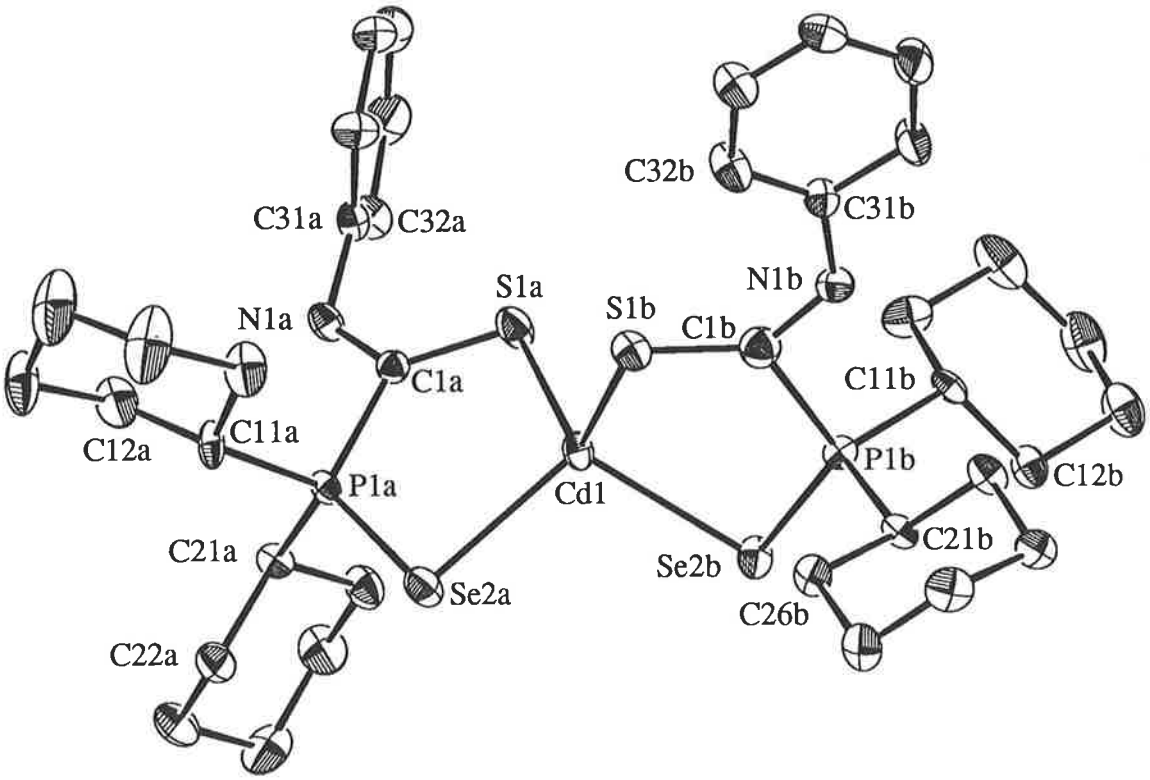

Fig. 6.4.2a The molecular structure of molecule *a* of $\{Cd[Cy_2P(Se)C(S)NPh]_2\}$

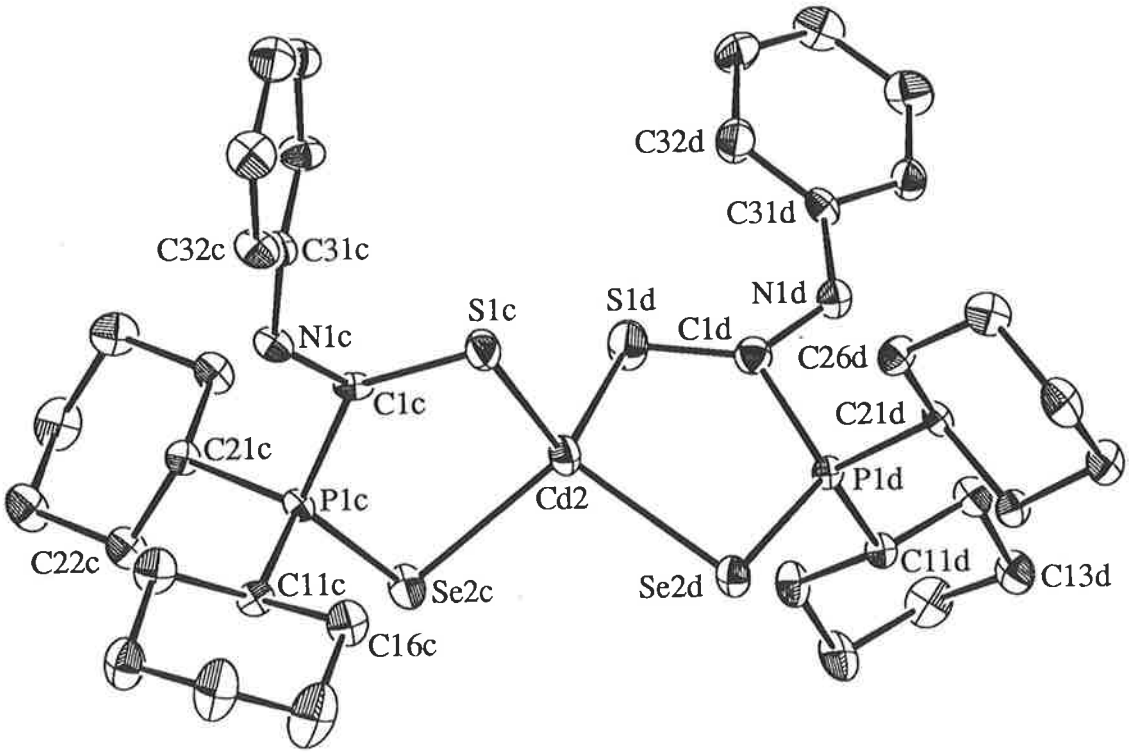

Fig. 6.4.2b The molecular structure of molecule *b* of $\{Cd[Cy_2P(Se)C(S)NPh]_2\}$

Table 6.4.2b: Selected bond distances (Å) and angles (deg.) for $\{Cd[Cy_2P(Se)C(S)NPh]_2\}$

	ligand *a*	ligand *b*	ligand *c*	ligand *d*
Cd-Se(2)	2.618(1)	2.623(1)	2.612(1)	2.624(1)
Cd-S(1)	2.486(3)	2.521(3)	2.508(3)	2.506(3)
Se(2)-P(1)	2.149(3)	2.153(3)	2.143(3)	2.152(3)
S(1)-C(1)	1.661(9)	1.63(1)	1.690(9)	1.592(9)
P(1)-C(1)	1.858(9)	1.87(1)	1.865(8)	1.898(9)
P(1)-C(11)	1.828(9)	1.844(9)	1.803(9)	1.839(9)
P(1)-C(21)	1.843(9)	1.849(9)	1.826(9)	1.835(9)
N(1)-C(1)	1.31(1)	1.33(1)	1.29(1)	1.37(1)
N(1)-C(31)	1.45(1)	1.42(1)	1.41(1)	1.44(1)

Se(2a)-Cd(1)-Se(2b)	107.11(5)	Se(2a)-Cd(1)-S(1a)	95.97(7)
Se(2a)-Cd(1)-S(1b)	127.00(7)	Se(2b)-Cd(1)-S(1a)	122.76(8)
Se(2b)-Cd(1)-S(1b)	95.27(7)	S(1a)-Cd(1)-S(1b)	111.3(1)
Se(2c)-Cd(1)-Se(2d)	105.10(5)	Se(2c)-Cd(2)-S(1c)	96.74(7)
Se(2c)-Cd(2)-S(1d)	119.69(9)	Se(2d)-Cd(2)-S(1c)	127.74(8)
Se(2d)-Cd(2)-S(1d)	95.40(8)	S(1c)-Cd(2)-S(1d)	113.9(1)
Cd(1)-Se(2a)-P(1a)	95.52(8)	Cd(1)-Se(2b)-P(1b)	93.52(8)
Cd(2)-Se(2c)-P(1c)	95.72(7)	Cd(2)-Se(2d)-P(1d)	94.47(8)
Cd(1)-S(1a)-C(1a)	105.6(4)	Cd(1)-S(1b)-C(1b)	102.9(4)
Cd(2)-S(1c)-C(1c)	104.2(3)	Cd(2)-S(1d)-C(1d)	103.5(4)
Se(2a)-P(1a)-C(1a)	115.0(3)	Se(2a)-P(1a)-C(11a)	107.5(4)
Se(2a)-P(1a)-C(21a)	110.9(3)	C(1a)-P(1a)-C(11a)	108.0(5)
C(1a)-P(1a)-C(21a)	106.5(4)	C(11a)-P(1a)-C(21a)	108.7(4)
Se(2b)-P(1b)-C(1b)	116.4(3)	Se(2b)-P(1b)-C(11b)	110.0(3)
Se(2b)-P(1b)-C(21b)	108.7(3)	C(1b)-P(1b)-C(11b)	107.9(4)
C(1b)-P(1b)-C(21b)	105.4(4)	C(11b)-P(1b)-C(21b)	108.1(4)
Se(2c)-P(1c)-C(1c)	115.9(3)	Se(2c)-P(1c)-C(11c)	107.9(3)
Se(2c)-P(1c)-C(21c)	110.7(3)	C(1c)-P(1c)-C(11c)	107.9(4)
C(1c)-P(1c)-C(21c)	105.3(4)	C(11c)-P(1c)-C(21c)	109.1(4)
Se(2d)-P(1d)-C(1d)	114.3(3)	Se(2d)-P(1d)-C(11d)	108.2(3)
Se(2d)-P(1d)-C(21d)	109.5(3)	C(1d)-P(1d)-C(11d)	107.7(4)
C(1d)-P(1d)-C(21d)	107.4(4)	C(11d)-P(1d)-C(21d)	109.5(4)
C(1a)-N(1a)-C(31a)	120.2(8)	C(1b)-N(1b)-C(31b)	127.2(9)
C(1c)-N(1c)-C(31c)	123.0(8)	C(1d)-N(1d)-C(31d)	125.4(8)

Table 6.4.2b continued

S(1a)-C(1a)-P(1a)	126.0(6)	S(1a)-C(1a)-N(1a)	127.1(7)
P(1a)-C(1a)-N(1a)	106.9(7)	S(1b)-C(1b)-P(1b)	123.4(6)
S(1b)-C(1b)-N(1b)	134.5(8)	P(1b)-C(1b)-N(1b)	101.9(7)
S(1c)-C(1c)-P(1c)	125.2(5)	S(1c)-C(1c)-N(1c)	129.1(7)
P(1c)-C(1c)-N(1c)	105.5(7)	S(1d)-C(1d)-P(1d)	125.6(6)
S(1d)-C(1d)-N(1d)	132.9(8)	P(1d)-C(1d)-N(1d)	100.9(6)

S bond distances of 2.642(2) to 2.774(2) Å have been found in cadmium xanthate complexes, $\{Cd[S_2COR']_2\}$ [162, 163], albeit with higher coordination numbers at the cadmium atoms. In cadmium dithiocarbamates, the Cd-S distances lie in a range of 2.509(7)-2.888(5) Å [164-168]. The Cd-S distances above involve the incorporation of the cadmium atom in a four-membered CdSCS ring system whereas in $\{Cd[Cy_2P(Se)C(S)NPh]_2\}$ there is a five-membered CdSePCS ring present and hence, shorter distances would be anticipated owing to the reduced strain in $\{Cd[Cy_2P(Se)C(S)NPh]_2\}$. The bite angles, Se-Cd-S, in the four ligands are similar and lie in a narrow range, 95.27(7)-96.74(7)°. The five-membered rings comprising the Cd, Se(2), P(1), C(1) and S(1) atoms deviate significantly from planarity as can be seen from the mean deviation from the least-squares plane through these atoms of 0.0976, 0.1946, 0.0913 and 0.1500 Å for ligands *a*, *b*, *c* and *d*, respectively. The structure of the complex $\{Cd[Cy_2P(Se)C(S)NPh]_2\}$ is the first instance in which a cadmium atom exists with a Se_2S_2 donor set that has been verified crystallographically. The cadmium atoms each exist in a distorted tetrahedral environment. The dihedral angle between the least-squares planes for rings *a* and *b* is 70.81° while the equivalent dihedral angle for rings *c* and *d* is very similar at 71.57°. From the torsion angles listed below it can be seen that ligand *a* is the most planar of the four ligands.

	ligand *a*	ligand *b*	ligand *c*	ligand *d*
Se(1)/P(1)/C(1)/S(1)	-4.3(8)°	16.7(8)°	-10.0(7)°	-16.0(8)°
Se(1)/P(1)/C(1)/N(1)	173.7(6)°	-168.0(5)°	174.1(5)°	172.3(5)°

The P(1)=Se(2) bond lengths, 2.143(3)-2.153(3) Å have elongated with respect to the separation of 2.098(1) Å found in the parent ligand $[Cy_2P(Se)C(S)N(H)Ph]$. The S(1)-C(1) separations of 1.661(9) Å ligand *a*, 1.63(1) Å ligand *b*, 1.690(9) Å ligand *c* and 1.592(9) Å ligand *d*, vary considerably amongst the ligands as do the P(1)-C(1) distances of 1.858(9) Å ligand *a*, 1.87(1) Å ligand *b*, 1.865(8) Å ligand *c* and 1.898(9) Å ligand *d*, notwithstanding the relatively high errors. The C(1)=N(1) distances for ligands *a-c* are equal within experimental error while the distance for ligand *d* is long at 1.37(1) Å. The S(1)-C(1) and

P(1)-C(1) distances are shorter and longer, respectively in ligand *a* compared to those found in ligand *b* on Cd(1). A similar trend was found for ligands *c* and *d*. Comparison of other parameters resulted in the conclusion that ligands *a* and *c* were similar to one another as were ligands *b* and *d*. The P-C(Cy) distances have elongated by approximately 0.025-0.035 Å compared with those found in the parent ligand. Similar variations have been noted earlier in the Chapter.

The S(1)-C(1)-P(1) angles are similar, i.e. 123.4(6)-126.0(6)°, but the angles S(1)-C(1)-N(1) and P(1)-C(1)-N(1) while being experimentally equivalent for ligands *a* and *c*, are different to those of ligands *b* and *d*.

The structure is molecular, there being no significant intermolecular contacts in the lattice; the closest non-hydrogen contact of 3.59(1) Å occurs between the Se(2c) and C(14b)' atoms (symmetry operation: -*x*, 1-*y*, 1-*z*) while the closest hydrogen contact of 3.006 Å is between atoms Se(2d) and H(14d)' (symmetry operation: -*x*, 1-*y*, 2-*z*). A view of the unit cell contents is shown in Fig. 6.4.2c.

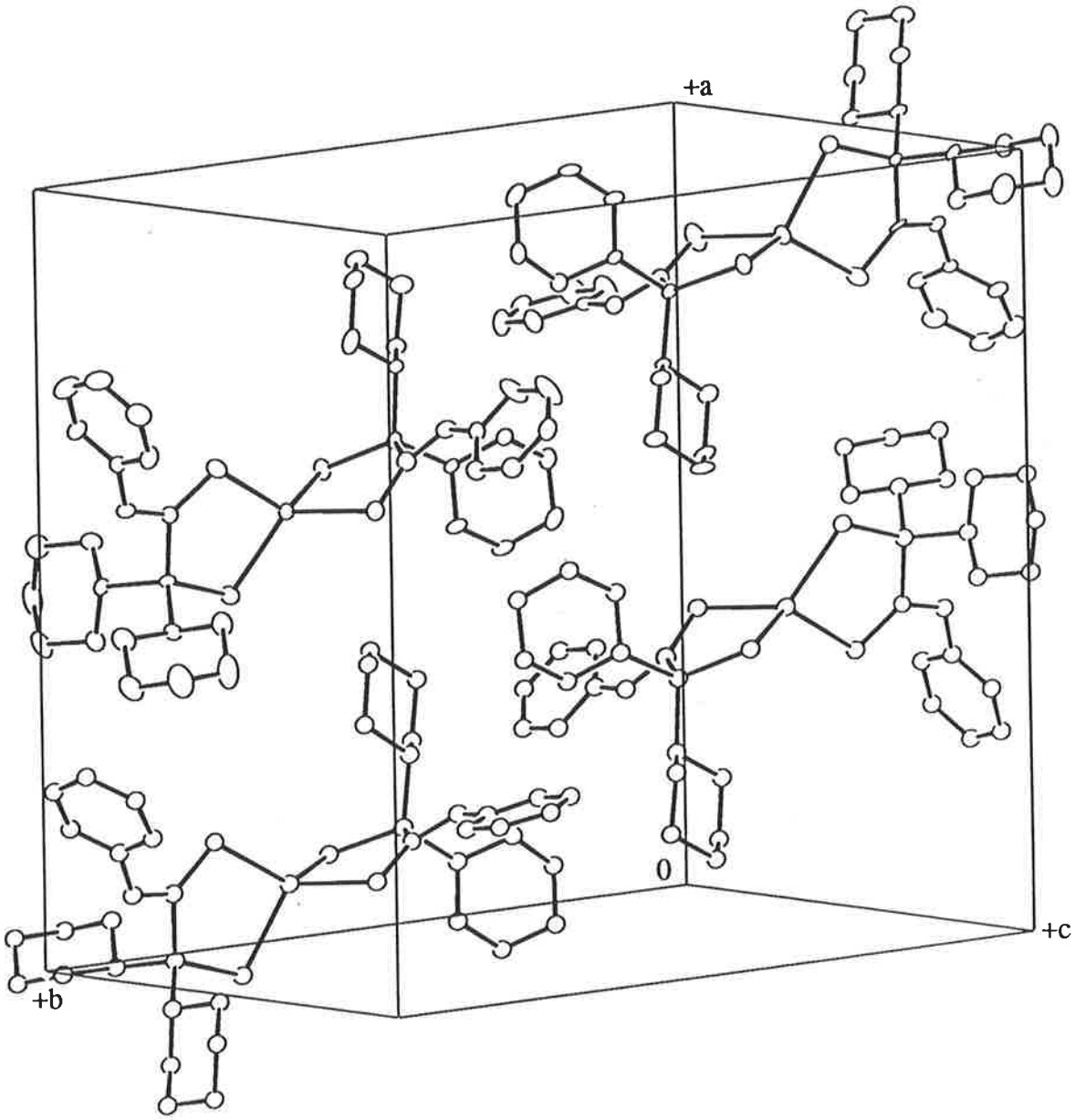

Fig. 6.4.2c The unit cell contents for $\{Cd[Cy_2P(Se)C(S)NPh]_2\}$

Chapter 7

CONCLUSION

This thesis has involved the characterisation of a series of potentially multidentate ligands of the type $R_2P(Y)C(S)N(H)R'$, Y = O, S or Se; R, R' = alkyl or aryl. Further, the coordination potential of a number of these ligands has been examined.

The Ligands

The preparation, characterisation and crystal structure determination of $R_2P(Y)C(S)N(H)R'$, Y= O, S or Se; R = Ph or Cy; R' = Ph or Me, as well as the crystal structure determination of $R_2P(Se)C(S)N(H)R'$, R = Ph or Cy; R' = Et or Cy has been achieved. All compounds featured a Z conformation about the C(1)-N(1) bond. The availability of a large data base of geometric parameters has enabled a systematic examination of these ligands and the determination of several trends which can be related to their chemical reactivity.

When the P-C bond distances of the phosphorus(V) compounds were compared with those of the parent phosphorus(III) compounds (where available) a systematic contraction was observed, as expected. While there was evidence for a general weakening in the P-C(1) bonds in the phosphorus(V) compounds, the weakening was more pronounced in the $Ph_2P(Y)C(S)N(H)R'$ derivatives. The crystallographic evidence suggested that the central P-C(1) bonds in the $Ph_2P(O)C(S)N(H)R'$ derivatives were significantly weaker than the comparable bonds in the $Cy_2P(O)C(S)N(H)R'$ compounds; a similar conclusion is true also for the $R_2P(S)C(S)N(H)R'$ and $R_2P(Se)C(S)N(H)R'$ analogues. This observation pointed to the reduced stability of the $Ph_2P(Y)C(S)N(H)R'$ compounds compared with the $Cy_2P(Y)C(S)N(H)R'$ compounds and is related to the greater electron withdrawing ability, i.e. greater inductive effect, of the phenyl substituents over that of the cyclohexyl groups.

The structural study of the $R_2P(Y)C(S)N(H)R'$ compounds reported showed that the P(1)-C(1) bond lengths increased in the following order $R_2P(O)C(S)N(H)R' < R_2P(S)C(S)N(H)R' < R_2P(Se)C(S)N(H)R'$. This trend may be correlated with the diminishing delocalisation of π-electron density over the P(1)Y(2)C(1)S(1)N(1) moieties in the order Y = O > S > Se which is in turn may be related to the decreased electronegativity of the Y substituent.

The Metal Complexes

The crystal and molecular structures of a number of metal complexes containing the $R_2P(Y)C(S)N(H)R'$, Y= 0, O, S or Se, ligands (both in their protonated and deprotonated forms) have been determined.

The diorganophosphinothioformamide ligands were shown to coordinate primarily *via* the phosphorus and sulfur atoms, normally in a chelating mode. In one instance, i.e. in the structure of $\{Co[Cy_2PC(S)NPh]_3\}$, two of the ligands coordinate in the common mode and the third ligand *via* the sulfur and nitrogen atoms. In the structure of $\{Au[Ph_2PC(S)NPh]\}_2$, the ligands were again bidentate, *via* the phosphorus and sulfur atoms, however they were bridging, rather than chelating.

A monodentate mode of coordination, i.e. *via* the thioamide sulfur atom, was found in the structure of $\{Au[Cy_2P(O)C(S)N(H)Me]Cl\}$.

In $\{Ni[Ph_2P(S)C(S)NPh]\}$, a S-, S- chelating mode was evident.

In both structures containing the $[R_2P(Se)C(S)NPh]$, R = Ph or Cy, a Se- and S-chelation mode of coordination was observed.

The structural studies demonstrate the flexibility of the $R_2P(Y)C(S)N(H)R'$, Y= 0, O, S or Se, ligands in their coordination towards a variety of metal centres. The coordination of the ligands are summarised in Fig. 7.1.

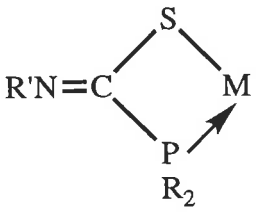

e.g. {Ni[$R_2PC(S)NR']_2$}, R = Ph or Cy, R' = Ph or Me, {Pd[$Cy_2PC(S)NPh]_2$}, {Co[$Cy_2PC(S)NPh]_3$}, {$Me_2Au[Cy_2PC(S)NCy]$}

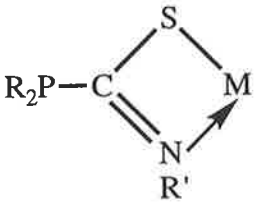

e.g. {Co[$Cy_2PC(S)NPh]_3$}

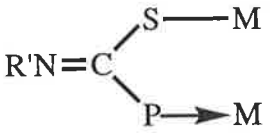

e.g. {Au[$Ph_2PC(S)NPh]$}$_2$

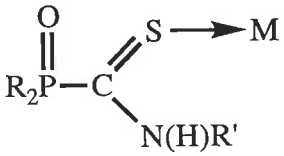

e.g. {Au[$Cy_2P(O)C(S)N(H)Me]Cl$}

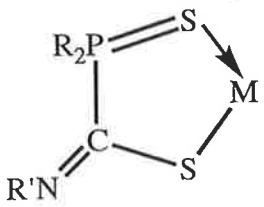

e.g. {Ni[$Ph_2P(S)C(S)NPh]_2$}

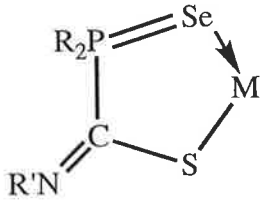

e.g. {Ni[$Ph_2P(Se)C(S)NPh]_2$}, {Cd[$Cy_2P(Se)C(S)NPh]_2$}

Fig. 7.1 Different modes of coordination observed for the protonated or deprotonated forms of the $R_2P(Y)C(S)N(H)R'$, Y = 0, O, S or Se; R = Ph or Cy; R' = Ph or Me, ligands

REFERENCES

1. Berners-Price, S.J. and Sadler, P.J.: *Struct. Bonding* **70** (1988) 27
2. Issleib, K. and Harzfeld, G.: *Chem. Ber.* **97** (1964) 3430
3. Issleib, K. and Harzfeld, G.: *Z. Anorg. Allg. Chem.* **351** (1967) 18
4. Schumann, H., Jutzi, P. and Schmidt, M.: *Angew. Chem., Int. Edit.* **4** (1965) 787
5. Satgé, J. and Couret, C.: *C. R. Acad. Sc. Paris Ser. C* **264** (1967) 2169
6. Schumann, H. and Jutzi, P.: *Chem. Ber.* **101** (1968) 24
7. Walther, B. and Bauer, S.: *J. Organomet. Chem.* **142** (1977) 177
8. Dubac, J., Escudié, J., Couret, J., Cavezzan, J., Satgé, J. and Mazerolles, P.: *Tetrahedron* **37** (1981) 1141
9. Dakternieks, D. and Rolls, C.L.: *Inorg. Chim. Acta* **87** (1984) 5
10. Carr, S.W., Colton, R. and Dakternieks, D.: *Inorg. Chem.* **23** (1984) 720
11. Dakternieks, D., Hoskins, B.F. and Rolls, C.L.: *Aust. J. Chem.* **41** (1988) 195
12. Hall, V.J. and Tiekink, E.R.T. (1993) unpublished results
13. Sutton, B.M., McGusty, E., Walz, D.T. and DiMartino, M.J.: *J. Med. Chem.* **15** (1972) 1095
14. Johnson, C.K.: ORTEPII. Report ORNL-5138, Oak Ridge National Laboratory, Tennessee (1976)
15. Cowan, S.W., Hoskins, B.F. and Tiekink, E.R.T.: *Aust. J. Chem.* **37** (1984) 1991
16. Pauling, L.: "The Nature of the Chemical Bond" 3rd Edn (Cornell University Press: New York 1960)
17. Just, B., Klein, W., Kopf, J., Steinhäuser, K.G. and Kramolowsky, R.: *J. Organomet. Chem.* **229** (1982) 49
18. Antoniadis, A., Hiller, W., Kunze, U., Schaal, H. and Strähle, J.: *Z. Naturforsch.* **37b** (1982) 1289
19. Gutierrez-Alonso, A., Ballester-Reventos, L., Perez-Garcia, V. and Ruiz-Valero, C.: *Polyhedron* **9** (1990) 2163
20. Dakternieks, D., Hoskins, B.F. and Rolls, C.L.: *Aust. J. Chem.* **41** (1988) 195
21. Huheey, J.E.: "Inorganic Chemistry" 2nd Edn (Harper and Row; New York 1978)
22. Ambrosius, H.P.M.M., Bosman, W.P. and Cras, J.A.: *J. Organomet. Chem.* **215**

(1981) 201

23. Allen, F.H., Kennard, O, Watson, D.G., Brammer, L., Orpen, A.G. and Taylor, R.: *J. Chem. Soc., Perkin Trans.* **II** (1987) S1
24. Ambrosius, H.P.M.M., van Hemert, A.W., Bosman, W.P., Noordik, J.H. and Ariaans, G.J.A.: *Inorg. Chem.* **23** (1984) 2678
25. Hiller, W., Wurst, K. and Kunze, U.: *Acta Crystallogr.* **C43** (1987) 2235
26. Albert, K., Bruns, A., Förster, H., Hiller, W. and Kunze, U.: *Angew. Chem., Int. Ed. Engl.* **24** (1985) 715
27. Kunze, U., Jawad, H., Hiller, W. and Naumer, R.: *Z. Naturforsch.* **40b** (1985) 512
28. Bosman, W.P., Noordik, J.H., Ambrosius, H.P.M.M. and Cras, J.A.: *Cryst. Struct. Comm.* **9** (1980) 7
29. Ambrosius, H.P.M.M.,Willemse, J., Cras, J.A., Bosman, W.P., and Noordik, J.H.: *Inorg. Chem.* **23** (1984) 2672
30. Ambrosius, H.P.M.M., Cotton, F.A., Falvello, L.R., Hintzen, H.T.J.M., Melton, T.J., Schwotzer, W.,Tomas, M. and Van der Linden, J.G.M.: *Inorg. Chem.* **23** (1984) 1611
31. Cowan, S.W., Dakternieks, D., Gable, R.W, Hoskins, B.F., Rolls, C.L. and Tiekink, E.R.T.: *Aust. J. Chem.* **39** (1986) 547
32. Dakternieks, D., Hoskins, B.F. and Rolls, C.L.: *Aust. J. Chem.* **39** (1986) 1221
33. Dakternieks, D., Corbett, M., Hoskins, B.F., Jackson, P.A. and Tiekink, E.R.T.: *Acta Crystallogr.* **C43** (1987) 2439
34. Nardelli, M., Pelizzi, C. and Pelizzi, G.: *J. Chem. Soc., Dalton Trans.* (1978) 131
35. Ng, S.W. and Kumar Das, V.G.: *Acta Crystallogr.* **C48** (1992) 1839
36. Gielen, M., Pan, H. and Tiekink, E.R.T.: *Bull. Soc. Chim. Belg.* **102** (1993) 447
37. Still, W.C., Kahn, M. and Mitra, A.: *J. Org. Chem.* **43** (1978) 2923
38. Sheldrick, G.M.: SHELX76. Program for crystal structure determination. University of Cambridge, England (1976)
39. teXsan Single crystal structure analysis software, Version 1.6. Molecular Structure Corporation, The Woodlands, Texas (1993)

40. Walker, N. and Stuart, D.: *Acta Crystallogr.* **A39** (1983) 158

41. Sheldrick, G.M.: SHELXS86. Program for the automatic solution of crystal structure. University of Göttingen, Germany (1986)

42. Zachariasen, W.H.: *Acta Crystallogr.* **23** (1967) 558

43. Hamilton, W.C.: *Acta Crystallogr.* **18** (1965) 502

44. Gee, W., Shaw, R.A. and Smith, B.C.: *Inorg. Synth.* **9** (1967) 19

45. M. Draeger: personal communication (1992)

46. Block, B.P.: *Inorg. Synth.* **4** (1953) 14

47. Ojima, I., Akiba, K. and Inamoto, N.: *Bull. Chem. Soc. Jpn.* **42** (1969) 2975

48. Al-Sa'ady, A.K., McAuliffe, C.A., Parish, R.V. and Sandbank, J.A.: *Inorg. Synth.* **23** (1985) 191

49. Bruns, A., Hiller, W. and Kunze, U.: Z. *Naturforsch.* **39b** (1984) 14

50. Fenske, D., Mattes, R., Löns, J. and Tebbe, K.-F.: *Chem. Ber.* **106** (1973) 1139

51. Siasios, G. and Tiekink, E.R.T.: Z. *Kristallogr.* **209** (1994) 547

52. Kunze, U., Bruns, A., Hiller, W. and Mohyla, J.: *Chem. Ber.* **118** (1985) 227

53. Hoskins, B.F. and Tiekink, E.R.T.: *Aust. J. Chem.* **41** (1988) 405

54. Codding, P.W. and Kerr, K.A.: *Acta Crystallogr.* **B35** (1979) 1261

55. Colton, R., Hoskins, B.F. and Panagiotidou, P.: *Aust. J. Chem.* **40** (1987) 1909

56. Iwaoka, M. and Tomoda, S: *J. Am. Chem. Soc.* **116** (1994) 4463

57. Vineyard, B.D., Knowles, W.S., Sabacky, M.J., Bachman, G.L. and Weinkauff, D.J.: *J. Am. Chem. Soc.* **99** (1977) 5946

58. Peters, G.: *J. Am. Chem. Soc.* **82** (1960) 4751

59. Maier, L.: *Helv. Chim. Acta* **49** (1966) 1000

60. Jensen, K.A. and Nielsen, P.H.: *Acta Chem. Scand.* **20** (1966) 597

61. Davies, M. and Jones, W.J.: *J. Chem. Soc.* (1958) 955

62. Jensen, K.A. and Nielsen, P.H.: *Acta Chem. Scand.* **17** (1963) 1875

63. Grim, S.O. and Walton, E.D.: *Inorg. Chem.* **19** (1980) 1982

64. Colton, R. and Panagiotidou, P.: *Aust. J. Chem.* **40** (1987) 13

65. Pouchert, C.J. and Campbell, J.R.: The Aldrich Library of ^{1}H NMR Spectra, Aldrich

Chemical Co. (1974)

66. Walter, W and Maerten, G.: *Liebigs Ann. Chem.* **712** (1968) 58
67. Walter, W and Schaumann, E.: *Chem. Ber.* **104** (1971) 4
68. Walter, W and Schaumann, E.: *Chem. Ber.* **104** (1971) 3361
69. Walter, W and Schaumann, E.: *Chem. Ber.* **109** (1976) 922
70. Antoniadis, A., Kunze, U. and Moll, M.: *J. Organomet. Chem.* **235** (1982) 177
71. Cookson, P.D.: MSc. Thesis, University of Adelaide (1993)
72. Pinnell, R.P., Megerle, C.A., Manatt, S.L. and Kroon, P.A.: *J. Am. Chem. Soc.* **95** (1973) 977
73. Carr, S.W. and Colton, R.: *Aust. J. Chem.* **34** (1981) 35
74. Allen, D.W. and Taylor, B.F.: *J. Chem. Soc., Dalton Trans.* (1982) 51
75. Allen, D.W., March, L.A. and Nowell, I.W.: *J. Chem. Soc., Dalton Trans.* (1984) 483
76. Allred, A.L.: *J. Inorg. Nucl. Chem.* **17** (1961) 215
77. Kunze, U. and Antoniadis, A.: *Z. Anorg. Allg. Chem.* **456** (1979) 155
78. Kunze, U. and Antoniadis, A.: *Z. Naturforsch.* **36b** (1981) 1588
79. Sutton, B.M.: *Gold Bull.* **19** (1986) 15
80. Parish, R.V. and Cottrill, S.M.: *Gold Bull.* **20** (1987) 3
81. Rodnan, G.P. and Benedek, T.G.: *Arthritis and Rheum.* **13** (1970) 145
82. Hart, P.D.: *Brit. Med. J.* **2** (1946) 805
83. Forestier, J.: *J. Lab. Clin. Med.* **20** (1935) 827
84. Gottleib, N.L. and Gray, R.G.: *Agents and Actions* **8** (1981) 529
85. Leibfarth, J.H. and Persellin, R.H.: *Agents and Actions* **11** (1981) 458
86. Lewis, A.J. and Walz, D.T.: *Prog. Med. Chem.* **19** (1982) 2
87. Walz, D.T., Dimartino, M.J., Griswold, D.E., Intoccia, A.P. and Flanagan, T.L.: *Am. J. Med.* (1983) 90
88. Graham, G.C., Haavisto, T.M., Jones, H.M. and Champion, G.D.: *Biochem. Pharmacology* **33** (1984) 1257
89. Tiekink, E.R.T. and Whitehouse, M.W.: *Chem. Aust.* **57** (1990) 346

90. Parish, R.V.: *Interdisc. Sci. Rev.* **17** (1992) 221

91. Reedijk, J., Fichtinger-Schepman, A.-M. J., van Oosterom, A.T. and van de Putte, P.: *Struct. Bonding* **67** (1987) 53

92. Berners-Price, S.J. and Sadler, P.J.: *Chem. Br.* (1987) 541

93. Mirabelli, C.K., Johnson, R.K., Sung, C.-M., Faucette, L.F., Muirhead, K. and Crooke, S.T.: *Cancer Res.* **45** (1985) 32

94. Mirabelli, C.K., Hill, D.T., Faucette, L.F., McCabe, F.L., Girard, G.R., Bryan, D.B., Sutton, B.M., O'Leary Bartus, J., Crooke, S.T. and Johnson, R.K.: *J. Med. Chem.* **30** (1987) 2181

95. Aritzi, M.P., Garcia-Orad, A., Somer, F., Silvestro, L., Massiot, P., Chevallier, P., Gutiérrez-Zorrilla, J.M., Colacio, E., Martinez de Pancorbo, M. and Tapiero, H.: *Anticancer Res.* **11** (1991) 625

96. Cookson, P.D., Tiekink, E.R.T. and Whitehouse, M.W.: *Aust. J. Chem.* **47** (1994) 577

97. Berners-Price, S.J., Mirabelli, C.K., Johnson, R.K., Mattern, M.R., McCabe, F.L., Faucette, L.F., Sung, C.-M., Mong, S.M., Sadler, P.J. and Crooke, S.T.: *Can. Res.* **46** (1986) 5486

98. Rush, G.F., Alberts, D.W., Meunier, D., Leffler, K. and Smith, P.F.: *Toxicologist* **7** (1987) 59

99. Cookson, P.D. and Tiekink, E.R.T.T.: *J. Chem. Soc., Dalton Trans.* (1993) 259

100. Pijpers, F.W., Dix, A.H. and Van der Linden, J.G.M.: *Inorg. Chim. Acta* **11** (1974) 41

101. Hussain, S.: *J. Cryst. Spectrosc.* Res. **16** (1986) 91

102. Schrauzer, G.N., Rhead, W.J. and Evans, G.A.: *Bioinorg. Chem.* **2** (1973) 329

103. Hesse, R. and Jennische, P.: *Acta Chem. Scand.* **26** (1972) 3855

104. Schmidbaur, H. and Franke, R.: *Inorg. Chim. Acta* **13** (1975) 85

105. Bardají, M., Connelly, N.G., Gimeno, M.C., Jiménez, J., Jones, P.G., Laguna, A. and Laguna, M.: *J. Chem. Soc., Dalton Trans.* (1994) 1163

106. Fernández, E.J., Gimeno, M.C., Jones, P.G., Laguna, A., Laguna, M and Lopez-de-

Luzuriaga, J.M.: *Angew. Chem., Int. Ed. Engl.* **33** (1994) 87

107. Liou, L.-S., Liu, C.-P. and Wang, J.-C.: *Acta Crystallogr.* **C50** (1994) 538
108. Davila, R.M., Elduque, A., Staples, R.J., Harlass, M. and Fackler Jr., J.P.: *Inorg. Chim. Acta* **217** (1994) 45
109. Crane, W.S. and Beall, H.: *Inorg. Chim. Acta* **31** (1978) L469
110. Pearson, W.B.: "Lattice Spacings and Structures of Metals and Alloys" (Pergamon: London 1951)
111. Siasios, G. and Tiekink, E.R.T.: *Z. Kristallogr.* **198** (1992) 139
112. Hall, V.J., Siasios, G. and Tiekink, E.R.T.: *Aust. J. Chem.* **46** (1993) 1
113. Faamau, J.W. and Tiekink, E.R.T.: *J. Coord. Chem.* **31** (1994) 93
114. Cookson, P.D. and Tiekink, E.R.T.: *J. Chem. Soc., Dalton Trans.* (1993) 259
115. Harker, C.S.W., Tiekink, E.R.T. and Whitehouse, M.W.: *Inorg. Chim. Acta* **181** (1991) 23
116. Siasios, G. and Tiekink, E.R.T.: *Z. Kristallogr.* **205** (1993) 261
117. Siasios, G. and Tiekink, E.R.T.: *Z. Kristallogr.* **204** (1993) 95
118. Usón, R., Laguna, A., Laguna, M., Fraile, M.N., Jones, P.G. and Erdbrügger, C.F.: *J. Chem. Soc., Dalton Trans.* (1989) 73
119. Ohba, S., Ito, M., Saito, Y. and Ishii, T.: *Acta Crystallogr.* **C39** (1983) 997
120. Alnaji, O., Peres, Y., Dahan, F., Dartiguenave, M. and Dartiguenave, Y.: *Inorg. Chem.* **25** (1986) 1383
121. Constable, E.C., Palmer, C.A. and Tocher, D.A.: *Inorg. Chim. Acta* **176** (1990) 57
122. Heeg, M.J., Blinn, E.L. and Deutsch, E.: *Inorg. Chem.* **24** (1985) 1118
123. Thewissen, D.H.M.W. and Van Gaal, H.L.M.: *J. Organomet. Chem.* **172** (1979) 69
124. Ambrosius, H.P.M.M., Van der Linden, A.H.I.M. and Steggerda, J.J.: *J. Organomet. Chem.* **204** (1980) 211
125. Thewissen, D.H.M.W., Noltes, J.G. and Steggerda, J.J.: *Inorg. Chim. Acta* **51** (1981) 135
126. Thewissen, D.H.M.W., Noltes, J.G., Willemse, J. and Diesveld, J.W.: *Inorg. Chim. Acta* **59** (1982) 181

127. Kramolowsky, R.: *Angew. Chem., Int. Ed. Engl.* **8** (1969) 202

128. Nakamoto, K.: "Infrared and Raman Spectra of Inorganic and Coordination Compounds" 3rd Edn (Wiley: New York 1978)

129. Kunze, U. and Antoniadis, A.: *J. Organomet. Chem.* **188** (1980) C21

130. Kunze, U., Antoniadis, A. and Moll, M.: *J. Organomet. Chem.* **215** (1981) 187

131. Kunze, U. and Bruns, A.: *J. Organomet. Chem.* **292** (1985) 349

132. Kunze, U. and Jawad, H.: *Z. Anorg. Allg. Chem.* **532** (1986) 107

133. Annan, T.A., Kumar, R. and Tuck, D.G.: *J. Chem. Soc., Dalton Trans.* (1986) 947

134. Kopf, J., Lenck, R., Olafsson, S. N. and Kramolowsky, R.: *Angew. Chem., Int. Ed. Engl.* **15** (1976) 768

135. Thewissen, D.H.M.W., Ambrosius, H.P.M.M., Van Gaal, H.L.M. and Steggerda, J.J.: *J. Organomet. Chem.* **192** (1980) 101

136. Usón, R., Forniés, J., Usón, M.A., Yagüe, J.F., Jones, P.G. and Meyer-Bäse, K.: *J. Chem. Soc., Dalton Trans.* (1986) 947

137. Palenik, G.J., Mathew, M., Steffen, W.L. and Beran, G.: *J. Am. Chem. Soc.* **97** (1975) 1059

138. Dakternieks, D.; Hoskins, B.F. and Tiekink, E.R.T.: *Aust. J. Chem.* **37** (1984) 197

139. Dakternieks, D.; Corbett, M.; Hoskins, B.F.; Jackson, P.A. and Tiekink, E.R.T.: *Acta Crystallogr.* **C43** (1987) 2439

140. Gal, A.W., Gosselink, J.W. and Vollenbroek, F.A.: *J. Organomet. Chem.* **142** (1977) 357

141. Gal, A.W. and Bolder, F.H.A.: *J. Organomet. Chem.* **142** (1977) 375

142. Kunze, U. and Antoniadis, A.: *Z. Naturforsch.* **36b** (1981) 1117

143. Thewissen, D.H.M.W.: *J. Organomet. Chem.* **192** (1980) 115

144. Kunze, U., Jawad, H. and Burghardt, R.: *Z. Naturforsch.* **41b** (1986) 1142

145. Tiekink, E.R.T. and Winter, G.: *Rev. Inorg. Chem.* **12** (1992) 183

146. Martin, J.M., Newman, P.W.G., Robinson, B.W. and White, A.H.: *J. Chem. Soc., Dalton Trans.* (1972) 2233

147. Newman, P.W.G. and White, A.H.: *J. Chem. Soc., Dalton Trans.* (1972) 2239

148. Healy, P.C., Connor, J.W., Skelton, B.W. and White, A.H.: *Aust. J. Chem.* **43** (1990) 1083

149. Dietzsch, W., Kaiser, J., Richter, R., Golic, L., Siftar, J. and Heber, R.: *Z. Anorg. Allg. Chem.* **477** (1981) 71

150. Dean, P.A.W., Vittal, J.J. and Payne, N.C.: *Inorg. Chem.* **26** (1987) 1683

151. Ueyama, N., Sugawara, T., Sasaki, K., Nakamura, A., Yamashita, S., Wakatsuki, Y., Yamazaki, H. and Yasuoka, N.: *Inorg. Chem.* **27** (1988) 741

152. Adel, J., Weller, F. and Dehnicke, K.: *Z. Naturforsch.* **43b** (1988) 1094

153. Krauter, G., Weller, F. and Dehnicke, K.: *Z. Naturforsch.* **44b** (1989) 444

154. Brennan, J.G., Siegrist, T., Carroll, P.J., Stuczynski, S.M., Brus, L.E. and Steigerwald, M.L.: *J. Am. Chem. Soc.* **111** (1989) 4141

155. Banda, R.M.H., Cusick, J., Scudder, M.L., Craig, D.C. and Dance, I.G.: *Polyhedron* **8** (1989) 1995

156. Lee, G.S.H., Fisher, K.J., Craig, D.C., Scudder, M.L. and Dance, I.G.: *J. Am. Chem. Soc.* **112** (1990) 6435

157. Bochmann, M., Webb, K.J., Hursthouse, M.B. and Mazid, M.: *J. Chem. Soc., Dalton Trans.* (1991) 2317

158. Magull, S., Dehnicke, K. and Fenske, D.: *Z. Anorg. Allg. Chem.* **608** (1992) 17

159. Hursthouse, M.B., Malik, M.A., Motevalli, M. and O'Brien, P.: *Polyhedron* **11** (1992) 45

160. Hursthouse, M.B., Malik, M.A., Motevalli, M. and O'Brien, P.: *J. Mater. Chem.* **2** (1992) 949

161. Vittal, J.J., Dean, P.A.W. and Payne, N.C.: *Can. J. Chem.* **70** (1992) 792

162. Hoskins, B.F. and Kelly, B.P.: *Inorg. Nucl. Chem. Lett.* **8** (1972) 875

163. Abrahams, B.F., Hoskins, B.F., Winter, G. and Tiekink, E.R.T.: *Inorg. Chim. Acta* **150** (1988) 147

164. Domenicano, A., Torelli, L., Vaciago, A. and Zambonelli, L.: *J. Chem. Soc. (A)* (1968) 1351

165. Casas, J.S., Sanchez, A., Bravo, J., Garcia-Fontan, S., Castellano, E.E. and Jones,

M.M.: *Inorg. Chim. Acta* **158** (1989) 119

166. Airoldi, C., De Oliveira, S.F., Ruggiero, S.G. and Lechat, J.R.: *Inorg. Chim. Acta* **174** (1990) 103

167. Glinskaya, L.A., Zemskova, S.M., Klevtsova, R.F., Gromilov, S.A. and Larionov, S.V.: *Zh. Neorg. Khim.* **36** (1991) 902

168. Baggio, R., Frigerio, A., Halac, E.B., Vega, D. and Perec, M.: *J. Chem. Soc., Dalton Trans.* (1992) 1887